ДОКЛАДЫ
АКАДЕМИИ НАУК СССР

Vol. 138, Nos. 1-6
May-June, 1961

PROCEEDINGS OF THE ACADEMY OF SCIENCES

OF THE USSR

(DOKLADY AKADEMII NAUK SSSR)

Physical Chemistry Section

M. I. T. Lincoln Laboratory
FEB 21 1962
Received-Library

IN ENGLISH TRANSLATION

c/b

CONSULTANTS BUREAU

RESEARCH BY SOVIET EXPERTS

Translated by Western Scientists

INSTABILITY CONSTANTS OF COMPLEX COMPOUNDS

by K. B. Yatsimirskii and V. P. Vasil'ev

Instability constants quantitatively characterize the equilibrium in solutions of complex compounds and, in this connection, are very widely used by chemists in different fields (analytical chemistry, electrochemistry, technology of nonferrous and rare metals, etc.) for appropriate calculations.

The instability constants of 1381 complex compounds are given. The authors have prefaced the summary of instability constants with an introductory section which examines methods of calculating instability constants from experimental data, the effect of external conditions (temperature and ionic strength) on the stability of complexes and the main factors determining the stability of complex compounds in aqueous solutions.

Cloth **200 pages** **$6.75**

SOVIET RESEARCH ON COMPLEXES AND CO-ORDINATION CHEMISTRY

This collection consists of 372 articles by Russian scientists in the general area of the chemistry of complexes. These reports have been complied from the Consultants Bureau translations of the following Soviet journals:

Journal of General Chemistry
Journal of Analytical Chemistry
Bulletin of the Academy of Sciences
Division of Chemical Sciences
Proceedings of the Academy of Sciences
Journal of Applied Chemistry
Soviet Journal of Atomic Energy

The articles have been grouped into five volumes, each of which may be purchased separately.

I. Inorganic Complexes—103 articles **$65.00**
II. Metal-Organic Complexes—86 articles **$45.00**
III. Thermodynamic and Kinetic Studies—57 articles .. **$37.50**
IV. Complexes in Analytical Chemistry—57 articles .. **$37.50**
V. Condensed Inorganic Systems; Miscellaneous —38 articles .. —31 articles .. **$45.00**

Complete collection .. **$200.000**

Tables of contents on request

Payment in sterling may be made to Barclays Bank in London, England

CONSULTANTS BUREAU

227 West 17th Street • New York 11, N. Y.

Vol. 138, Nos. 1-6
May-June, 1961

PROCEEDINGS OF THE ACADEMY OF SCIENCES

OF THE USSR

(DOKLADY AKADEMII NAUK SSSR)

Physical Chemistry Section

A publication of the Academy of Sciences of the USSR

IN ENGLISH TRANSLATION

Year and issue of first translation:
Vol. 112, Nos. 1-6 Jan.-Feb. 1957

Annual subscription	*$160.00*
Single issue	*35.00*

Copyright © 1961
CONSULTANTS BUREAU ENTERPRISES, INC.
227 West 17th Street, New York, N. Y.

A complete copy of any paper in this issue may be purchased from the publisher for $5.00

Note: The sale of photostatic copies of any portion of this copyright translation is expressly prohibited by the copyright owners.

Printed in the United States of America

PROCEEDINGS OF THE ACADEMY OF SCIENCES OF THE USSR
Physical Chemistry Section

Vol. 138, Nos. 1-6 May-June, 1961

CONTENTS

	PAGE	RUSS. ISSUE	RUSS. PAGE
The Coagulating Action of Electrolyte Mixtures on Lyophobic Sols. The Effect of Counterion Adsorption. V. M. Barboi, Yu. M. Glazman, and I. M. Dykman	383	1	139
Isothermal Distillation in a System Consisting of a Fog from Water and a Fog from a Weak Solution. M. V. Bulkov	387	1	143
The Effect of Co^{60} γ-Rays on the Isotopic Exchange between Hydrocarbon Polymers and Gaseous Deuterium. Z. S. Bulanovskaya, Ya. M. Varshavskii, V. L. Karpov, and I. Ya. Petrov	390	1	146
The Kinetics of Caprolactam Hydrolysis in Aqueous KOH Solutions. M. I. Vinnik, Yu. V. Moiseev, and L. V. Palagina	393	1	149
The Photochemical Reduction of Ferric Chloride in Aromatic Hydrocarbons. A. I. Kryukov and B. Ya. Dain	396	1	153
Contact Potential Differences between Some Liquid Metals and Their Alloys. V. A. Kuznetsov, L. S. Zagainova, N. P. Loginova, I. Ya. Lyubimtseva, N. S. Onoprienko, and L. E. Tsimbal	399	1	156
Determination of Curves on the Formation of Centers of Crystallization and on the Velocity of Crystal Growth in Glass by Means of Density Measurements. É. M. Rabinovich	402	1	159
Atom-Scattering Factors and the Distribution of Electron Density in Gallium Antimonide. N. N. Sirota and E. M. Gololobov	405	1	162
The Polymerization of Methyl Methacrylate by the Electrolytic Reduction of Oxygen. A. I. Fedorova, I. V. Shelepin, and N. B. Moiseeva	408	1	165
Radiation Transformations of Fe^{2+} and Fe^{3+} Mixtures in Acid Solutions Saturated with Hydrogen under Pressure. V. N. Shubin and P. I. Dolin	412	1	169
The Separation of Silicon Isotopes by the Fractional Distillation of Silane. G. G. Devyatykh, G. K. Borisov, and A. M. Pavlov	416	2	402
The Adsorption of Nitrogen, Argon, and Krypton on Various Surfaces and the Determination of Surface Areas. M. G. Kaganer	419	2	405
The Effect of Overstoichiometric Oxygen on the Catalytic, Adsorption, and Electrical Properties of Nickel Oxide. L. N. Kutseva	423	2	409
The Variation of the Surface Tension of Thallium with Temperatures. O. A. Timofeevicheva and V. B. Lazarev	425	2	412
An Investigation of Thin Benzene Films on a Mercury Surface. A. Sheludko and D. Platikanov	428	2	415
A Study of the Properties of the Surface of Crystalline Titanium Dioxide. L. G. Ganichenko and V. F. Kiselev	431	3	608
The Hyperfine Structure of the Electron Paramagnetic Resonance Line in Aqueous Solutions of V^{2+} Salts. N. S. Garif'yanov	435	3	612
The Relation between the Mechanical Properties of Crystalline Polymers and Their Supermolecular Structures. A. V. Ermolina, L. A. Igonin, L. A. Nozova, I. I. Farberova, and K. N. Vlasova	437	3	614

CONTENTS (continued)

	PAGE	RUSS. ISSUE	RUSS. PAGE
The Structure of the Surface Compounds Formed by Carbon Monoxide on Palladium from Adsorption Measurements and Infrared Spectral Data. N.N.Kavtaradze and V. I. Lygin	439	3	616
Polymerization of Nitroethylene with γ-Radiation. V. N. Sokolov, I. Ya. Poddubnyi, V. V. Perekalin, and V. F. Evdokimov	442	3	619
A Rule Concerning Interatomic Distances in Halogenide Molecules of Different Groups of the Periodic System. V. M. Tatevskii, V. P. Spiridonov, and P. A. Akishin	444	3	621
The Electron Spectrum in a Polymer Chain. A. B. Almazov	448	4	863
Composition of the Unit Cells and Maximum Adsorption Volumes of Dehydrated Synthetic Zeolite Crystals. M. M. Dubinin	450	4	866
Selective Sorption on Porous Glasses. S.P.Zhdanov and E.V.Koromal'di	454	4	870
Relation between Spontaneous Ignition and Laminar and Turbulent Burning Velocities of Paraffin Hydrocarbons. V. P. Karpov and A. S. Sokolik	457	4	874
The Adsorptive and Ion-Exchange Properties of Silica Modified by a Radical with Acid Functions. I. E. Neimark and V. M. Chertov	460	4	877
The Formation of Hydrazine by the γ-Ray Irradiation of Liquid and Solid Ammonia. Yu. A. Sorokin and S. Ya. Pshezhetskii	463	4	880
The Applicability of Allen's Model to the Radiolysis of Aqueous Solutions. V. G. Firsov and B. V. Ershler	466	4	884
The Adsorption of Hexane and Benzene Vapors on Inactive and Radioactive Barium Sulfate. L. D. Belyakova, V. V. Gromov, A. V. Kiselev, and Vikt. I. Spitsyn	468	5	1139
The Radio-Thermal Cracking of Liquid Hydrocarbons. A. M. Brodskii, K. P. Lavrovskii, and V. B. Titov	472	5	1143
Electrical Double Layer Resulting from Donor-Acceptor Bonding at the Contact Surface between Amorphous Solids. V. P. Smilga	476	5	1147
A Study of the Surface of an Iron Electrode by Measuring the Potential Decay after Switching of the Current. V. V. Sobol' and Z. A. Iofa	480	5	1151
The Retarding Effect of the Uranyl Ion in the Radiation-Chemical Oxidation of Bivalent Iron. V. G. Firsov	483	5	1155
Adsorption Isosteres in the Potential Theory. B.P.Bering, M. M. Dubinin, and V. V. Serpinskii	486	6	1373
The Effects of Alkali Metal Cations on the Hydrogen Overvoltage at a Mercury Electrode in Acid Solutions. É. A. Maznichenko, B. B. Damaskin, and Z. A. Iofa	490	6	1377
The Photoconductivity Kinetics of Chlorophyll and Green Leaf Pigments. E. K. Putseiko	494	6	1381
The Separation of the Hydrogen Isotopes on a Palladium Cathode. G. N. Trusov, N. A. Aladzhalova, and V. I. Veselovskii	498	6	1385
The Thermal Expansion of Water in Microcapillaries. N. N. Fedyakin	502	6	1389

THE COAGULATING ACTION OF ELECTROLYTE MIXTURES ON LYOPHOBIC SOLS

THE EFFECT OF COUNTERION ADSORPTION

V. M. Barboi, Yu. M. Glazman, and I. M. Dykman

Kiev Technological Institute of Light Industry
(Presented by Academician P. A. Rebinder, December 20, 1960)
Translated from Doklady Akad. Nauk SSSR, Vol. 138, No. 1,
pp. 139-142, May, 1961
Original article submitted November 17, 1960

The present communication, unlike the previous ones [1, 2] in which strongly charged sols were discussed, is devoted to clarifying the effect of adsorption phenomena on the regularities found in the coagulation of lyophobic colloids by electrolyte mixtures. In this study we will investigate one of the limiting cases of coagulation: that where as a result of counterion adsorption the potential of the colloidal particles has been depressed so strongly that the following expression, which is the criterion for the stability of weakly charged sols [3], becomes applicable

$$\psi_a^2/\varkappa \geqslant a_1 = \text{const.} \tag{1}$$

Here $\varkappa$ represents the inverse thickness of the ionic atmosphere in the solution; ψ_a is taken by us to be the potential at the boundary of the adsorbed layer on the colloidal particles.

To simplify the calculations, several assumptions are introduced:

1. The particle concentration in the colloidal system is supposed to be so small that the additional adsorption of the ions which determine the potential, such as takes place when indifferent electrolytes are added to the sol [4], practically does not change the concentration of the ions in the solution. Thanks to this, the value of the potential ψ_0 at the surface of the disperse phase remains constant when the coagulating electrolytes are added.

2. It is supposed that the adsorption of the coagulating electrolyte ions obeys the very simple equation of Langmuir

$$\Gamma_i' = \Gamma_\infty \frac{C_i'/b_i}{1 + \sum_{i=1}^{n} C_i'/b_i}, \tag{2}$$

where Γ_i' represents the adsorption of the i-th ion from the electrolyte mixture,* C_i' the concentration of the i-th ion in the solution; b_i and Γ_∞ are constants of Langmuir's equation.

In addition, we take into account only the adsorption of counterions and do not pay attention to the adsorption of indifferent ions having a charge of the same sign as that on the colloidal particles [5, 6].

3. As a first approximation we postulate that the potential Ψ_a on the boundary of the adsorbed layer changes linearly with the adsorbed amount Γ of the coagulating electrolyte ion

$$\psi_a = \psi_0 - k\Gamma z, \tag{3}$$

where z is the valence of the counterion and k a constant at a given ionic strength of the solution.

* Here and further all values marked by a prime refer to the case where coagulation is effected by an electrolyte mixture; the absence of a prime corresponds to coagulation by a single electrolyte.

When we denote the charge density in electrons (after the coagulating electrolyte has been added to the sol) at the boundary of the adsorbed layer by Q_a and that on the surface of the disperse phase by Q_0, we may obviously write down the equality

$$Q_a = Q_0 - \Gamma z. \tag{4}$$

When one takes into account that at $\Gamma z = Q_0$, $\psi_a = 0$, then by using the relations (3) and (4) one may easily get the equation

$$Q_a / Q_0 = \psi_a / \psi_0. \tag{5}$$

From this it follows that relation (3) is equivalent to the assumption that counterion adsorption has no noticeable effect on the capacity of the double layer as a whole.

Since the capacity of the double layer is inversely proportional to its thickness or to the radius of the ionic atmosphere ($1/\varkappa$), which in its turn is inversely proportional to the square root of the ionic strength J of the solution [7], then

$$Q_0 / \psi_0 = Q_a / \psi_a = \alpha J^{1/2}, \tag{6}$$

where α is a constant.

When coagulation of the sol is effected by a mixture of two electrolytes, combination of the equality (1) with relations (4) and (6) gives

$$\alpha\psi_0 (J_c')^{1/2} - \alpha a^{1/2} (J_c')^{3/4} = \Gamma_{1c}' z_1 + \Gamma_{2c}' z_2, \tag{7}$$

where here and further the index c indicates the "critical" value of the corresponding property.

It is expedient to modify somewhat the equation obtained. For this purpose we write down the expression (7) separately for each of the electrolytes considered and determine the values of the constants $\alpha a^{\frac{1}{2}}$ and $\alpha\psi_0$. By substituting the relations found into equation (7), we get

$$\frac{(J_{1c}/J_{2c})^{3/4} - (\Gamma_{1c} z_1)/(\Gamma_{2c} z_2)}{(J_{1c}/J_{2c})^{3/4} - (J_{1c}/J_{2c})^{1/2}} (J_c'/J_{2c})^{1/2} -$$
$$- \frac{(J_{1c}/J_{2c})^{1/2} - (\Gamma_{1c} z_1)/(\Gamma_{2c} z_2)}{(J_{1c}/J_{2c})^{3/4} - (J_{1c}/J_{2c})^{1/2}} (J_c'/J_{2c})^{3/4} = \frac{\Gamma_{1c}' z_1 - \Gamma_{2c}' z_2}{\Gamma_{2c} z_2}. \tag{8}$$

Equation (8) may be used in this form for calculating the coagulation curve for a mixture of two electrolytes, if the coagulation concentration of each of the separate electrolytes and the adsorbability (that is, the constants b_i in Langmuir's equation) of both coagulating ions are known. It should, however, be noted that the general character of the regularities found for the coagulating effect of an electrolyte mixture may be established, even if one does not resort to a complete calculation of the curve. For this purpose, it suffices to determine the values of the derivatives

$$\Phi = \lim_{C_1'=0} (dC_2')/(dC_1'),$$
$$F = \lim_{C_2'=0} (dC_2')/(dC_1'),$$

which characterize the course of the curve at its ends.

Equation (8) can be differentiated more easily, if by using (1), (4), and (6) it is transformed into

$$\frac{1}{1-K_{2c}} \left(\frac{J_c'}{J_{2c}}\right)^{1/2} - \frac{K_{2c}}{1-K_{2c}} \left(\frac{J_c'}{J_{2c}}\right)^{3/4} = \frac{\Gamma_{1c}' z_1 + \Gamma_{2c}' z_2}{\Gamma_{2c} z_2}, \tag{9}$$

where $K = \psi_a/\psi_0$.

When one differentiates (9), it should be taken into consideration that the coagulating concentration of the electrolyte is related to the adsorbability of the counterion by the relation

$$\frac{(1-K_{1c})\,K_{1c}^2}{\Gamma_{1c}\,z_1} = \frac{(1-K_{2c})\,K_{2c}^2}{\Gamma_{2c}\,z_2} = \text{const}, \tag{10}$$

which is obtained by combining (1), written in the form $\psi_a^2 = \text{const} \cdot J^{\frac{1}{2}}$, with (4) and (6). Although we do not give here the rather cumbersome formulas for the limits of the derivatives, Φ and F, we note one very important fact. The relations mentioned contain only the values K_1, K_2, z_1, and z_2 as variables. So, by assigning various values to the potential drop in the adsorbed layer separately for each of the electrolytes, it is possible to calculate the values of the derivative limits Φ and F. Calculations done in this way have shown that the equation derived expresses all types of regularities usually found in the experiments in the coagulation of lyophobic sols by electrolyte mixtures, namely, antagonism, superadditivity and synergism.

To carry out a complete calculation of the entire coagulation curve for a mixture of two electrolytes, one must assume numerical values for the four variables entering into the corresponding equation. From these, however—because of (10)—only three values may be assigned arbitrarily. The numerical value of the constants in (10) may be estimated by starting from the following considerations.

The numerator at the left side of this equality has a maximum at the value $K = \frac{2}{3}$. If we assume that among the electrolytes with univalent coagulating ions the case which satisfies the condition $K = \frac{2}{3}$ will certainly occur, we get for this case

$$\text{const} = \frac{4/27}{\Gamma}.$$

If we examine only coagulation phenomena where in the critical state of the sol the coverage of the colloidal particle surface by counterions is limited by the condition

$$\Gamma \leqslant \tfrac{1}{2}\,\Gamma_\infty, \tag{11}$$

we find that

$$\text{const} \cdot \Gamma_\infty = \gamma \geqslant 8/27. \tag{12}$$

It can be easily proved that (11) corresponds to a coagulation which sets in when during the addition of electrolyte to the sol the potential of the colloidal particles drops to a certain (critical) value, which depends upon the ionic strength of the solution. At the same time, the following formula can be obtained from (4) and (6)

$$\psi_a = \psi_0 \left(1 - \frac{\Gamma z}{\beta J^{1/2}}\right). \tag{13}$$

This expresses the way in which the potential at the boundary of the adsorbed layer depends upon the electrolyte concentration in the solution. An analysis of this equation shows that the curve $\psi_a = f(C)$ goes through a minimum which corresponds to an electrolyte concentration C = b (figure). Therefore, the restriction (11) means that in this study we investigate only the coagulation in the falling branch of the curve in the figure, namely at electrolyte concentrations $C \leq b$.

Since the value of γ, as is evident from (10), does not depend upon the kind of electrolyte, (12) remains valid for any electrolyte. We calculated all coagulation curves for the various electrolyte mixtures with the value $\gamma = 8/27$, since at $\gamma > 8/27$ the coagulation law remains qualitatively unchanged.

As a result of the calculations, it has been established that a positive deviation from additivity in the coagulated effect (antagonism or superadditivity) will occur in those cases where the critical values of the ionic strength in the solution for each of the separate electrolytes differ considerably from each other; as these differences are raised the tendency to superadditivity and antagonism increases. Synergism can be observed only when the potential of the col-

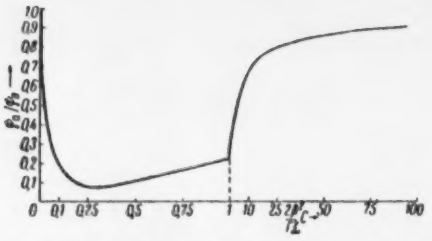

The change in the potential of the colloidal particle plotted against the electrolyte concentration in the solution (beyond one the scale of the abscissa axis has been reduced 100 times).

loidal particles is sufficiently small not only in the critical but also in the original state of the sol. It should be noted specially that antagonism in the coagulation of lyophobic sols turns out to be possible even in the case where one of the counterions added to the colloidal solution is not adsorbed at all. It is quite evident that here the phenomenon of antagonism is not connected with mutual depression of the adsorption of the coagulating ions; it results, probably, because at the addition of electrolytes to the sol besides adsorption of counterions there still takes place, as is well known [4], additional adsorption of the ions which determine the potential of the colloidal particles.

The authors consider it their pleasant duty to express their gratitude to B. V. Deryagin, Corresponding Member, Academy of Sciences, USSR, for his critical discussion of the results and many very valuable comments.

LITERATURE CITED

1. Yu. M. Glazman and I. M. Dykman, Doklady Akad. Nauk SSSR 100, 299 (1955); Kolloid. Zhur. 18, 13 (1956).
2. Yu. M. Glazman, I. M. Dykman, and E. A. Strel'tsova, Doklady Akad. Nauk SSSR 117, 829 (1957); Kolloid. Zhur. 20, 149 (1958).
3. B. V. Deryagin, Kolloid. Zhur. 7, 285 (1941); Trans. Farad. Soc. 36, 730 (1940).
4. Yu. M. Glazman, D. N. Strazhesko, and others, Kolloid. Zhur. 21, 263 (1959).
5. Yu. M. Glazman and D. N. Strazhesko, Doklady Akad. Nauk SSSR 75, 411 (1950); Yu. M. Glazman. D. N. Strazhesko, and B. É. Tartakovskaya, Kolloid. Zhur. 15, 161 (1953).
6. Yu. M. Glazman, D. N. Strazhesko, and N. A. Bisikalova, Zhur. Neorg. Khim. 3, 115 (1958).
7. H. Falkenhagen, Electrolytes [Russian translation] (Leningrad, 1935) p. 133.

All abbreviations of periodicals in the above bibliography are letter-by-letter transliterations of the abbreviations as given in the original Russian journal. *Some or all of this periodical literature may well be available in English translation.* A complete list of the cover-to-cover English translations appears at the back of this issue.

ISOTHERMAL DISTILLATION IN A SYSTEM CONSISTING OF A FOG FROM WATER AND A FOG FROM A WEAK SOLUTION

M. V. Buikov

Institute of General and Inorganic Chemistry, Academy of Sciences, Ukr. SSR
(Presented by Academician A. N. Frumkin, December 20, 1960)
Translated from Doklady Akad. Nauk SSSR, Vol. 138, No. 1,
pp. 143-145, May, 1961
Original article submitted November 29, 1960

In many problems connected with the study of mixtures of different fogs, the kinetics of the distillation resulting from the difference in saturated water vapor pressure over the drops of the various components in the fog is of great importance. In particular, the kinetics of distillation from water droplets to small ice crystals has been studied thoroughly [1-3].

The subject of the present note is a study of the distillation from water droplets to drops of a weak solution. The set of equations which describe the distillation has the form

$$\rho_1 r_1 \frac{dr_1}{dt} = D(u - u_1),$$

$$\rho_2 r_2 \frac{dr_2}{dt} = D(u - u_2), \tag{1}$$

$$\frac{du}{dt} + 4\pi D n_1 r_1 (u - u_1) + 4\pi D n_2 r_2 (u - u_2) = 0,$$

where the following denotations have been introduced: r_1, ρ_1, n_1 and r_2, ρ_2, n_2 represent the radius, density, and concentration of the pure water drops and those of the solution, respectively; u the density of water vapor; u_1 and u_2 the corresponding densities of saturated water vapor; D the diffusion coefficient of water vapor in air.

By substituting into (1) the value of u_2 according to Raoult's law

$$u_2 = u_1(1 + \gamma r_2^{-3}); \quad \gamma r_2^{-3} \ll 1; \quad \gamma = \frac{3m\mu_W}{4\pi\rho_1\mu_P}$$

(where m is the weight of substance dissolved in one drop of the solution; μ_W, μ_P are the molecular weights of water and the dissolved substance, respectively), introducing the new function $u' = u - u_1$ and dropping the prime, we obtain

$$\rho_1 r_1 \frac{dr_1}{dt} = Du,$$

$$\rho_2 r_2 \frac{dr_2}{dt} = D(u + u_1\gamma r_2^{-3}), \tag{2}$$

$$\frac{du}{dt} + 4\pi D n_1 r_1 u + 4\pi D n_2 r_2 (u + u_1\gamma r_2^{-3}) = 0.$$

The initial conditions are:

$$r_1 = r_{10}, \quad r_2 = r_{20}, \quad u = 0 \quad \text{for} \quad t = 0.$$

For solving the set (2), we use the so-called "quasistationary" approximation [1, 2], that is, in a first approximation we take the water vapor density to be constant. By assuming in the third equation of the set (2) that $du/dt \approx 0$, we get

$$u = -u_1\gamma r_2^{-3}\left(1 + \frac{n_1 r_1}{n_2 r_2}\right)^{-1}. \tag{3}$$

From (3) it is evident that the initial condition u = 0 is approximately met for weak solutions. By differentiating (3) with respect to time, we obtain

$$\left|\frac{du}{dt}\frac{T}{u_1}\right| = \frac{u}{u_1}\left[T\cdot\frac{dr_1}{dt}\frac{n_1}{n_1r_1+n_2r_2} + T\frac{dr_2}{dt}\left(\frac{2}{r_2}+\frac{n_1}{n_1r_1+n_2r_2}\right)\right], \tag{4}$$

where T is the time at which the drops of the water fog have evaporated completely; it is the characteristic time for the problem. From (4) it follows that the applicability condition of the approximation used: $|(du/dt)\cdot(T/u_1)| \ll 1$ is satisfied, since $u \ll u_1$ and all terms enclosed in brackets are of the order of one.

Since time does not enter explicitly into (2), we may take r_2 to be a function of r_1 : $r_2(r_1)$. By this and using (3), one may easily get

$$r_2^2 dr_2 = -\nu r_1^2 dr_1;\quad r_2 = r_{20} \quad \text{at} \quad r_1 = r_{10};\quad \nu = \frac{\rho_1 n_1}{\rho_2 n_2}. \tag{5}$$

By integrating (5) and using the initial condition, we obtain

$$r_2 = r_m\left(1-\nu r_1^3 r_m^{-3}\right)^{1/3};\qquad r_m = r_{20}\left(1+\alpha\right)^{1/3};\quad \alpha = \frac{n_1\rho_1 r_{10}^3}{n_2\rho_2 r_{20}^3}, \tag{6}$$

where r_m is the radius attained by the solution droplets at the moment when the water droplets disappear.

From the first equation of the set (2), we find:

$$\int_{r_{10}}^{r_1}\frac{r'dr'}{u(r')} = \frac{D}{\rho_1}t. \tag{7}$$

By simple algebra, using (3) and (6), we obtain from (7) an implicit relation $r_1(t)$:

$$t = t_0 J\left(\frac{r}{r_{10}}\right).$$
$$J(x) = {}^1/_2\left(1-x^2\right)\beta\left(1+\alpha\right)^{-4/3} - {}^1/_5\left(1-x^5\right)\alpha\beta\left(1+\alpha\right)^{-4/3} +$$
$$+\frac{\rho_2}{5\rho_1}\left(1-\frac{\alpha}{1+\alpha}x^3\right)^{5/3} - \frac{\rho_2}{5\rho_1}\left(1+\alpha\right)^{-4/3}; \tag{8}$$
$$t_0 = \frac{r_m^3}{\gamma}\frac{\rho_1 r_m^3}{Du_1};\quad \beta = \frac{r_{10}^2}{r_{20}^2}.$$

The time T required for completely evaporating the droplets of the water fog is determined by the equation

$$T = t_0 J\left(\frac{r_1}{r_{10}}\right)\Big|_{r_1=0}. \tag{9}$$

It is evident from (8) that J(x) and also J(0) depend upon two parameters: the ratio α between the amount of water fog and that of solution per unit volume and the ratio β of the water drop surface to that of the solution at the beginning. Depending upon the magnitude of these parameters, one may obtain some simple formulas for the time of completely evaporating the water droplets: at $\alpha \gg 1$, that is, when the amount of solution added is much smaller than that of water and $\beta \lesssim 1$,

$$T = \frac{r_{20}^3}{\gamma}\frac{\rho_2 r_{20}^2}{5Du_1}\alpha^{5/3}. \tag{10}$$

The same formula is valid at $1 \ll \beta \ll \alpha^{2/3}$. At $1 \ll \alpha^{2/3} \ll \beta$ we have the formula

$$T = 0{,}3\frac{r_{20}^3}{\gamma}\frac{\rho_1 r_{10}^2}{Du_1}\alpha. \tag{11}$$

From (10) and (11) it follows that by keeping α, r_{10} constant and taking smaller solution droplets we may decrease T. In the opposite limiting case $\alpha \ll 1$ and $\beta \gtrsim 1$, we have

$$T = \frac{r_{20}^3}{\gamma} \frac{\rho_1 r_{10}^3}{2Du_1}. \tag{12}$$

The latter formula is also valid at $1 \gg \beta \gg \alpha$. In the case where $1 \gg \alpha \gg \beta$, we get

$$T = \frac{r_{20}^3}{\gamma} \frac{\rho_2 r_{20}^3}{3Du_1} \alpha, \tag{13}$$

and in this case, too, a decrease in the initial radius of the solution droplets results in a lowered T. We note that formula (12) gives the time required to evaporate one water drop located between solution droplets.

Because the problem has been solved for monodisperse fogs and actual fogs are polydisperse, it is of interest to discuss distillation in a mixture of polydisperse fogs; this is the subject of a separate communication.

I thank S. S. Dukhin for helpful discussions.

LITERATURE CITED

1. K. S. Shifrin, Trudy Glavn. Geofiz. Obs. 31, 93 (1951).
2. K. S. Shifrin and N. Ya. Perel'man, Doklady Akad. Nauk SSSR 132, 1148 (1960).
3. K. S. Shifrin and N. Ya. Perel'man, Izvest. Akad. Nauk SSSR, Ser. Geofiz. No. 6, 839 (1960).

All abbreviations of periodicals in the above bibliography are letter-by-letter transliterations of the abbreviations as given in the original Russian journal. *Some or all of this periodical literature may well be available in English translation.* A complete list of the cover-to-cover English translations appears at the back of this issue.

THE EFFECT OF Co^{60} γ-RAYS ON THE ISOTOPIC EXCHANGE BETWEEN HYDROCARBON POLYMERS AND GASEOUS DEUTERIUM

Z. S. Bulanovskaya, Ya. M. Varshavskii, V. L. Karpov, and I. Ya. Petrov

L. Ya. Karpov Physicochemical Institute

(Presented by Academician V. A. Kargin, December 12, 1960)
Translated from Doklady Akad. Nauk SSSR, Vol. 138, No. 1, pp. 146-148, May, 1961
Original article submitted December 8, 1960

In the paper [1] it was shown that under the action of ionizing irradiation there is isotopic exchange between some polymers and gaseous deuterium. It is known that this process, which in the absence of irradiation does not take place, was explained by the fact that the decomposition of the polymer molecule to radicals and hydrogen by irradiation appears to be reversible to some extent so that deuterium atoms enter into the polymer molecule. In the study [1] the active zone of a water–solution reactor was used as radiation source; the experiments were done in sealed glass ampoules at a deuterium pressure of about one atmosphere.

The purpose of the present study was to investigate the said phenomenon in more detail by using pure Co^{60} γ-radiation and also to examine whether exchange is possible between several liquid hydrocarbons (n-pentane, cyclopentane, n-hexane, cyclohexane, and benzene) and gaseous deuterium under the action of Co^{60} γ-radiation, since such exchange reactions, just as the reaction with hydrocarbon polymers as is well known, under normal conditions do not take place in the absence of irradiation. In a first approximation we have studied how the effect observed depends upon the magnitude of the polymer surface area, the irradiation dose, the deuterium pressure, and the temperature.

Methods. The experiments were carried out in metallic ampoules at deuterium pressures up to 150 atm. A weighed portion of the sample to be tested (0.3 - 0.5 g) was put into the hermetically sealed ampoule having about 20-ml capacity and provided with a valve. The ampoule was evacuated and filled with gaseous deuterium (~99.6% D) from a cylinder, the pressure of which exceeded 150 atm. The packings and the glands of the valves were made of polyethylene. The pressure was checked by means of a calibrated standard manometer connected to the filling system. After it had been filled, the ampoule was disconnected and the valve covered by a special cap with a plug to prevent the leaking of deuterium through the valve, which might occur as a result of the action of the irradiation on the gland. The ampoules prepared in this way were exposed to irradiation by a source of Co^{60} γ-radiation. After the irradiation the pressure in the ampoule was checked; the sample tested was drawn out and its deuterium content determined.

For this purpose a weighed portion (~0.15 g) was burned in an oxygen atmosphere at 900°, the water formed was collected, purified from possible impurities and CO_2 by sublimation in vacuum after BaO had been added, and the deuterium concentration was determined by the drop method [2]. The accuracy of the isotope analysis was ±0.02%. The value obtained gives the average concentration of deuterium in the substance. By blank experiments it has been shown that a long contact between the polymer and gaseous deuterium in the absence of irradiation does not result in the appearance of heavy water in the combustion products of the polymer. This proves that the presence of deuterium in the polymer, as is found in irradiation experiments, is not connected with the adsorption of hydrogen on the film surface but originates from the entering of deuterium into the molecule studied.

Results and discussion. To examine the effect of pure Co^{60} γ-radiation we have investigated the isotopic exchange between gaseous deuterium on the one hand and two polymers – polyethylene and polymethylmethacrylate – on the other hand. Among the polymers investigated in the study [1], maximum exchange is found in the case of polyethylene, whereas for polymethylmethacrylate the fraction of exchange is the smallest. In both experiments the irradiation dose was $4 \cdot 10^8$ r; the deuterium pressure was 150 atm. For polymer samples of the order of 1 g and an ampoule volume of 70 ml the deuterium concentration was 0.55 at. % in the case of polyethylene and 0.27 at. % in the

case of polymethylmethacrylate. These data show that the type of the ionizing radiation has no substantial influence upon the hydrogen exchange studied. The reason why in the study [1] no noticeable entering of deuterium into polymethylmethacrylate was found probably lies in the fact that the irradiation dose was not high enough.

As the experiment shows, the amount of deuterium entered strongly depends upon the magnitude of the polyethylene surface area. So, at a dose of $2 \cdot 10^8$ r and a deuterium pressure of 150 atm the deuterium concentration in the case of a 0.3-mm-thick polyethylene film was 0.45 at. %, whereas in an experiment with powdered polyethylene the deuterium concentration was 1.55 at. %. The main reaction characteristics were studied with a nonstabilized polyethylene in the form of a 0.07- to 0.08-mm film.

The results obtained when studying the concentration of deuterium entering into the polymer as a function of the integral irradiation dose are shown in Fig. 1. The curve indicates how the deuterium concentration in the sample rises at increased doses. At an irradiation dose of $2 \cdot 10^8$ r we have studied the deuterium concentration in polyethyl-

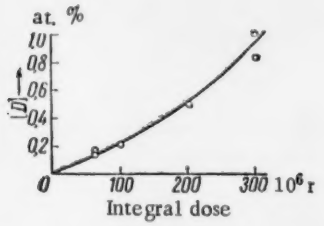

Fig. 1.

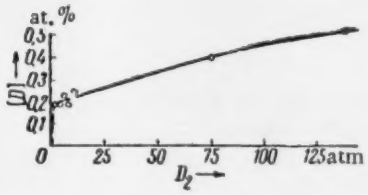

Fig. 2.

ene as a function of the deuterium pressure in the ampoule. The corresponding data are shown in Fig. 2. They indicate that in the range from 2 to 140 atm the deuterium concentration increases altogether only by 2-2.5 times. It is evident that at a deuterium pressure close to zero, exchange will not occur. Therefore, in the pressure region below 2 atm we have extrapolated the experimental curve in the form of the dashed line shown in Fig. 2.

So, the rapid rise of the deuterium concentration in the polymer at increasing deuterium pressures in the region of small pressures (up to 2 atm) and the relative slow rise in the region of higher pressures (up to 150 atm) are characteristic features of the process studied.

To find out how the effect observed depends upon temperature, besides the experiments at room temperature, we have also done experiments at 100° (boiling water) and −196° (liquid nitrogen). The irradiation dose in both experiments was $8 \cdot 10^7$ r, the deuterium pressure ~100 atm. In the experiment done at t = 100° the deuterium concentration in the polymer was 0.25 at. %, in that at t = −196° it was 0.08 at. %.

The results of experiments on the isotopic exchange between several low-molecular hydrocarbons and gaseous deuterium are given in the table. The data obtained prove that at a dose of $2 \cdot 10^8$ r and a deuterium pressure of 10 atm deuterium is found to enter from the gas phase into the CH bonds of the hydrocarbons studied.*

Raising the pressure to ~145 atm results in all cases in a considerably increased deuterium concentration in the hydrocarbon.

So, the previously discovered initiation of isotopic exchange between the C−H bonds of some polymers and gaseous deuterium under the action of ionizing radiation has been confirmed. It has been shown that the type of irradiation has no noticeable influence upon the exchange found, and such an exchange is characteristic not only for high-molecular compounds but also for low-molecular hydrocarbons. For hydrocarbons of various structures the fraction of exchange has been studied as a function of temperature and deuterium pressure.

The results obtained throw light on the mechanism of isotopic exchange in the case where radioactive isotopes (for instance, tritium) are used; in this case the radioactivity of the isotope itself, analogously to irradiation from the outside, may serve as the factor initiating the exchange.

* The hydrocarbons were identified by means of the boiling point, which did not change by the irradiation.

Substance	Amount of hydrocarbon, g	Deuterium pressure, atm		Deuterium concentration, at. %	Yield in moles per 100 ev	Substance	Amount of hydrocarbon, g	Deuterium pressure, atm		Deuterium concentration, at. %	Yield in moles per 100 ev
		before irradiation	after irradiation					before irradiation	after irradiation		
n-Pentane	0.80	10	10	0.09	0.8	n-Hexane	0.55	142	135	0.26	2.2
n-Pentane	0.70	147	141	0.46	3.9	Cyclohexane	0.43	10	10	0.02	0.1
Cyclopentane	0.50	10	10	0.18	1.3	Cyclohexane	0.50	142	142	0.21	1.6
Cyclopentane	0.70	147	125	0.55	4.0	Benzene	0.80	10	10	0.05	0.2
n-Hexane	0.46	10	10	0.10	0.8	Benzene	0.55	147	141	1.32	5.2

The effect observed should be taken into account when radioactive indicators are used in chemistry or biology; here the activation energies of exchange reactions may be rather small, and the values found when one uses stable and radioactive isotopes of one and the same element may be different.

LITERATURE CITED

1. Ya. M. Varshavskii, G. Ya. Vasil'ev, V. L. Karpov, Yu. S. Lazurkin, and I. Ya. Petrov, Doklady Akad. Nauk SSSR 118, 315 (1958).
2. A. I. Shatenshtein and Ya. M. Varshavskii, Zhur. Anal. Khim. 11, 746 (1956).

All abbreviations of periodicals in the above bibliography are letter-by-letter transliterations of the abbreviations as given in the original Russian journal. *Some or all of this periodical literature may well be available in English translation.* A complete list of the cover-to-cover English translations appears at the back of this issue.

THE KINETICS OF CAPROLACTAM HYDROLYSIS IN AQUEOUS KOH SOLUTIONS

M. I. Vinnik, Yu. V. Moiseev, and L. V. Palagina

Institute of Chemical Physics, Academy of Sciences, USSR
(Presented by Academician V. N. Kondrat'ev, December 15, 1960)
Translated from Doklady Akademii Nauk SSSR, Vol. 138, No. 1,
pp. 149-152, May, 1961
Original article submitted December 8, 1960

It is well known that solutions of alkalis in water, alcohols, and other organic solvents are effective catalysts. The literature on the catalytic action of alkalis (NaOH and KOH), while extensive, is mainly of a qualitative character. Quantitative studies have been concerned with investigations in dilute and moderately concentrated alkali solutions. Because of the lack of quantitative data on the kinetic course of chemical reactions in concentrated alkali solutions, it has not been possible as yet to come to conclusions of a general nature concerning the mechanism of catalytic activity in such media.

Based on the experimental results of the kinetics of hydrolysis in dilute alkali solutions, a number of authors [1-3] have concluded that the limiting stage is the interaction between an hydroxyl ion and a reagent molecule B. In such a case

$$W = K_{\text{eff}} \cdot C_B = K_{\text{true}} \cdot a_{OH^-} \cdot C_B \frac{f_B}{f^*}; \quad K_{\text{eff}} = K_{\text{true}} \cdot a_{OH^-} \cdot \frac{f_B}{f^*}, \tag{1}$$

where a_{OH^-} is the activity of the hydroxyl and f_B, f^* are the activity coefficients of the reagent and the activated complex.

At present the direct experimental proofs are that for an entire series of processes the catalytic action of acidic media results in conversion of the reagent into an ionic form and the limiting stage is the conversion stage of the ionized form. By analogy with catalysis in acid media it is possible to assume that in alkaline media also, the reagent will be subject to ionization whereby equilibrium between the ionized and un-ionized forms will be rapidly established. The results of Edward and Terry [2] on the hydrolysis of diacetylamine and succinimide and of Taft and co-workers [3] on the hydrolysis of trifluoroacetanilide can be considered as evidence for this viewpoint. We define the dissociation equilibrium of caprolactam B by K_p expressed in activity constants

$$B + OH^- \rightleftarrows BOH^-; \quad K_p = \frac{a_B \cdot a_{OH^-}}{a_{BOH^-}}.$$

For the condition that the degree of dissociation is small, the equation for K_{eff} is correctly

$$W = K_{\text{eff}} \cdot C_B = \frac{K_{\text{true}}}{K_p} a_{OH^-} \cdot C_B \cdot \frac{f_B}{f^*}; \quad K_{\text{eff}} = \frac{K_{\text{true}}}{K_p} a_{OH^-} \cdot \frac{f_B}{f^*} \tag{2}$$

and it is not possible, by the formal kinetic rules, to distinguish the two mechanisms mentioned.

In both cases the rate constant being observed varies directly proportionally to the hydroxyl ion activity.

If a molecule of water takes part in the limiting stage of the amide hydrolysis, then

$$\frac{K_{\text{eff}}}{a_{H_2O} \cdot a_{OH^-}} = K' \cdot \frac{f_B}{f^*},$$

where $K' = K_{\text{true}}$ for mechanism (1) and $K' = K_{\text{true}}/K_p$ for mechanism (2).

In the present work the catalytic activity of aqueous KOH solutions on the hydrolysis of caprolactam for example was studied. Kinetic measurements were carried out with a SFD-1 spectrophotometer. Utilization of the spectrophotometric method proved to be possible owing to the fact that in the ultraviolet region of the spectrum the absorption coefficients of caprolactam and of its hydrolysis product – aminocaproic acid – greatly differed. KOH of chemically pure quality was used for the experiments.

TABLE 1

KOH, wt. %	Temp. °C	K_{eff}, min^{-1}	KOH, wt. %	Temp. °C	K_{eff}, min^{-1}
1,037	90	$0{,}570 \cdot 10^{-2}$	12,41	90	$0{,}676 \cdot 10^{-1}$
	80	$0{,}315 \cdot 10^{-2}$		80	$0{,}405 \cdot 10^{-1}$
	70	$0{,}170 \cdot 10^{-2}$		70	$0{,}191 \cdot 10^{-1}$
	60	$0{,}075 \cdot 10^{-2}$		60	$0{,}108 \cdot 10^{-1}$
2,250	90	$0{,}993 \cdot 10^{-2}$		50	$0{,}506 \cdot 10^{-2}$
	80	$0{,}464 \cdot 10^{-2}$		40	$0{,}199 \cdot 10^{-2}$
	70	$0{,}310 \cdot 10^{-2}$		25	$0{,}474 \cdot 10^{-3}$
	60	$0{,}132 \cdot 10^{-2}$	15,76	60	$0{,}147 \cdot 10^{-1}$
4,184	90	$0{,}207 \cdot 10^{-1}$		50	$0{,}690 \cdot 10^{-2}$
	80	$0{,}120 \cdot 10^{-1}$		40	$0{,}314 \cdot 10^{-2}$
	70	$0{,}610 \cdot 10^{-2}$		25	$0{,}745 \cdot 10^{-3}$
	60	$0{,}320 \cdot 10^{-2}$	20,45	60	$0{,}244 \cdot 10^{-1}$
8,056	90	$0{,}403 \cdot 10^{-1}$		50	$0{,}112 \cdot 10^{-1}$
	80	$0{,}221 \cdot 10^{-1}$		40	$0{,}479 \cdot 10^{-2}$
	70	$0{,}112 \cdot 10^{-1}$		25	$0{,}123 \cdot 10^{-2}$
	60	$0{,}503 \cdot 10^{-2}$	26,95	50	$0{,}214 \cdot 10^{-1}$
	50	$0{,}230 \cdot 10^{-2}$		40	$0{,}980 \cdot 10^{-3}$
	40	$0{,}109 \cdot 10^{-2}$		25	$0{,}227 \cdot 10^{-2}$
	25	$0{,}295 \cdot 10^{-3}$	33,16	50	$0{,}384 \cdot 10^{-1}$
				40	$0{,}176 \cdot 10^{-1}$
				25	$0{,}410 \cdot 10^{-2}$
			37,25	50	$0{,}588 \cdot 10^{-1}$
				40	$0{,}350 \cdot 10^{-1}$
				25	$0{,}651 \cdot 10^{-2}$
			45,78	25	$0{,}159 \cdot 10^{-1}$

Since aqueous KOH solutions attack glass, the alkali solutions were prepared immediately before the experiments. The experiments were carried out in a similar way as in the investigation of the dehydration of orthobenzoylbenzoic acid [4].

The concentration of the lactam in the experiments was $3\text{-}6 \cdot 10^{-3}$ M/liter. In very concentrated solutions (KOH above 46%) the lactam was very difficultly soluble (its solubility apparently was less than $1 \cdot 10^{-3}$ M/liter); therefore, the attempt to study the process in such media was abandoned. In the range of KOH concentrations studied the caprolactam was completely hydrolyzed. As might be expected, the lactam process was comparatively unimolecular. In the figure is shown the kinetic curve and its logarithmic anamorphosis of the hydrolysis of caprolactam in a 20.45% KOH medium at t = 60°. The rate constant remained unimolecular down to the complete conversion of caprolactam into aminocaproic acid. In cases where the rate of hydrolysis was small ($K_{eff} \ll 2.5 \cdot 10^{-3}$ min^{-1}), the experiment proceeded at the given temperature with only 40-70% conversion. The cell was then heated to 70-90° C, during which the reaction was completed. The cell was then cooled to the original temperature and the value of the optical density of the solution D_∞ measured. In Table 1 are shown the rate constants for the hydrolysis of caprolactam at different temperatures in media of different KOH content. These results fit the Arrhenius dependence quite well. In Table 2 the K_{eff} rate constants at 25° are given. For KOH concentrations of 1.037 to 12.41% the effective constants were calculated by extrapolation from high temperatures by means of the Arrhenius equation. Values of the activation energies were practically independent of the KOH concentration and equalled 16.6 ± 0.3 kcal/mole.

As seen from Table 2, the rate constant for hydrolysis of caprolactam K_{eff} in concentrated aqueous KOH solutions increased more rapidly than the hydroxyl ion concentration. For example, with increase of the alkali concentration from 1.037 to 45.78% the rate constant at 25° increased by a factor of 417. This fact indicates that the cata-

TABLE 2.

KOH, wt. %	lg [K_{eff}] at 25°C	lg a_{KOH}	lg $a_{OH_\pm}$	lg a_{H_2O}	lg $\frac{K_{eff}}{a_{OH_\pm} \cdot a_{H_2O}}$	E_{eff}, kcal/mole
1,037	—4,42	—1,62	—0,81	—0,002	—3,61	16,9
2,250	—4,16	—1,04	—0,52	—0,005	—3,64	16,7
4,184	—3,85	—0,50	—0,25	—0,011	—3,59	16,7
8,056	—3,56	0,21	0,105	—0,025	—3,64	16,7
12,41	—3,27	0,76	0,38	—0,040	—3,61	16,5
15,76	—3,10	1,15	0,575	—0,054	—3,63	16,6
20,45	—2,91	1,70	0,85	—0,090	—3,67	16,7
26,95	—2,64	2,47	1,235	—0,134	—3,74	16,7
33,16	—2,39	3,22	1,61	—0,240	—3,76	16,3
37,25	—2,19	3,76	1,88	—0,320	—3,75	16,5
45,78	—1,80	4,96	2,48	—0,580	—3,70	—

Note. Values of a_{KOH} taken from [5] and values of a_{H_2O} from [6].

lytic activity of KOH is determined not only by the OH^- ion concentration, but it also depends on the properties of the hydroxyl ion in the given solutions. Schwarzenbach [7], by analogy with the acidity function for acid solutions, suggested characterization of alkaline media by alkalinity functions determined by an indicator method. However, his results could not be used for quantitative characterization since during his measurements the indicator and the solution under study were present as different phases. Besides that, Schwarzenbach did not show how the indicators added to them were ionized in the alkaline media. The experimental results obtained in the present work for the hydrolysis of caprolactam fit the following equation with satisfactory precision:

$$\frac{K_{eff}}{a_{H_2O} \cdot a_{\pm}} = \text{const}, \qquad (3)$$

where $a_\pm$ is the mean ionic activity of the aqueous KOH solutions. In view of the fact that equation (3) is valid for a wide range of alkali concentrations, there are grounds for making the following conclusions.

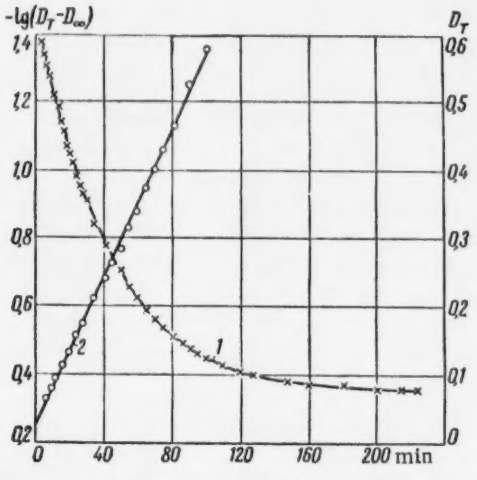

The kinetic curve (1) and its logarithmic anamorphosis (2) of the hydrolysis of caprolactam in a 20.45% KOH medium at 60°.

The limiting stage of hydrolysis of amides involves a molecule of water. By variation of the concentration of aqueous KOH solutions, the activity of the hydroxyl ions changes in a similar way as the activity of the potassium ions (by variation of the KOH concentration, the activities of the OH^- and K^+ ions change by equal factors). This conclusion may also be justified by the fact that it is consistent with the calculations of Bernal and Fowler that potassium and hydroxyl ions in solution have the same radius [8].

LITERATURE CITED

1. C. K. Ingold, Mechanism of Reactions and Structure of Organic Compounds [Russian translation] (IL, 1960).
2. J. T. Edward and K. A. Terry, J. Chem. Soc., 3527 (1957).
3. S. S. Biechler and R. W. Taft, J. Am. Chem. Soc. 79, 4927 (1957).
4. M. I. Vinnik, R. S. Ryabova, and N. M. Chirkov, Zhur. Fiz. Khim. 33, 1993 (1959).
5. R. A. Robinson and R. M. Stokes, Trans. Farad. Soc. 45, 612 (1949).
6. E. Shibata, J. Kabayschi, and S. Furukawa, J. Chem. Soc. Japan 52, 404 (1931).
7. D. Schwarzenbach and R. Sulzberger, Helv. Chim. Acta 27, 348 (1944).
8. J. O. Bernal and R. H. Fowler, J. Chem. Phys. 1, 515 (1933).

THE PHOTOCHEMICAL REDUCTION OF FERRIC CHLORIDE IN AROMATIC HYDROCARBONS

A. I. Kryukov and B. Ya. Dain

L. V. Pisarzhevskii Institute of Physical Chemistry, Academy of Science, USSR
(Presented by Academician A. N. Terenin, December 19, 1960)
Translated from Doklady Akademii Nauk SSSR, Vol. 138, No. 1,
pp. 153-155, May, 1961
Original article submitted December 12, 1960

As is known, the solubility of ferric chloride in benzene and other aromatic hydrocarbons under the usual damp atmospheric conditions is extremely small. However, by careful removal of moisture, dilute solutions of this salt in benzene (concentration of the order 10^{-3} M) can be obtained, satisfactorily stable under vacuum. In the spectrum of these solutions a single absorption band with a maximum at 340 mμ was detected. It was assumed [1] that it corresponded to the "forbidden" transition from the fundamental singlet state of benzene to the lowest triplet state, the probability of which is greatly increased owing to the perturbing action of the paramagnetic ferric chloride molecules. However, another explanation of the origin of this band is also possible, to which A. N. Terenin [2] draws attention. Since the bond between $FeCl_3$ and C_6H_6 molecules has a donor–acceptor character, then it is reasonable to assume that the observed absorption band belongs to the type of "charge-transfer spectra", analogous to the ultraviolet spectrum of complexes of iodine with aromatic hydrocarbons [3].

If this explanation of the spectrum is correct, then it may be expected that the absorption of a quantum of ultraviolet light by the $FeCl_3 \cdot C_6H_6$ complexes, corresponding to the absorption band at 340 mμ, must lead to an intracomplex electron transfer more profound than that already existing in the normal state. The observed band must thus correspond to the process of photoreduction of ferric chloride by benzene. The same photoprocesses ought to be observed in solutions of $FeCl_3$ in other aromatic hydrocarbons. In addition to this, in a series of these hydrocarbons, depending on their electron-donor properties, a definite regularity ought to be observed, both in the position of the corresponding absorption bands and also in the magnitude of the photochemical effect. The investigation that we have carried out of the spectra of ferric chloride in benzene, toluene, and p-xylene, and also of the effect of ultraviolet light on these systems, confirmed these theoretical conclusions. In the present article the results of this investigation are briefly reported.

The experiments were carried out with solutions deaerated under high vacuum (for the photochemical investigations) or prepared in a dry-box (for measuring the absorption spectra). The hydrocarbons used for the work were subjected to careful purification and drying by the methods described in [4]. The $FeCl_3$ concentration in the solutions was determined spectrophotometrically at $\lambda = 470$ mμ as the complex with sulfosalicylic acid. Solutions containing the ferric salt in concentrations of $1 \cdot 10^{-4}$ to $8 \cdot 10^{-4}$ M were employed for the work. Absorption spectra were measured in quartz cells by means of the SF-4 photoelectric spectrophotometer. Exposure was made with a PRK-7 mercury vapor lamp using a cobalt light filter, providing light with $\lambda = 365$ mμ. The quantum yields of the photoreaction were determined by means of an uranyl oxalate actinometer.

The experiments showed that solutions of $FeCl_3$ in all the hydrocarbons possess in the near ultraviolet one broad absorption band of great intensity. The maximum of this band was displaced in the long-wave direction with the changeover from benzene to its derivatives. The bands also encroach to some extent on the visible region, and the inherent yellow-brown color of all such solutions is connected with this. The corresponding spectra are given in Fig. 1*. Values of ε_{max} for the solutions in benzene, toluene, and p-xylene equalled respectively 6700, 6200, and 5600. These values were obtained without taking account of dimerization of ferric chloride, which is assumed by some authors. In Fig. 2 is shown the relationship appearing between the position of the absorption maxima of the respective bands and the ionization potentials of the hydrocarbon solvents. The values of the latter were taken from [5]. Clearly

* In the case of mesitylene the optical densities of only one solution were determined. Therefore, the results of the light absorption in this solvent are given conditionally.

the observed linear character of this relationship is connected with the donor function of the solvent in respect of the intermolecular bond and may also be considered as one proof that the spectral bands of the respective complexes are due to intermolecular transfer of an electron according to the scheme:

$$C_6H_6 \cdot FeCl_3 \overset{h\nu}{\rightleftarrows} C_6H_6^+ \cdot FeCl_3^- \qquad (1)$$

Even more convincing support of this is the fact that the absorption of a quantum corresponds to a photochemical reduction process of ferric chloride in all the cases examined. This is borne out first of all by the decrease in intensity of the absorption band with irradiation of the deaerated ferric chloride solutions with monochromatic light, $\lambda = 365$ mμ (Fig. 3a). At the same time, the formation of divalent iron occurs, which can be detected in the solution after exposure by reaction with o-phenanthroline.

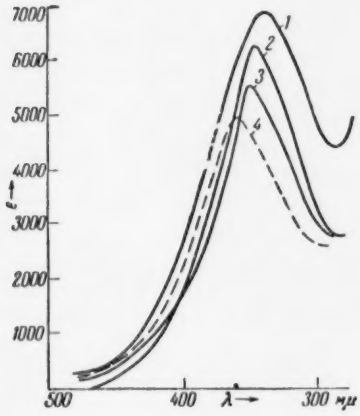

Fig. 1. Absorption spectra of ferric chloride. 1) In benzene, 2) in toluene, 3) in p-xylene, 4) in mesitylene.

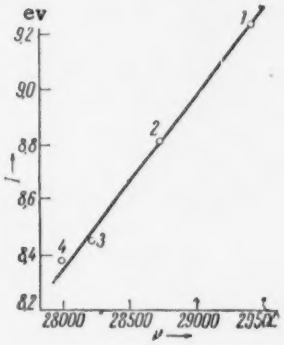

Fig. 2. Dependence of the position of absorption maxima of ferric chloride solutions on the solvent ionization potential. 1) Benzene, 2) toluene, 3) p-xylene, 4) mesitylene.

It must be assumed that as a result of absorption of a quantum of light the system $C_6H_6^+ \cdot FeCl_3^-$ formed is unstable and has the possibility of dissociation, both into the original components and also according to the equation:

$$C_6H_6^+ \cdot FeCl_3^- \rightarrow C_6H_5^{\cdot} + FeCl_2 + HCl. \qquad (2)$$

The latter course promotes a further development of the reaction. It is obvious that the stronger are the electron-donor properties of the hydrocarbon, the less probable is reversion of the reaction system (1) to the original state. Correspondingly, the greater must be the yield of the photochemical reaction.

Indeed, measurements of the quantum yields of the photoreduction reaction, carried out at $\lambda = 365$ mμ gave the following values of γ (in $FeCl_3$): for benzene $6.1 \cdot 10^{-2}$; for toluene $13.6 \cdot 10^{-2}$; for p-xylene $18.8 \cdot 10^{-2}$.

These results are the mean values from several experiments. As separate experiments showed, the quantum yields hardly change with a temperature increase from 20 to 40°. The low values of γ indicate that the probability of reversion to the original state in all the cases studied was very great. In the series of the three systems studied it was observed that the increase in the yield which occurred corresponded with a decrease in the ionization potential of the hydrocarbon.

From data given in the literature, it is known [6] that reduction of ferric chloride by aromatic hydrocarbons with simultaneous chlorination of the latter can be observed during boiling in the absence of light. However, as is apparent from the results presented in Fig. 3 b, the rate of the dark reaction at room temperature is so low that it can

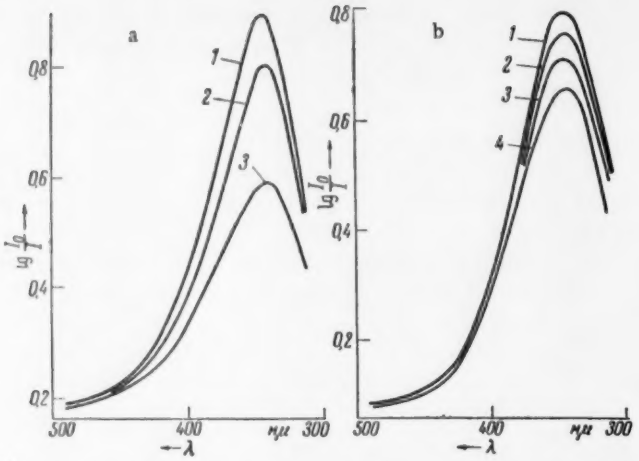

Fig. 3. a) Reduction of ferric chloride in benzene through irradiation at λ = 365 mμ: 1) Absorption curve before irradiation, 2) after 5-min irradiation, 3) after 23-min irradiation. b) Reduction of ferric chloride in benzene in the dark: 1) Absorption curve of initial solution, 2) after 4.5 hours, 3) after 17 hours, 4) after 65 hours.

be neglected in determining the quantum yields. On the other hand, from these results it follows that chlorination of aromatic hydrocarbons by ferric chloride would have to be considerably intensified by the action of light for the possibility of providing favorable conditions for its utilization.

LITERATURE CITED

1. D. D. Eley and P. J. King, J. Chem. Soc., 4972 (1952).
2. A. N. Terenin, Uspekhi Khim. 24, 121 (1955).
3. R. S. Mulliken, J. Am. Chem. Soc. 74, 811 (1952).
4. A. Weissberger, E. Proskauer, et al., Organic Solvents [Russian translation] (IL, 1958).
5. F. I. Vilesov and A. N. Terenin, Doklady Akad. Nauk SSSR 115, 744 (1957); W. C. Price, R. Bralsford, et al., Spectrochim. Acta 14, 44 (1959).
6. V. Thomas, C. r. 126, 157 (1898); I. M. Dang'yan, Zhur. Obshch. Khim. 8, 1780 (1938); P. Kovacic and N. O. Brace, J. Am. Chem. Soc. 76, 5491 (1954); U. S. A. Pat. 2719074; Chem. Abstr. 50, 2136 (1956).

All abbreviations of periodicals in the above bibliography are letter-by-letter transliterations of the abbreviations as given in the original Russian journal. *Some or all of this periodical literature may well be available in English translation.* A complete list of the cover-to-cover English translations appears at the back of this issue.

CONTACT POTENTIAL DIFFERENCES BETWEEN SOME LIQUID METALS AND THEIR ALLOYS

V. A. Kuznetsov, L. S. Zagainova, N. P. Loginova,

I. Ya. Lyubimtseva, N. S. Onoprienko, and L. E. Tsimbal

A. M. Gor'kii Ural State University

(Presented by Academician A. N. Frumkin, December 10, 1960)
Translated from Doklady Akademii Nauk SSSR, Vol. 138, No. 1,
pp. 156-158, May, 1961
Original article submitted November 25, 1960

Mention was made in a previous paper [1] that the contact potential differences between liquid metals have as yet been insufficiently investigated and the results obtained in some cases are not very reliable. Continuing our studies along these lines, we have measured the contact potential differences between some liquid metals and their alloys.

Unfortunately the choice of experimental materials for study is not very wide, as may be seen at a glance. For the determination of the contact potential differences, we used the thermal electron method, which essentially involves taking the volt ampere curves of a diode, in which the pure metal first serves as the anode, and then its alloy. In this case the magnitude of the contact potential difference may be determined by the displacement of the volt ampere curves in the direction of the axis of the potentials. In order to increase the reliability of the results, it would be desirable to use metals and their alloys between which the contact differences are as large as possible. It is well known [1] that the greatest differences in null charge potential (NCP) are found between Zn, Cd, Tl, and Bi on the one hand, and Te on the other. Insofar as the contact potential differences are supposed to be close to the differences in null charge potential [3], it is advisable to carry out the measurements between the above-mentioned metals (Zn, Cd, Tl, Bi) and their alloys, and Te. In preparing the experiment, however, liquid metals are subjected to prolonged pumping out in a vacuum. For this reason, it is difficult to use Zn and Cd, since they have a high vapor pressure. Moreover, many metals, including Bi, form chemical compounds with Te which have fairly high melting points, and this makes it difficult to obtain alloys concentrated in Te.

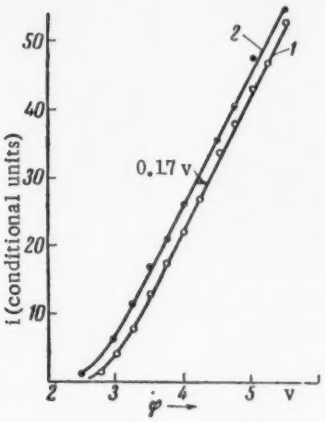

Fig. 1. Volt ampere curves: 1) Sn; 2) Sn–Tl alloy (23.8% Tl).

Below are shown the results of measurements of the contact differences between Sn and the alloy Sn–Tl (23.8% Tl), Tl and the alloy Tl–Sn (49.8% Sn), Tl and the alloy Tl–Te (50.5% Te), and also Bi and the alloys Bi–Te (3.6% and 9% Te). All concentrations are given in atomic percents. The results of these measurements are compared with the difference of the null charge potential of the metals and of the corresponding alloys. Such a comparison, as is well known [3], is of great interest in connection with the development of a theory of electromotive forces of galvanic elements.

The Bi and Sn used in the study had a purity of class B–3; the Tl contained impurities of Fe, Pb, and Cd amounting to about 0.02%*. The Te was obtained by double distilling chemically pure Te in vacuo. The method of measurement was described in detail in [1]. All measurements were carried out at a temperature of 450°.

The volt ampere curves for Sn and the alloy Sn–Tl (23.8% Tl) are shown in Fig. 1, and those for Tl and the alloy Tl–Sn (49.8% Sn) in Fig. 2A. The contact potential difference in the first case was 0.17 v, and in the second, 0.25 v.

* The spectrographic analysis of Tl was made by R. Gutkin, to whom the authors express their thanks.

In order to compare the contact potential differences with the difference in null charge potential, we determined null charge potential from electrocapillary measurements. The results of these measurements are shown in Fig. 3,

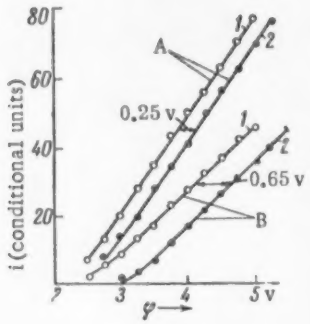

Fig. 2. Volt ampere curves: A: 1) Tl, 2) Tl–Sn alloy (49.8% Sn); B: 1) Tl, 2) Tl–Te alloy (50.5% Te).

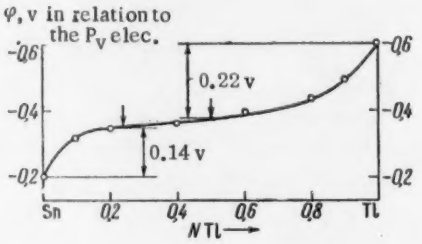

Fig. 3. Dependence of the null charge potential of Sn–Tl alloys on composition.

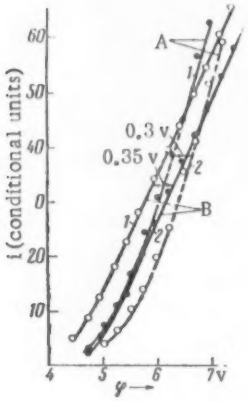

Fig. 4. Volt ampere curves: A: 1) Bi, 2) Bi–Te alloy (3.6% Te); B: 1) Bi, 2) Bi–Te alloy (9% Te).

which shows the dependence of null charge potential on alloy composition. As may be seen in Fig. 3, the null charge potentials of the alloys are displaced by 0.14 and 0.22 v in relation to the null charge potentials of Sn and Tl–in the first case in a negative direction and in the second case in a positive one.

The volt ampere curves for Tl and the alloy Tl–Te (50.5% Te) are shown in Fig. 2. The contact potential difference in this case is equal to 0.65 v. Data on the null charge potentials of Te–Tl alloys have been published [4]. From this it can be seen that the null charge potential of the Tl–Te alloy containing 50.5% Te is displaced by 0.67 v in a positive direction in comparison with the null charge potential of Tl.

The volt ampere curves for Bi and Bi–Te alloys containing 3.6 and 9% Te are shown in Fig. 4. As can be seen from the figure, the contact potential differences between Bi and Bi–Te alloys of the given composition are equal to 0.3 and 0.35 v, respectively. The electrocapillary measurements that we made showed that the null charge potentials of these alloys of Bi–Te are displaced by 0.25 v and 0.33 v, respectively, in a positive direction in relation to the null charge potential of pure Bi.

From the results obtained it follows that the contact potential differences between the metals and their alloys which we studied are actually close to the differences of null charge potential of the corresponding metals and their alloys. Thus, the assumption in regard to the approximate correspondence of these magnitudes predicted by A. N. Frumkin [3] has received additional confirmation from this study.

The following fact requires attention. The volt ampere curves of the alloys Tl–Sn, Tl–Te, and Bi–Tl are displaced in the direction of more positive potentials in comparison with the volt ampere curves of Tl and Bi (Figs. 2 and 4). This apparently means that the work for an electron to escape from the alloys mentioned is greater than that for the corresponding pure metals. In this connection, the null charge potentials of alloys are displaced in a positive direction in a magnitude approximately equal to the contact potential differences. On the other hand, the volt ampere curve of the Sn–Tl alloy is displaced in the direction of less positive potentials (Fig. 1), which gives evidence of a smaller amount of energy for the escape of an electron from the alloy than from Sn. At the same time, the null charge potential of the alloy is displaced in a positive direction. This confirms the existence of a parallelism between the null charge potentials of metals and the escape energy of electrons from them, which had been determined in a previous study [5].

In conclusion, we wish to express deep appreciation to Academician A. N. Frumkin for his exceptional interest in our work and for his valuable advice.

LITERATURE CITED

1. V. A. Kuznetsov, M. P. Klevtsova, and others, Zhur. Fiz. Khim. 34, 1349 (1960).
2. S. V. Karpachev and A. G. Stromberg, Zhur. Fiz. Khim. 18, 47 (1944).
3. A. N. Frumkin and A. B. Gordetskaya, Z. Phys. Chem. A136, 451 (1928).
4. B. A. Kuznetsov, V. I. Aksenov, and M. P. Klevtsova, Doklady Akad. Nauk 128, 763 (1959).
5. B. M. Novakovskii, E. A. Ukshe, and A. I. Levin, Zhur. Fiz. Khim. 29, 1847 (1955).

All abbreviations of periodicals in the above bibliography are letter-by-letter transliterations of the abbreviations as given in the original Russian journal. *Some or all of this periodical literature may well be available in English translation.* A complete list of the cover-to-cover English translations appears at the back of this issue.

DETERMINATION OF CURVES ON THE FORMATION OF CENTERS OF CRYSTALLIZATION AND ON THE VELOCITY OF CRYSTAL GROWTH IN GLASS BY MEANS OF DENSITY MEASUREMENTS

É. M. Rabinovich

State Scientific Research Institute for Electrotechnical Glass
and Technological Equipment
(Presented by Academician A. V. Shubnikov, December 13, 1960)
Translated from Doklady Akademii Nauk SSSR, Vol. 138, No. 1,
pp. 159-161, May, 1961
Original article submitted November 29, 1960

The construction of Tamman curves showing the dependence of the number of centers of crystallization (KV) and of the linear velocity of crystal growth (KG) on temperature [1] for silicate glasses requires the use of extremely laborious methods. In the case of the formation of a fine crystalline structure under the influence of mineralizers, such a study can be accomplished only with the aid of an electron microscope, which makes the practical application of these curves for controlling crystallization even more difficult.

In the present paper are presented the results of a study of crystallization and a method of constructing curves, analogous to KV and KG, for glasses containing mineralizers, by measuring the density, the value of which depends on the compactness of the packing of the substance, and consequently also on the relationship of the crystalline and glass phases. For a glass whose composition corresponds with the composition of a definite chemical compound and which has not been subjected to polymorphic conversion, this dependence may be stated by the following expression:

$$\Delta\rho = \rho - \rho_g = (\rho_g - \rho_c)\, p, \tag{1}$$

where ρ is the density of the substance whose degree of crystallization (in volume parts) is equal to p; ρ_g is the density of the substance in the glassy state; ρ_c is the density of the substance in the crystalline condition; $\rho_c > \rho_g$ [2, 3].

It is easy to show that

$$p = kl^3n, \tag{2}$$

where l is the average length of the crystal; n is the number of crystals in unit volume; k is a constant dependent on the form of the crystals.

In the case of complex glasses, the value ρ_c is the average weighted value of the densities of all crystalline phases, in connection with which equation (1) for all these glasses may be used if the degree of crystallization is sufficiently large (of the order of 0.3-0.5).

The following glasses, synthesized in the Institute, were chosen for investigation: multicomponent aluminosilicate glasses I (ρ_g = 2.610 g/cm^3) and II (ρ_g = 2.875 g/cm^3), containing TiO_2 as a mineralizer, and a light-sensitive glass III (ρ_g = 2.360 g/cm^3), containing small additions of silver. The lower temperatures at which external signs of crystallization appear in these glasses are as follows: Glass I 830° 1-8 hours; Glass II 930° one hour, 900° four hours. 850° eight hours; Glass III 550-600° one to two hours (depending on illumination).

The density was determined by hydrostatic weighing on an analytical balance. Not less than three samples of glass per determination were twice subjected to thermal treatment [1]. The purpose of the first treatment, after which no external signs of crystallization could be seen in the samples, was the formation of invisible centers of crystallization; the purpose of the second was to make them grow.

Fig. 1 gives the curves of changes in density of Glass I after crystallization with a constant temperature of secondary thermal treatment (curve 1) which corresponds with the temperature of the first maximum exothermic effect on the thermogram (930°) and with a constant temperature of primary treatment (curve 2 and curve $\sqrt[3]{\Delta\rho}$); the

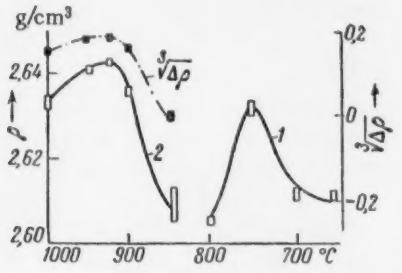

Fig. 1. Changes in the density of Glass I as a result of thermally treating it twice. On the abscissa are given the temperatures of the primary thermal treatment for curve 1 (one hour, secondary treatment 30 minutes at 930°) and the temperatures of the secondary treatment for curve 2 and curve $\sqrt[3]{\Delta\rho}$ (one hour, primary treatment one hour at 750°).

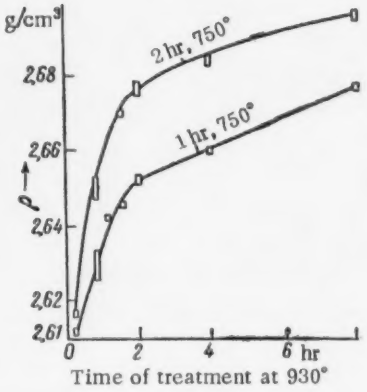

Fig. 2. Changes in density of Glass I related to the time of primary (750°) and secondary (930°) thermal treatment.

time of each treatment was constant for one curve. If we assume that the average dimensions of the crystals are not dependent on the primary treatment, then each value of $\rho-\rho_c$ on curve 1 is proportional, in accordance with (1) and (2), to the number of centers of crystallization in unit volume, i.e., curve 1 is analogous to KV; each value on curve 2 is proportional to the average crystal volume, and on curve $\sqrt[3]{\Delta\rho}$ to the average length (or rate of growth) of a crystal; i.e., curve $\sqrt[3]{\Delta\rho}$ is analogous to KG. However, the condition of independence of crystal dimension on primary treatment, i.e., on the number of centers in unit volume, is fulfilled only in the case of a not very high degree of crystallization, when each crystal is located fairly far from its neighbor. This is especially essential to take into consideration for glasses in which the centers of crystallization are located at distances of the order of 1-2 μ from each other. The curves of Fig. 2 serve as confirmation of the fact that the conditions of the preceding experiment were chosen correctly. If the time of treatment at 930° does not exceed 1½ hours, then a twofold increase in the difference $\rho-\rho_c$ results from a twofold increase in the time of primary treatment at 750° and consequently a twofold increase in the number of centers of crystallization. With a longer time of secondary treatment this proportionality breaks down and the conditions for correct construction of curves analogous to KV and KG do not exist.

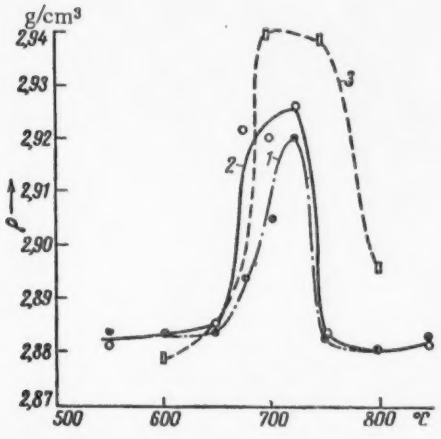

Fig. 3. Changes in the density ρ of Glass II as a result of twofold thermal treatment. Primary treatment one hour; secondary treatment: 1) One hour at 850°; 2) two hours at 850°; 3) 30 minutes at 950°.

Fig. 3 shows that incorrectly chosen conditions of secondary treatment of Glass II, which result in too high a degree of crystallization, lead to changes in the form of curves 2 and 3 in comparison with curve 1 and also to a displacement of the maximum.

Fig. 4 shows a curve of changes in density, analogous to KV, for Glass III which was subjected to preliminary exposure to ultraviolet light. In this glass Li_2SiO_3 separates out as the first crystalline silicate phase. Extremely tiny crystals of silver, formed previously [4], apparently serve as

centers of crystallization; at a lower temperature of secondary treatment (500-550°) they give rise to a colloidal coloring of the glass without crystallization of the fundamental phase. The primary temperature, to which the maximum intensity of coloration is related, corresponds with the maximum temperature on the curve of density change (Fig. 4). This correspondence, as well as the correspondence between the maximum temperature of curve 2 ($\sqrt[3]{\Delta\rho}$) for Glass I (Fig. 1) and the temperature of maximum crystallization on the thermogram (930°), confirms the correctness of using the measurement of density for the quantitative determination of crystallization in glasses containing mineralizers.

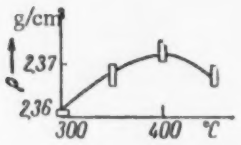

Fig. 4. Changes in the density ρ of irradiated Glass III as a result of twofold thermal treatment. Primary treatment, one hour; secondary treatment, 30 minutes at 720°.

The dimensions of the areas under curves of the type of curves 1 and 2 in Fig. 1 are identical (g·degree/cm³), and consequently they may conditionally characterize the ability of a glass to crystallize. In order to correct for the formation and growth of new centers at temperatures of secondary treatment, it is necessary to limit these areas below by curves giving the values of the density of samples which have been subjected only to secondary treatment without the primary. In the case of Glass I values are obtained which are equal or slightly lower for ρ_c (2.609 g/cm³ after four hours at 930°, 2.612 after eight hours). These curves also serve to some degree as a correction for equation (1).

The curves of Fig. 2 and calculations according to (1) and (2) permit us to determine the kinetics of the decrease in the linear velocity of crystal growth, resulting from the low rate of diffusion, with time when a constant number of centers of crystallization is present.

Density measurements may also be utilized for studying the influence of irradiation on light-sensitive glass under constant conditions of thermal treatment.

LITERATURE CITED

1. G. Tamman, The Glasslike State [in Russian] (Moscow-Leningrad, 1935).
2. G. G. Sentyurin, Tr. Mosk. Khim.-Tekhnol. Inst. im. D. I. Mendeleeva 19, 178 (1954).
3. S. I. Sil'vestrovich and É. M. Rabinovich, Zhurn. Vsesoyuzn. Khim. Obshch. im. D. I. Mendeleeva 5, 2, 186 (1960).
4. S. D. Stookey, Glastech. Ber., Sonderband V, Intern. Glaskongress, 32K, 5 (1959) p. 1.

All abbreviations of periodicals in the above bibliography are letter-by-letter transliterations of the abbreviations as given in the original Russian journal. *Some or all of this periodical literature may well be available in English translation.* A complete list of the cover-to-cover English translations appears at the back of this issue.

ATOM-SCATTERING FACTORS AND THE DISTRIBUTION OF ELECTRON DENSITY IN GALLIUM ANTIMONIDE

Academician N. N. Sirota (Academy of Sciences, BelorusSSR)

and E. M. Gololobov

Division of Solid State Physics and Semiconductors, Academy of Sciences, BelorusSSR

Translated from Doklady Akademii Nauk SSSR, Vol. 138, No. 1,
pp. 162-164, May, 1961
Original article submitted December 12, 1960

The present study is the beginning of a cycle of work on the distribution of electron density in the antimonides of elements of the third group in the Mendeleev periodic system. Gallium antimonide as a semiconductor is characterized by a considerable mobility of the conductors of current – electrons and holes. Among other compounds $A^{III}B^{V}$ it possesses the lowest value of the ratio of these mobilities. The width of the forbidden zone in GaSb has a magnitude of the order of 0.8 ev [1] – somewhat larger than in germanium. The study of the distribution of electron density in gallium antimonide is of great scientific interest in connection with the character of the interatomic bond in semiconductors of the type $A^{III}B^{V}$.

The gallium antimonide used in this study was prepared in the laboratory of the Institute of Rare Metals by immediate fusion in quartz ampoules and then subjected to zone refining. The polycrystalline sample was ground in an agate mortar. Then the powder was washed with toluene. The powder, with particle dimensions of 5-8 μ, was used for the investigation. Particle size was determined under the microscope.

The roentgenographic survey was carried out on a URS-50I apparatus with emission from Cu K_{α}-. The elementary cell constant $a = 6.087$ A which we determined corresponds very well with values in the literature [2]. The survey method and calculations were similar to those previously described [3-5]. On the basis of the determination of absolute values of the reflex intensities, reflected from planes with even indexes the sum of which is divisible by four, from planes with odd indexes and from planes with even indexes the sum of which is not divisible by four, were constructed curves of the structural amplitude, attributed to the unit formula of GaSb (Fig. 1a). The values of the atom-scattering factors of the ions of antimony and gallium were calculated from the squares of the amplitudes (Fig. 1b).

The logarithms of the values of the atom-scattering factors of the ions of antimony and gallium, beginning with the value $\sum_{i=1}^{3} h_i^2 > 8$, lie on straight lines (Fig. 2). For the logarithms of the atom-scattering factors, only the first two points in the case of antimony ions and the first three points in the case of gallium ions deviate significantly from straight lines and thus cause a difference in the interionic distribution of electron density from the Gauss type distribution.

From data on the values of f_{Sb} and f_{Ga} the electron density [3] was calculated. In the calculation the edge of the elementary cell was divided into 60 equal parts. In Fig. 3 are shown the curves of the distribution of electron density in the direction [111], in plane (110) (Fig. 3a) and in direction [113] in the same plane (Fig. 3b).

It is possible to determine the values of the ionic radii of the ions of antimony and gallium from the data obtained. At the level of electron density equal to one electron per cubic angstrom, the ionic radius of gallium is approximately equal to 0.5 A, and that of antimony to 0.8 A. At the level of electron density equal to 0.5 electrons per cubic angstrom, the ionic radius of gallium is 0.75 A, and that of antimony 0.8 A. These values for the ionic radii may be compared with the number of electrons located in a volume of an ion of given radius, and consequently with the number of electrons located between the ions. At the same time, the values obtained give information both for an understanding of the ionic radii themselves and for concepts concerning the structures of dense packing. The character of the distribution of electron density between ions of antimony and gallium in the [111] direction requires attention (Fig. 3a). A matter deserving attention is the fact that in domains distributed at approximately half the

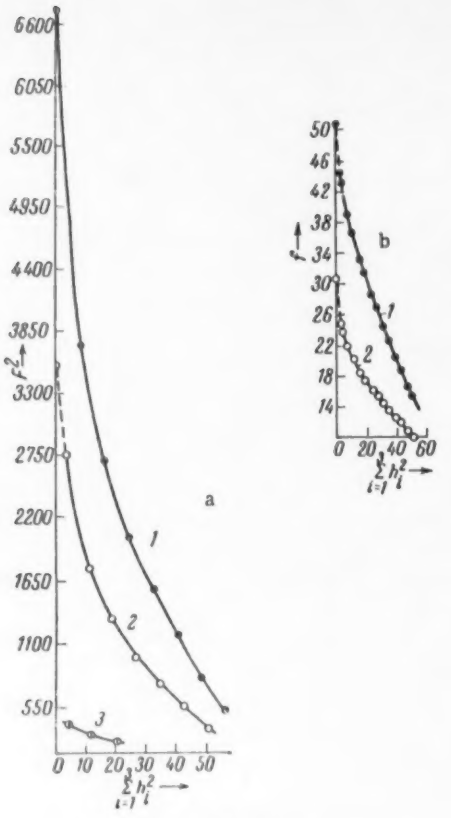

Fig. 1. a) Change of F^2 relative to $\sum_{i=1}^{3} h_i^2$: 1) For reflexes with even indexes the sum of which is divisible by four; 2) for reflexes with odd indexes; 3) for reflexes with even indexes the sum of which is not divisible by four. b) Change in the atom-scattering factors of the ions of antimony (1) and gallium (2) relative to $\sum_{i=1}^{3} h_i^2$.

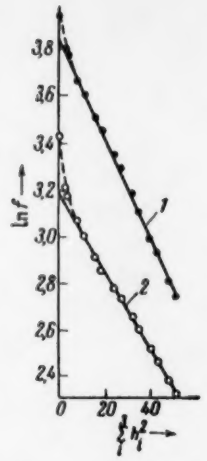

Fig. 2. Change of the logarithm of the atom-scattering factors of the ions of antimony (1) and gallium (2) relative to $\sum_{i=1}^{3} h_i^2$.

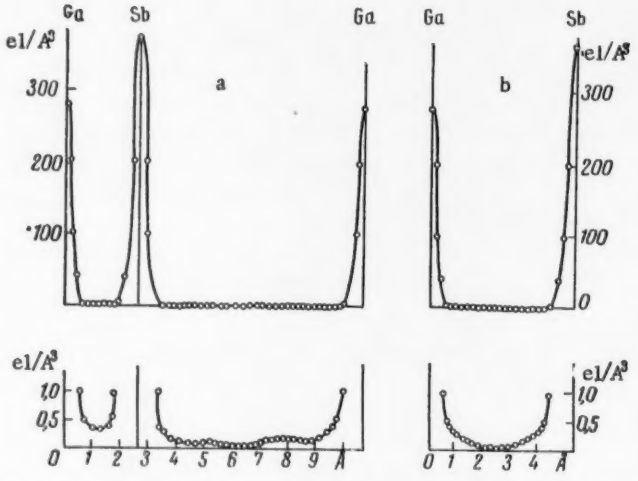

Fig. 3. Distribution of the electron density in an elementary cell in plane (110): a) In the [111] direction; b) in the [113] direction.

distance ($^5/_8$ $^5/_8$ $^5/_8$) between the ions of gallium and antimony in the [111] direction and the [113] direction in the (110) plane, the electron density falls practically to zero. Between closer gallium and antimony ions the electron density near the points $^1/_8$ $^1/_8$ $^1/_8$ decreases to 0.36 electrons per cubic angstrom, forming a "little bridge" of electron density.

In the direction [111], between Sb and Ga, near the points $^3/_4$ $^3/_4$ $^3/_4$ there is observed a region of somewhat increased electron density (from 0.12 to 0.16 electrons per cubic angstrom). Near the points $^1/_2$ $^1/_2$ $^1/_2$ there is also observed a region of somewhat increased electron density – from 0.08 to 0.12 electrons per cubic angstrom.

Fig. 4 is a chart of the distribution of the electron density in plane (110) of the elementary cell of GaSb. In analyzing the character of this distribution, some peculiarities must be mentioned. In the chart one can readily see

the above-mentioned "little bridges" of increased electron density between the nearest ions of Sb and Ga with an electron density of 0.36 electrons per cubic angstrom (see lower part of Fig. 4.) Between the Ga ions, distributed in the upper part of the chart, and the ions of antimony and gallium in the lower part of the chart, there appears a band of lowered electron density in which, however, it is possible to observe the well-known differences in the distribution of electrons.

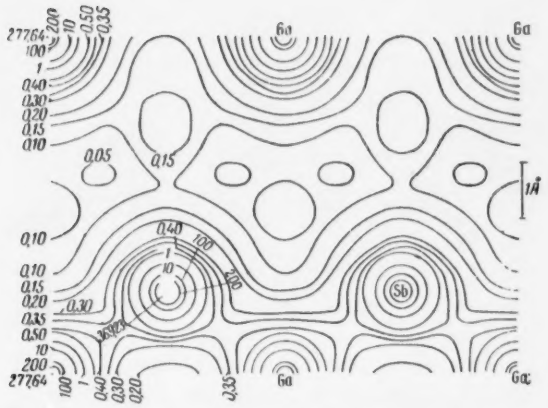

Fig. 4. Chart of the distribution of electron density in the (110) plane of the elementary cell of GaSb.

The atom-scattering factors of the ions of gallium and antimony which were determined in the present study and the resulting picture of the distribution of electron density in the lattice of the semiconductor GaSb may be useful in discussing the peculiarities of the character of the interatomic action and the physical properties of this compound.

LITERATURE CITED

1. G. Walker and G. Weise,* New Semiconductor Materials [Russian translation] (1958).
2. G. Giesecke and H. Pfister, Acta Cryst. 11, No. 5 (1958).
3. N. N. Sirota, N. M. Olekhnovich, and A. U. Sheleg, DAN SSSR 132, 1, 160 (1960).
4. N. N. Sirota and A. U. Sheleg, DAN SSSR 135, No. 5 (1960).
5. N. N. Sirota and N. M. Olekhnovich, DAN SSSR 136, No. 3 (1960); 136, No. 4 (1960).

All abbreviations of periodicals in the above bibliography are letter-by-letter transliterations of the abbreviations as given in the original Russian journal. *Some or all of this periodical literature may well be available in English translation.* A complete list of the cover-to-cover English translations appears at the back of this issue.

---

*Names not verified.

THE POLYMERIZATION OF METHYL METHACRYLATE BY THE ELECTROLYTIC REDUCTION OF OXYGEN

A. I. Fedorova, I. V. Shelepin, and N. B. Moiseeva

M. V. Lomonosov Moscow State University

(Presented by Academician A. N. Frumkin, December 29, 1960)
Translated from Doklady Akademii Nauk SSSR, Vol. 138, No. 1,
pp. 165-168, May, 1961
Original article submitted December 13, 1960

In the literature there are a number of papers on the polymerization of unsaturated organic compounds initiated at a cathode [1-6]. An essential shortcoming of these papers is the absence of measurements of the electrode potential and the absence of information on how the medium in which the experiments were conducted was freed from oxygen. As will be shown in this paper, the electrode potential and the presence of oxygen play an important role in electrochemical initiation. Control of the degree of freedom of the electrolyte from oxygen is especially necessary because, in the opinion of the authors of a number of papers, the basic initiator of polymerization in electrolytic reduction reactions is atomic hydrogen.

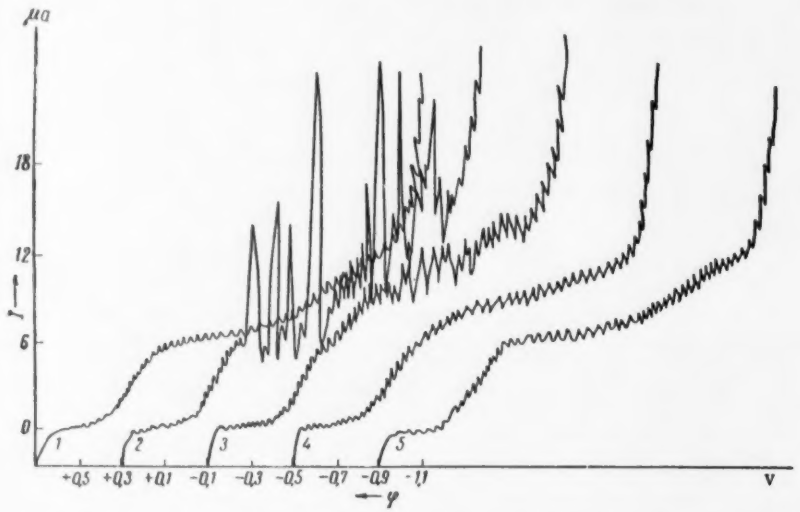

Fig. 1. Dependence of the form of the polarograms of the reduction of oxygen in a solution of 1 N H_2SO_4 in the presence of methyl methacrylate on time. The value of each division on the abscissa is 0.2 v; the beginning of each curve is moved 0.4 v. The concentration of methyl methacrylate was 0.02 M. 1) Without the addition of methyl methacrylate. 2, 3, 4, 5) curves under similar conditions 1, 16, 31, and 90 minutes after the addition of methyl methacrylate.

The purpose of the present investigation was to explain the conditions of polymerization of the methyl ester of methacrylic acid (methyl methacrylate) in acid solutions at a mercury cathode. Among electrochemical reactions which initiate the polymerization of methyl methacrylate we studied the reduction of molecular oxygen, hydrogen peroxide, and ionic hydrogen [7]. In the present paper we give the results obtained with the electrolytic reduction of oxygen.

The experiments were carried out at 20° in acid water and water-alcohol solutions of methyl methacrylate in thermostatically controlled electrochemical cells, in which the cathode space was separated from the anode area by a closed ground glass stopcock. All connections between individual parts of the cell, and also of the apparatus for the distillation of the reactants, were made of ground glass. The construction of the cells and of the apparatus for the distillation of the reactants guaranteed that they were hermetically tight. A platinum-palladium electrode served as anode and was saturated with hydrogen in such a way that during the course of the experiment no oxygen was released in the anode area. The monomer was introduced without allowing it to come into contact with the air. Ampoules containing methyl methacrylate were broken inside the cell in a hydrogen medium with the aid of an electromagnet. The purity of the mercury cathode and the electrolyte were controlled in accordance with the overvoltage of the reduction of the hydrogen ions, which was measured before each experiment.

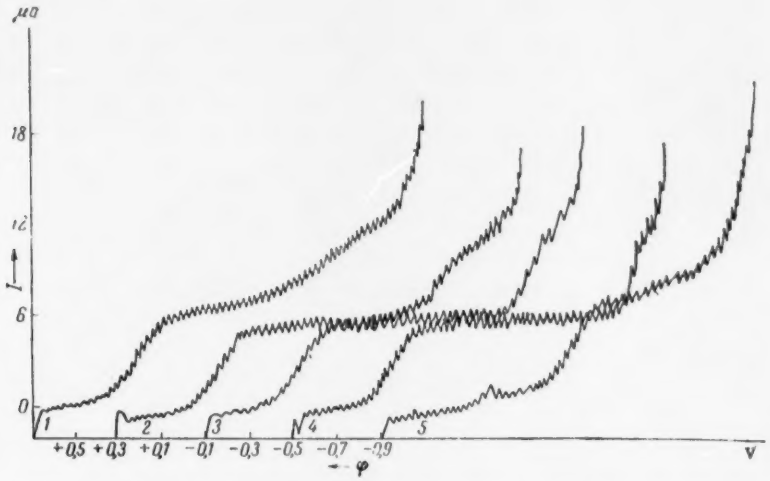

Fig. 2. Influence of the concentration of methyl methacrylate on the reduction wave of oxygen at a mercury dropping electrode in a solution of 1 N H_2SO_4: 1) Without methyl methacrylate; 2) 0.033 M methyl methacrylate; 3) 0.066 M methyl methacrylate; 4) 0.1 M methyl methacrylate; 5) 0.4 M methyl methacrylate with the addition of methyl alcohol. The value of a division on the abscissa is 0.2 v; the beginning of each curve is moved 0.4 v.

Reactants and gases were subjected to careful purification. Commercial chemically pure methyl methacrylate was distilled in an atmosphere of nitrogen freed from traces of oxygen in a 400-mm glass column for precise rectification. The second fraction, boiling at 43-43.5°/90 mm, was distilled directly from the receiver into the ampoules while still under 40 mm of nitrogen. These were frozen and sealed and kept in a refrigerator at −20°. The monomer prepared in this way must not contain traces of peroxides [8]. Analysis for traces of polymer gave a negative result; n_D^{25} 1.4148, d_4^{20} 0.946. For the preparation of the electrolyte, twice distilled water, sulphuric acid, and methyl alcohol that had been twice distilled in nitrogen were used. The mercury was chemically purified and then distilled twice in vacuo.

For the purpose of selecting an electrode potential for conducting the experiments on the initiation of polymerization in methyl methacrylate by the electrolytic reduction of oxygen, we first made a preliminary study, using an automatic polarograph, of the influence of methyl methacrylate on the process of reduction of O_2 at a mercury drop electrode in acid solutions.

The polarograms obtained with solutions of methyl methacrylate show the unique character of the action of the latter on the reduction of oxygen at a mercury electrode in acid solutions. If freshly distilled methyl methacrylate is quickly introduced into the reaction medium up to a concentration of $2.0 \cdot 10^{-2}$ M and the polarogram measured, strong fluctuations of the current at an interval of from $\varphi = +0.3$ v* up to the potential of hydrogen ion reduction are

*The potential of the electrode studied is always given in relation to the normal hydrogen electrode.

observed (Fig. 1). These fluctuations decrease with time, and finally the curve takes its initial form with the difference that the second wave of oxygen is somewhat displaced in the direction of more negative values of the potential.

This action of methyl methacrylate is apparently connected with the fact that methyl methacrylate on being introduced into the solution polymerizes in an adsorbed layer and forms a film which causes a change in the rate of dropping. The damping of the current fluctuations with time may be explained by the fact that the methyl methacrylate introduced in a given time period reacts with the dissolved oxygen in the electrolyte, and as a result of the chemical reactions taking place, polymerization on freshly formed surfaces on the dropping electrode ceases.

In accordance with what was said above, polarograms of solutions of methyl methacrylate prepared in air for some hours before measurement do not show current fluctuations (Fig. 2). However, the displacement of the reduction wave of hydrogen peroxide in the direction of more negative potential values remains. The slowing down of the reduction of hydrogen peroxide depends on the concentration of the monomer; as the latter increases, this effect gets stronger. At a concentration of approximately 0.1 M of the monomer in the solution, the reduction wave of hydrogen peroxide is not observed on the polarogram since the reduction of the latter takes place at the reduction potential of hydrogen ions. Higher concentrations of the monomer in a water-alcohol solution of sulphuric acid also displace the reduction wave of oxygen in the direction of more negative potential values (Fig. 2, 5).

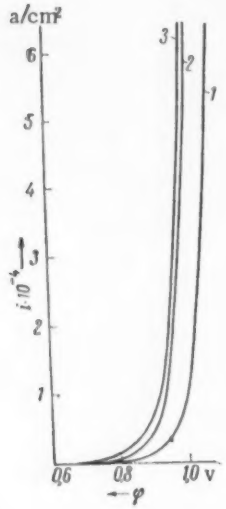

Fig. 3. Polarization curve at 18°. 1) 1 N H_2SO_4; 2) 50% 1 N H_2SO_4 + + 50% CH_3OH; 3) solution of the monomer in 50% 1 N H_2SO_4 + 50% CH_3OH after three-hour standing in air. Concentration of methyl methacrylate 0.4 M.

The initiation of the polymerization of methyl methacrylate, with accumulation of the polymer, was carried out at a stationary mercury cathode (S 10 cm^2) during the reduction of O_2, which, as is well known, takes place in an acid environment through the following steps:

$$O_2 + \bar{e} + H^+ \rightarrow HO_2. \qquad \text{(a)}$$

$$HO_2 + \bar{e} + H^+ \rightarrow H_2O_2. \qquad \text{(b)}$$

The electrode potential had a value of 0.2 v, i.e., approximately 0.1 v more negative than the potential of the half-wave of oxygen reduction in the presence of methyl methacrylate. The potential was determined on introducing the monomer and thereafter remained constant for three hours; changes in the dependence of current strength on time and visual observations of the solution made it possible to determine the time of appearance of the solid polymer. After completion of the experiment the polymer was separated from the solution, washed with water and alcohol, dried in a vacuum desiccator, and weighed.

In addition to the basic experiments on the accumulation of polymer, control experiments were carried out under the same conditions, but without the electrochemical reduction of oxygen and in the absence of oxygen, or without the superimposing of polymerization. In neither case was the formation of the polymer observed. The polarization curves as measured under the conditions of the experiment did not show the presence of admixtures which were reduced at the controlled potential (Fig. 3).

The results of the experiments showed that in saturated aqueous solutions (of approximately 0.1 M sulphuric acid) of methyl methacrylate, no deposit of the polymer was formed for a period of three hours after the introduction of the monomer. With increased concentration of the monomer up to 0.4 M and utilizing water-alcohol (sulphuric acid) solutions of the monomer, it was found that in solutions containing O_2 in concentrations of $1.25 \cdot 10^{-4}$ M and above, and also in the complete absence of oxygen, polymerization was not observed during the same time interval. With concentrations of oxygen that were from 20 to 100 times lower, i.e., at concentrations of oxygen corresponding to $6.25 \cdot 10^{-6}$ M and $1.25 \cdot 10^{-6}$ M, under the same reaction conditions formation of the polymer was observed; moreover, in the first case the polymerization took place more rapidly than in the second case. During the three-hour period, the strength of the current, which showed fluctuations, gradually fell to zero, which was related to the decrease in the concentration of oxygen.

We carried out prolonged experiments, the purpose of which was to obtain larger quantities of the polymer (0.035-0.05 g) for further study. In this case, not only the potential but also the concentration of oxygen were held approximately constant; the strength of the current did not decrease and it was possible to continue the accumulation of polymer for a considerable time.

Through repeated determinations by measuring the viscosity of a solution of the polymer in benzene, it was possible to calculate the average molecular weight of the polymer, which was found to be $2.5\text{-}3 \cdot 10^6$.

The results obtained on the initiation of polymerization of methyl methacrylate by the electrolytic reduction of oxygen indicate the twofold character of the action of the latter on the polymerization of methyl methacrylate. On the one hand, oxygen inhibits the process; on the other hand, it takes part in its initiation, probably through HO_2 radicals formed at the electrode during the reduction of O_2 in the first stage (a). The polymerization of methyl methacrylate under the given experimental conditions may also be considered as experimental confirmation of the formation of radicals as intermediate products during the electrolytic reduction of oxygen.

The influence of the agitation of the electrolyte at 700 rpm on the process of initiation of the polymerization of methyl methacrylate by the electrolytic reduction of oxygen under the conditions described was also studied. These experiments were carried on both in the field of diffusion and of kinetics in relation to this reaction, during which the concentration of oxygen was maintained at the same level as in the case of experiments with an unstirred electrolyte. It was shown that when the electrolyte is stirred polymerization does not take place. It is possible that this is related to the disruption of the conditions for the formation of polymeric chains on the surface of the electrode, or their growth, if the latter start from the electrode. This question, however, demands further study.

We express sincere thanks to Academician A. N. Frumkin for the interest he showed during the work, and for his valuable advice.

LITERATURE CITED

1. E. Dineen, T. Schwan, and C. Wilson, Trans. Electrochem. Soc. 96, 226 (1949).
2. C. Walling, Free Radicals in Solutions (1957) p. 591.
3. G. Parravano, J. Am. Chem. Soc. 73, 628 (1951).
4. J. Kolthoff and L. Ferstandig, J. Polym. Sci. 6, 563 (1951).
5. W. Kern and H. Qast, Makromolek. Chem. 10, 202 (1953).
6. J. W. Breitenbach and H. Gabler, Monatsh. Chem. 91, 202 (1960).
7. A. I. Fedorova, I. V. Shelepin, and N. B. Moiseeva, Tezisy Doklady na II soveshch. po élektrokhim. organich. soedinenii (Moscow, 1959).
8. J. C. Schoonover, G. M. Brauer, and W. T. Sweency, J. Res. Nat. Bur. Stand. 49, No. 6, 359 (1952); C. E. Barnes, J. Am. Chem. Soc. 67, 217 (1945); W. Kern, Makromolek. Chem. 1, 199 (1948).

All abbreviations of periodicals in the above bibliography are letter-by-letter transliterations of the abbreviations as given in the original Russian journal. *Some or all of this periodical literature may well be available in English translation.* A complete list of the cover-to-cover English translations appears at the back of this issue.

RADIATION TRANSFORMATIONS OF Fe^{2+} AND Fe^{3+} MIXTURES IN ACID SOLUTIONS SATURATED WITH HYDROGEN UNDER PRESSURE

V. N. Shubin and P. I. Dolin

Institute of Electrochemistry, Academy of Sciences, USSR
(Presented by Academician A. N. Frumkin, July 19, 1960)
Translated from Doklady Akademii Nauk SSSR, Vol. 138, No. 1,
pp. 169-172, May, 1961
Original article submitted July 19, 1960

In previous work [1-3] the oxidation of Fe^{2+} and the reduction of Fe^{3+} in solutions saturated with hydrogen under pressure were studied and some kinetic characteristics of the oxidation and reduction processes were determined. A study of the radiolysis of Fe^{2+} and Fe^{3+} mixtures in solutions under H_2 pressure enables these data to be obtained in several ways by varying the concentrations of the solution components, and makes possible more reliable conclusions about the mechanism of the process, on the basis of comparison of these data.

The $Fe^{2+} + Fe^{3+}$ system has already been studied [4, 5]. However, [4] and [5] were restricted to the determination of one type of relationship, and it is impossible to arrive at definite conclusions about the radiolysis mechanism, and consequently also the rate constants of the reactions which take place, on the basis of the obtained data.

It is obvious that when molecular hydrogen is present in the solution, a portion of the OH radicals is transformed into H atoms in accordance with the reaction

$$H_2 + OH \rightarrow H_2O + H \qquad (I)$$

competing with the reaction

$$Fe^{2+} + OH \rightarrow F^{3+} + OH^-. \qquad (II)$$

Because of the occurrence of Reaction (I), H atoms, able to participate in both oxidation and reduction reactions, appear in place of the oxidizing OH radicals. This extends the range of transformation yields and enables more accurate relationships to be derived.

In the present work the yields from Co^{60} γ-ray oxidation of Fe^{2+}, in the presence of different concentrations of Fe^{3+}, H_2, and Fe^{2+} in 0.8 N H_2SO_4 solutions, were measured.

METHOD

The glass cell and the procedure for saturating the solutions with hydrogen were described in detail previously [1, 2]. The solutions were prepared from c..p. grade reagents in twice-distilled water. The dose intensity amounted to $\sim 2 \cdot 10^{15}$ ev/cm^3·sec. The Fe^{2+} concentrations were determined spectrophotometrically with o-phenanthroline.

RESULTS AND DISCUSSION

The dependence of the oxidation yields on Fe^{3+} concentration was determined for $\sim 10^{-3}$ M Fe^{2+} solutions in 0.8 N H_2SO_4 saturated with H_2 at 100 atm. The initial portion of the oxidation curve was recorded for each Fe^{3+} concentration; the maximum change in the initial concentrations did not exceed 10%. The initial oxidation yields in relation to Fe^{3+} in the solution ($[Fe^{2+}] = 1.05 \cdot 10^{-3}$ M; $P_{H_2} = 100$ atm), calculated from these data, are given in Table 1.

TABLE 1

Fe^{3+} concentration, mole/liter	10^{-3}	$2 \cdot 10^{-3}$	$8.6 \cdot 10^{-3}$	$8.6 \cdot 10^{-2}$	$8.6 \cdot 10^{-1}$
G (Fe^{3+}), moles/100 ev	5.8	4.2	−1.05*	−4.2	−5.8

* The minus sign indicates that reduction occurs.

As is evident from the table, with increase in $[Fe^{3+}]$ the oxidation yield falls to zero, and with further increase in $[Fe^{3+}]$, reduction commences. Such a relationship may probably be explained by competition for H atoms in the following two reactions:

$$H + Fe^{3+} \rightarrow H^+ + Fe^{2+}; \quad \text{(III)}$$

$$H + H^+ \rightarrow H_2^+. \quad \text{(IV)}$$

The resulting H_2^+ ions are removed by the reaction

$$Fe^{2+} + H_2^+ \rightarrow Fe^{3+} + H_2. \quad \text{(V)}$$

Assuming that the initial yield is determined by the occurrence of reactions (I)-(V), and also

$$Fe^{2+} + H_2O_2 \rightarrow Fe^{3+} + OH^- + OH, \quad \text{(VI)}$$

we get the following expression for the oxidation yield:

$$G(Fe^{3+}) = G_H + G_{OH} + 2G_{H_2O_2} - \left[G_H + \frac{G_{OH} + G_{H_2O_2}}{1 + \frac{k_2[Fe^{2+}]}{k_1[H_2]}}\right] \frac{2}{1 + \frac{k_4[H^+]}{k_3[Fe^{3+}]}} \equiv$$
$$\equiv A - \frac{2\alpha}{1 + \frac{k_4[H^+]}{k_3[Fe^{3+}]}}. \quad \text{(1)}$$

We convert this into the following form:

$$1 + \frac{k_4[H^+]}{k_3[Fe^{3+}]} = \frac{2\alpha}{A - G(Fe^{3+})}. \quad \text{(2)}$$

Since only $[Fe^{3+}]$ changes in the solution, the right-hand side of the expression is a linear function of the ratio $[H^+]/[Fe^{3+}]$. Such a relationship is depicted in Fig. 1, plotted from the data in Table 1. According to Eq. (2), the slope of the line equals $k_4/k_3 = 9 \cdot 10^{-3}$, and the intercept $b_1 = 1$. From Fig. 1 we find $b_1 = 0.142$ $\alpha = 1$, from whence $\alpha = \left[G_H + \frac{G_{OH} + G_{H_2O_2}}{1 + \frac{k_2[Fe^{2+}]}{k_1[H_2]}}\right] = 7.05$. Hence, using the known magnitudes of the yields G_H, G_{OH}, and $G_{H_2O_2}$, and the concentration ratio $[Fe^{2+}]/[H_2] = 0.013$, we get $k_1/k_2 = 0.125 \pm 0.3$. This quantity can also be ascertained from the dependence of the oxidation yield on hydrogen pressure. For this, we transform Eq. (1) into the form

$$\frac{k_1[H_2]}{k_2[Fe^{2+}]} = \left[\frac{G_{OH} + G_{H_2O_2}}{\frac{1}{2}[A - G(Fe^{3+})]\left(1 + \frac{k_4[H^+]}{k_3[Fe^{3+}]}\right) - G_H} - 1\right]^{-1} \equiv X. \quad \text{(3)}$$

TABLE 2

H_2 pressure, atm	1	10	25	50	100
$G(Fe^{3+})$, moles/100 ev	2.9	0.85	−0.25	−0.75	−1.05

If only P_{H_2} changes, X is a linear function of the ratio $[H_2]/[Fe^{2+}]$. The dependence of X on $[H_2]/[Fe^{2+}]$, for the solution $[Fe^{2+}] = 1.05 \cdot 10^{-3}$ M, $[Fe^{3+}] = 8.6 \cdot 10^{-3}$ M, is depicted in Fig. 2, plotted from the experimental data (Table 2).

The slope of the line gives the value of $k_1/k_2 = 0.138$. We had previously determined this quantity by radiolysis of Fe^{2+} solutions in 0.8 N H_2SO_4 solutions saturated with H_2 and O_2, and it was found to be equal to 0.135. Values of k_1/k_2 obtained from data conforming to the third radiolysis method agreed well with that obtained for radicals origi-

nating in accordance with Reaction (VI), free from radiation effects [6]. This confirms that the radicals originating in accordance with Reaction (VI) and during radiolysis are identical.

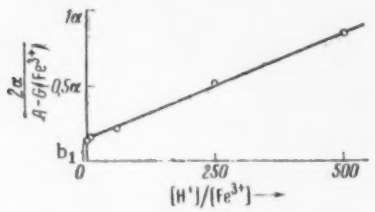

Fig. 1. Graphical representation of Eq. (2) from the data in Table 1.

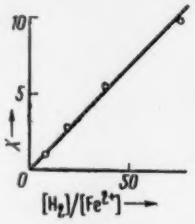

Fig. 2. Graphical representation of Eq. (3) from the data in Table 2.

Many authors consider that Reaction (IV) and the ensuing Reaction (V) should be substituted by the reaction [7]:

$$Fe^{3+}(H_2O)_n + H \rightarrow Fe\,OH^{2+}(H_2O)_{n-1} + H_2 \qquad \text{(IVa)}$$

or [8]

$$Fe^{2+} + H \rightarrow FeH^{2+} \xrightarrow{+H^+} Fe^{3+} + H_2. \qquad \text{(IVb)}$$

In this case evidently, $[Fe^{2+}]$ appears in place of the H^+ concentrations in Eqs. (1) and (2). The dependence of the oxidation yields on $[Fe^{2+}]$ was determined in $\sim 10^{-2}$ M Fe^{3+} solution with a constant $[Fe^{2+}]/[H_2]$ ratio. The results are presented in Table 3 ($[Fe^{3+}] = 8.6 \cdot 10^{-3}$ M; $[Fe^{2+}]/[H_2]$ = const).

TABLE 3

Fe^{2+} concentration, mole/liter	$1.15 \cdot 10^{-4}$	$2.3 \cdot 10^{-4}$	$1.05 \cdot 10^{-3}$	$1.05 \cdot 10^{-2}$
$G(Fe^{3+})$, moles/100 ev	0	0.3	0.85	1.25

Since only $[Fe^{2+}]/[Fe^{3+}]$ changes, the right-hand side of Eq. (2) should be a linear function of this ratio. The sought relationship, plotted from the data in Table 1 (dotted line) and Table 3 (solid line), is depicted in Fig. 3. The

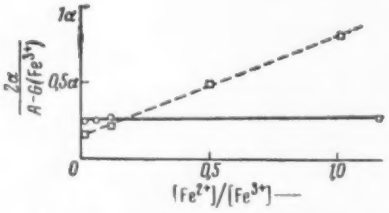

Fig. 3. Graphical representation of Eq. (2) as a function of the ratio $[Fe^{2+}]/[Fe^{3+}]$ from the data in Table 1 (dashed line) and Table 3 (solid line).

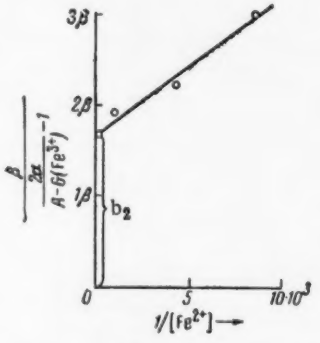

Fig. 4. Graphical representation of Eq. (4) from the data in Table 3.

slopes of the curves and the results calculated from the ratios of their constants do not agree, as they would have done in the case of the occurrence of Reactions (IVa) and (IVb). Thus, the experimental results do not confirm the occurrence of Reactions (IVa) and (IVb).

The experimentally observed dependence of the yields on $[Fe^{2+}]$ (see Table 3) is probably explained by not all the H_2^+, originating in accordance with Reaction (IV), reacting with Fe^{2+} at low Fe^{2+} concentrations: a portion of the H_2^+ ions is lost in accordance with the reaction

$$H_2^+ \rightarrow H^+ + H. \qquad \text{(VII)}$$

In this case, as is easily verified, it is necessary to replace the term k_4/k_3 by $\frac{k_4}{k_3} \Big/ \left(1 + \frac{k_7}{k_5[Fe^{3+}]}\right)$ in Eq. (1) and (2). In order to determine k_7/k_5 and k_4/k_3, we rewrite Eq. (2) in the following form:

$$1 + \frac{k_7}{k_5[Fe^{3+}]} = \frac{k_4[H^+]/k_3[Fe^{3+}]}{\frac{2\alpha}{A - G(Fe^{3+})} - 1} \equiv \frac{\beta}{\frac{2\alpha}{A - G(Fe^{3+})} - 1}. \qquad (4)$$

The right-hand side of the expression is a linear function of the quantity $1/[Fe^{2+}]$. The sought relationship is depicted in Fig. 4, plotted from the data in Table 3. The slope of the line equals $k_7/k_5 = 1.5 \cdot 10^{-4}$ mole/liter. The intercept $b_2 = 1$, from which $k_4/k_3 = 1.03 \cdot 10^{-2}$.

In conclusion, it is necessary to note that the effective Fe^{3+} concentrations in sulfuric acid solutions may be considerably lower than the total, as was shown before [3], because of the formation of complexes, which must be taken into account for the determination of the absolute values of the k_4/k_3 ratios.

LITERATURE CITED

1. V. N. Shubin and P. I. Dolin, Doklady Akad. Nauk SSSR 125, No. 6, 1294 (1959).
2. V. N. Shubin and P. I. Dolin, Zhur. Fiz. Khim. 34, No. 11 (1960).
3. V. N. Shubin and P. I. Dolin, Doklady Akad. Nauk SSSR 134, No. 4, 891 (1960).
4. W. G. Rothschild and A. O. Allen, Rad. Res. 8, No. 2, 101 (1958).
5. P. Riesz and E. J. Hart, J. Phys. Chem. 63, No. 6, 858 (1959).
6. D. Bunn, F. Dainton, et al., Trans. Farad. Soc. 55, No. 10, 1760 (1959).
7. T. W. Davis, S. Gordon, and E. J. Hart, J. Am. Chem. Soc. 80, 4487 (1958).
8. J. Halpern, G. Czapski, et al., Nature 186, 629 (1960).

All abbreviations of periodicals in the above bibliography are letter-by-letter transliterations of the abbreviations as given in the original Russian journal. *Some or all of this periodical literature may well be available in English translation.* A complete list of the cover-to-cover English translations appears at the back of this issue.

THE SEPARATION OF SILICON ISOTOPES BY THE FRACTIONAL DISTILLATION OF SILANE

G. G. Devyatykh, G. K. Borisov, and A. M. Pavlov

Chemical Scientific Research Institute, N. I. Lobachevskii Gorky State University
(Presented by Academician A. N. Frumkin, January 9, 1961)
Translated from Doklady Akademii Nauk SSSR, Vol. 138, No. 2,
pp. 402-404, May, 1961
Original article submitted September 29, 1960

There are three stable isotopes of silicon with a natural abundance of: Si^{28} = 92.27%, Si^{29} = 4.68%, and Si^{30} = = 3.05% [1].

A small scale separation of silicon isotopes has been achieved by the electromagnetic method [2, 3].

One might have expected that physicochemical methods used successfully for the isotopic separation of other light elements would also be applicable to silicon. Yet so far no method of this kind has been worked out. Attempts to separate the isotopes of silicon by the fractional distillation of silicon tetrachloride were unsuccessful [4]. Calculations have also shown that the equilibrium constant for the isotopic exchange reaction

$$Si^{28}F_4 + Si^{30}F_6^{2-} \rightleftarrows Si^{30}F_4 + Si^{28}F_6^{2-},$$

which could have been used for the desired separation, is very small, 1.002 at 27° C [5].

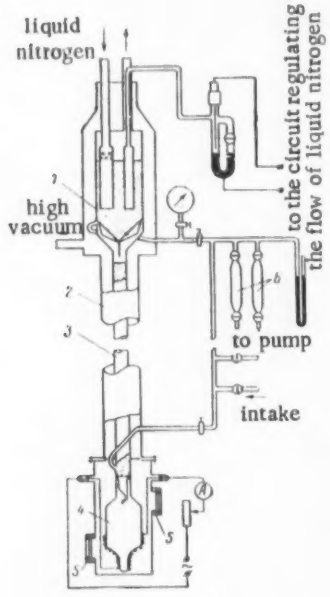

Fig. 1. The design of the fractionating column. 1) Condenser; 2) vacuum jacket; 3) column; 4) glass boiler; 5) viewing windows; 6) receiver tubes.

The purpose of this work was to see if the silicon isotopes could be separated by the fractional distillation of silane. Silane has a very low boiling point, and the relative difference between the masses of the various isotopic forms is larger than that for any other silicon compound. Hence, one would expect the differences between the vapor pressures of isotopically different silanes to be more pronounced than in the case of other compounds.

Silane was fractionated in the packed metal column described in Fig. 1. The packing consisted of 0.18-mm nichrome wire coils (2 × 2 mm). The packing was 240 cm long. The column was 10 mm in diameter. The column had an efficiency of 60 theoretical plates, which was determined from the separation of carbon isotopes through fractional distillation of carbon monoxide. The fractionation was carried out under a 560-mm silane pressure, which is equivalent to a temperature of −117° C. The silane fractions collected for mass-spectroscopic isotopic analysis were converted into silicon tetrafluoride.

The conversion was achieved in the following way. Silane was burned in an atmosphere of oxygen and converted to silicon dioxide, which was then dissolved in hydrofluoric acid; addition of barium chloride to this solution yielded a precipitate of barium hexafluorosilane, which was subsequently converted to silicon tetrafluoride by thermal decomposition.

Silane-oxygen mixtures containing less than 50% silane are stable under atmospheric pressure at room temperature, but mixtures with more than 50% silane are highly explosive under these conditions [6-8]. In order to achieve a smooth reaction between silane and oxygen, we used hydrogen peroxide to initiate the reaction. The solution of silicon dioxide and the pre-

Results from the Fractionation of Silane

Sample No.	Duration of work, hr	F_{29}	F_{30}	Sample No.	Duration of work, hr	F_{29}	F_{30}
1	2,3	1,006 ± 0,004	1,011 ± 0,004	5	20,75	1,019 ± 0,003	1,030 ± 0,004
2	7,1	1,010 ± 0,003	1,012 ± 0,003	6	27	1,012 ± 0,002	1,029 ± 0,002
3	12,3	1,007 ± 0,003	1,016 ± 0,003	7	31	1,022 ± 0,004	1,037 ± 0,004
4	16,3	1,012 ± 0,002	1,024 ± 0,002	8	33,5	1,020 ± 0,004	1,035 ± 0,004

cipitation of barium hexafluorosilane were carried out in polyethylene beakers. The precipitate was washed with distilled water, transferred into a porcelain crucible, and dried at 120° C. After that, the precipitate was placed in a stainless steel test tube. To remove the last traces of water we heated the test tube to 250° and pumped it out with a mercury diffusion pump until the pressure was reduced to $\sim 5 \cdot 10^{-5}$ mm Hg; subsequently, the pump was disconnected and the evacuated tube heated to ~800° C. At this temperature barium hexafluorosilane decomposed and silicon tetrafluoride was evolved.

The isotopic analysis of our samples was done in an MI-1305 mass spectrometer. The measurements were based on the $Si^{28}F_3^+$, $Si^{29}F_3^+$, and $Si^{30}F_3^+$ peaks (masses of 85, 86, and 87, respectively). At least 8-10 peaks of each mass were used in the analysis.

In analyzing our mass spectra we interpolated the heights of peaks with mass 36 and 87 to the instant at which the mass peak was recorded in order to take into account the small gradual changes in the intensity of ion currents [4].

From the mass spectra we determined the isotopic ratios

$$A_1 = I_{86}/I_{85} \; ; \quad A_2 = I_{87}/I_{85},$$

where I_{85}, I_{86}, and I_{87} are the current intensities for ions of mass 85, 86, and 87, respectively.

The separation factor was determined from the ratio of the isotopic ratios in samples taken simultaneously from the boiler and the condenser of the column,

$$F_{29} = A_1^b / A_1^c \; , \quad F_{30} = A_2^b / A_2^c \; ,$$

where F_{29} is the separation factor for the Si^{29} isotope, and F_{30} for the Si^{30} isotope.

The results of our fractionation are presented in the table and Fig. 2.

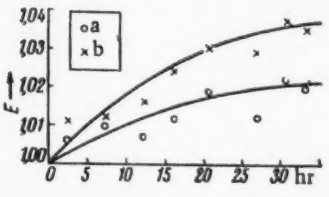

Fig. 2. The fractionation curves of isotopic silanes: a) $Si^{29}H_4$; b) $Si^{30}H_4$.

As can be seen in the table and Fig. 2, stationary conditions were achieved in the column. From the fractionation data we calculated the separation factors, which are equal to the relative vapor pressures of the various isotopic forms of silane

$$\alpha_{29} = P_{Si^{28}H_4}/P_{Si^{29}H_4} = 1{,}00035 \pm 0{,}00007,$$
$$\alpha_{30} = P_{Si^{28}H_4}/P_{Si^{30}H_4} = 1{,}00061 \pm 0{,}00010.$$

In conclusion, we would like to express our gratitude to L. P. Korovin for his assistance in the experimental work.

LITERATURE CITED

1. Short Encyclopedia, Atomic Energy [in Russian] (Moscow, 1958).
2. W. Groth, Z. Elektrochem. u. angew. phys. Chem. 54, 5 (1950).
3. C. P. Keim, J. Appl. Phys. 24, 1255 (1953).
4. V. P. Orlov and N. M. Zhavoronkov, Zhur. Priklad. Khim. 29, 959 (1956).

5. J. Bigeleisen and M. G. Mayer, J. Chem. Phys. 15, 261 (1947).
6. P. S. Schantorowitch, Acta phys.-chim. URSS 2, 633 (1935).
7. P. S. Schantorowitch, Acta phys.-chim. URSS 6, 65 (1937).
8. H. J. Emeleus and K. Stewart, J. Chem. Soc., No. 9, 1182 (1935).

All abbreviations of periodicals in the above bibliography are letter-by-letter transliterations of the abbreviations as given in the original Russian journal. *Some or all of this periodical literature may well be available in English translation.* A complete list of the cover-to-cover English translations appears at the back of this issue.

THE ADSORPTION OF NITROGEN, ARGON, AND KRYPTON ON VARIOUS SURFACES AND THE DETERMINATION OF SURFACE AREAS

M. G. Kaganer

All-Union Scientific Research Institute of Oxygen Technology
(Presented by Academician M. M. Dubinin, December 15, 1960)
Translated from Doklady Akademii Nauk SSSR, Vol. 138, No. 2, pp. 405-408, May, 1961
Original article submitted December 15, 1960

The adsorption of nitrogen on various surfaces has been investigated quite thoroughly over a wide range of relative pressures. Nitrogen is frequently used to determine specific surfaces by the BET method. The author of this paper has recently proposed [1] a new method for the determination of surface areas from the adsorption of unimolecular layers; the method was based on the equations derived by M. M. Dubinin and L. V. Radushkevich. In the above-mentioned paper nitrogen was used as adsorbate.

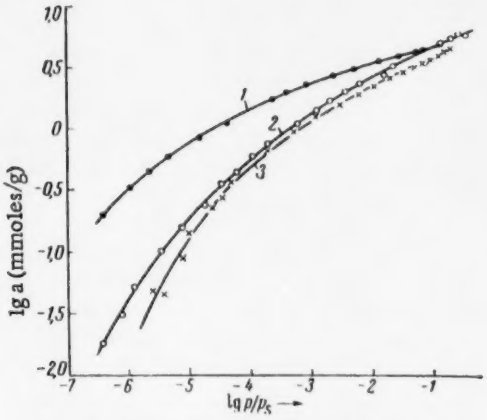

Fig. 1. Adsorption isotherms on S-U silica gel. 1) Nitrogen; 2) argon; 3) krypton. T = 90.1° K.

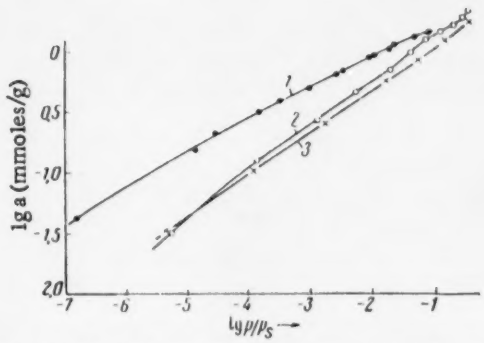

Fig. 2. Adsorption isotherms on silicoaerogel. 1) Nitrogen; 2) argon; 3) krypton. T = 90.1° K.

The main purpose of the current work was to study the adsorption of other gases, particularly argon and krypton, over a wide range of pressures and to see if they could be used for the determination of surface areas by the new method. The adsorption of N_2, A, and Kr was investigated* at 90° K over a range of pressures from $1 \cdot 10^{-4}$ to 500 mm Hg on four adsorbents: silica gel, silicoaerogel, aluminagel, and activated charcoal. Measurements were carried out in the same apparatus as before [1]. The experimental results are plotted in Figs. 1-4 in logarithmic co-ordinates.

According to the potential theory of adsorption, the adsorption potential can be determined from the equation

$$\varepsilon = RT/\ln (p_s/p)$$

where R is the gas constant, p and T are the pressure and temperature, respectively, during the adsorption, and p_s is the saturated vapor pressure of the adsorbate. According to the potential theory, when a is plotted vs. ε (where a is the amount of adsorbed material) the adsorption isotherms of different vapors on any one adsorber should be very similar. M. M. Dubinin and D. P. Timofeev have shown [2] that the affinity coefficient, in the first approximation at least, is equal to the ratio of the molar volumes in the condensed phase of the adsorbates.

*G. P. Tikhonova participated in the experimental work.

Since all the adsorption isotherms in our work were determined at the same temperature, the curves plotted in Figs. 1-4 should be related. The molar volume of liquid nitrogen at 90° K is greater than that of either the liquid argon or solid krypton. Therefore, the adsorption isotherm of N_2 should lie below the isotherms of A and Kr. As one can see in the figures, this relationship holds on charcoal at relative pressures above 0.001; similar relationships were obtained in the case of N_2 and A [3], and N_2 and Kr [4] on charcoal. On other adsorbents (Figs. 1-3) the adsorption isotherms of nitrogen lie considerably above the curves for the other gases, and the curves tend to diverge with decreasing pressure. A similar relationship is observed when N_2 and A are adsorbed on crystals (see [5, 6]). No satisfactory explanation was given for this last effect.

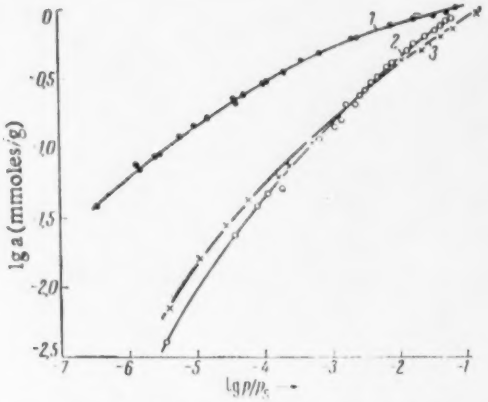

Fig. 3. Adsorption isotherms on activated alumina. 1) Nitrogen; 2) argon; 3) krypton. T = 90.1° K.

An important property, which distinguishes nitrogen from several other gases, is the presence of a large and permanent quadrupole moment [7, 8]. In nitrogen it is $1.5 \cdot 10^{-26}$ cgs esu (p), while in oxygen it does not exceed $0.5 \cdot 10^{-26}$ cgs esu (p), but in monoatomic gases it is zero. This moment does not exert any appreciable effect on the intermolecular interactions at larger distances, and that is why the thermodynamic properties of gaseous nitrogen are very similar to those of A, Kr, O_2, and several other gases [9].

Theoretical calculations have shown [10] that the energy of interaction between the nitrogen quadrupole moment and the electrostatic field of the solid surface is quite large and in several cases it is close in magnitude to the Van der Waals interaction energy. It has been established [8, 11] that the interaction of the quadrupole moment with the solid surface makes the heat of adsorption of N_2 and CO greater than that of A and O_2 on crystalline surfaces at low relative pressures. The fact that N_2 is more strongly adsorbed on silica gel and on alumina gel at low relative pressures than A and Kr are can also be attributed to an interaction of the quadrupole moment with the surface, since the hydroxyl groups found on the surface of these adsorbents have very large dipole moments. Activated charcoal is an amorphous form of carbon, and hence the adsorption interaction depends mainly on Van der Waals forces. That is why the adsorption isotherm of N_2 on charcoal lies closely to the isotherms of A and Kr (Fig. 4). The divergence which appears at surface coverages $\theta < 0.3$ can apparently be attributed to the presence of a certain number of activated sites on the surface with a sharply inhomogeneous structure.

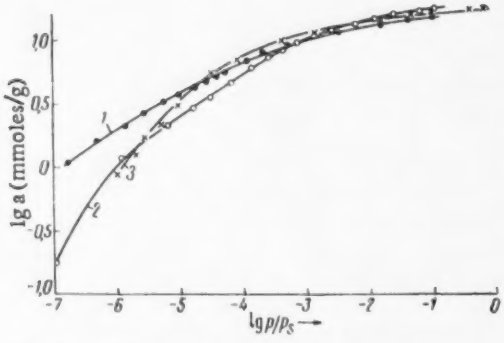

Fig. 4. Adsorption isotherms on SKT charcoal. 1) Nitrogen; 2) argon; 3) krypton. T = 90.1° K.

These peculiarities in the adsorption of nitrogen indicate a need for a critical re-examination of surface determination methods based on nitrogen adsorption. A comparative determination of surface areas from the adsorption of N_2, A, Kr, and other gases has been reported by several workers [12-18]. The area of a nitrogen molecule, calculated from the density of liquid nitrogen at 77.4° K (16.2 A^2), was used as reference value in these calculations. Measurements have shown that in order to get results consistent with the data determined from the adsorption of nitrogen one would have to assume that the cross section of the other gases is 1.2-1.5 times as large as the values calculated from their densities in the liquid state. The calculated ratio of the area occupied by an adsorbate molecule to the area of a nitrogen molecule, σ_x/σ_{N_2}, at 77.4° K is 0.88 in the case of A and 0.94 in the case of Kr, whereas the experimental adsorption data yield σ_x/σ_{N_2} of 0.95-1.05 for A and 1.20-1.35 for Kr. In the opinion of several investigators, the reason for the discrepancy is that molecules adsorbed on a solid surface occupy an area greater than that calculated from the density in the condensed phase.

The surface data obtained from the adsorption isotherms plotted in Figs. 1-4 are presented in Table 1. We have also listed values calculated for AG-2 charcoal from the data given in [3]. The symbol a_m gives the amount of nitrogen adsorbed in a unimolecular layer. The surface area of an adsorber can be determined from this number in the usual way. The ratios σ_x/σ_{N_2} were obtained by dividing the value of a_m for N_2 by the corresponding number for A and Kr.

TABLE 1. Surface Areas Determined From the Adsorption of N_2, A, and Kr at 90° K

Adsorber	a_m, mmoles/g		σ_x/σ_{N_2}			
	nitrogen		argon		krypton	
	BET method	the new method	BET method	the new method	BET method	the new method
S-U silica gel	3.87	3.89	1.01	1.04	1.13	1.16
Silicoaerogel	1.19	–	0.99	–	1.25	–
Activated alumina	1.09	1.12	1.00	0.97	1.23	1.24
SKT charcoal	–	15.1	–	0.84	–	0.94
AG-2 charcoal [3]	8.45	8.35	0.86	0.86	–	–

First of all, we would like to point out that the results obtained by the BET method are in good agreement with those calculated by the method proposed by the author of this paper [1]; the differences do not exceed 3%. Hence in calculating the surface area by the new method one can use the adsorption isotherms of A and Kr as well as N_2. Calculations based on the experimental data of other workers [3, 6] indicate that when O_2 and Xe are used the surface areas determined by the new method are also in good agreement with those calculated by the BET method.

TABLE 2. Surface Areas Occupied by Adsorbed Molecules

Adsorbate	Area occupied by one molecule, A^2			
	90° K		78° K	
	from adsorption data	from density in condensed state	from adsorption data	from density in condensed state
Argon	14.4	14.4	13.8	–
Nitrogen	14.4•	14.6•••	13.7•	14.6•••
	17.0••	17.0	16.1••	16.2
Krypton	18.0	17.5••••	17.0	17.5••••
				15.2
Oxygen	13.7	14.1	13.3	13.5

• Polar surfaces.
•• Nonpolar surfaces.
••• Density of solid at the melting point.
•••• Density of liquid at the melting point.

The σ_x/σ_{N_2} ratios for the first three adsorbents lie within the range of values reported by other workers, with the exception of Kr on S-U silica gel. But in the case of carbon (activated charcoal) the values are close to those calculated from the density of the adsorbate. Similar results have been reported by other workers for the adsorption of N_2, Kr, Xe, and other gases on various forms of charcoal [4].

Our and some earlier work yield an average value of 1.25 for σ_{Kr}/σ_A, but the ratio is 1.15 on S-U silica gel and 1.12 on SKT charcoal. The deviation from the average may be due to the microporous nature of the two above-mentioned adsorbers: the average pore radius (calculated from the formula r = 2v/s) in S-U silica gel is 10 A, and in SKT charcoal 8 A.

On the basis of the experimental data, with the pore effect taken into account, one can safely presume that the difference between the surface areas calculated from N_2 adsorption and those determined using other gases is mainly due to the fact that on surfaces with strong dipoles and ions nitrogen molecules are more tightly packed due to the interaction of the N_2 quadrupole with the surface. The packing apparently resembles more that encountered in the solid phase than that in the liquid. Therefore, the calculated areas of N_2 molecules should be much smaller. A similar explanation was recently proposed as a result of comparative surface area determinations in which adsorption and electron-microscopic techniques [16] were used.

As a starting point it is best to use the area occupied by a monoatomic gas, such as A, which is independent of the chemical or geometrical surface modifications. It is preferable to carry out the measurements at 90°K instead of 78° K since argon solidifies at 84° K and there is some evidence [19] that the adsorbed film may be in the liquid form even at 78° K. The area of an argon molecule calculated from the density of the liquid is 14.4 A^2.

Adsorption data indicate that N_2 occupies about the same area as A, which would correspond to the packing in nitrogen crystals. This fact strongly supports the mechanism proposed above. We suggest that the molecular areas listed in Table 2, which were calculated from the adsorption data on the basis of the given argon area, be used for the determination of surface areas of adsorbers. They are in good agreement with the values determined from the densities in the condensed phase.

We wish to thank A. I. Moroz for his valuable advice during the discussion of this work.

LITERATURE CITED

1. M. G. Kaganer, Zhur. Fiz. Khim. 33, 2202 (1959).
2. M. M. Dubinin and D. P. Timofeev, Zhur. Fiz. Khim. 21, 1213 (1947).
3. V. G. Fastovskii and A. E. Rovinskii, Trudy Vsesoyuz. Elektrotekh. Instituta, No. 61, 48 (1958).
4. K. M. Nikolaev and M. M. Dubinin, Izvest. Akad. Nauk SSSR, Otdel Khim. Nauk,1165 (1958).
5. A. G. Keenan and J. M. Holmes, J. Phys. Coll. Chem. 53, 1309 (1949).
6. J. M. Honig and L. H. Reyerson, J. Phys. Chem. 56, 140 (1952).
7. J. O. Hirschfelder, C. F. Curtiss, and R. B. Bird, Molecular Theory of Gases and Liquids (New York, 1954) p. 1028.
8. G. L. Kington and A. C. Macleod, Trans. Farad. Soc. 55, 1799 (1959).
9. M. G. Kaganer, Zhur. Fiz. Khim. 30, 2691 (1956).
10. L. E. Drain, Trans. Farad. Soc. 49, 650 (1953)
11. L. E. Drain and J. A. Morrison, Trans. Farad. Soc. 49, 654 (1953).
12. R. A. Beebe, J. B. Beckwith, and J. M. Honig, J. Am. Chem. Soc. 67, 1554 (1945).
13. P. H. Emmett and M. Cines, J. Phys. Coll. Chem. 51, 1248 (1947).
14. M. L. Corrin, J. Am. Chem. Soc. 73, 4061 (1951).
15. H. L. Pickering and H. C. Eckstrom, J. Am. Chem. Soc. 74, 4775 (1952).
16. K. Kodera and J. Onishi, Bull. Chem. Japan 32, 356 (1959).
17. M. M. Dubinin, E. G. Zhukovskaya, et al., Izvest. Akad. Nauk SSSR, Otdel Khim. Nauk,588 (1960).
18. G. L. Gaines and P. Cannon, J. Phys. Chem. 64, 997 (1960).
19. V. Daneš and J. Nováková, Coll. Czechosl. Chem. Commun. 24, 874 (1959).

All abbreviations of periodicals in the above bibliography are letter-by-letter transliterations of the abbreviations as given in the original Russian journal. *Some or all of this periodical literature may well be available in English translation.* A complete list of the cover-to-cover English translations appears at the back of this issue.

THE EFFECT OF OVERSTOICHIOMETRIC OXYGEN ON THE CATALYTIC, ADSORPTION, AND ELECTRICAL PROPERTIES OF NICKEL OXIDE

L. N. Kutseva

Institute of Physical Chemistry, Academy of Sciences, USSR
(Presented by Academician P. A. Rebinder, September 30, 1960)
Translated from Doklady Akademii Nauk SSSR, Vol. 138, No. 2,
pp. 409-411, May, 1961
Original article submitted July 25, 1960

This paper is the outcome of an investigation of the catalytic, adsorption, and electrical properties of various nickel oxide samples with different electrical conductivities [1]. Nickel oxide samples prepared in air at elevated temperatures retain varying amounts of oxygen in excess of stoichiometric, and the higher the decomposition temperature of the initial salt the less excess oxygen retained. As the relative amount of excess oxygen increases, the nickel oxide changes in color from green to black; this is also accompanied by changes in the electrical conductivity, magnetic susceptibility, catalytic activity, and other properties [1].

TABLE 1. Specific Surface and the Initial Composition of NiO Samples Prepared at Various Temperatures

Catalyst	S_1, m^2/g (from Krypton)	Initial composition
NiO (900°)	2,0	$Ni_1O_{0,997}$
NiO (800°)	3,5	—
NiO (700°)	13,0	$Ni_1O_{1,07}$
NiO (600°)	17,5	—
NiO (500°)	30,5	$Ni_1O_{1,13}$

1. Nickel oxide samples were prepared by pyrolyzing nickel carbonate pellets (compressed at 4000 atm) for 3 hrs at 500, 600, 700, 800, and 900° C in a stream of pure air. The samples ranged in color from black (500°) to light green (900° C). The specific surface areas were determined by the BET method from the equilibrium isotherms for the physical adsorption of krypton at liquid nitrogen temperature (−195°).

The amount of oxygen in excess of stoichiometric was determined by reducing NiO in a stream of hydrogen at 400° C. The data are compiled in Table 1. The method used for the determination of electrical conductivity has been described elsewhere [2].

In Table 2 we have listed the specific electrical conductances at 25° and the electrical conductivity activation energies of various NiO samples determined in vacuo at temperatures ranging from room temperature to 300°. One can see that the electrical conductivity of the two extreme samples differs by two orders of magnitude, while the activation energy changes by 15 kcal/mole.

TABLE 2

Catalyst	E, kcal/mole	R, ohm·cm
NiO (900°)	30	$7,0 \cdot 10^5$
NiO (800°)	25	$6,8 \cdot 10^4$
NiO (700°)	21	$4,0 \cdot 10^4$
NiO (600°)	—	$8,9 \cdot 10^3$
NiO (500°)	15	$6,9 \cdot 10^3$

TABLE 3

Catalyst	K_0	K_1 at 24°	E, kcal/mole
NiO (900°)	$2 \cdot 10^3$	0,11	5,7
NiO (800°)	$6,4 \cdot 10$	0,37	3,0
NiO (600°)	$3,4 \cdot 10$	0,20	3,0
NiO (500°)	$2,2 \cdot 10$	0,11	3,0

2. The catalytic oxidation of CO (in a stoichiometric mixture of $2CO + O_2$) was investigated in a vacuum apparatus at a pressure of 0.5 mm Hg under stationary conditions. The resulting CO_2 was trapped in a U-tube cooled to the liquid nitrogen temperature. In all cases the reaction followed first-order kinetics. The lines plotted in Fig. 1 show how the specific rate of CO oxidation on various catalysts varies with temperature. The activation energy for the oxidation of CO, the frequency factor, and the rate constant K_1 at 24° are given in Table 3.

Table 3 shows that the activation energies on all the NiO catalysts prepared by pyrolysis at temperatures between 500 and 800° are about the same, but the initial rates are different. The rate constant K_1 at 24° on the 800° NiO is three times as large as that on the 500° NiO. The rate constant in this case increases as a result of increasing frequency factor K_0. On the 900° NiO, the composition of which is closest to the stoichiometric, the activation energy for the oxidation of CO is about 3 kcal/mole higher than on the other samples.

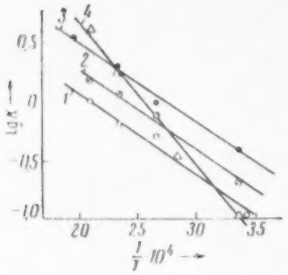

Fig. 1. The logarithms of the rate constant for the oxidation of CO on NiO samples prepared at various temperatures as a function of 1/T. 1) 500°; 2) 600°; 3) 800°; 4) 900°.

The adsorption of O_2, CO, and acetylene on the 800° NiO and the 500° NiO were measured. The electron configuration makes O_2 an acceptor of electrons while CO and C_2H_2 act as donors. The adsorption of CO was investigated at room temperature, and the plot in Fig. 2 shows that the adsorption rate and the amount adsorbed both are slightly smaller on the 500° NiO than on the 800° NiO. The adsorption of C_2H_2 proceeded very similarly. The adsorption of oxygen, measured at 300°, was practically the same on the 800° NiO as on the 500° NiO (see Fig. 3).

3. When the initial nickel carbonate was pyrolyzed at different temperatures, the resulting catalysts differed in their composition relative to the stoichiometric. As we have already shown, the deviations from stoichiometric composition are due to an excess of oxygen. The excess oxygen might be localized in the lattice nodes in the form of divalent anions. For each such anion a cationic vacancy would arise in the nickel oxide lattice, and if the lattice is to remain neutral two Ni^{+++} have to form near each vacancy.

As the amount of excess oxygen and consequently the number of Ni^{+++} increases, the rate of CO oxidation declines in the same way as in the case of solid solutions of lithium oxide in NiO [3]. However, whereas on $NiO(Li_2O)$ the reaction rate decreases due to a decline in the activation energy, in our present case the decrease is due to a reduced frequency factor K_0. The change in K_0 seems to be accompanied by a parallel change in the adsorption of the main reactant (CO). Presumably the

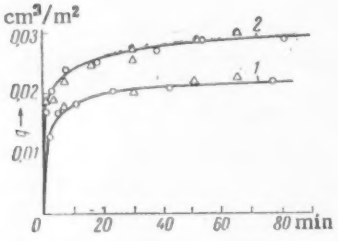

Fig. 2. Rate curves for the adsorption of CO on various types of NiO at t = 24°. 1) 500° sample; 2) 800° sample.

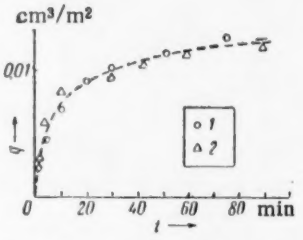

Fig. 3. Rate curves for the adsorption of oxygen on various types of NiO at t = 300°. 1) 500° sample; 2) 800° sample.

adsorption of CO is the rate-determining step in the reaction. The fact that in the temperature range from 500-800° there seems to be no correlation between the activation energy for the catalytic reaction (E_{cat}) and the activation energy for the electrical conductivity (E_σ) indicates that in the present system the two phenomena are not interrelated in the usual manner.

LITERATURE CITED

1. N. P. Keier, S. Z. Roginskii, and I. S. Sazonova, Doklady Akad. Nauk SSSR 106, 859 (1956); N. P. Keier and L. N. Kutseva, Doklady Akad. Nauk SSSR 117, No. 2, 259 (1957).
2. W. Klemm and K. Hass, Zs. anorg. Chem. 219, 82 (1934); M. Le Blanc and H. Sachse, Zs. anorg. Chem. 168, 15 (1927); Phys. Zs. 32, 887 (1931); M. Prasad and M. G. Tendulkar, J. Chem. Soc.,1403, 1407 (1931).
3. N. P. Keier and L. N. Kutseva, Izvest. Akad. Nauk SSSR, Otdel Khim. Nauk, No. 5, 797 (1959).
4. I. S. Sazonova, Dissertation [in Russian], Institute of Phys. Chem., Acad. Sci. USSR (1957).

THE VARIATION OF THE SURFACE TENSION OF THALLIUM WITH TEMPERATURE

O. A. Timofeevicheva and V. B. Lazarev

N. S. Kurnakov Institute of General and Inorganic Chemistry,
Academy of Sciences, USSR
(Presented by Academician I. V. Tananaev, December 24, 1960)
Translated from Doklady Akademii Nauk SSSR, Vol. 138, No. 2,
pp. 412-414, May, 1961
Original article submitted December 21, 1960

We decided to investigate the variation of the surface tension (σ) of thallium with temperature in order to clarify certain problems connected with the preparation of semiconductors [1]. The surface tension of thallium has been previously investigated by Sauerwald and Schmidt [2], but the authors were unable to obtain reproducible results, since they report that the σ of thallium at 320° C increased from 357.0 to 496.0 dynes/cm over a period of 1-2 hours; it is quite apparent that their method was unsatisfactory.

To measure the value of σ of thallium at different temperatures we used the maximum pressure technique, which has a very sound theoretical basis. The theory was developed by Cantor [3] and the method demands that the capillaries have infinitesimally thin walls at the tip. Since thallium is extremely toxic, we decided to carry out the surface tension investigation in a sealed glass apparatus. However, it is very difficult to make the type of capillaries required by the theory [3] out of glass. But if we were to use the maximum drop pressure method for the determination of σ of liquids which do not wet the capillary material and the maximum bubble pressure method for liquids which do wet the capillary then it is permissible to use capillaries with finite wall dimensions.

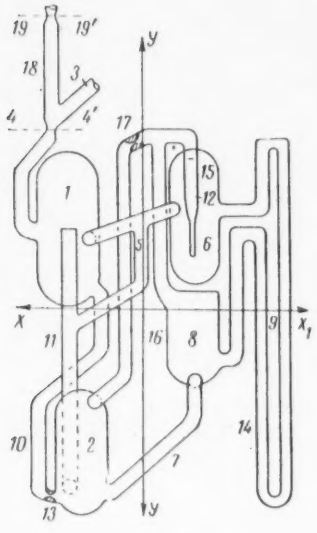

Fig. 1.

Since we did not know whether thallium would wet glass at the experimental temperatures, we were faced with a choice between the two variations of the maximum pressures technique. In order to eliminate this problem, one of us (O. A. Timofeevicheva) designed a rotating sealed glass apparatus which, unlike the apparatus described previously [4, 5], enabled us to not only measure σ by the maximum drop pressure method, but also to switch over to the maximum gas-bubble pressure method at any stage of the experiment and back without having to open the apparatus.

After the apparatus was evacuated and degassed by heating and attached to a rotating frame (Fig. 1), the desired amount of the molten metal was introduced into the bulbs 1 and 2 through tube 18, and the T-tube was sealed off along the dashed line 19 – 19'; an inert gas was introduced into the apparatus through tube 3 under a pressure slightly under atmospheric; the apparatus was detached from the vacuum system by sealing along the line 4 – 4' and placed in an air-circulating thermostat. If the surface tension is to be determined by the method of maximum gas-bubble pressure, the apparatus is rotated clockwise in the plane of the diagram until some of the metal flows through tube 5 into reservoir 6, covering the tip of capillary 12, and also through tube 7 into vessel 8, and from it into manometer 9. After the apparatus is returned to its original position, it is rotated by more than 90° (away from the viewer) about the XX_1 axis, forcing the metal left over in vessel 2 into vessel 1 through tubes 10 and 11, and returned to the position shown in the diagram. After that, the metal is forced through constriction 13 by the force of gravity and it gradually seals tubes 11 and 7; this creates an enclosed volume of gas within the apparatus sealed by the metal surfaces in vessel 2, in capillary 12, and in bend 14 of manometer 9. As more and more metal

flows into vessel 2, the pressure increases in the enclosed space and decreases in reservoir 6 and the connected volume; a gas bubble then begins to form at the tip of capillary 12, which is immersed in the liquid. The pressure difference between the bubble and the metal surface in reservoir 6 (which is recorded on manometer 9) expands the gas bubble and detaches it from the tip of capillary 12 when the maximum pressure is attained. When the apparatus is rotated again by more than 90° about the XX_1 axis (away from the viewer), the pressure throughout the apparatus is equalized and the metal flows out of vessel 2 into vessel 3. After the apparatus is returned to the original position, the measurements are carried out as before and the entire process can be repeated many times. Since the distance from the mark 15 to the tip of capillary 12 is known, by measuring the distance from the mark to the surface of the liquid in vessel 6 one can determine the depth to which the capillary is submerged. In order to get σ from the Cantor equation, the only other data we need is the difference between the liquid levels in the manometer, the radius of capillary 12, and the density of the liquid at the experimental temperature.

If measurements are to be done by the maximum drop pressure method, the apparatus is simply rotated by 180° about the XX_1 axis. Since vessel 2 is now in the upper position, the metal will gradually flow through tube 16 and constriction 17 into capillary 12 and the manometer tube 8. Due to the various connections, the gas pressure remains constant throughout the apparatus. When the maximum drop pressure is attained, liquid droplets will begin to fall from the tip of capillary 12. Since we already know the liquid density at the experimental temperature and the capillary radius and can determine the pressure maintained by the metal column by measuring the distance from the tip of capillary 12 to the liquid surface in manometer tube 8, we can calculate the surface tension by means of Cantor's equation. To repeat the measurements, we tilt the apparatus by 90° (from the upside-down position) so that the liquid flows from vessels 8 and 6 back to vessel 2, and tilt it back to the initial (upside down) position before carrying out the next set of measurements.

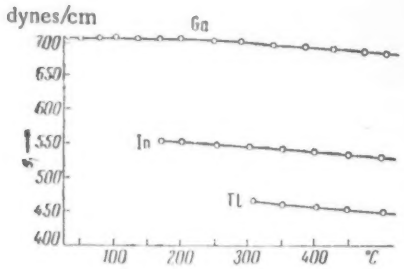

Fig. 2.

Quite frequently it becomes obvious in the course of an experiment that the liquid introduced into the apparatus does not wet glass; in a case like that, to simplify the determination of σ we can always seal off and detach the apparatus from the vacuum system before filling it with inert gas and carry out the measurements by the maximum drop pressure method only under high vacuum, i.e., as in the gravitational apparatus [4]. We encountered this situation in our investigation of the surface tension of thallium.

After we filtered the molten metal in vacuo ($\sim 1 \cdot 10^{-5}$ mm Hg) to remove the oxides and poured it into the apparatus, we found that in the 303-500° temperature range thallium does not wet glass. We were therefore able to seal off the evacuated apparatus and measure the surface tension of liquid thallium in equilibrium with its own vapor pressure (in vacuo) by the maximum drop pressure method.

The densities of molten thallium at the experimental temperatures were taken from Ref. [6] (the density is a variable in the Cantor equation for σ).

In contrast with the results reported by Sauerwald and Schmidt [2], the surface tension of thallium remained constant in our experiments over a period of 7 days. Within the investigated temperature range (310° to 500°) the σ of thallium is a linear function of temperature and can be expressed by the equation

$$\sigma = 464{,}5 - 0{,}080\,(t - 303°). \qquad (1)$$

The parameters in Equation (1) were evaluated by the method of least squares, and the maximum deviation of any experimental point from the straight line given by Eq. (1) was less than 0.2 dynes/cm, i.e. $\approx 0.05\%$.

As one can see in Fig. 2, where we have plotted our results and the corresponding relationships for gallium and indium [7, 8], the surface tension of the gallium subgroup elements decreases with increasing atomic weight; the same was observed in the case of the alkali metal subgroup [9].

The authors would like to acknowledge the help rendered by V. S. Bryushkov and V. A. Murlykov in the course of this work.

LITERATURE CITED

1. A. P. Vyatkin, Zhur. Tekh. Fiz. 27, No. 6 (1957); Izvest. Vysshykh Ucheb. Zaved., Fizika 2, 48 (1959).
2. F. Sauerwald and B. Schmidt, Zs. anorg. u. allgem. Chem. 213, 314 (1933).
3. M. Cantor, Ann. Phys. 47, 399 (1892).
4. P. P. Pugachevich, Zhur. Fiz. Khim. 25, 365 (1951).
5. P. P. Pugachevich and O. A. Timofeevicheva, Doklady Akad. Nauk SSSR 79, 831 (1951).
6. A. Schneider, A. Stauffer, and G. Heimer, Naturwiss. 41, 326 (1954).
7. O. A. Timofeevicheva and P. P. Pugachevich, Doklady Akad. Nauk SSSR 124, 1093 (1959).
8. O. A. Timofeevicheva and P. P. Pugachevich, Doklady Akad. Nauk SSSR 134, 840 (1960).
9. J. W. Taylor, Phil. Mag. 46, 379, 867 (1955).

All abbreviations of periodicals in the above bibliography are letter-by-letter transliterations of the abbreviations as given in the original Russian journal. *Some or all of this periodical literature may well be available in English translation.* A complete list of the cover-to-cover English translations appears at the back of this issue.

AN INVESTIGATION OF THIN BENZENE FILMS ON A MERCURY SURFACE

A. Sheludko and D. Platikanov

Institute of Physical Chemistry, Bulgarian Academy of Sciences
(Presented by Academician A. N. Frumkin, January 3, 1961)
Translated from Doklady Akademii Nauk SSSR, Vol. 138, No. 2,
pp. 415-418, May, 1961
Original article submitted December 21, 1960

A method for investigating bilateral (free) films, with automatic recording of the film thickness in a time function, enabled us to derive wedge pressure isotherms in a series of works [1], during which, since the film was unstable not only in the region where the wedge pressure was negative, other, static methods [2, 3] could not be used for determination of the magnitude of the wedge pressure. In the present work the application of this method to the investigation of liquid films on an extraneous substrate is described; thus, it is an extension of the works of B. V. Deryagin and M. M. Kusakov [2] and A. N. Frumkin [4]. Mercury was chosen as the substrate in view of the homogeneity of its surface. The apparatus did not differ in principle from that used for the investigation of bilateral films (see [1]; the method was described in greater detail in [5]). The main difference consisted of the design of the measuring cell, which allowed the mercury surface to be wetted by the film of liquid. A microscopic film c was formed on the mercury surface by drawing off the liquid through the capillary d (Fig. 1). All the cells were placed in an enclosed space saturated with vapor of the liquid under investigation. The thickness of the thin film was measured interferometrically in reflected monochromatic light. The intensity of the reflected light was recorded as a function of time t, which enabled the curve h = h(t) (h is the film thickness) to be plotted. The intense background caused by the light reflected from the mercury surface was compensated with the aid of a second photoamplifier illuminated from the same source (high-pressure mercury lamp), which was necessary in order to weaken the effect of fluctuations of the latter light.

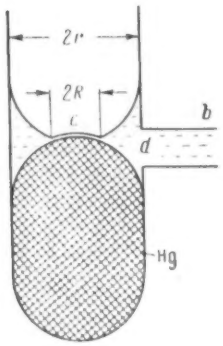

Fig. 1.

It was necessary to calculate the film thickness–time curve from the experimentally produced photocurrent–time curves, as previously [1]. In the case under investigation, because the reflective powers of the two surfaces were different, more complex formulas had to be used:

$$\sin^2\left(\frac{2\pi n_0 h}{\lambda}-\frac{\delta}{2}\right)=\frac{\Delta}{1+\dfrac{4\sqrt{RG}}{(1-\sqrt{RG})^2}(1-\Delta)},$$

$$\Delta=\frac{I-I_{min}}{I_{max}-I_{min}},\quad \operatorname{tg}\delta=\frac{2n_0k}{n_0^2-n^2-k^2},\quad R=\left(\frac{n_0-1}{n_0+1}\right)^2,\quad G=\frac{(n-n_0)^2+k^2}{(n+n_0)^2+k^2}. \qquad (1)$$

Here I is the instantaneous value of the intensity of the light reflected from the thin liquid film; I_{max} and I_{min} are the maximum and minimum values of this intensity; h is the film thickness; λ is the monochromatic light wavelength; n_0 is the refractive index of the liquid; n and k are optical constants of mercury; δ is the phase difference due to reflection from the mercury surface; R is the coefficient of light reflection from the liquid surface; and G is the coefficient of light reflection from the lower surface of the film at the boundary with mercury. It was possible to calculate the magnitude of the phase difference δ by using literature data relating to n_0, n, and k, or else by making use of the value of I in the case when h approached zero on purging the cell with air. According to the agreement between both values, it was possible to test to what extent the mercury surface under the liquid in question remained unaltered and consequently to what degree of reliability it was possible to calculate the film thickness

from the intensity of the reflected light. In this respect, we tried ethyl and propyl alcohols, glycerine, aniline, xylene, toluene, benzene, and aqueous KNO_3 solution (0.1 mole/liter). Unfortunately, in all cases except with benzene a coating appeared on the mercury surface, the reflectivity of which changed. It may be that this was brought about in some cases by impurities in the liquids, or else because the work was carried out in air. With benzene it was easy to get full agreement between the δ magnitudes found by both methods, and also the reproducibility of the measurements was very good; therefore all measurements described below were carried out with benzene.

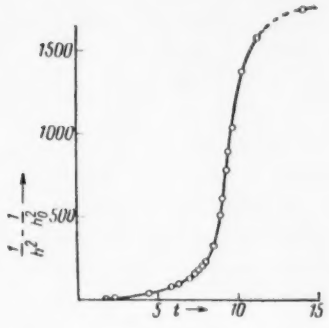

Fig. 2.

The photocurrent–time curves were plotted after the measuring cell had been completely saturated with benzene vapor (with saturation the average rate of thinning of the film was a minimum). The film thickness h for different moments of time was calculated from these data in accordance with formula (1). In Fig. 2 is depicted the relationship found by this means, $(1/h^2)-(1/h_0^2) = f(t-t_0)$, where h_0 is the value of the film thickness at moment t_0 and equalled 1960 A. The following values of the constants were used: λ = 4358 A, n_0 = 1.5235, n = 0.878, and k = 3.36 (the last two values were taken from [6]).

In order to calculate the wedge pressure Π from the relationship $(1/h^2)-(1/h_0^2) = f(t-t_0)$, it was necessary to know the theoretical dependence of $d(1/h^2)/dt$ on the total pressure $P = P_0-\Pi$, causing thinning of the film, and also the capillary pressure P_0. Reynolds' relationship

$$\frac{d(1/h^2)}{dt} = aP, \quad a = \frac{4}{3\eta R^2} \tag{2}$$

(η is the viscosity of the liquid, and R is the radius of the discoid film; see Fig. 1), used by us for bilateral films [7], was inapplicable in the case under examination because a fixed surface tension gradient, ensuring zero rate of tangential flow in the absorption layer, was not developed at the benzene/air boundary (the bilateral foam film always broke instantaneously during attempts to form it from benzene, as we and Ekserov established). Therefore, we calculated the dependence of $d(1/h^2)/dt$ on P for the case when the rate of flow at one surface of the film (benzene/mercury) equalled zero, and at the other (benzene/benzene vapor) the border condition, corresponding to the free surface, was realized, to wit $(\partial v_r/\partial z)_h = 0$ (v_r is the radial flow velocity, z axis perpendicular to the surface), by the method used for bilateral films [8]. As a result, a relationship similar to (2) was obtained, but the value of the coefficient in front of P was four times larger than in (2):

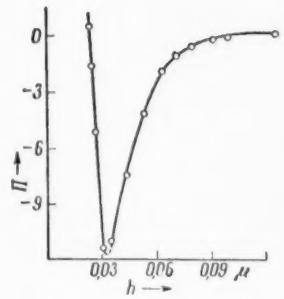

Fig. 3.

$$\frac{d(1/h^2)}{dt} = 4aP. \tag{3}$$

The capillary pressure was calculated in accordance with the formula discovered by B. V. Deryagin and A. E. Titievskaya [3], which we additionally proved [5], to wit

$$P_0 = \frac{4\sigma_1}{r}\frac{\sigma_2}{\sigma_1+\sigma_2}, \tag{4}$$

where σ_1 and σ_2 are the surface tensions at the benzene/vapor and mercury/benzene boundaries and r is the radius of the tube containing the biconcave drops of benzene on mercury, in the center of which the film formed (Fig. 1). By means of graphical differentiation of the relationship $(1/h^2)-(1/h_0^2) = f(t-t_0)$, the relationship $d(1/h^2)/dt = \varphi(h)$ was obtained, and from this with the aid of formulas (3) and (4) the wedge pressure isotherm $\Pi = \Pi(h)$ (Fig. 3) for the benzene film on mercury was calculated. The isotherm ends at the equilibrium film thickness h_e = 240 A when Π = P_0. This value of h_e was reproduced with an accuracy of ± 30 A. The value of the thickness corresponding to the maximum negative wedge pressure and this wedge pressure, i.e. h_{min} = 340 A and Π_{min} = 11,500, were reproduced still better (h_{min} with an accuracy of about ± 10 A). In this isotherm the part corresponding to positive wedge pressures at larger film thicknesses ($h > 10^{-5}$ cm) is unreliable because the values of these pressures are small and

close to the errors of measurement. The theory of I. E. Dzyaloshchiskii, E. M. Lifshits, and L. P. Pitaevskii [9] for the case of a nonmetallic liquid on a metallic substrate for films of large thickness always gives a positive wedge pressure, as is easily calculated, and so confirms our results for this range of thicknesses. In the other limiting case of thin films, this theory concerning a nonmetallic liquid on a metal also gives a positive value for the wedge pressure. Thus, the portions in the regions of small and large film thicknesses of the wedge pressure isotherm which we obtained experimentally for a benzene film on mercury agrees with the theory. The main part of our results, encompassing the sizable negative wedge pressure, evidently corresponds to the transition region between the limiting thick and limiting thin films, and at the present time it cannot be compared with the theory because the latter contains the unknown function $\varepsilon(\xi)$.

We also conducted qualitative observations on films of other liquids on mercury. In all cases (ethyl and propyl alcohols, glycerine, aniline, xylene, toluene, and benzene) except water the films steadily thinned down after their formation until they attained equilibrium thickness, which, for the above-mentioned reasons, we could not easily measure. In films of aqueous solutions of KNO_3 (0.1 mole/liter) spherical "holes", which expanded at different and nonreproducible rates, unexpectedly appeared at a specific film thickness. This phenomenon, evidently occurring as an elementary flotation adherence act, in view of its importance will be specially studied by us.

LITERATURE CITED

1. A. Sheludko, Doklady Akad. Nauk SSSR 123, 1074 (1958); A. Sheludko and D. Ekserova, Kolloid Zs. 165, 148 (1959); 168, 24 (1960); A. Sheludko and D. Ekserova, Doklady Akad. Nauk SSSR 127, 149 (1959); Izvest. Khim. Inst. Bolgar. Akad. Nauk 7, 116 (1959); 7, 105 (1959).
2. B. V. Deryagin and M. M. Kusakov, Izvest. Akad. Nauk SSSR, Ser. Khim. 5, 1119 (1937).
3. B. V. Deryagin and A. E. Titievskaya, Kolloid. Zhur. 15, 416 (1953).
4. A. N. Frumkin, Zhur. Fiz. Khim. 12, 337 (1938).
5. A. Sheludko and D. Platikanov, Kolloid Zs. (in the press).
6. E. Lange, Zs. Physik. 94, 650 (1935).
7. A. Sheludko, Kolloid Zs. 155, 39 (1957).
8. A. Sheludko, G. Desimirov, and K. Nikolov, Ezhegodnik. Sofiisk. Univ., 1954/55, 49, Book 2 (1956) p. 129.
9. I. E. Dzyaloshchinskii, E. M. Lifshits, and L. P. Pitaevskii, Zhur. Éksptl. i Teoret. Fiz. 37, 229 (1959).

All abbreviations of periodicals in the above bibliography are letter-by-letter transliterations of the abbreviations as given in the original Russian journal. *Some or all of this periodical literature may well be available in English translation.* A complete list of the cover-to-cover English translations appears at the back of this issue.

A STUDY OF THE PROPERTIES OF THE SURFACE OF CRYSTALLINE TITANIUM DIOXIDE

L. G. Ganichenko and V. F. Kiselev

M. V. Lomonosov Moscow State University
(Presented by Academician M. M. Dubinin, January 11, 1961)
Translated from Doklady Akademii Nauk SSSR, Vol. 138, No. 3,
pp. 608-611, May, 1961
Original article submitted January 7, 1961

In the large number of studies on adsorption on titanium dioxide, the problems of the nature of the surface have not been the object of special study. The authors of [1, 2] consider that the adsorption centers on a TiO_2 surface are the ions of the lattice, and on this assumption they calculate the energy of the van der Waals interaction between an adsorbed molecule and the ions, which they compare with the experimentally determined heat of adsorption. In an examination of dehydration and dehydrogenation reactions in the presence of TiO_2 as catalyst, the authors of [3] also assumed that the active centers are the O and Ti ions of the surface. However, studies of the irreversible adsorption of water vapor on titanium dioxide [4] indicate that, in addition to physical adsorption of water on the surface, hydration processes are also possible. The presence in titanium dioxide of a small quantity of water which is not removed up to high temperatures is indicated by data [5] for the loss in weight on ignition. In [5], however, the nature of this water was not discovered. Hydration of a surface may lead to a marked change in the nature of the adsorption interactions compared with the case considered in [1, 2] of purely electrostatic and dispersion interactions. No quantitative determinations of the degree of hydration of the surface were carried out in any of the works cited [1-4].

The aim of the present work was to study the degree of hydration of a titanium dioxide surface subjected to treatment at different temperatures. In addition, measurements were made of the adsorption of water vapor. This adsorption, as has already been shown [6], provides a sensitive indication of the state of a surface. The few studies [7-9] of the specific adsorption of water vapor on titanium dioxide were not accompanied by an analysis of the surface of the specimen on which the adsorption measurements were carried out. The material taken for study was the low-temperature modification of titanium dioxide – anatase – obtained by igniting $TiCl_4$. In order to obtain maximum hydration of the surface, the specimen was kept beforehand for a prolonged period in saturated water vapor. The measurements of the adsorption of water vapor and nitrogen were carried out on a volume adsorption apparatus. The specific surface values were determined by the BET method from the low-temperature adsorption of nitrogen. In order to determine the structural water, the water evolved during ignition of the specimen was frozen out, and determinations were made of the pressure of nonfrozen gases and afterward of the total pressure of gas and unfrozen water in the volume apparatus. The results are given in Figs. 1 and 2.

Figure 1c shows that the structural water content per unit surface area of the titanium dioxide evacuated at room temperature is very high. The magnitude of the hydration of the TiO_2 surface approximates to that of a quartz surface (qu-5, degree of hydration 11.5 $\mu M/m^2$ [10]) treated under the same conditions. In the range of ignition temperatures 25-400° the structural water content relative to unit mass of the adsorbent (Fig. 1a) and relative to unit surface area (Fig. 1c) decreases sharply. In this temperature range titanium dioxide loses three times more water than quartz (qu-5). The specific surface increases slightly with increase in the temperature to 460° (Fig. 1b). One of the reasons for this is possibly the exposure of part of the surface as a result of the removal of surface hydrate from surface defects and dislocations. A slight increase in the specific surface at these temperatures has been observed on titanium dioxide films [11]. The adsorption of water vapor on a specimen evacuated at 25° is reversible (Fig. 2). It should be noted that the reproducibility of the original state of the titanium dioxide surface is much lower than that for silica specimens [6] and depends to a marked extent on the duration of the evacuation of the specimen. This also is apparently related to the instability of the surface hydrate of the TiO_2. Figure 2 shows that the reversible isotherm for titanium dioxide is very close to the corresponding isotherm for quartz with almost the same surface hydration [10]. For a high water content on the surface, the differences in the adsorptive powers of the titanium and silicon oxides are smoothed out. The adsorption of water vapor on these surfaces is due chiefly to the formation of hydrogen

bonds between the adsorbed water molecules and the structural water on the surface. The suggestion that the centers of water adsorption on a TiO_2 surface are hydroxide groups has been put forward by a number of authors [4, 11, 12], but no experimental confirmation of their existence or estimation of their quantity has been given. Recently [13] experiments have detected bands for the valence vibrations of OH groups and the deformational vibrations of water in the infrared absorption spectrum recorded for films of TiO_2 heated in the temperature range 25-190°.

The specific values of the primary adsorption in the initial section of the isotherm increase with increase in the temperature of treatment of the specimens from 25 to 260° (Fig. 2). Earlier, in a study of the adsorption of water vapor on titanium dioxide films, the authors of [11] also noted an increase in the adsorptive activity with increase in the temperature of treatment of the specimen. Figure 2 shows that the isotherm for a TiO_2 specimen ignited at 260° is almost three times higher than the corresponding isotherm for K-2 silica gel with practically the same degree of hydration [6]. After the specimens had been kept for two days in saturated water vapor, as in [4], irreversible adsorption was observed. The values of the irreversible adsorption increase with increase in the temperature of treatment of the specimen (150° 6.4 $\mu M/m^2$, 260° 7.75 $\mu M/m^2$). In the temperature range studied, the values of the irreversible adsorption on TiO_2 are more than 5-10 times greater than the corresponding values for crystalline silica [10]. The dehydration and rehydration processes are reversible. Figure 2 shows that the initial sections of the secondary adsorption isotherms for a specimen ignited at 260° show satisfactory agreement with the reversible isotherm for the original specimen. It is interesting to note that rehydration of the surface of specimens dehydrated at the temperatures studied takes place completely even at low vapor pressures. Figure 2 shows that at almost zero pressure the adsorption isotherms for specimens treated at 150 and 260° reach values close to the values of the irreversible adsorption noted above. No appreciable decrease in the rate of adsorption of water vapor was observed in this region of the isotherm, in contrast to the case of the rehydration of ignited silicas, where the process of rehydration at low pressures takes place extremely slowly [14]. The ease with which the surface gives up its water and is rehydrated indicates the absence of any significant rearrangement of the surface lattice in this temperature range.

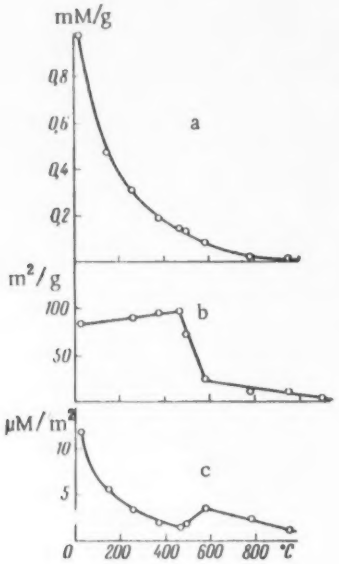

Fig. 1. Dependence of the concentration of structural water in TiO_2, calculated per unit mass (a) and per unit surface area (c), and of the specific surface (b), on the temperature of treatment of the specimen.

The specific surface of the specimen undergoes a sharp decrease with increase in the temperature of ignition above 460°. A marked decrease in the surface area at high temperatures was observed earlier [13, 15]. The authors of [3] attributed this decrease to a phase change taking place in the specimen. It is known that the phase change from the low-temperature modification of TiO_2 – anatase – to the more stable modification – rutile – takes place at high temperatures. The literature [16] gives different values for the temperature of this change (from 825 to 1000°). The authors of [3, 5] note correctly that rearrangement of the lattice to the rutile structure begins on the surface at much lower temperatures*. In the temperature range corresponding to the sharp change in the specific surface by a factor of four (Fig. 1b) the structural water content per g of the specimen decreases slightly (Fig. 1a). The structural water content calculated per unit surface area increases slightly (Fig. 1c). The observed increase in the concentration of structural water on the surface is probably related to rearrangement of the anatase surface to the more compact rutile structure. It should be noted that sharp changes in the catalytic activity and selectivity of catalysis on TiO_2 are observed at the same temperatures [3]. Our experimental results show good agreement with the data given in [3] and confirm the viewpoint held by the authors of [3] regarding the part played by polymorphic changes in the TiO_2 in determining the physicochemical properties of its surface. These data show that surface properties provide a sensitive indication of phase changes taking place in a solid body.

Further dehydration of the surface takes place with increase in the ignition temperature above 600°. At an ignition temperature of 400°, the TiO_2 specimen begins to acquire a marked gray color. At the same time, the dehydration products are found to contain a small quantity (0.2-0.3 $\mu M/m^2$) of a gas which is not frozen out in a liquid

*In a study of the phase conversion of γ-Al_2O_3 to α-Al_2O_3, it was shown that the change begins at much lower temperatures on the surface than in the bulk [17].

nitrogen trap. It has been shown in earlier studies [15, 18] that evolution of oxygen takes place when TiO_2 is ignited and, conversely, that oxygen can be absorbed by the specimen at high temperatures. The authors of [15] assume that at high temperatures the oxygen is evolved as a result of the conversion of TiO_2 to titanium monoxide TiO. Chemical analysis of our specimens ignited at 1100° showed the presence of approximately 0.3% of trivalent titanium—in contrast to the case described in [15], no divalent titanium ions were detected. Measurements of the magnetic properties [19] have shown that during the reduction of TiO_2 a fairly high concentration of Ti^{3+} ions is produced on the surface. These Ti^{3+} ions are present in the natural mineral anosovite [20, 21].

At the present time it is difficult to give a complete interpretation of the nature of the water evolved from titanium dioxide during its ignition. The authors of [5] describe the water present in titanium dioxide as "osmotically" combined water. The dissolution of water in the compact anatase lattice appears unlikely, however. No crystal hydrate forms are known in the anatase—rutile series. It is more probable that the water evolved from the TiO_2 comes from the surface. This is indicated by the fact that the kinetics of water absorption are not retarded, although a retardation is observed when vapor diffuses inside the lattice of a solid body. The Ti atoms in the TiO_2 structure have a coordination number of 6. On the surface, the coordination sphere of the titanium—oxygen octahedra will be unsaturated. According to [22], the optimum screening of Ti ions can be brought about, in particular, both by saturation with hydroxide groups combined by valence forces and also by water molecules, as takes place in the case of the oxides SiO_2 and Al_2O_3 [10, 17]. With increase in temperature during the ignition of a specimen, the coordination water will be removed first. With further increase in the temperature, when the surface begins to undergo the phase change, accompanied by deformation and then by rearrangement of the anatase lattice [3], the hydroxide groups more firmly bound to the surface will also be removed. In the high-temperature range, decrease in the degree of hydration of the surface may also, to some extent, be brought about by a change in the valence of the Ti^{4+} ion. The presence of structural water on the surface up to temperatures at which catalytic processes take place must be taken into account in the examination of the elementary catalytic process. It is possible that, together with the catalytic reaction schemes considered in [3] for the decomposition of alcohol on the surface atoms of oxygen and titanium, the dehydration of the alcohol may also take place by the formation of surface esters by reaction between the alcohol molecules and the hydroxide groups of the surface, as takes place, for example, in the dehydration of alcohols on aluminosilicates [23]. Ester compounds of Ti are well known. In the theoretical calculations of the energy of the adsorption interactions, which the authors of [1, 2] compared with the values of the heats of adsorption measured on the specimens (treated at comparatively high temperatures), no allowance was made for hydration processes taking place on the surface or for changes in the valence of part of the Ti^{4+} ions. It should be noted that it is hardly possible to consider the adsorption energy strictly as local interactions of the adsorbed molecule and the ions of the TiO_2 lattice. In the case of TiO_2, which is a semiconductor [18], it is necessary to consider the adsorbed molecules and the lattice of the adsorbent as a single quantum-mechanical system [24].

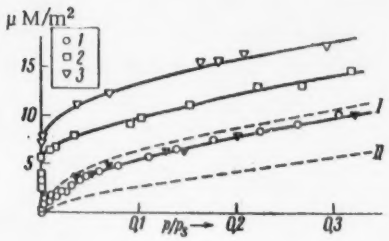

Fig. 2. Specific isotherms for the primary adsorption on TiO_2 specimens evacuated at 25° (1), 150° (2), and 260° (3), qu-5 quartz at 25° (I) and K-2 silica gel at 25° (II) [10]. The solid symbols correspond to the secondary adsorption.

The authors wish to express their sincere thanks to S. G. Moinov for providing and analyzing the specimens.

LITERATURE CITED

1. F. H. Healey, J. J. Chessick, et al., J. Phys. Chem. 58, 887 (1954).
2. J. J. Chessick, A. C. Zettlemoyer, et al., Canad. J. Chem. 33, 251 (1955).
3. A. M. Rubinshtein and S. G. Kulikov, Izvest. Akad. Nauk SSSR, Otdel Khim. Nauk, No. 1, 84 (1950); No. 2, 133 (1951).
4. K. S. Rao, J. Phys. Chem. 45, 500 (1941).
5. G. F. Hüttig and K. Kosterhon, Kolloid Zs. 89, 202 (1939).
6. M. M. Egorov, T. S. Egorova, K. G. Krasil'nikov, and V. F. Kiselev, Zhur. Fiz. Khim. 32, 2624 (1958).
7. H. K. Livingston, J. Am. Chem. Soc. 66, 569 (1944).
8. G. Yura and W. D. Harkins, J. Am. Chem. Soc. 66, 1356 (1944).

9. E. H. Loeser and W. D. Harkins, J. Phys. Chem. 57, 591 (1953).
10. L. G. Ganichenko, M. M. Egorov, V. F. Kiselev, K. G. Krasil'nikov, and G. S. Khodakov, Doklady Akad. Nauk SSSR 131, 597 (1960).
11. D. P. Dobychin and Yu. N. Andreev, Zhur. Fiz. Khim. 28, 22 (1954).
12. S. P. Zhdanov and Yu. N. Andreev, Trudy Gos. Optich. Inst. 24 (145), 210 (1956).
13. Yu. N. Andreev, Zhur. Fiz. Khim. 33, 2295 (1959).
14. S. P. Zhdanov, Surface Chemical Compounds and Their Role in Adsorption Phenomena [in Russian] (Moscow, 1957) p. 129.
15. A. W. Czanderna and J. M. Honig, J. Phys. Chem. 63, 620 (1959).
16. A. V. Pamfilov and E. G. Ivancheva, Zhur. Obshch. Khim. 7, 2774 (1937); 10, 154 (1940).
17. M. M. Egorov, V. F. Kiselev, K. G. Krasil'nikov, and Yu. P. Simanov, Izvest. Vysshykh Ucheb. Zaved., Khimiya 2, 360 (1959).
18. L. H. Reyerson and J. M. Honig, J. Am. Chem. Soc. 75, 3917 (1953).
19. T. J. Gray, C. C. McCain, and N. G. Masse, J. Phys. Chem. 63, 472 (1959).
20. A. A. Rusakov and G. S. Zhdanov, Doklady Akad. Nauk SSSR 77, 411 (1951).
21. N. E. Filonenko, V. I. Kudryavtsev, and I. V. Lavrov, Doklady Akad. Nauk SSSR 86, 561 (1952).
22. W. A. Weyl and E. S. Marboe, Some Mechanical Properties of Glasses and Crystals as Affected by Changes in Chemical Binding Forces (Munich, 1959).
23. K. V. Topchieva, K. Yung-P'in, and I. V. Smirnova, Surface Chemical Compounds and Their Role in Adsorption Phenomena [in Russian] (Moscow, 1957) p. 311.
24. F. F. Vol'kenshtein, The Electronic Theory of Catalysis on Semiconductors [in Russian] (Moscow, 1960).

All abbreviations of periodicals in the above bibliography are letter-by-letter transliterations of the abbreviations as given in the original Russian journal. *Some or all of this periodical literature may well be available in English translation.* A complete list of the cover-to-cover English translations appears at the back of this issue.

THE HYPERFINE STRUCTURE OF THE ELECTRON PARAMAGNETIC RESONANCE LINE IN AQUEOUS SOLUTIONS OF V^{2+} SALTS

N. S. Garif'yanov

Physicotechnical Institute, Kazan Branch of the Academy of Sciences, USSR
(Presented by Academician A. E. Arbuzov, January 19, 1961)
Translated from Doklady Akademii Nauk SSSR, Vol. 138, No. 3,
pp. 612-613, May, 1961
Original article submitted January 17, 1961

The hyperfine structure (hfs) of the electron paramagnetic resonance (epr) line of salts of paramagnetic ions of the iron group elements in liquid solutions under strong fields has been investigated only for Mn^{2+}, VO^{2+}, and Cu^{2+} [1-8]. Hyperfine structure was not obtained for other paramagnetic ions of this group in liquid solutions either because of the large epr line width (Co^{2+}, V^{3+}) or because of the smallness of the nuclear magnetic moments.

Our investigations of the epr of violet solutions of VCl_2 were carried out with the 9598 Mc frequency in the temperature range 295-400° K. Water, alcohol, and glycerine were employed as solvents. The solution under examination was sealed by means of a special heating device into a glass barometric tube, which was then placed at the antinode of the magnetic lines of force of a rectangular H_{103} resonator. The method of making these measurements was described in reference [9]. In aqueous VCl_2 solutions of concentrations from 0.5-0.05 M at room temperature a single epr line of width $\Delta H = 800$ oe with a spectroscopic splitting factor $g = 1.96 \pm 0.01$ was observed. The width of this line was determined by the unresolved hfs.

With a rise of the solution temperature up to 400° K there were detected 8 peaks with nearly isotropic hfs corresponding to a nuclear spin $I = {}^7/_2$ V^{51}. The shape of the hfs spectra at 400° K was practically unchanged over the concentration range 0.5-0.05 M. As seen from Fig. 1, the spectrum of the hfs is incompletely resolved.

It may be noted that heating the VCl_2 solutions does not cause strong oxidation since with repeated rise or fall of the temperature the corresponding intensity of the epr lines remains practically unchanged.

A graphical analysis of the spectra showed that the width of the ΔH component of the hfs lines of the absorption of 0.05 M VCl_2 in water with T = 400° K was ~100 oe. At room temperature the width of the unresolved components of the hfs must be ~300 oe. The position of the 8 resonance lines of the hfs can be described by the expression

$$H^{*} = H_0 - Am - \frac{A}{2H_0}[I(I+1) - m^2] - \frac{A^2 m}{2H_0}(2M - 1); \qquad (1)$$

where H^{*} is the resonance value of the static magnetic field H, A is the hyperfine splitting constant, m and M are the magnetic quantum numbers of the nucleus and of the electronic shell of the ion under study, respectively, and $H_0 = h\nu/g\beta$; good agreement with the experiment was obtained with the values A = 96 oe and $g = 1.965 \pm 0.002$. Equation (1) follows from the general theory of paramagnetic resonance line structure with the assumption that fine resolutions of the lines due to the action of local electric fields were absent or very small in comparison with the hyperfine splitting.

In some solid solutions of V^{2+} salts, possessing the fundamental state $^4F_{3/2}$, the fine splitting constant was greater than or equal to the constant A. In these solid solutions the g-factor was isotropic.

In 0.05 M aqueous solutions of VCl_2 the width ΔH of the hfs components of the epr lines was almost an order greater in comparison with the ΔH components of the hfs in aqueous solutions of Mn^{2+} and VO^{2+} at the corresponding concentrations. Therefore it may be concluded that for violet aqueous solutions of VCl_2 the width of the hfs components is determined in the main by the fine splitting. This conclusion also explained the absence of concentration dependence of the width of the ΔH component of the hfs of the epr lines for VCl_2 solutions. We have assumed that

the electric field on the V^{2+} ion in violet aqueous solutions of VCl_2 is mainly of cubic symmetry with a small admixture of fields of axial symmetry which are set up to some extent by the distorted octahedron of the water, owing to the Jahn-Teller effect. These moving electric fields are not completely neutralized. Additionally there is also superimposed on the V^{2+} ion a small admixture of fields of lower symmetry due to the influence of particles of the second coordination sphere. According to the increase of the solution temperature this crystal field of low symmetry on the V^{2+} ion is neutralized by movement and the epr line is narrowed.

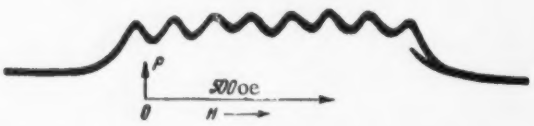

Spectrum showing hfs of epr line of an aqueous 0.05 0.005 M VCl_2 solution; ν = 9598 Mc, T = 400°K.

In alcohol and glycerine solutions of VCl_2 in the temperature range T = 295-400° K the epr line was not detected. Such a large width of these lines in the organic solvents mentioned is explained by the presence of a strong axial component of the crystal field, which is due to the ionic molecules [9, 10].

An epr line with ΔH = 1000 oe was detected in these organic solvents when supercooled [11, 12].

Finally, it may be noted that the constant A in aqueous VCl_2 solutions has the same value as that in solid V^{2+} salt solutions [13] and is 22 oe less than A in aqueous $VOCl_2$ solutions [14].

In conclusion, the author expresses thanks to B. M. Kozyrev for a discussion of the results and N. F. Usacheva for help with the experiments.

LITERATURE CITED

1. T. S. England and E. E. Schneider, Physica 17, 221 (1951).
2. M. Tinkham, R. Weinstein, and A. F. Kip, Phys. Rev. 84, 848 (1951).
3. M. A. Garstens and S. H. Libson, J. Chem. Phys. 20, 1677 (1952).
4. N. S. Garif'yanov and B. M. Kozyrev, Doklady Akad. Nauk SSSR 98, 929 (1954).
5. N. S. Garif'yanov and B. M. Kozyrev, Uch. zap. Kazansk. gos. univ. im Lenina 114, 83 (1954).
6. B. M. Kozyrev, Doctoral Dissertation [in Russian] (FIAN, 1957).
7. S. R. McGarvey, J. Phys. Chem. 60, 71 (1956).
8. A. I. Rivkind, Doklady Akad. Nauk SSSR 135, 65 (1960).
9. V. I. Avvakumov, S. N. Garif'yanov, B. M. Kozyrev, and P. G. Tishkov, Zhur. Éksp. i Teor. Fiz. 37, 1564 (1959).
10. V. I. Avvakumov, N. S. Garif'yanov, and E. I. Semenova, Zhur. Éksp. i Teor. Fiz. 39, 1215 (1960).
11. N. S. Garif'yanov, Doklady Akad. Nauk SSSR 103, 41 (1955).
12. N. S. Garif'yanov, Doklady Akad. Nauk SSSR 109, 725 (1956).
13. B. Bleaney, D. J. E. Ingram, and H. D. E. Scovil, Proc. Phys. Soc. A 64, 39 (1951).
14. R. N. Rogers and G. E. Pake, J. Chem. Phys. 33, 1107 (1960).

All abbreviations of periodicals in the above bibliography are letter-by-letter transliterations of the abbreviations as given in the original Russian journal. *Some or all of this periodical literature may well be available in English translation.* A complete list of the cover-to-cover English translations appears at the back of this issue.

THE RELATION BETWEEN THE MECHANICAL PROPERTIES OF CRYSTALLINE POLYMERS AND THEIR SUPERMOLECULAR STRUCTURES

A. V. Ermolina, L. A. Igonin, L. A. Nozova,

I. I. Farberova, and K. N. Vlasova

Scientific Research Institute for Plastics

(Presented by Academician V. A. Kargin, January 6, 1961)
Translated from Doklady Akademii Nauk SSSR, Vol. 138, No. 3,
pp. 614-615, May, 1961
Original article submitted December 15, 1960

Structural, mainly electron microscopic, investigations in recent years [1-7] have shown that polymers are not a chaotically entangled system of molecular chains but a highly ordered system of small bundles. Side by side with the bundles in a number of crystalline polymers, part of the substance is present in a globular state. The polymer bundles, being independent structural units, are able to form more highly ordered morphological forms.

It is obvious that the macroscopic properties of polymeric materials are closely linked not so much with the relative proportion of ordered and disordered material but with how much formation and development of one or the other secondary structures there is in the polymer. Formation of a molecular bundle with a definite regularity of the chains, the appearance of lamellar forms, and other supermolecular structures are important factors determining largely the macroscopic, partly the mechanical, properties of the polymers.

We have examined, for example, the polyamide resin 68 by comparing some of its structural and mechanical properties in order to clarify the relative roles of local regularity of the segments ("degree of crystallinity") and of secondary supermolecular structures in determining the macroscopic properties of polymers. For the investigation we used the commercial polyamide resin 68 (polyhexamethylene sebacamide), which is widely employed in technical practice, especially for making slide bearings, and which wears well in service. Test samples in the form of blocks 4 × 6 × 55 mm were cast under pressure in the LM-3 die casting machine by normal foundry procedure and then subjected to thermal treatment in inert media (silicone oils) at different temperatures and times of exposure. For each set of samples a determination was made of the changes both of the "degree of crystallinity" and of the spherulitic structure of the polyamide.

The "degree of crystallinity" was determined in the usual way, from the integrated intensities of the most characteristic interferences on the intensity curve of the material examined. We recorded the intensity curves for the angle of scatter of x rays on the URS-50-I x-ray diffractometer using filtered copper radiation. We derived the spherulitic structure of the polyamide by photomicrographing the surfaces of the sample, which were first polished and then etched with tricresol. Photomicrographs of the surfaces of the samples were obtained by means of the MIM-8 metallographic microscope with 1000 × magnification.

At the same time each set of samples was examined for wear resistance, which was determined as the value of reciprocal wear (the wear was estimated from the loss in volume through abrasion), according to the scale on a Grasselli type testing machine.

As the technological thermal treatment procedures, the temperatures of 150 and 190° C and different periods of heating of 15 min to 30 hours for each temperature were chosen. As a result of the heating, we observed a transition of the original sample from one form, characterized by hexagonal cells, into another, a triclinic form, well known and described in the literature [8, 9]. The structure with triclinic cells was already developed after 15 minutes heating. Further thermal treatment brought about progressive development of the x-ray picture characterized by marked growth of the (100) and (010) intensities and, thus, also of the "degree of crystallinity." At the same time, the interesting observation was made that for longer periods of heating there appeared again between the (100) and

(010) reflections of the triclinic cell an interference characteristic for a hexagonal cell. After 8 hours heating at 190° and 12 hours at 150° the increase of crystallinity ceased, and perceptible change in the structure, according to the x-ray results, was not observed up to 30 hours thermal treatment.

It was established that the spherulite structure of the polyamide was more sensitive to changes in the thermal treatment procedures than the "degree of crystallinity." For short periods of heating appreciable growth of the size of the spherulites (from 1 to 5 μ) was observed, individual formations were considerably larger. After 8 hours heating at 190° and 10 hours at 150° a gradual breakdown of the spherulitic structure began, and the surface of the samples after 30 hours thermal treatment did not give pictures typical for spherulite formations.

Comparison of the structural data with the results of the tests of the polyamide for durability showed that there was no definite correlation between the "degree of crystallinity" and the wear resistance of the plastic. Thus, for example, samples with the same "degree of crystallinity" but treated under different conditions of temperature did not have the same wear resistance. For samples for which the values of the "degree of crystallinity" did not change on lengthy thermal treatment, an appreciable reduction of the wear resistance, depending on the period of heating, was observed.

The preliminary investigations showed that the greatest resistance to wear was possessed by samples the spherulitic formations of which were characterized by uniform dimensions in the 2-3 μ range. Thus, the uniformity of size and fine structure of the supermolecular formations play an essential part for the durability of the polyamide. Therefore, the study of the relation between the mechanical properties and the structure of crystalline polymers has its principal value in clarification of the role of secondary supermolecular formations in molding these properties.

The authors express their best thanks to Academician V. A. Kargin for a discussion of the results and also to S. B. Ratner for assistance in the work.

LITERATURE CITED

1. V. A. Kargin, N. F. Bakeev, and Kh. Vergin, Doklady Akad. Nauk SSSR 122, 97 (1958).
2. V. A. Kargin and T. A. Koretskaya, Vysokomolek soed. 1, 1721 (1959).
3. V. A. Kargin and N. F. Bakeev, Kolloid Zhurn. 19, 133 (1957).
4. P. V. Kozlov, Li Pan-Tun, and N. F. Bakeev, Vysokomolek soed. 1, 1848 (1959).
5. P. V. Kozlov, M. M. Iovleva, and Li Pan-Tun, Vysokomolek soed. 2, 284 (1960).
6. P. V. Kozlov, N. F. Bakeev, Li Pan-Tun, and A. S. Kaftanova, Vysokomolek soed. 2, 421 (1960).
7. A. Keller, Proceedings of the International Conference of Crystal Growth (New York, 1958); Khimiya i Tekhnologiya Polimerov, No. 7, 3 (1959).
8. I. Sandeman and A. Keller, J. Polym. Sci. 19, 401 (1956).
9. G. Bunn and E. Garner, Proc. Roy. Soc. London A 189, 39 (1947).

All abbreviations of periodicals in the above bibliography are letter-by-letter transliterations of the abbreviations as given in the original Russian journal. ***Some or all of this periodical literature may well be available in English translation.*** **A complete list of the cover-to-cover English translations appears at the back of this issue.**

THE STRUCTURE OF THE SURFACE COMPOUNDS FORMED BY CARBON MONOXIDE ON PALLADIUM FROM ADSORPTION MEASUREMENTS AND INFRARED SPECTRAL DATA

N. N. Kavtaradze and V. I. Lygin

Physical Chemistry Institute, Academy of Sciences, USSR
(Presented by Academician V. I. Spitsyn, December 30, 1960)
Translated from Doklady Akademii Nauk SSSR, Vol. 138, No. 3,
pp. 616-618, May, 1961
Original article submitted December 28, 1960

The adsorption of CO has been studied at temperatures from −195° to 100° and pressures from 10^{-6} to $2\text{-}4 \cdot 10^{-2}$ mm Hg on layers of palladium condensed at $1\text{-}2 \cdot 10^{-7}$ mm Hg and on palladium deposited on an aerosil. The construction of the apparatus used, the method of preparing the layers, and the measurement of the pressure and adsorption have been described earlier [1]. The specimens for the spectral study were prepared by soaking the aerosil with an aqueous solution of $PdCl_2 \cdot 2H_2O$ [2]. Weighed specimens of 150 mg of the aerosil powder were then compressed to form discs of diameter 28 mm under a pressure of 50 kg/mm^2. The discs were placed in a special vacuum cell [3], evacuated at 300° to 10^{-5} mm Hg, and reduced at 300° in an atmosphere of hydrogen at a pressure of 100 mm Hg. The final purification of the palladium surface was carried out by treating the specimen at 300° and a pressure of 10^{-5} mm Hg for 5 hours. The transmission of discs with composition 10% Pd and 90% SiO_2 in the 2000 cm^{-1} range amounted to 10%.

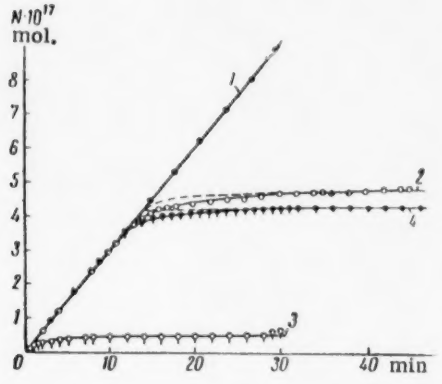

Fig. 1. The adsorption of CO at −195° on a layer of Pd of thickness 1160 A: 1) Accumulation in an empty reaction vessel; 2) total adsorption; 3) reversible adsorption; 4) strong adsorption.

X-ray diffraction studies showed that the palladium prepared in this way is distributed in the aerosil in the form of crystals with the normal face-centered cubic lattice, the average crystal dimensions being 140 A. The spectra were recorded at 25° on an IKS-12 single-beam infrared spectrometer with NaCl prism.

Study of the adsorption of CO on Pd showed that the qualitative features are similar to those characteristic of the adsorption of hydrogen on Cr, Fe, Ni, and Pd [1]. Even at −195° carbon monoxide is adsorbed extremely rapidly and the rate of adsorption is difficult to measure (Fig. 1). Adsorption of more than 90% of the total quantity of carbon monoxide adsorbed in the experiment takes place in the first minute after the introduction of the gas. The adsorption is complete in 15-20 minutes. At higher temperatures the rate of adsorption is even higher.

The total adsorption at the temperatures studied is made up of a strong irreversible adsorption and a weak reversible adsorption. The strong adsorption takes place rapidly and the reversible adsorption almost instantaneously. The strong adsorption of CO decreases with increase in temperature, while the reversible adsorption increases with increase in temperature and pressure. The fact that the weak adsorption takes place instantaneously and is completely reversible at all temperatures enables us to regard it as a function of pressure. The initial section of the isotherms for the weak adsorption follows the logarithmic relationship found by A. N. Frumkin and A. N. Shlygin [4], and the final section follows the Langmuir equation. On the whole (Fig. 2), the total adsorption is practically independent of the sequence of temperature changes since the adsorption curves on going from low (−195°) to high temperatures (100°) and back to low show good reproducibility. These facts indicate that the adsorption reaches equilibrium.

We estimated the proportions of strong and weak adsorption (its saturation limit was calculated by the method of linear anamorphoses of the Langmuir equation). The proportions of strong and weak adsorption (from the saturation limit), respectively, in the total adsorption had the values 92 and 8% at −78°, 84 and 16% at 0°, and 75 and 25% at 50°. In [5] it was found that the weak adsorption amounts to 5% at 0° and a pressure of 10^{-2} mm Hg.

The adsorption of CO on palladium deposited on an aerosil retains all the features of the adsorption of the gas on condensed layers of the metal. In this case also there is equilibrium coexistence of strong adsorption and weak reversible adsorption, with increase in the reversible adsorption and decrease in the strong adsorption with increase in temperature. The reversible adsorption at 25° and a pressure of $2 \cdot 10^{-2}$ mm Hg is approximately 10%. The fact that adsorption of carbon monoxide on palladium takes place above the critical temperature of the gas (−140.2°) and the existence of both strong and reversible types of adsorption throughout the whole range of temperatures studied indicate that the adsorption is chemical in character. The existence of two types of chemisorption—strong and weak—indicates that the chemisorbed molecules may exist in at least two forms. In order to study these forms we used the method of infrared spectroscopy, which was first applied to the study of surface compounds on metals by Terenin [6] and was subsequently used by Eischens [7, 9] and Gryaznov [8].

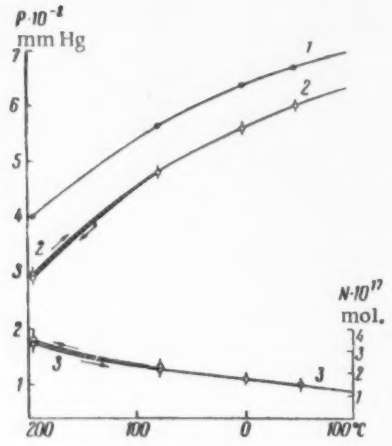

Fig. 2. The adsorption of CO (for a constant quantity of CO in the system) by a layer of Pd of thickness 510 A: 1) Calibration curve giving the change in the CO pressure in the reaction vessel; 2) the change in CO pressure in the presence of a layer of Pd; 3) the adsorption of CO on Pd.

The spectrum of the compounds formed by carbon monoxide on a palladium surface at high pressures (Fig. 3, 1) shows bands at 2085 and 1990 cm^{-1}. Evacuation of the specimen to a pressure of 10^{-4} mm Hg decreases the intensity of the bands and the spectrum shows bands with maxima at 2085 and 1960 cm^{-1} (Fig. 3, 2). Absorption bands in this region, due to the firmly chemisorbed CO molecules, were observed by Eischens [7, 9], and on the basis of a comparison of the spectrum of the surface compounds formed by the CO with the spectrum of carbonyls of known structure these bands were ascribed to two different forms of bond between the CO molecules and the surface atoms of the Pd. It may be assumed that the 2085 cm^{-1} band belongs to the valence vibrations of a CO group combined with one surface Pd atom, the so-called linear structure, and the 1960 cm^{-1} band to the valence vibrations of a CO group combined with two surface Pd atoms, the so-called bridge structure. The ratio of the band intensities on the spectrograms (Fig. 3, 4, 1) indicates that the surface compounds on the palladium exist predominantly as the bridge forms. The change in the spectrum (Fig. 3, 1, 2) when the specimen is evacuated to a pressure of 10^{-4} mm Hg indicates the removal, for the most part, of the linear forms (decrease in the intensity of the 2085 cm^{-1} band) and of part of the CO molecules of the bridge form more weakly combined with the surface (decrease in the intensity and displacement of the 1960 cm^{-1} band). It is not possible to detect a separate absorption band for the reversibly sorbed molecules, apparently due to the low magnitude of the reversible adsorption at the temperatures and pressures studied and possibly also as a result of the weak localization of the reversibly adsorbed molecules on the Pd surface atoms.

The introduction of oxygen at a pressure of 8 mm Hg and 25° brings about practically no change in the spectrum of the surface compounds formed by the CO. This indicates the existence of an induction period in the oxidation reaction [5]. Treatment of the CO surface compounds with oxygen at 200° accelerates this process (Fig. 3, 4). At the same time, the spectrum still shows absorption bands of low intensity at 1995 and 2120 cm^{-1}, which can be attributed to CO compounds remaining on the surface and excited by the chemisorbed O_2.

The reaction of the surface CO groups with hydrogen takes place more slowly (Fig. 4). As a result of the reaction, there is a decrease in the intensity of the absorption bands of the linear and bridge structures and a displacement of these bands toward longer wavelengths: the band for the bridge forms is displaced to 1940 cm^{-1} (Fig. 4, 3). The displacement in opposite directions of the absorption bands for the CO surface compounds in the reactions with oxygen and hydrogen is observed on other metals [7] and is due to a change in the electronic state of the metal surface as a result of the difference in the electron-acceptor properties of the O_2 and H_2 adsorbed on the surface during the reaction.

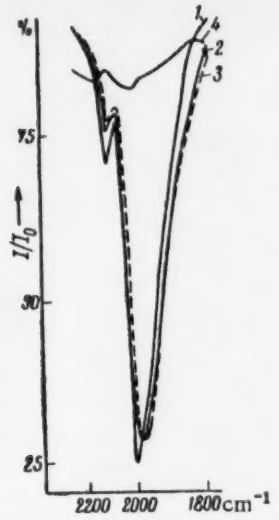

Fig. 3. Spectrum of the compounds formed by carbon monoxide on the palladium surface: 1) At a CO pressure of 1.5 mm Hg; 2) after evacuation to a pressure of 10^{-4} mm Hg; 3) in the presence of O_2 at a pressure of 8 mm Hg; 4) after treatment with O_2 at a pressure of 8 mm Hg and 200° for 5 min.

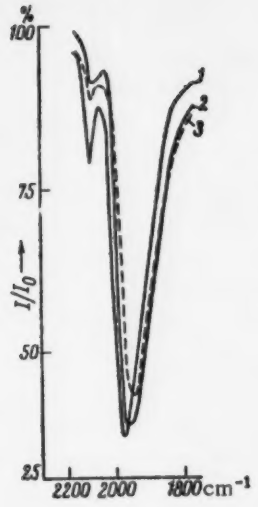

Fig. 4. Spectrum of the compounds formed by carbon monoxide on a palladium surface: 1) After evacuation to 10^{-4} mm Hg; 2) after treatment with H_2 at a pressure of 1 mm Hg and 200° for 15 min; 3) after treatment for 30 min.

Thus, the adsorption data enable us to distinguish between two forms of adsorption on the surface: a weak reversible form and a strong irreversible form. The infrared spectra indicate that the strongly adsorbed carbon monoxide molecules are present chiefly in the form of bridge structures.

LITERATURE CITED

1. N. N. Kavtaradze, Doklady Akad. Nauk SSSR 114, No. 4, 822 (1957).
2. V. I. Lygin, N. N. Kavtaradze, and E. G. Boreskova, Zhur. Fiz. Khim. 35, No. 4 (1961).
3. N. N. Kavtaradze and V. I. Lygin, Zhur. Fiz. Khim. 34, 462 (1960).
4. A. N. Frumkin and A. N. Shlygin, Doklady Akad. Nauk SSSR 2, 176 (1934).
5. S. J. Stephens, J. Phys. Chem. 63, 188 (1959).
6. A. N. Terenin, Zhur. Fiz. Khim. 14, 1362 (1940).
7. R. P. Eischens and W. A. Pliskin, Advances in Catalysis 10, 1 (1958).
8. V. M. Gryaznov, V. D. Yagodovskii, A. M. Bogomol'nyi, and Huo Tiu Ok, Doklady Akad. Nauk SSSR 121, 499 (1958).
9. R. P. Eischens, S. A. Francis, and W. A. Pliskin, J. Phys. Chem. 60, 194 (1958).

All abbreviations of periodicals in the above bibliography are letter-by-letter transliterations of the abbreviations as given in the original Russian journal. *Some or all of this periodical literature may well be available in English translation.* A complete list of the cover-to-cover English translations appears at the back of this issue.

POLYMERIZATION OF NITROETHYLENE WITH γ-RADIATION

V. N. Sokolov, I. Ya. Poddubnyi, V. V. Perekalin,

and V. F. Evdokimov

(Presented by Academician N. N. Semenov, December 20, 1960)
Translated from Doklady Akademii Nauk SSSR, Vol. 138, No. 3,
pp. 619-620, May, 1961
Original article submitted December 17, 1960

Unsaturated nitro compounds are interesting as there is the possibility of converting them to polymeric materials that are resistant to the action of various solvents and have a satisfactory thermostability. The polymerization of the simplest nitroalkene, nitroethylene, under the action of water [1, 8], aqueous solutions of alkali and alkaline earth metal carbonates [2, 3], and inorganic and organic bases, which proceeds by an ionic mechanism [4], forms a powdery, low-molecular polymer (mol. weight up to 2000). Some physical properties of this polymer (heat of explosion, sensitivity to impact, and energy of explosion) have been studied [8].

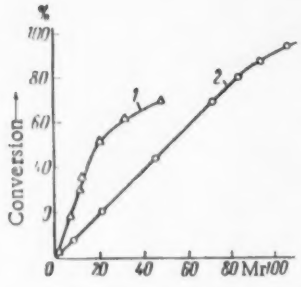

Fig. 1.

Polymerization in solvents that dissolve both nitroethylene and its polymer (N, N-dimethylformamide and tetrahydrofuran) yielded high-molecular products [5], which, however, consisted of a powdery polymer.

The literature data presented show that the polymerization of nitroethylene in the presence of an initiator in a solvent yields powdery products that are contaminated by the initiator and the solvent. In polymerization by ionizing radiation, the purity of the polymer is known to correspond to the purity of the starting monomer. In addition, radiation polymerization is readily effected in the absence of a solvent, as the polymerization rate may be controlled accurately by changing the radiation intensity.

In this connection, we undertook to determine the possibility of and find conditions for the preparation of high-molecular polynitroethylene by block polymerization with γ-radiation.

The radiation source was Co^{60}. The construction of the radiation apparatus used in the present work was described by Breger et al. [9]. The activity of the source equaled 1450 g-equiv. Ra and provided a dose strength of 0.28 to 0.72 million r per hr. The nitroethylene for the polymerization was obtained by dehydration of 1-nitroethanol-2 with phthalic anhydride [6, 7]. The monomer was fractionated repeatedly and fractions with b.p. 36°/100 mm were collected. The glass ampoules were first flushed with hot nitrogen, weighed, and filled with freshly distilled nitroethylene. The normal operations of freezing and melting were carried out to remove occluded atmospheric oxygen. The ampoules were sealed under vacuum and placed in the working chamber of the radiation apparatus. Irradiation was carried out at 20°. After irradiation, the ampoules were opened and the monomer removed in vacuum. The polymer yield was determined by weighing.

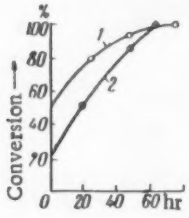

Fig. 2.

Figure 1 shows the relation of the degree of monomer conversion to the integral radiation doese at dose strengths of 0.28 (1) and 0.49 (2) Mr/hr.

In the initial irradiation period ($1 \cdot 10^6$ r) the clear monomer became turbid, and a white precipitate then formed ($5 \cdot 10^6$ r), which was identical with the polymer obtained by the action of organic bases [4].

With further irradiation, the pasty mass of polymer and monomer formed was converted into a clear, pale-yellow block polymer. The formation of the block polymer was apparently connected with secondary reactions, namely the addition of growing polymer chains to previously formed polymer with an increase in its molecular weight. It is interesting to note that the formation of block poly-

nitroethylene did not occur at dose stengths > 0.3 Mr/hr. In this case the polymer remained powdery right up to 100% conversion and its color changed from white to light brown. It should be noted that the formation of clear block polynitroethylene is an extremely complex physichochemical process, depending on many factors, and therefore a partly powdery polymer was sometimes formed at 100% conversion.

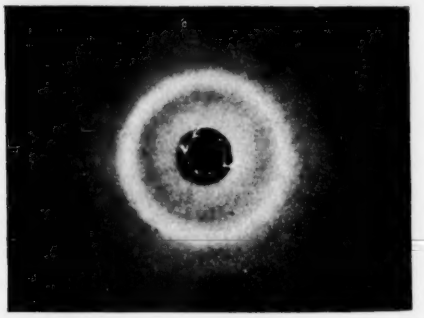

Fig. 3.

It was established that partly polymerized samples of nitroethylene continued to polymerize when irradiation had been stopped. This led to the conclusion that comparatively long-lived polymer radicals were formed under the action of γ-radiation.

The nature of the postirradiation polymerization with initial conversions of 50% (1) and 20% (2) is shown in Fig. 2.

Block polynitroethylene was also formed by postirradiation polymerization.

The polymerization of nitroethylene by γ-radiation was inhibited by hydroquinone and oxygen, which also indicates its radical nature. The radiation polynitroethylene obtained was insoluble in the usual solvents but dissolved readily in N,N-dimethylformamide; its characteristic viscosity in this solvent equaled 0.38, which corresponds to a molecular weight of 38,000 [5]. The density of block polynitroethylene d_{20} equaled 1.535 and the decomposition point was 150°.

Elementary analysis of the polymer showed that there was no denitration during irradiation: $(-CH_2-CHNO_2^-)_n$. Calculated: N 19.2%. Found: N 19.19%.

X-ray diffraction analysis of the polymer showed that it did not contain a crystalline phase. The intense narrow halo and the weak wide halo corresponded to the parameters of closest order 5.15 A and 3.73 A* (see Fig. 3).

It was also established that nitroethylene readily copolymerizes with other unsaturated nitro compounds, for example, 1,4-dinitrobutadiene-1,3, under the action of γ-radiation.

LITERATURE CITED

1. H. Wieland and E. Sakkellarios, Ber. 52, 898 (1919).
2. A. Smith, Pat. USA 2385037 (1945); Chem. Abstr. 40, 347 (1946).
3. A. Smith, C. W. Scaise, and R. H. Stanley, Pat. USA 2384049 (1945); Chem. Abstr. 40, 348 (1946).
4. D. Vofsi and A. Katchalsky, J. Polym. Sci. 26, 127 (1957).
5. Yu. Grodzinskii, A. Katchalsky, and D. Vofsi, International Symposium on Macromolecular Chemistry. Reports and Abstracts [Russian translation] Section 2 (1960) p. 221.
6. G. Buckley and C. Scaife, J. Chem. Soc. 1947, 1477.
7. G. Buckley and C. Scaife, Brit. pat. 595282 (1947); Chem. Abstr. 42, 37775 (1948).
8. J. Csaba and G. Janos, Magyar kem. folyóirat 64, No. 12, 468 (1958).
9. A. Kh. Breger et al., Action of Ionizing Radiations on Inorganic and Organic Polymer Systems [in Russian] Izd. AN SSSR (1958).

All abbreviations of periodicals in the above bibliography are letter-by-letter transliterations of the abbreviations as given in the original Russian journal. *Some or all of this periodical literature may well be available in English translation.* A complete list of the cover-to-cover English translations appears at the back of this issue.

*The x-ray structural analysis of the polymer was carried out by S. G. Strunskii.

A RULE CONCERNING INTERATOMIC DISTANCES IN HALOGENIDE MOLECULES OF DIFFERENT GROUPS OF THE PERIODIC SYSTEM*

V. M. Tatevskii, V. P. Spiridonov, and P. A. Akishin

M. V. Lomonosov Moscow State University

(Presented by Academician A. N. Frumkin, January 4, 1961)
Translated from Doklady Akademii Nauk SSSR, Vol. 138, No. 3,
pp. 621-624, May, 1961
Original article submitted December 28, 1960

From an examination of experimental data, one of us previously [4] concluded that the geometrical configuration of the molecule AX_n (where X is a halogen) does not qualitatively change when the central atom A is substituted by an atom A' of another element from the same group (or subgroup) of the periodic system with retention by A' of the valency, in sequence as well as number of bonds, characteristic of atom A. The configuration of the molecule AX_n also does not change with substitution of one or several X atoms, linked with the given central atom by other halogen atoms. Therefore, molecules of type AX_n can be assembled into sets of similar molecules in which a specific rule concerning the values of the interatomic distances is displayed.

We renumbered the group (subgroup) of the periodic system in which element A belongs with the index k, element A in the k group (subgroup) with the index i (or l), and element X in the halogen group with the index j (or m). Thus, for example, if A is a group-two element $A^{(21)} \equiv Be$, $A^{(22)} \equiv Mg$, $A^{(23)} \equiv Ca$, etc.; for the halogens, $X^{(1)} \equiv F$, $X^{(2)} \equiv Cl$, $X^{(3)} \equiv Br$, and $X^{(4)} \equiv I$. We fixed the k group, examined the interatomic distances $A^{(ki)}-X^{(j)}$ in the AX_n halogenide sets, and compiled Table 1, in which the number of lines equals the number of $A^{(ki)}$ elements in the k group (subgroup) and the number of columns equals the number of $X^{(j)}$ halogens. Here there are the following sets of similar molecules: sets of molecules along the lines, differing one from the other by atoms of element $A^{(ki)}$, and sets of molecules in the columns, differing by the halogen atoms $X^{(j)}$.

We examined the sets of similar halogenide molecules AX_n along the lines in Table 1. The relationships between the interatomic distances A–X in halogenide molecules of groups one to four and the atomic number Z_j of the halogen atoms are graphically depicted in Fig. 1**. This results in a family of graphs of approximately similar form. Similar graphs were obtained for halogenides of the elements of the other groups of the periodic system. Evidently the dependence of the interatomic distances A–X in these molecules on the atomic number of the halogen atoms can be approximately expressed by some function, having one and the same form for all sets of similar molecules, and a collection of constants. More precisely, it is possible to write down for the interatomic distances $A^{(ki)}-X^{(j)}$ in these sets

$$\begin{aligned} r_{1j}^{(k)} &= a_1^{(k)} + b_1^{(k)}\varphi^{(k)}(z_j), \\ &\cdots\cdots\cdots \\ r_{ij}^{(k)} &= a_i^{(k)} + b_i^{(k)}\varphi^{(k)}(z_j), \\ &\cdots\cdots\cdots \\ r_{lj}^{(k)} &= a_l^{(k)} + b_l^{(k)}\varphi^{(k)}(z_j) \\ &\cdots\cdots\cdots \end{aligned} \qquad (1)$$

* The described work was carried out by the authors several years ago as part of a larger investigation. Their results were used during the last three years in the "Structure of Molecules" course delivered in the Moscow University Chemistry faculty (see also [1, 2]). Other authors [3] independently arrived at similar conclusions.

** The interatomic distances A–X for halogenides of group one elements were derived from microwave work [5], whereas for lithium, sodium, potassium, and rubidium fluorides were used values evaluated in this work in accordance with a semiempirical formula; for the halogenides of group two elements and also for lithium, lanthanum, and neodymium halogenides—from electronographic work [6, 7]; for the remaining halogenides—from [8].

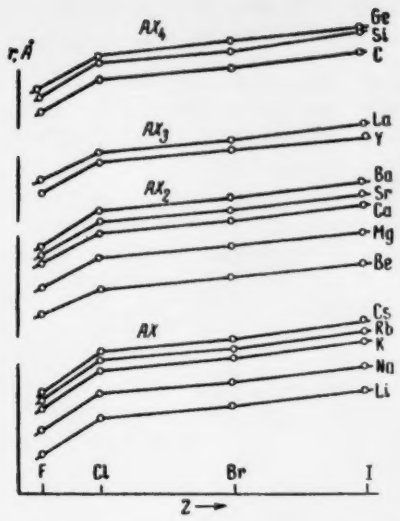

Fig. 1. Dependence of interatomic distances A–X in AX_n molecules on the atomic number of the halogen atoms.

where $\varphi^{(k)}(Z_j)$ is a function which is similar for all of the sets. Evidently for all such sets, differing by atoms $A^{(ki)}$, in conformance with (1) we will have

$$\varphi^{(k)}(z_j) = \frac{r_{ij}^{(k)} - a_i^{(k)}}{b_i^{(k)}} = \frac{r_{lj}^{(k)} - a_l^{(k)}}{b_l^{(k)}}, \tag{2}$$

from where

$$r_{ij}^{(k)} = c_{il}^{(k)} r_{lj}^{(k)} + d_{il}^{(k)}, \tag{3}$$

where $c_{il}^{(k)}$ and $d_{il}^{(k)}$ are independent of j, i.e., the interatomic distances $A^{(ki)}-X^{(j)}$ of the molecules in the i'th line of Table 1 can be described by a linear function of the interatomic distances of the molecules in the l'th line.

If the sets of AX_n molecules in Table 1 are examined column by column it is possible, in a similar manner as before, to derive the equation

$$r_{ij}^{(k)} = c_{mj}^{\prime(k)} r_{im}^{(k)} + d_{mj}^{\prime(k)}, \tag{4}$$

i.e., the interatomic distances $A^{(ki)}-X^{(j)}$ of the molecules in the j'th line of Table 1 can be described by a linear function of the interatomic distances of the molecules in the m'th column.

The observed rule can be illustrated graphically (Fig. 2) for halogenides of different groups of the periodic system (see the more detailed [1, 2]).

Thus, there is an approximate linear relationship between the A–X interatomic distances in the sets of specified AX_n halogenides. Since the sequence and number of A–X bonds are similar and the valency state of the central A atoms is one and the same in these sets, the change of A–X interatomic distances in the sets in conformance with the rule is explained by the periodicity of the changes in properties of the atoms of elements belonging to one group (or subgroup) of the periodic system, i.e., D. I. Mendeleev's law of periodicity is the principle of this rule. The periodicity of molecular properties was studied by D. I. Mendeleev [9] as a means of predicting a number of the properties (e.g. specific weight, boiling point, etc.) of compounds of elements which had still not been isolated. In order to calculate these properties, the arithmetic average of the corresponding properties of the compounds of the elements situated in the periodic table to the right and to the left above and below the element in question was taken, i.e., to all intents and purposes a linear dependence on the atomic number of the element was assumed. Subsequently, attempts were repeatedly made to use the law of periodicity in order to determine the properties of a set of compounds from the corresponding properties of another set of compounds. In the Soviet Union this method was developed in the works of V. A. Kireev [10, 11] and, recently, in the works of M. Kh. Karapet'yants [12-15].

TABLE 1

$A^{(k1)}X_n^{(1)}$,	$A^{(k1)}X_n^{(2)}$,	$A^{(k1)}X_n^{(3)}$,	$A^{(k1)}X_n^{(4)}$
. . . . .	. . . . .	. . . . .	. . . . .
$A^{(ki)}X_n^{(1)}$,	$A^{(ki)}X_n^{(2)}$,	$A^{(ki)}X_n^{(3)}$,	$A^{(ki)}X_n^{(4)}$
. . . . .	. . . . .	. . . . .	. . . . .
$A^{(kl)}X_n^{(1)}$,	$A^{(kl)}X_n^{(2)}$,	$A^{(kl)}X_n^{(3)}$,	$A^{(kl)}X_n^{(4)}$
. . . . .	. . . . .	. . . . .	. . . . .

One particular case of the above-discussed rule is of interest. It is evident that if in Eq. 1 the coefficients $b_i^{(k)}$ for all atoms of the $A^{(ki)}$ elements are equal, i.e., $b_i^{(k)} = b_l^{(k)}$, Eq. 3 acquires the form:

$$r_{ij}^{(k)} = r_{lj}^{(k)} + a_i^{(k)} - a_l^{(k)}. \tag{5}$$

Because $a_i^{(k)}$ and $a_l^{(k)}$ are independent of index j, the differences in the interatomic distances $A^{(ki)}-X^{(j)}$ for two sets of similar molecules, differing by the atoms $A^{(ki)}$, do not depend on what kind of halogen atoms are linked

to the atoms of the $A^{(ki)}$ elements. Consequently, under these conditions it is possible to ascribe certain constant effective radii to the $A^{(ki)}$ atoms. Precisely similar arguments can be applied to the $X^{(j)}$ halogen atoms.

Thus, in the particular case of the sets of molecules which were investigated it is possible to introduce the effective atomic radii, which are constant for the whole series of molecules under consideration, the sums of which equal the corresponding interatomic distances. This is illustrated for molecules of the alkali elements' halogenides in Table 2, examination of which shows that the corresponding differences in the interatomic distances are maintained constant, with maximum divergence from the mean by ± 0.03-0.04 A. Consequently, the interatomic distances in these molecules can be represented with adequate accuracy as the sums of certain constant effective atomic radii.

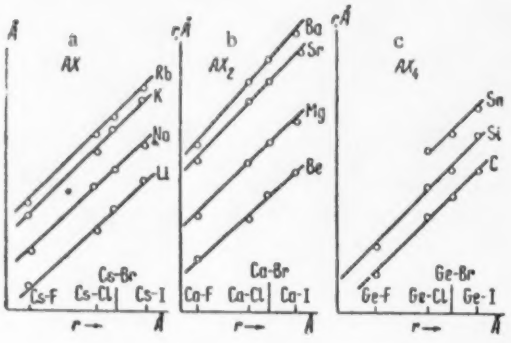

Fig. 2. The rule concerning the values of the interatomic distances A−X: a) For halogenides of group one elements (the interatomic distances in cesium halogenides are laid off along the axis of abscissas); b) for halogenides of group two elements (the interatomic distances in calcium halogenides are laid off along the axis of abscissas); c) for halogenides of group four elements (the interatomic distances in germanium halogenides are laid off along the axis of abscissas).

However, the equations adduced above do not enable us to determine the numerical values of the effective atomic radii, since the number of independent equations is one less than the number of unknowns. Therefore, in order to construct a scale of effective atomic radii it is always necessary to enlist the aid of additional suppositions. In many cases this leads to the necessity to introduce specific corrections, by one or another means (e.g., the well-known Schomaker-Stevenson equations [16]), into the interatomic distances in unstudied molecules which have been estimated with the aid of the effective atomic radii. The value of the above-examined rule for estimating the interatomic distances in molecules for which experimental data are deficient lies in the fact that the linear relationship of the interatomic distances in the sets of similar molecules is independent of whether it is possible to introduce a system of constant effective atomic radii so that the interatomic distance equalled their sum in the appropriate molecules. However, the possibility of using the comparative method described is somewhat limited because in order to estimate the interatomic distances in some molecules it is necessary to know the interatomic distances for all the molecules in one set and the interatomic distances for two (or one in the discussed exceptional case) members of the set to which the molecule in question belongs.

TABLE 2. Differences in Interatomic Distances in Diatomic Halogenide Molecules of the Alkali Elements

Element	F	$\Delta r_{Cl,F}$	Cl	$\Delta r_{Br,Cl}$	Br	$\Delta r_{I,Br}$	I	Average
Li		0,49		0,15		0,22		
$\Delta r_{Na,Li}$	0,31		0,34		0,33		0,32	0,33
Na		0,52		0,14		0,21		
$\Delta r_{K,Na}$	0,29		0,31		0,32		0,34	0,31
K		0,54		0,15		0,23		
$\Delta r_{Rb,K}$	0,12		0,12		0,12		0,13	0,12
Rb		0,54		0,16		0,23		
$\Delta r_{Rb,Cs}$	0,10		0,12		0,13		0,14	0,12
Cs		0,56		0,17		0,24		
Average		0,53		0,15		0,23		

The discussed rule concerns interatomic distances in sets of similar molecules. But this rule may have a wider significance if the idea is applied to sets of different types (or subtypes) of compounds in which a linear change in interatomic distances is also found.

LITERATURE CITED

1. V. P. Spiridonov, Thesis for a Master's Degree, Chemistry Faculty, Moscow State University (1958).
2. V. A. Naumov, Thesis for a Master's Degree, Chemistry Faculty, Moscow State University (1959).
3. M. Kh. Karapet'yants and Ling Ting-Ching, Zhur. Strukturn. Khim. 1, 277 (1960).
4. V. M. Tatevskii, Doklady Akad. Nauk SSSR 101, 515 (1955).
5. A. Honig, M. Mandel, et al., Phys. Rev. 96, 629 (1954).
6. P. A. Akishin and V. P. Spiridonov, Kristallografiya 2, 475 (1957).
7. P. A. Akishin, V. A. Naumov, and V. M. Tatevskii, Vestnik Moskov. Gosudarst. Univ., Ser Matem., Astron., Fizika i Khim., No. 1, 229 (1959).
8. Tables of Interatomic Distances and Configurations in Molecules and Ions (London, 1958).
9. D. I. Mendeleev, Principles of Chemistry [in Russian] (Moscow-Leningrad, 1947).
10. V. A. Kireev, Zhur. Fiz. Khim. 2, 233 (1931).
11. V. A. Kireev, Zhur. Priklad. Khim. 7, 1 (1934).
12. M. Kh. Karapet'yants, Zhur. Fiz. Khim. 27, 934 (1953).
13. M. Kh. Karapet'yants, Zhur. Fiz. Khim. 29, 1132, 1328 (1955).
14. M. Kh. Karapet'yants, Zhur. Fiz. Khim. 30, 2218 (1956).
15. M. Kh. Karapet'yants, Zhur. Fiz. Khim. 32, 306 (1958).
16. V. Schomaker and D. Stevenson, J. Am. Chem. Soc. 63, 37 (1941).

All abbreviations of periodicals in the above bibliography are letter-by-letter transliterations of the abbreviations as given in the original Russian journal. *Some or all of this periodical literature may well be available in English translation.* A complete list of the cover-to-cover English translations appears at the back of this issue.

THE ELECTRON SPECTRUM IN A POLYMER CHAIN

A. B. Almazov

N. S. Kurnakov Institute of General and Inorganic Chemistry,
Academy of Sciences, USSR
(Presented by Academician I. V. Tananaev, April 22, 1960)
Translated from Doklady Akademii Nauk SSSR, Vol. 138, No. 4,
pp. 863-865, June, 1961
Original article submitted April 22, 1960

In the theory of ideal crystals it is shown that the set of natural values relating to the motion of an electron in a periodic lattice field is resolved into bands, i.e. regions of energy in which the values are situated very close to one another. These regions, generally speaking, are separated by intervals in which there are no natural values. The existence of semiconductors and insulators is also usually explained by the presence of these forbidden bands. However, numerous examples of substances are known which do not possess a periodic structure and at the same time are semiconductors or insulators. Therefore, the existence of permitted and forbidden bands is apparently a consequence of some more profound reason than the assumption of the ideal periodicity of the field in which the electron moves. In these cases, when in the immediate vicinity of almost every atom the periodicity is approximately preserved (near order), the existence of bands is merely due to the fact that for small changes in the form of the operator and of the limiting conditions the electron spectrum is changed very little [1]. In the present work it is shown, with a polymer as example, that the spectrum can be banded also in a completely isotropic substance when some regularity is absent in the immediate zones.

Usually [2] a polymer chain of N units is represented by a series of N vectors of equal length: $\mathbf{l}_1, \mathbf{l}_2, \ldots \mathbf{l}_N$. By this the vector $\mathbf{l}_{i+1}$ is obtained from vector $\mathbf{l}_i$ by the transformation

$$\mathbf{l}_{i+1} = A_{i+1,i}\mathbf{l}_i, \tag{1}$$

where $A_{i+1,i}$ are the matrices set down in rotation. The vectors $\mathbf{l}_i$ are situated in space so that the end of vector $\mathbf{l}_i$ coincides with the origin of vector $\mathbf{l}_{i+1}$. Then the radius-vector $\mathbf{R}_i$ connecting the origin of vector $\mathbf{l}_1$ with the origin of vector $\mathbf{l}_i$ equals:

$$\mathbf{R}_i = \sum_{k=1}^{i-1} \mathbf{l}_k. \tag{2}$$

Thus, the matrices $A_{i+1,i}$ completely define the chains.

To elucidate the character of the electron spectrum, it is necessary to solve the Schrodinger equation with the potential describing the field of all the polymer nuclei and the self-consistent field of all the other electrons. A perturbation function of an electron in a polymer can be constructed in a general form by the same method, which is made by consideration of the motion of an electron within a crystal lattice [3, 4]. Namely, let $\Phi(\mathbf{r})$ be some function of the three-dimensional coordinates. We define the function $\Phi_i(\mathbf{r})$ $i = 1, 2, \ldots, N$, so that

$$\Phi_i(\mathbf{r}) = \Phi(A_{i,i-1}A_{i-1,i-2}\ldots A_{21}\mathbf{r} + \mathbf{R}_i). \tag{3}$$

Without limiting the generality, the function $\Phi_i(\mathbf{r})$ can be considered orthonormalized. We will seek a solution of the Schrodinger equation $H\psi = E\psi$ as the linear combination of the functions $\Phi_i(\mathbf{r})$. Then the natural values are the essential roots of the secular equation

$$|H_{ik} - E\delta_{ik}| = 0, \tag{4}$$

where $H_{ik} \doteq \int \Phi_i H \Phi_k dV$. In agreement with Gershgorin's theorem [5], the roots of equation (4) lie in a restricted region formed by the circles with radii

$$\rho_i(N) = \sum_{k=1}^{N}{}' |H_{ik}|, \tag{5}$$

where the prime denotes that for summation the component $|H_{ii}|$ is omitted. The centers of these circles are at the points H_{ii}. In the case under consideration the roots of equation (4) are real. Therefore, the region in which all the roots are found is a segment of the real axes. Thus, the set of natural values relating to the motion of an electron in the field of a chain is limited top and bottom, i.e. it forms a band.

The spectrum of an electron in an infinite chain is banded then, when the limits are:

$$\rho_i = \lim_{N\to\infty} \rho_i(N) = \sum_{k=1}^{\infty}{}' |H_{ik}|, \tag{6}$$

for the condition that the sequence of values H_{ii} is limited top and bottom.

Both for a finite and for an infinite chain the distribution density of levels per band can be very different. In particular, there must be intervals in the band in which there are no levels. Such a splitting of the bands can already occur by breakdown of the far order [1].

More detailed information on the properties of the bands can be obtained by assuming that the matrices $A_{i+1,i}$ are determined statistically and the vectors $\mathbf{l}_1, \mathbf{l}_2, \ldots$ form a Markov chain.

The system of functions $\Phi_i \mathbf{r})$ is incomplete. Therefore, in order to find all solutions of the Schrodinger equation it is necessary to start from some experimental functions chosen so that the set of all the solutions will form a complete system. Depending on whether the valence band is separated from the conduction bands by a more or less wide gap, or overlaps with them, the polymer will be an insulator, semiconductor, or metal.

Thus, the band character of the spectrum is not a specific feature of periodic structures: by very general assumptions concerning the properties of the Hamiltonian and the wave functions it is found that for polymers not possessing even approximately periodic properties the spectrum can be banded. The representation of a quasi-impulse as a number, together with the energies characterizing the states of an electron in the band, can of course be introduced only in the case of periodic structures when the determinant (4) is converted to a cyclic determinant. The existence of bands for polymers is connected with the fact that the roots of the secular equation are groups in some finite region not only for cyclic determinants but also for the considerably wider class of secular equations.

The conditions (6) for the existence of bands are sufficient but not requisite.

Numerous experimental results and theoretical considerations indicate that the electrical properties of substances are determined in the main by the near order [1, 6]. With this, by the electrical properties is understood the whole set of environment characteristics determining the conductivity: the effective mass of the carriers, width of the forbidden band, etc. The preceding discussions are only an indication that for the specified conditions the existence of forbidden bands does not depend on any assumptions of regularity. Therefore, destruction of the near order can radically change the electrical (and generally the electronic) properties of a substance.

LITERATURE CITED

1. A. B. Almazov, Collection. Solid State Physics [in Russian] (1959) Vol. 2, p. 158.
2. M. V. Vol'kenshtein, Configurational Statistics of Polymer Chains [in Russian] (Moscow-Leningrad, 1959).
3. R. Peierls, Quantum Theory of Solids [Russian translation] (IL, 1955).
4. A. B. Almazov, Doklady Akad. Nauk SSSR 131, No. 3, 529 (1960).
5. S. A. Gershgorin, Izvest. Akad. Nauk SSSR, OMEN, 749 (1931).
6. A. F. Ioffe, Jubilee Collection Akad. Nauk SSSR (Acad. Sci. USSR Press) (1947) Vol. 1, p. 305.

COMPOSITION OF THE UNIT CELLS AND MAXIMUM ADSORPTION VOLUMES OF DEHYDRATED SYNTHETIC ZEOLITE CRYSTALS

Academician M. M. Dubinin

Institute of Physical Chemistry, Academy of Sciences, USSR
Translated from Doklady Akademii Nauk SSSR, Vol. 138, No. 4,
pp. 866-869, June, 1961
Original article submitted March 8, 1961

Type A and X synthetic zeolites have in recent years acquired an increasing practical application as highly effective adsorbents, especially for separating gaseous mixtures, and for highly purifying and drying gases. Zeolites are prepared by hydrothermal synthesis as crystals with dimensions of the order of a micron. In technical practice, zeolites of the A and X types are normally used as granules, pellets, or beads, consisting of the crystalline powder of natural zeolites and added binder (10-15%). By rational granulation the practically inert (adsorptionwise) binder which is added causes, proportionally to its content, a decrease in the adsorption properties of the granules by comparison with the original crystalline zeolite. Therefore, consideration of the structures and adsorption properties of dehydrated zeolite crystals is of fundamental scientific interest.

Synthetic zeolites of the A and X types in the completely hydrated form are uniform crystalline substances possessing a rigid aluminosilicate framework. As a result of dehydration at 350° under vacuum, holes or cavities of strictly defined dimensions for each type of zeolite are formed in the zeolite crystals. These holes constitute the primary porous structure of dehydrated zeolite crystals. The parameters of the primary porous structure (shape and dimensions of the pores and narrower inlets in them or the "windows") are well known from X-ray structural investigations. Therefore, the total volume of the primary pores or the maximum adsorption volume of dehydrated zeolites can be calculated on the basis of their known chemical composition and crystal structure.

The chemical composition of dehydrated synthetic A or X zeolites in the oxide form can be expressed as:

$$Na_2O \cdot Al_2O_3 \cdot x\,SiO_2, \tag{1}$$

where the molar ratio SiO_2/Al_2O_3 is denoted by $\underline{x}$. Both types of zeolite have crystals with cubic unit cells the a_0 (side of cube) parameters of which are known from X-ray structural data. Then the composition of the unit cell in the oxide form is expressed as:

$$n\,[Na_2O \cdot Al_2O_3 \cdot x\,SiO_2], \tag{2}$$

where the number $\underline{n}$ of Na, Al, Si, and O atoms (ions) of the aluminosilicate framework of the unit cell is in accordance with the X-ray structural data. The composition of the unit cell of a zeolite crystal according to (2) can be expressed in an atomic form:

$$[2n\,Na \cdot 2n\,Al \cdot nx\,Si \cdot 2n\,(2 + x)\,O]. \tag{3}$$

From X-ray structural data the unit cell of a synthetic zeolite A crystal contains one cubic octahedral (sodalite) structural unit, consisting of 24 (Al + Si) ions and 36 oxygen ions, and 3 tetrameric oxygen bridges in which the total content of oxygen ions is 12. Altogether the aluminosilicate framework of the unit cell of zeolite A contains 24 (Al + Si) ions and 48 oxygen ions [1-3].

From analogous X-ray structural data, the unit cell of synthetic zeolite X contains 8 cubic octahedral units composed of $24 \cdot 8 = 192$ (Al + Si) ions and $36 \cdot 8 = 288$ oxygen ions. In addition, 96 oxygen ions are contained in the 16 hexameric oxygen bridges present in one unit cell [3, 4]. Altogether the unit cell of zeolite X contains 192 (Al + + Si) ions and 384 oxygen ions. Fourier analysis was not able to determine the position of all the ion-exchanged cations nor, therefore, the total number in the unit cells of zeolites A and X.

On the basis of the chemical composition of the unit cell of a zeolite in the form (3) and the number of (Al + Si) and O ions contained in it, derived from X-ray structural measurements, it is possible to obtain a relationship between x and n for each type of zeolite. We will consider the results of this relationship with zeolite X as the example. According to the formula of the unit cell composition (3), the number of (Al + Si) ions is 2n + nx = 192 or

$$n(2+x)=192. \tag{4}$$

In an analogous way we obtain the same relationship (4) by consideration of the number of oxygen ions in the unit cell. We arrive at the same result from the electroneutrality of a unit cell containing positive Na^+, Al^{3+}, and Si^{4+} ions and negative O^{2-} ions:

$$2n\cdot 1+2n\cdot 3+nx\cdot 4=384\cdot 2, \tag{5}$$

from which (4) results.

According to (4) for the zeolite NaX it follows that

$$n=\frac{192}{2+x}. \tag{6}$$

The analogous formula for zeolite NaA has the form:

$$n=\frac{124}{2+x}. \tag{7}$$

In the table examples are given of the characteristic compositions and parameters of the unit cells of zeolite crystals, types A and X (Linde Company) from the results of various investigations. The formulas of the zeolites shown in the table satisfy the X-ray structural data for the total content of (Al + Si) ions and O ions in the unit cells of the crystals. Obviously, the value of n is essentially a mean statistical quantity.

Zeolite	Lit. source	x	n	a_0, A	Type 3 formula of unit cell
NaA	(1)	2,00	6	12,32	12 Na·12 Al·12 Si·48 (O)
	(3)	2,00	6	12,30±0,01	12 Na·12 Al·12 Si·48 (O)
	(2)	1,87	6,205	12,273±0,003	12,40 Na·12,40 Al·11,60 Si·48 (O)
NaX	(3)	2,8	40	24,91±0,02	80 Na·80 Al·112 Si·384 (O)
	(4)	2,67	41,11	24,94	82,22 Na·82,22 Al·109,78 Si·384 (O)

From the data of the table, the main difference in chemical composition of the aluminosilicate frameworks of A and X zeolites consists in: 1) the different relative content of Al and Si ions present in the aluminum-oxygen and silicon-oxygen tetrahedra from which the cubic octahedral structural units are built up and 2) the variation of the inter bonding of the cubic octahedral units – by tetrameric oxygen bridges in zeolite A and correspondingly by hexameric oxygen bridges in zeolite X. Thus, the cubic octahedral unit of zeolite A contains 12 Al^{3+}, 12 Si^{4+}, and 36 O^{2-}, and the cubic octahedral unit of zeolite X contains 10 Al^{3+}, 14 Si^{4+}, and 36 O^{2-}. By calculation 12 O^{2-} per cubic octahedral unit of the zeolites A and X comprise oxygen bridges. The excess negative charges of the cubic octahedral units due to their oxygen bridges are compensated by Na^+, which also determines their number in the zeolite.

The variable values of x, in particular it being somewhat less than 2 for NaA, can be explained: 1) according to Barrer for NaA [2] by occlusion of $NaAlO_2$ molecules in the cavities of the zeolite and 2) in our view by an unusual isomorphic substitution of part of the silicon-oxygen tetrahedra in the cubic octahedral structural units by aluminum-oxygen tetrahedra. The cubic octahedra of NaA and NaX zeolites are concrete examples of cubic octahedral units with different relative contents of Al and Si ions. We assume the possibility of small deviations from Lowenstein's rule for NaA ($x<2$), which must give rise to reduced stability of the aluminosilicate framework of the zeolite.

Such isomorphic substitution is not substantially revealed by the a_0 parameters of the unit crystal cell. Thus, the calculated a_0 parameter of NaX per cubic octahedral unit (24.92 : 2 = 12.46 A) differs very little from the a_0 values for NaA given in the table.

In certain cases, particularly for zeolite samples obtained by laboratory methods, the ratio of the numbers of Na and Al atoms from the result of chemical analysis is somewhat less than one, usually not more than by 10%. It is not excluded that this occurs as a result of ion exchange of a small proportion of Na^+ by H^+ owing to the presence of a considerable amount of carbonic acid in ordinary distilled water which is used for washing the zeolite crystals. From previous observations, this effect is shown in greater degree on lengthy washing of the zeolite.

The shape and dimensions of the cavities of the unit cell of synthetic crystals of type A zeolites, known from X-ray structural data, permit ready calculation of the total volume of the cavities of the unit cell and the maximum adsorption volume per unit mass of the dehydrated crystals, available for absorbing molecules of varying dimensions. This problem proves more difficult to solve for type X zeolites owing to the arrangement of the centers of the cubic octahedral units at the points of the crystal lattice characteristic for diamond, i.e. an unsymmetrical arrangement of the cavities in the unit cell. In the present work an attempt to solve this problem was made by calculating the apparent volume of a cubic octahedral unit from the X-ray structural data for the unit cell of zeolite A and by calculating the volumes of the tetrameric and hexameric oxygen bridges in the aluminosilicate frameworks of the unit cells of A and X zeolites.

According to the model of the aluminosilicate framework of zeolite NaA [2], the crystal unit cell contains one cubic octahedral structural unit and corresponding to it 3 tetrameric oxygen bridges. On the other hand, in a single unit cell there is present one large cavity of practically spherical shape of diameter 11.4 A [1, 2] and volume 776 A^3, and one small cavity inside the cubic octahedron of diameter 6.6 A [1, 2] and volume 150 A^3. If a_0 is the parameter of the unit cell of NaA, then the apparent volume of a cubic octahedral structural unit V_{oct} in the aluminosilicate framework of the zeolite is given by:

$$V_{oct} = a_0^3 - (776 + 3V_{4B}), \tag{8}$$

where V_{4B} is the volume of the tetrameric oxygen bridge.

A model is readily constructed of the tetrameric oxygen bridge connecting the (Al, Si) ions through oxygen ions situated at the vertices of tetrameric windows of adjoining cubic octahedral units. By taking the length of the (Al, Si)−O bond as 1.67 A [3] and therefore the length of the side of the tetrameric window as 3.34 A and the position of the oxygen ions of the bridge at the center of the straight lines connecting the (Al, Si) ions of adjoining cubic octahedra, we obtain, with the radius of the oxygen ion as 1.4 A, the radius describing the circumference of a normal cross section of the central portion of the tetrameric oxygen bridge as 3.7 A. If such an oxygen bridge is considered to be a cylinder with radius 3.7 A and height equal to the diameter of an oxygen ion, 2.8 A, then its volume will be 116 A^3. According to (8) with $a_0 = 12.273 \pm 0.003$ A [2], i.e. with the volume of the unit cell as 1848 A^3, the apparent volume of the cubic octahedral unit will equal 724 A^3.

In the unit cell of a NaX zeolite with $a_0 = 24.94$ A [4] and volume 15513 A^3, there are 8 cubic octahedral units and binding them 16 hexameric oxygen bridges. If V_{6B} is the volume of one hexameric bridge, then the total volume of the 8 large cavities ("super-cages") V_L contained in the unit cell is given by:

$$V_L = 15513 - 8 \cdot 724 - 16V_{6B} \tag{9}$$

In an analogous way as for the tetrameric oxygen bridge, the radius of a constructed model of the hexameric bridge with the same parameters (length of (Al, Si)−O bond, radius of the oxygen ion) describing the circumference of a normal cross section of the central portion of the bridge will be 4.8 A. If such an oxygen bridge is considered to be a cylinder with radius 4.8 A and height equal to the diameter of an oxygen ion 2.8 A then its volume V_{6B} will equal 202 A^3. Substituting this value in formula (9), we obtain $V_L = 6490$ A^3. Only the volume of these cavities is accessible to the majority of molecules of adsorbed substances such as nitrogen, hydrocarbons, etc.

For water molecules, apart from large cavities, their internal or small cavities of volume 150 A for each cubic octahedron are accessible through "windows" in the cubic octahedra. The total volume of the small cavities in the unit cell of zeolite NaX is $V_s = 150.8 = 1200$ A^3. The total volume of the cavities of the unit cell of zeolite NaX accessible to water molecules is:

$$V = V_L + V_s = 6490 + 1200 = 7690 Å^3. \tag{10}$$

According to Barrer, a single unit cell of completely hydrated zeolite NaX contains 256 water molecules [4]. This number of water molecules corresponds to the volume of liquid of normal density or maximum adsorption volume 7670 A^3, practically coincident with the calculated volume V.

In conclusion, the author is pleased to express his thanks to N. A. Shishakov for discussion of the results obtained.

LITERATURE CITED

1. T. B. Read and D. B. Breck, J. Am. Chem. Soc. 78, 5972 (1956).
2. R. M. Barrer and W. M. Meier, Trans. Farad. Soc. 54, 1074 (1958).
3. L. Broussard and D. P. Shoemaker, J. Am. Chem. Soc. 82, 1041 (1960).
4. R. M. Barrer, F. W. Bultitude, and J. W. Sutherland, Trans. Farad. Soc. 53, 1111 (1957).

SELECTIVE SORPTION ON POROUS GLASSES

S. P. Zhdanov and E. V. Koromal'di

The Institute of Silicate Chemistry of the Academy of Sciences of the USSR
(Presented by Academician M. M. Dubinin, January 20, 1961)
Translated from Doklady Akademii Nauk SSSR, Vol. 138, No. 4,
pp. 870-873, June, 1961
Original article submitted January 20, 1961

Selective sorption, dependent on the molecular sieve action of the adsorbent, is usually considered to be a specific property of porous crystals, such as zeolites. However, our previous investigations [1, 2] and the present paper on the sorption of various substances by porous glasses show that a capacity for selective sorption is also characteristic of certain porous glasses which behave as typical molecular sieves. Such porous glasses can be obtained by leaching two-component alkali silicate and certain alkali borosilicate glasses with acid.

Figures 1 and 2 show sorption isotherms for water, alcohols, nitrogen, and certain hydrocarbons on porous glasses No. 2 and 3, obtained by treatment with 1N HCl of two potassium silicate glasses which differed in K_2O content. Figure 3 refers to porous glass No. 1, obtained in a similar way from sodium silicate glass. Figure 3a separately shows sorption isotherms for water and nitrogen on another sample of porous glass No. 1. Adsorption measurements were carried out at 18° for water, alcohols, and hydrocarbons, and at −195.6° for nitrogen, by weight for water and alcohols and by volume for hydrocarbons and nitrogen, using vacuum adsorption equipment. The porous glass samples* were heated in vacuo to 100 or 200° before adsorption.

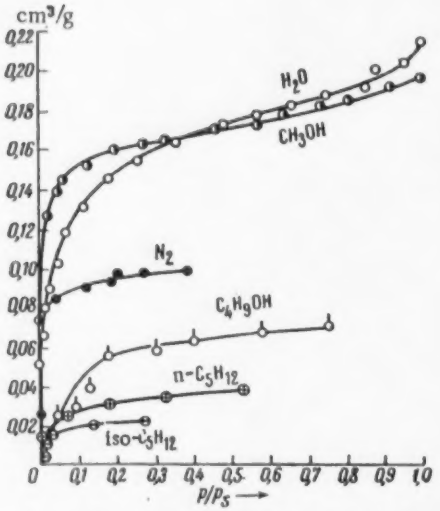

Fig. 1. Selective sorption on porous glass No. 2, prepared from potassium silicate glass.

We investigated the sorption of C_2H_5OH, as well as of CH_3OH and C_4H_9OH. The corresponding isotherms are not shown in Figs. 1-3 because, as a result of very slow C_2H_5OH adsorption, the points did not represent true equilibrium. For the same reason, some of the points on the butanol sorption isotherm of glass No. 2 may not correspond to true equilibrium.

The ethanol volumes** adsorbed at $p/p_s = 0.2$ on porous glasses No. 1, 2, and 3 were approximately 0.042, 0.120, and 0.032 cm^3/g, respectively. It is clear from the figures and the above data that water and methyl alcohol, whose molecules were the smallest of the substances investigated, were adsorbed to a considerably greater extent than the substances with larger molecules, such as C_2H_5OH, hydrocarbons, and particularly C_4H_9OH. Hence it follows that the selective sorption shown by these porous glasses is due to the existence in them of very fine pores, of diameter comparable with the dimensions of simple molecules. Estimates of the pore dimensions of glasses No. 1 and 3 can be obtained from the sorption data for water and nitrogen. These porous glasses are similar to the molecular sieve Linde 4 A; they take up water well and hardly adsorb nitrogen at all (at −196°). It is clear that these porous glasses are like the zeolite porous crystals in that they have uniform pores with an extremely narrow diameter distribution curve. Since the diameter of an H_2O molecule is about 2.8 A, and that of an N_2 molecule about 4 A, the pore diameter of these porous glasses must be in the range 2.8-4 A. Porous glass No. 2 has somewhat larger pores, but they are still

*Most of the porous glass samples were prepared and kindly presented to us by Yu. A. Shmidt. We take this opportunity of thanking him.

**Expressed as cubic centimeters of liquid of normal density.

so fine that a large part of their volume remains unoccupied even by such relatively small molecules as C_4H_9OH (d = = 5.8 A [3]) and C_5 hydrocarbons.

The problem arises as to how we can explain the formation of such uniform small pores in porous glasses. The voids and channels of molecular dimensions in crystalline zeolites represent the gaps in the crystalline lattice between the silica and alumina structural elements and their groupings, which form the lattice but are not very densely packed. The alkali and alkaline earth metal cations, which compensate for the negative charges on the alumina and silica tetrahedral elements, are present in these cavities but do not occupy the whole space, so that a considerable part of it remains free and is filled by water molecules. Removal of water from the zeolite by heating leaves free cavities and is not accompanied by any change in crystalline structure.

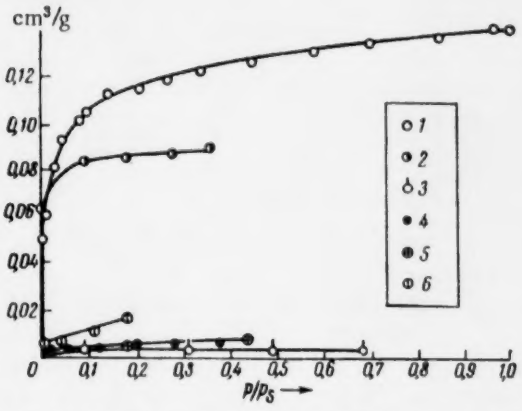

Fig. 2. Selective sorption on porous glass No. 3, obtained from potassium silicate glass. 1) H_2O, 2) CH_3OH, 3) C_4H_9OH, 4) N_2, 5) n-C_5H_{12}, 6) iso-C_8H_{18}.

The structure of an alkali silicate glass is also formed by associated silica tetrahedral elements, the gaps between being filled by alkali metal cations. However, the packing of the oxygen in the glasses is so dense that not only the sites occupied by alkali metal cations but also the free gaps in the silicon oxygen lattice are inadequate for the sorption of even such small molecules as water. The glass becomes porous and acquires its sorptive capacity only after leaching by acid solutions. The leaching process begins with replacement of alkali metal cations by protons from the acid. For example, for a sodium silicate glass, the process can be represented by the scheme:

$$\begin{array}{l} | \\ -\mathrm{Si}-\mathrm{O^-Na^+} + \mathrm{H^+} \rightarrow \\ | \end{array} \quad \begin{array}{l} | \\ -\mathrm{Si}-\mathrm{OH} + \mathrm{Na^+} \\ | \end{array}$$

glass solution glass solution

When there is a high enough SiO_2 content in the glass, leaching with acid solution is not accompanied by rupture of the Si−O−Si bonds in the silica glass lattice. There are a number of important considerations which favor this picture [2, 4, 5]. One of the most convincing confirmations is the production of a silica hydrate−disilicic acid $H_2Si_2O_5$ −by leaching of crystalline sodium disilicate $Na_2Si_2O_5$.

Thus, the formation of very fine channels in the silica lattice of a glass as the result of leaching is not due to rupture of Si−O−Si bonds or their arrangement. These channels must be the direct result of the extraction, during the leaching process, of large alkali metal ions and of their replacement, according to the above scheme, by the much smaller protons. We should therefore expect an increase in the pore volume with increasing content of alkali metal oxide in the glass and with increasing ionic radius of the alkali metal cation. In fact, both these expectations have been confirmed for porous glasses obtained by leaching lithium, sodium, and potassium silicate glasses of various compositions.

Thus, an increase in the Na_2O content of glass from 20 to 25 to 33% resulted in an increase in the pore volume of the product of leaching from 0.062 to 0.076 to 0.157 cm^3/g, as measured by the limiting value of water sorption. The pore volumes of porous glasses obtained from potassium silicate glasses of analogous compositions were 0.120, 0.140, and 0.210 cm^3/g. A lithium glass containing 33% of Li_2O gave a porous glass with a pore volume of 0.068 cm^3/g, i.e. considerably less than corresponded to a sodium and particularly to a potassium glass.

However, the pore volumes, as determined by the water sorption isotherms, were in all cases 2-3 times the total volumes of the cations extracted from the glass in the leaching process. This is not only because the total space in the glass freed by the dissolution of an alkali metal cation must always be greater than the actual volume of the cation. There is a much more pronounced effect due to the secondary process of water synthesis from closely placed hydroxyl groups, formed in the glass when the randomly distributed alkali metal cations are replaced by protons. The water formed in this way at low temperatures remains in the glass, but comes off on evacuation at room temperature and frees additional pore space in the glass; this is because the water is made up from some of the oxygen atoms

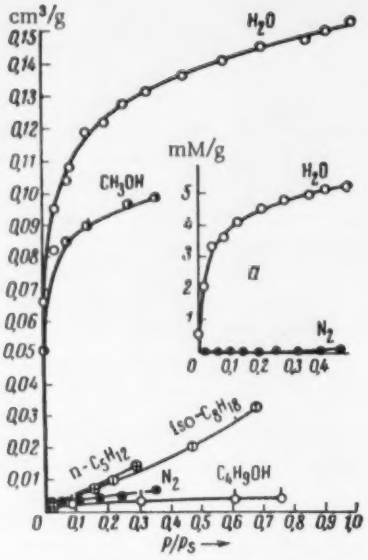

Fig. 3. Selective sorption of porous glass No. 1, obtained from sodium silicate glass. The section a shows isotherms for sorption of water and nitrogen on another sample of porous glass No. 1.

originally present in the glass. The conception of low temperature dehydration of porous glasses obtained by leaching sodium silicate glasses follows from analysis of the curves for dehydration in vacuo [2].

Thus, the appearance of fine channels of molecular dimensions in alkali silicate glasses after treatment with acid solutions is due to extraction from the glass of alkali metal cations located at sites in the silicon-oxygen lattice, and the subsequent removal as water of part of the oxygen originally present in the glass. Porous glasses showing a capacity for selective sorption are inferior to porous crystals (zeolites) in sorptive capacity, but because of certain specific features and the possibility of deliberately controlling their structure, porous glasses can be considered as extending the range of molecular sieves and may be suitable for separating mixtures when porous crystals cannot be used.

LITERATURE CITED

1. S. P. Zhdanov and E. V. Koromal'di, Izv. AN SSSR, OKhN 1959, No. 4, 626; 1959, No. 5, 811.
2. S. P. Zhdanov, Dissertation, Inst. Silicate Chem. AN SSSR (Leningrad, 1959).
3. S. Brunauer, Adsorption of Gases and Vapors [Russian translation] (1948).
4. Yu. A. Shmidt, Izv. AN SSSR, OKhN 1954, No. 5, 778.
5. S. K. Dubrovo and Yu. A. Shmidt, Izv. AN SSSR, OKhN 1953, No. 4, 597.

All abbreviations of periodicals in the above bibliography are letter-by-letter transliterations of the abbreviations as given in the original Russian journal. *Some or all of this periodical literature may well be available in English translation.* A complete list of the cover-to-cover English translations appears at the back of this issue.

RELATION BETWEEN SPONTANEOUS IGNITION AND LAMINAR AND TURBULENT BURNING VELOCITIES OF PARAFFIN HYDROCARBONS

V. P. Karpov and A. S. Sokolik

Institute of Chemical Physics, Academy of Sciences of the USSR
(Presented by Academician V. N. Kondrat'ev, January 23, 1961)
Translated from Doklady Akademii Nauk SSSR, Vol. 138, No. 4, pp. 874-876, June, 1961
Original article submitted January 1, 1961

In a new model of a turbulent flame the turbulent burning velocity is directly determined by the ignition lag with a mixture of unburnt and burning gases [1]. In this connection, it is of practical interest to compare the turbulent burning velocity with the known kinetic characteristics of spontaneous ignition, e.g., for methane and for propane and butane, since a different relation between the spontaneous ignition lag and the composition of the hydrocarbon-air mixture at a given temperature has been reported [2]. At temperatures of 700-750° the ignition lag for methane is reduced by diluting the mixture, but in the case of propane and butane it is reduced by enriching the mixture with the combustible (for more detail see the book of Brunauer, p. 73 [3]). Unfortunately; the fact that there is an important fundamental difference in the high-temperature spontaneous ignition of methane and the higher hydrocarbons of the paraffin series, as has been known for some thirty years, has not been investigated in more detail.

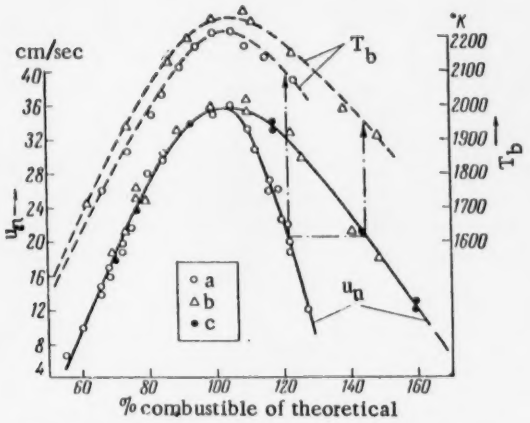

Fig. 1. a) Methane, b) propane, c) butane.

In the present paper the differences between laminar and turbulent burning velocities are compared (for mixtures of methane, propane, and butane with air) with the variation in the ignition lag in relation to the composition of the mixture, using a constant-volume bomb method. In determining the turbulent burning velocity in a sealed volume a photographic record is used for the propagation of the laminar flame in order to measure the volume of the laminar flame, which gives the equivalent increase in pressure from the combustion (the method is described elsewhere [4]). The laminar burning velocity is determined by recording the apparent flame velocity $u_a = dr/dt$ from the equation $u_b = u_a/\varepsilon$. In addition, the degree of expansion ε may be determined as $\varepsilon \simeq T_{ad}/T_0$ by substituting the actual temperature of the flame T_f by the calculated adiabatic temperature and by neglecting the variation in the number of moles during combustion n/n_0.

Since $n/n_0 > 1$ in hydrocarbon flames, and $T_f < T_{ad}$, by substituting $\varepsilon = (T_f/T_0)(n/n_0)$ by $\varepsilon \simeq T_{ad}/T_0$, the permissible error is reduced and does not exceed the limits of experimental error. Comparison of the normal burning velocities u_n with the composition of the mixture for methane and C_3 and C_4 hydrocarbons shows that there is a definite difference in the region of rich mixtures—for methane there is a considerably reduced velocity and reduced upper limit for flame propagation as compared to propane and butane (Fig. 1). Since in each case the burning temperatures T_b of all three flames which are examined are very close but the transfer coefficient (thermal diffusivity and diffusion) for rich methane mixtures is higher than for propane and butane this difference in normal flame velocities may be due only to the difference in the rates of the reaction in the flame, with a significantly greater rate of reaction for propane and butane in comparison with methane.

An even more definite difference for the two similar types of fuel is observed with variation in composition of the mixture for the turbulent burning velocity, u_T. As can be seen from Fig. 2, with a constant absolute intensity of

turbulence u'_{Σ} = 4.2 m/sec (for the determination of u'_{Σ} see our earlier paper [4]) both the values of u_T and the limit of propagation with rich mixtures are considerably higher for propane and butane than for methane. On the other hand, with lean mixtures, there is a noticeable increase of u_T for methane in comparison with propane and butane, although to a lesser extent. Correspondingly, the maximum turbulent velocities for propane and butane shift considerably in the region of rich mixtures (about 120% excess combustible) in comparison with methane, for which the maximum lies close to the stoichiometric composition. Analogous differences in the position of the maximum turbulent velocities for methane and butane air mixtures were observed in the investigation by Wohl and Shore [5].

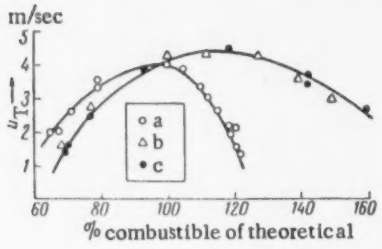

Fig. 2. For notation of points, see Fig. 1. u'_{Σ} = 4.2 m/sec.

The observed parallelism in relation to the velocities of laminar and turbulent flames for the two types of hydrocarbons in different ranges of mixtures of the components cannot be considered as evidence that turbulent burning itself is obtained in laminar flames, i.e., as indirect proof of the surface-laminar model. That this conclusion is incorrect may easily be established by comparing the turbulent burning velocity with variation of the normal flame velocity in Fig. 3. In the range of lean mixtures different turbulent burning velocities correspond to each value of the normal velocity: The value is higher for methane and lower for propane and butane. Let us note that according to the data of Fig. 1, for this range of compositions the values of the burning temperatures which correspond to a given value of the normal velocity are close. Thus, for lean mixtures the velocities of turbulent combustion for methane are higher than the velocities for propane and butane at the same values of u_n and T_b.

In the range of rich mixtures, even more different values of u_T correspond to each value of the normal velocity of the flame: lower for methane and higher for propane and butane. Hence, there is a higher burning temperature for methane (by approximately 100-150°), corresponding to the determined value of the normal velocity, than for propane (Fig. 1). Thus, in the range of rich mixtures for a given value of the normal velocity the turbulent burning velocity of methane proves to be significantly lower than propane and butane despite the higher temperature for methane.

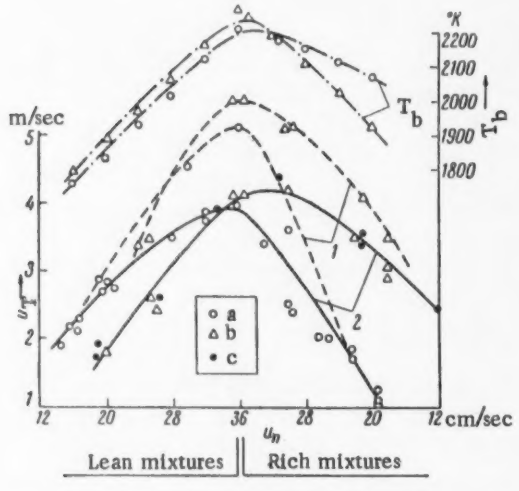

Fig. 3. For notation of points, see Fig. 1. 1) u'_{Σ} ~ ~ 5.6 m/sec; 2) u'_{Σ} ~ 4.2 m/sec.

It is therefore possible to assume that there are certain kinetic differences for methane and for the higher alkanes which manifest themselves by facilitating high-temperature spontaneous ignition and by accelerating the propagation of laminar and turbulent flames – for methane with a lean mixture and for C_3 and C_4 hydrocarbons with an enriched mixture.

In any case, these kinetic differences cannot be linked with the stage of chain formation since there is no basis whatsoever for assuming a significant difference in the rate of reaction in the generation of active centers for methane and higher alkanes. Moreover, this stage, limiting the high-temperature spontaneous ignition of hydrocarbons ([3], p. 64), is eliminated in reactions of laminar and turbulent flames: firstly, due to the diffusion of the active centers from their zone of maximum concentration; secondly, due to turbulent mixing of burning and unburnt gases.

It is not possible to consider the effect of the composition of the mixture on the ignition and on the velocities of the flames as being due to chain branching. The mechanism of chain branching at high-temperature ignition of hydrocarbons takes place through the degeneration of the branching with aldehydes by the formation of an intermediate active product. At the same time, from general considerations and from experimental results it follows that degeneration of branching does not take part in the development of reactions in flames. Both in laminar and in

turbulent flames for hydrogen and also hydrocarbons, branching obviously is realized through one and the same reaction: $H + O_2 \rightarrow HO + O$, as shown by Sokolik [3] (p. 188 et ff.) and by the authors of the present paper [1].

It remains possible to assume that the difference in the ignition properties and in the velocities of the laminar and turbulent flames for methane and the C_3 and C_4 alkanes in relation to the composition of the mixture is determined by the difference in the stage of chain propagation for these two types of hydrocarbons, i.e., in this stage the reaction rate increases in the case of methane when the mixture is diluted and increases in the case of the higher alkanes when the mixture is enriched. There is therefore special interest in investigating the mechanism of this stage, both in the process of high-temperature spontaneous ignition and in the development of reactions in flames. From the results derived it also follows that in laminar and turbulent flames the reaction begins by a similar mechanism under analogous conditions in the mixing of the burning and unburnt gases, but the reaction is propagated by an essentially different mechanism: in laminar flames, by a continuous molecular transfer of heat and mass; in turbulent flames, by turbulent mixing.

LITERATURE CITED

1. A. S. Sokolik and V. P. Karpov, Doklady Akad. Nauk SSSR 129, 1, 168 (1959).
2. C. A. Naylor and R. W. Wheeler, J. Chem. Soc. 1931, 2456; 1933, 1240.
3. A. S. Sokolik, Spontaneous Ignition, Flame, and Detonation in Gases [in Russian] (Izd. AN SSSR, 1960).
4. V. P. Karpov, E. S. Semenov, and A. S. Sokolik, Doklady Akad. Nauk SSSR 128, 6, 1220 (1959).
5. K. Wohl and L. Shore, Ind. and Eng. Chem. 47, 828 (1955).

All abbreviations of periodicals in the above bibliography are letter-by-letter transliterations of the abbreviations as given in the original Russian journal. *Some or all of this periodical literature may well be available in English translation.* A complete list of the cover-to-cover English translations appears at the back of this issue.

THE ADSORPTIVE AND ION-EXCHANGE PROPERTIES OF SILICA MODIFIED BY A RADICAL WITH ACID FUNCTIONS

I. E. Neimark and V. M. Chertov

L. V. Pisarzhevskii Institute of Physical Chemistry, Academy of Science, USSR
(Presented by Academician M. M. Dubinin, January 25, 1961)
Translated from Doklady Akademii Nauk SSSR, Vol. 138, No. 4,
pp. 877-879, June, 1961
Original article submitted January 23, 1961

By giving silica gel specificity with respect to adsorption of various substances, with acidic or basic properties for example, its range of application could be considerably widened. With this aim chemical modification of silica gel by organic radicals with various functional groups is proposed. Substitution of the hydroxyls of silica gel by radicals with acidic or basic properties could lead to the creation of new types of nonswelling ion-exchangers and acid-base catalysts. In this direction we synthesized earlier [1] silica gels with basic properties.

TABLE 1. Principal Characteristics of Silica Gel and Aerosil

Sample	V_s, cm^3/g	S, m^2/g	r, A	OH, meq/g
Silica gel	1.0	276	56	3.7
Aerosil	–	120	–	1.27

In the present work the aim was to prepare silica gels modified by a radical with acidic functions which should make it specific for the adsorption of substances with basic properties. As such a radical with well-defined acidic properties the sulfonic acid group was chosen. A uniformly porous particulate silica gel prepared in the laboratory, as well as a highly dispersed preparation of nonporous silica–aerosil, were employed for modification; their main characteristics are given in Table 1. The value of the specific surface area was determined from the adsorption isotherm of methanol, the structural water content by a thermal method.

Sulfonation of silica gel and aerosil was carried out in two stages. First of all, the samples, dried under vacuum for 2 hours at 200° C, were phenylated by treatment with diphenyldichlorosilane. Interaction thereby occurred between the hydroxyl groups of the adsorbent and the diphenyldichlorosilane, as a result of which phenyl groups were covalently bound to the surface of the sample. In the second stage of modification the phenyl groups present on the surface were sulfonated with sulfuric acid. After sulfonation the samples were carefully washed free of acid with distilled water and dried at 180-200°. The reactions which occur during modification can be presented by the following scheme*:

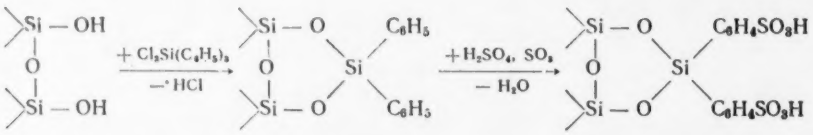

As a result, a proportion of the hydroxyl groups on the surfaces of the silica gel and aerosil were substituted by a complex surface compound with sulfonic acid groups. The number of attached phenylsilyl groups was determined by the increase in weight, the number of attached sulfonic groups from ion-exchange results and by chemical analysis. The ion-exchange properties of the sulfonated samples were characterized by the value of the static exchange capacity from the results of exchange in 1N aqueous NaCl solution [3]. At the same time, the equilibrium pH of the solution was recorded, arising from the exchange of the H^+ of the sulfonic groups with the Na^+ of the solution; the pH was determined by means of a glass electrode.

*Other schemes of the reaction of diphenyldichlorosilane with the surface are possible (e.g. see [2]).

In Table 2 are given ion-exchange data for the original and sulfonated samples of silica gel and aerosil. As seen from the table, the ion-exchange properties of the sulfonated samples greatly exceed the original values. For these, the equilibrium pH of the solution was 1.8-2.1, i.e. exchange occurred in strongly acid media. As is known

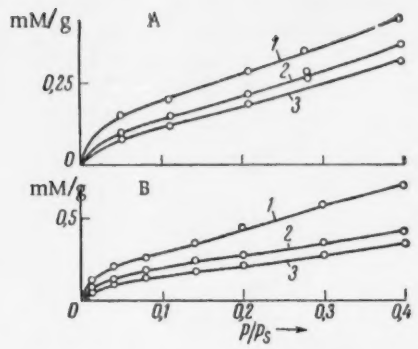

Fig. 1. Isotherms of the adsorption of heptane (A) and benzene (B) vapors at 20° for the original (1), sulfonated (2), and phenylated (3) aerosil.

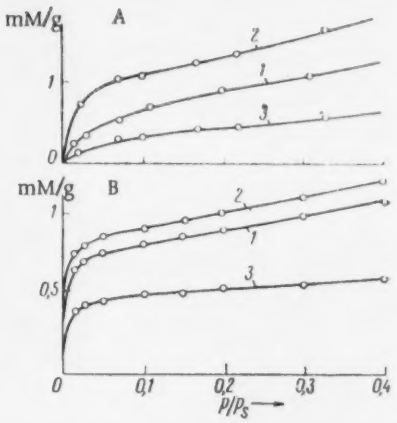

Fig. 2. Isotherms of the adsorption of methyl alcohol (A) and diethylamine (B) vapors at 20° for the original (1), sulfonated (2), and phenylated (3) aerosil.

[4], exchange has not been detected at such pH values on unmodified silanol silica gel. Only at a pH around 4 is exchange noticeably established, but its value is some orders less than for sulfonated silica gel. Thus, the static exchange capacity of sulfonated silica gel is 510 μ eq/g at an equilibrium solution pH of 1.8, and the ion-exchange capacity of the original silica gel at pH 4.0 is only 11.2 μeq/g.

TABLE 2. Ion Exchange on the Original and Sulfonated Silica Gel and Aerosil in 1N NaCl Solution (pH of original solution 6.6)

Sample	Exchange capacity μeq/g	Equilibrium pH of solution
Silica gel	11.2	4.0
Sulfonated silica gel	510	1.8
Aerosil	6.3	4.3
Sulfonated aerosil	250	2.1

Thus, the presence on the surfaces of the silica gel and aerosil of the covalently bound strongly acid ionogenic sulfonic groups ensures ion exchange on such samples in strongly acid media, whereas the hydrogen of the outer surface of the double layer of the silica gel, owing to its protonization being considerably smaller in comparison with the hydrogen of the sulfonic groups, is unable to dissociate and exchange.

A change of the adsorption properties as a result of modification can be caused by a change both of the porosity of the sorbents and of the chemical nature of their surfaces. For that purpose, in order to study the adsorption properties of sulfonated samples so as to isolate the effect of porosity, a nonporous preparation of silica-aerosil was examined. The adsorption isotherms of the vapors of benzene, heptane, methyl alcohol, and diethylamine on the original, the phenylated, and the sulfonated aerosil samples were measured. These results are given in Figs. 1 and 2. As seen from the figures, phenylation of aerosil caused a substantial decrease in the adsorption of all the vapors used. A different picture was observed for sulfonated aerosil. The adsorption isotherms of benzene and heptane were situated somewhat above the isotherm for phenylated aerosil (this can be explained by partial breakdown of the phenylsilyl layer during sulfonation), and the adsorption isotherms of methyl alcohol and diethylamine lie above not only the phenylated sample but even the original aerosil.

The decrease of the adsorption of benzene and heptane on sulfonated and phenylated aerosil is connected with the decrease of the dispersion component of the van der Waals interaction. This is explained mainly by the remoteness of the adsorbed molecules from the surface of the adsorbent due to substitution of the hydroxyl groups by the larger

phenylsilyl or sulfonic phenylsilyl groups [5-10]. For benzene this effect is heightened by the decrease in the electrostatic interaction energy with the hydroxyls. The increase in adsorption of methyl alcohol and diethylamine on sulfonated aerosil compared with the phenylated and original materials is due to the interaction of the molecules of these substances with the sulfonic groups present on the surface. It is known that compounds containing oxygen such as alcohols and ethers, as well as organic bases containing nitrogen are able to interact with strong mineral acids [11]. Such an interaction obviously takes place also on sulfonated aerosil since the sulfonic group has the properties of a strong mineral acid. This is also supported by the fact that desorption from sulfonated samples shows that the amount of irreversibly bound diethylamine and methanol is greater than in the case of the phenylated and original materials. Hence, the adsorption of CH_3OH and $(C_2H_5)_2NH$ on sulfonated aerosil has a chemisorption character. For these molecules the sulfonic groups are the active adsorption centers, and therefore the adsorption of methanol and diethylamine is increased. For the C_6H_6 and C_7H_{16} molecules the sulfonic groups are not active centers, and this leads to a decrease of the adsorption potential of the modified aerosil with respect to the vapors of these substances.

Thus, by modifying silica gels with organic radicals with acidic or basic functions it is possible to prepare specific adsorbates and catalysts. In particular, sulfonated silica gels can be used as nonswelling ion-exchangers in strong acid media. As the matrix of such ionites is thermally stable, they can be employed at higher temperatures at which the matrix of the usual synthetic ion-exchange resins is subject to degradation [12].

LITERATURE CITED

1. I. E. Neimark, V. M. Chertov, and others, Doklady Akad. Nauk 132, 1356 (1960).
2. L. G. Ganichenko, M. M. Dubinin, and others, Izvest. Akad. Nauk SSSR, Otdel Khim. Nauk, 1355 (1960).
3. A. A. Vansheidt, A. A. Vasil'ev, and O. I. Okhrimenko, Collection: Theory and Practice of the Utilization of Ion-Exchange Materials [in Russian] (Acad. Sci. USSR Press, 1955) p. 110.
4. B. P. Nikol'skii and O. N. Grigorov, Doklady Akad. Nauk 50, 325 (1945); K. G. Miesserov, Zhur. Obshch. Khim. 24, 947 (1954); C. J. Plank, J. Phys. Chem. 57, 284 (1953).
5. I. Yu. Babkin, V. S. Vasil'eva, and others, Doklady Akad. Nauk 129, 131 (1959).
6. I. Yu. Babkin and A. V. Kiselev, Doklady Akad. Nauk 129, 357 (1959).
7. V. M. Dubinin, Izvest. Akad. Nauk SSSR, Otdel Khim. Nauk, 1739 (1960).
8. A. V. Kiselev, A. Ya. Korolev, and others, Koll. Zhur. 22, 671 (1960).
9. K. H. Ebert, Monatsh. f. Chem. 88, 275 (1957).
10. M. M. Dubinin, V. G. Zhukovskaya, and others, Izvest. Akad. Nauk SSSR, Otdel Khim. Nauk, 588 (1960).
11. T. I. Temnikova, Course of the Theoretical Basis of Organic Chemistry [in Russian] (Leningrad, 1959) p. 211.
12. H. Lux, Anorganisch-chemische Experimentierkunst (Leipzig, 1959) p. 262.

All abbreviations of periodicals in the above bibliography are letter-by-letter transliterations of the abbreviations as given in the original Russian journal. *Some or all of this periodical literature may well be available in English translation.* A complete list of the cover-to-cover English translations appears at the back of this issue.

THE FORMATION OF HYDRAZINE BY THE γ-RAY IRRADIATION OF LIQUID AND SOLID AMMONIA

Yu. A. Sorokin and S. Ya. Pshezhetskii

L. Ya. Karpov Physico-Chemical Institute

(Presented by Academician S. S. Medvedev, January 20, 1961)
Translated from Doklady Akademii Nauk SSSR, Vol. 138, No. 4,
pp. 880-883, June, 1961
Original article submitted October 20, 1960

As is well known, in a number of cases a change in phase has very pronounced effects on the outcome of radiochemical reactions. The differences between liquid-phase and gas-phase reactions are quite well known, but much less work has been done in comparing solid-phase with liquid-phase reactions. However, it is even hard to compare the already available data for reactions in these two phases, since the work was frequently done at different temperatures. Therefore the effects observed might have equally been due to differences between the properties of liquid and solid phases as to some differences in the rates of various stages on account of temperature variations.

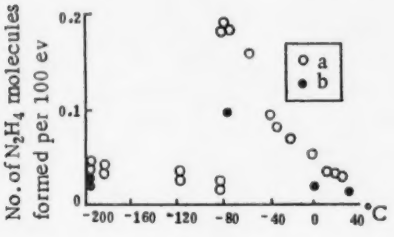

Fig. 1. The quantum yield of hydrazine as a function of temperature. Exposure to radiation was 4 hr. a) An intensity of $1.2 \cdot 10^{16}$ ev/g·sec; b) intensity of $4.1 \cdot 10^{16}$ ev/g·sec.

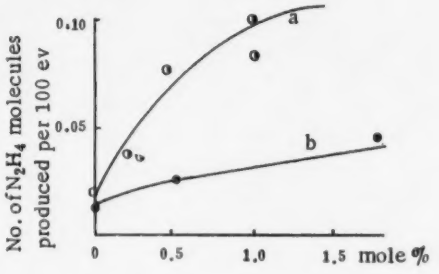

Fig. 2. The quantum yield of hydrazine as a function of the concentration of material introduced into the solid phase. The radiation intensity was 200 g/sec. Exposure to radiation was 4 hr. The temperature was -80° C. a) Propylene; b) propane.

Of course, it is best to study the effects of phase state on radiochemical reactions at temperatures not too widely apart. It is also important that the reactions be not too complicated, and that it be possible to correlate the observed effects with any of the primary or secondary reaction steps. The formation of hydrazine by the radiolysis of ammonia represents one such reaction.

We investigated the formation of hydrazine in liquid and solid ammonia induced by γ-rays. Some of the data pertaining specifically to the effect of phase on the reaction are reported here.

Ammonia was irradiated in quartz tubes by exposure to γ-rays from a Co^{60} source with an activity of $2 \cdot 10^4$ C. The radiation intensity was varied from 25 to 790 r/sec. The amount of energy absorbed was determined by means of a ferrous sulfate dosimeter. The exposure to radiation ranged from 10 to 10^4 min.

After irradiation the ammonia was evaporated. Hydrazine was determined photocolorimetrically in a solution of HCl in p-dimethylaminobenzaldehyde. Using this method we could determine hydrazine with an accuracy of 0.1 mg/ml.

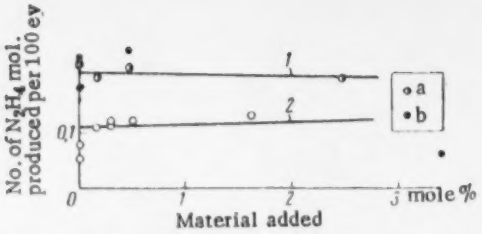

Fig. 3. The quantum yield of hydrazine as a function of the concentration of material introduced into the liquid phase. Radiation intensity was 200 r/sec. Exposure time 4 hr. 1) t = −70° C; 2) t = −35° C; a) Propylene; b) propane.

The effect of temperature on the yield of hydrazine is shown in Fig. 1.

In the liquid phase the yield of hydrazine increases as temperature is decreased. But below the melting point of ammonia (−78°) the yield of hydrazine drops; the yield in the solid phase is about one tenth as large as in the liquid phase. Thus, the transition from the liquid to the solid state produces an abrupt change in the yield of hydrazine. From the variation of yield with temperature one can determine the activation energy for the formation of hydrazine in liquid ammonia, 3-4 kcal/mole.

The observed phase effect can be attributed to altered conditions for the formation of $\dot{N}H_2$ radicals.

It seems that the principal reactions leading to the formation of hydrazine are:

$$1.\ NH_3 \rightleftarrows \begin{cases} NH_2 + H \\ NH + H_2 \end{cases}$$
$$2.\ NH_2 + NH_2 \rightarrow N_2H_4.$$
$$3.\ NH + NH_3 \rightarrow N_2H_4.$$

The concentration of NH_2 radicals depends on the rate of recombination with hydrogen atoms. In the liquid phase it is much easier for a hydrogen atom to depart from the vicinity of "its own" NH_2 radical than in the solid phase. This apparently constitutes one reason why hydrazine is formed more readily in the liquid phase.

If our explanation is right, then a hydrogen acceptor should enhance the yield of hydrazine. The acceptor should also be more effective in the solid phase than in the liquid phase, since in the latter the removal of hydrogen is much easier to begin with, and hence the capture of hydrogen atoms by the acceptor should have a relatively less pronounced effect on the yield of hydrazine.

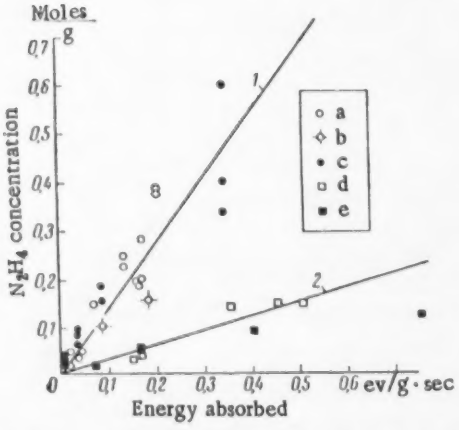

Fig. 4. The dependence of hydrazine yield on the amount of absorbed γ-ray energy. 1) Liquid ammonia, t = −75° C: a) Radiation intensity = $1.17 \cdot 10^{16}$ ev/g · sec; b) radiation intensity = $4.1 \cdot 10^{16}$ ev/g · sec (in a and b exposure time was varied; in c) exposure was constant, intensity was varied). 2) solid ammonia, t = −196° C: d) radiation intensity = $1.17 \cdot 10^{16}$ ev/g · sec; e) radiation intensity = $4.1 \cdot 10^{16}$ ev/g · sec (in d and e the exposure time was varied).

We used propylene in our experiments as hydrogen atom acceptor. The experimental results are presented in Figs. 2 and 3. In order to correct for possible side effects which might result from the slight distortion of the solid ammonia crystal lattice by the acceptor molecules, we carried out a parallel set of experiments in which equal amounts of propane were added to the ammonia (propane cannot act as an acceptor of hydrogen atoms). Figure 2 shows that the yield of hydrazine increases as the concentration of propylene in solid ammonia is increased. No comparable effect was detected when propane was used instead of propylene. Addition of propylene to liquid ammonia (Fig. 3) also fails to produce a comparable increase in the yield of hydrazine.

Thus, it seems that the principal effect of a phase change is to alter the conditions for the recombination of H atoms and NH_2 radicals. However, it is quite possible that this is not the sole cause of the observed effects.

It is obvious that any change in the conditions responsible for the dimerization of NH_2 radicals, which leads to the formation of hydrazine, must also be important; the same applies to reaction of NH radicals

with NH_3 molecules. Apparently, the conditions in the liquid phase are more favorable not only to the formation but also to the dimerization of NH_2 radicals on account of higher mobility. In the solid state the radicals cannot move around freely. There are data showing that in a true solid there is practically no dimerization of NH_2 radicals and even less reaction between NH radicals and NH_3. It should be pointed out that low temperatures do not favor these reactions either. This becomes quite apparent if one compares the number of radicals formed in solid ammonia (as determined by p.m.r.) with the amount of hydrazine formed (table).

	Energy absorbed, ev/g	No. of molecules per 1 g of NH_3	Quantum yield G, molecules/100 ev
Formation of radicals	$0.37-0.39\cdot10^{21}$	$0.53-0.59\cdot10^{18}$	0.14
Formation of hydrazine	$0.35\cdot10^{21}$	$0.14\cdot10^{18}$	0.038

As our data show, the yield of hydrazine is of the same order of magnitude as the amount expected from the number of frozen radicals. This indicates that, under our conditions at least, practically no reaction takes place in the solid state. The reaction apparently occurs when the irradiated samples are melted and the molecules acquire a greater mobility.

The reciprocal relationship between the temperature and the yield of hydrazine in liquid ammonia may be attributed to several factors. One such possible factor is the decomposition of hydrazine. Since at low hydrazine concentrations the amount of radiation absorbed by the hydrazine is insignificantly small in comparison with the amount absorbed by ammonia, the decomposition of hydrazine must result primarily from its reaction with the reactive intermediates such as NH_2 and NH radicals. The rates of these reactions depend on the activation energy for the interaction of the radicals with N_2H_4, and consequently as the temperature is raised the decomposition rate increases and the concentration of hydrazine declines.

Analysis reveals that if the formation of hydrazine (as in reaction 2) were combined with such decomposition reactions the concentration of hydrazine would not be a linear function of the radiation dosage, and at fairly high dosages the N_2H_4 concentration would attain a constant value due to an equilibrium between the formation and decomposition rates. Yet, the experimental results (see Fig. 4) fail to reveal any deviations from the straight line within the range of investigated dosages.

Another possibility is that the reciprocal relationship between yield and temperature is somehow connected with the fact that the diffusion rate of NH_2 radicals increases with increasing temperature and consequently the probability of dimerization to yield N_2H_4 decreases. This mechanism would be consistent with the effective (negative) activation energy of 3–4 kcal/mole.

The observed yields of about 0.2 molecules/100 ev are of the same order of magnitude as those determined previously by one of us in cooperation with E. V. Bol'shun and I. A. Myasnikov [1] when liquid ammonia was bombarded by fast electrons (about 0.7 molecule /100 ev).

LITERATURE CITED

1. E. V. Bol'shun, S. Ya. Pshezhetskii, and I. A. Myasnikov, Coll. The Effects of Ionizing Radiation on Organic and Inorganic Systems [in Russian] (Izd. AN SSSR, 1958) p. 184.

THE APPLICABILITY OF ALLEN'S MODEL TO THE RADIOLYSIS OF AQUEOUS SOLUTIONS

V. G. Firsov and B. V. Érshler

Institute of Theoretical and Experimental Physics, Academy of Sciences, USSR
(Presented by Academician A. I. Alikhanov, January 23, 1961)
Translated from Doklady Akademii Nauk SSSR, Vol. 138, No. 4,
pp. 884-885, June, 1961
Original article submitted January 23, 1961

Radiolysis rate equations for aqueous solutions are usually set up on the basis of a model for the irradiated solution which was first clearly formulated by A. O. Allen [1]. According to this model, some of the H and OH radicals generated in regions of high ionization density ("hot spots" in Allen's terminology) will recombine to yield H_2, H_2O_2, and H_2O; others will diffuse into the bulk of the liquid avoiding recombination. The initial yields of H_2, H_2O_2, H, and OH generated in this primary reaction when water is irradiated by γ-rays from Co^{60} were also first reliably established by Allen [2, 3].

When Allen's model is used it is customary to use homogeneous kinetic equations, and hence it is obvious that the following two approximations are implied: 1) the yields of H_2, H_2O_2, H, and OH are assumed to be independent of the composition and concentration of the solution; 2) the uneven distribution of primary radiolysis products is neglected, i.e., it is assumed that H_2, H_2O_2, H, and OH are distributed uniformly throughout the solution.

The validity of approximation 1 in dilute solutions of a number of weak radical acceptors exposed to X rays and γ-radiation is well supported by experiments and by theoretical calculations based on Allen's model ([4-7] et al.).* However, the validity of approximation 2 has never been tested experimentally and its theoretical treatment (done by B. V. Érshler and G. G. Myasicheva) is confined to the radiolysis of solutions containing H_2O_2, H_2, and O_2.

One of the authors of this paper has shown [8] that if Allen's model correctly describes the radiolytic reactions and if homogeneous reaction kinetics hold, then the following two relationships should be observed: 1) If the irradiated liquid attains a steady state and for a given intensity I_1 of the absorbed radiation we determine certain curves relating the logarithm of the concentration of all the species found in solution to the logarithm of the concentration of any one of them, then if the intensity is changed to I_2 all the curves will be shifted along both axes by the amount $\log (I_2/I_1)^{1/2}$ without any change in shape; 2) If in a given radiolytic reaction we plot the yield of any one particle against the logarithm of the concentration of another particle when the intensity is I_1, then if the radiation intensity is changed to I_2 the curve will be shifted without any change in shape along the log axis by the amount $\log (I_2/I_1)^{1/2}$. The two "$I^{1/2}$ laws" should hold in any radiolytic reaction which satisfies Allen's model, provided the equilibrium concentrations or yields in the given solution are single-valued functions of the concentration of any of the particles. Other cases have been examined in more detail elsewhere [8].

In our present work we have attempted to use these $I^{1/2}$ laws to find out if approximation 2 of the Allen's model is applicable to the radiolysis of titanium salts in solution, assuming that approximation 1 is applicable as in the case of many other weak acceptors in solution.

In the figure we have plotted two curves showing the oxidation yield of radiolyzed solutions of trivalent titanium as a function of $\log [Ti^{3+}]$; the radiolysis was carried out in the absence of oxygen using radiation from a cobalt source. Curve 1 was recorded at a radiation intensity $I_1 = 0.0364 \cdot 10^{19}$ ev/liter·sec, curve 2 at $I_2 = 1.00 \cdot 10^{19}$ ev/liter·sec. Measurements show that the oxidation yield at first increases slowly with concentration and then sharply drops. One can see in the figure that the two curves obtained at different intensities are indeed very similar in shape, and their separation along the log axis ranges from 0.70 to 0.72, which agrees very well with the value of $\log (I_2/I_1)^{1/2} = 0.72$. The fact that the $I^{1/2}$ law is observed in this case indicates that Allen's model is a good approximation to solutions of salts of trivalent titanium.

* These theoretical calculations have also revealed that Allen's model accounts satisfactorily for the observed relationship between the initial yields and the radiation ionization density.

The observed relationship between the yield and radiation intensity provides direct evidence for the interaction between particles generated along different ionization paths, whereas the fact that the $I^{1/2}$ law is obeyed indicates that the interaction in this case can be described satisfactorily by equations of homogeneous reaction kinetics. It is obvi-

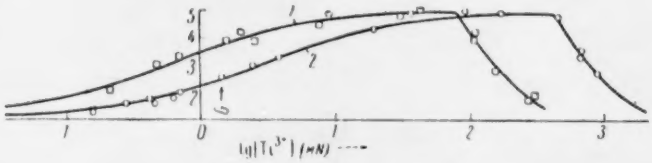

Applicability of the $I^{1/2}$ law to solutions of Ti^{3+}. The curves of G (number of Ti^{3+} ions oxidized per 100 ev) versus log $[Ti^{3+}]$ recorded at an intensity $I_1 = 0.0364 \cdot 10^{19}$ ev/liter · sec (1) and $I_2 = 1.00 \cdot 10^{19}$ ev/liter · sec (2).

ously desirable to extend the study of Allen's model by using the $I^{1/2}$-law and to determine in this way to which systems and over what concentration and intensity range one can use the model for analyzing the mechanisms of radiolytic reactions. We are currently engaged in research along these lines.

LITERATURE CITED

1. A. O. Allen, J. Phys. and Coll. Chem. 52, 479 (1948).
2. A. O. Allen, C. J. Hochanadel, J. A. Ghormley, and T. W. Davis, J. Phys. Chem. 56, 575 (1952).
3. A. O. Allen, Rad. Res. 1, 85 (1954).
4. A. H. Samuel and J. L. Magee, J. Chem. Phys. 21, 1080 (1953).
5. S. C. Ganguly and J. L. Magee, J. Chem. Phys. 25, 129 (1956).
6. P. J. Dyne and J. M. Kennedy, Canad. J. Chem. 36, 1518 (1958).
7. P. J. Dyne and J. M. Kennedy, Canad. J. Chem. 38, 61 (1960).
8. B. V. Ershler, Doklady Akad. Nauk SSSR 129, 866 (1959).

All abbreviations of periodicals in the above bibliography are letter-by-letter transliterations of the abbreviations as given in the original Russian journal. *Some or all of this periodical literature may well be available in English translation.* A complete list of the cover-to-cover English translations appears at the back of this issue.

THE ADSORPTION OF HEXANE AND BENZENE VAPORS ON INACTIVE AND RADIOACTIVE BARIUM SULFATE

L. D. Belyakova, V. V. Gromov, A. V. Kiselev, and

Academician Vikt. I. Spitsyn

Institute of Physical Chemistry, Academy of Sciences, USSR,
and M. V. Lomonosov Moscow State University
Translated from Doklady Akademii Nauk SSSR, Vol. 138, No. 5,
pp. 1139-1142, June, 1961
Original article submitted February 24, 1961

Although it is known that the physical chemical properties of solid substances are altered by the introduction of radioactive isotopes [1-5], the nature of the processes involved here is not entirely clear. Interest attaches to a study of the adsorptional properties of radioactive substances with respect to the vapor phase take-up of materials of various structural types, especially polar and nonpolar. Indication of the possibility of increasing the adsorption of

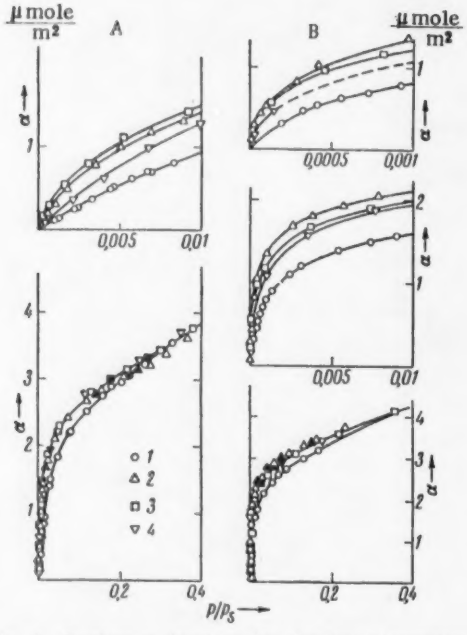

Fig. 1. Isotherms showing the absolute adsorption of vapors of n-hexane at 20° (A) and benzene at 50° (B) on inactive $BaSO_4$ (200°) (1), and on the radioactive specimens: $BaSO_4$-1 (200°) (2), $BaSO_4$-2 (200°) (3), and $BaSO_4$-3 (200°) (4). Points shown in black, here and in Figs. 3 and 4, designate desorption. Initial segments of these isotherms are indicated above.

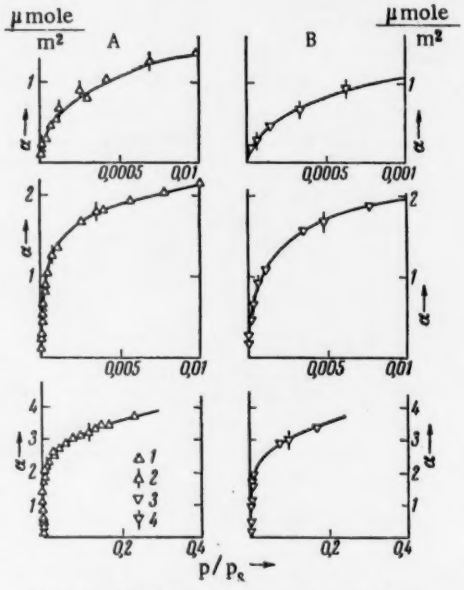

Fig. 2. Isotherms showing the absolute adsorption of benzene vapors at 50° on radioactive specimens: $BaSO_4$-1 (200°) (A) and $BaSO_4$-3 (200°) (B). Points 1 and 3 designated initial measurements on the adsorption isotherms; points 2 and 4, repeat measurements made after holding each specimen for two months.

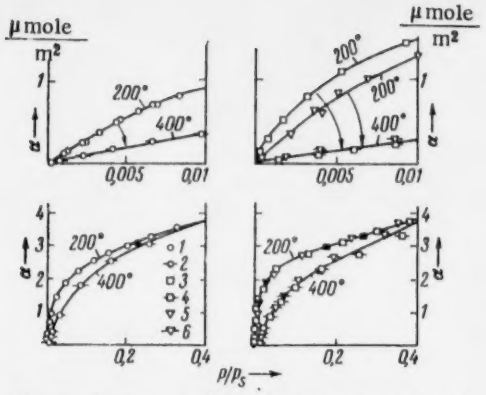

Fig. 3. Isotherms of the absolute adsorption of hexane vapors at 20° on specimens of $BaSO_4$ which had been degassed at 200° (1, 3, 5) and 400° (2, 4, 6). Points 1 and 2 represent the inert specimen of $BaSO_4$; points 3, 4, 5, 6, radioactive specimens: $Ba^{*}SO_4$-2 (3, 4) and $Ba^{*}SO_4$-3 (5, 6).

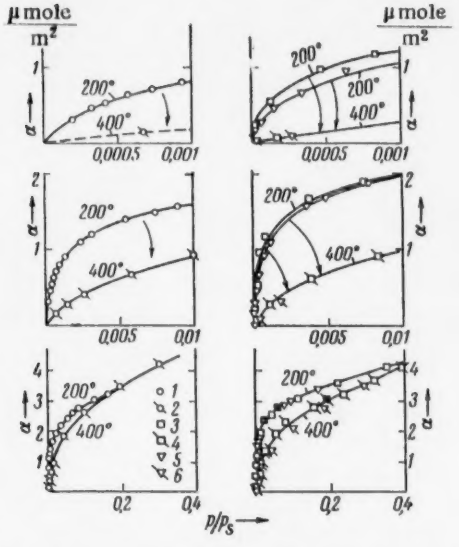

Fig. 4. Isotherms of the absolute adsorption of benzene vapors at 50° on specimens of $BaSO_4$ which had been degassed at 200° (1, 3, 5) and 400° (2, 4, 6). Points 1 and 2 designate the inert specimen of $BaSO_4$; points 3, 4, 5, 6, radioactive specimens: $Ba^{*}SO_4$-1 (3, 4) and $Ba^{*}SO_4$-3 (5, 6).

methanol on powdered K_2SO_4 through the introduction of radioactive sulfur was reported in [6] although the accuracy of the results obtained there was limited by the low value of the surface area. Barium sulfate precipitates containing radioactive sulfur were employed as adsorbents in the present work since a form of this material having an extensively developed surface can be prepared readily.

These $BaSO_4$ precipitates were obtained by the interaction of $BaCl_2$ solutions with a solution of Na_2SO_4 containing S^{35}. The $Na_2^{*}SO_4$ solution had a pH of 7, contained the stable carrier at a concentration of 3.9 mg/liter, and had a specific activity of 10 mC /ml with respect to S^{35}. There was practically no contamination from foreign salts, and contamination from radioactive phosphorous did not exceed 0.01%. The precipitated $BaSO_4$ was washed with successive portions of a 10% solution of C_2H_5OH in distilled water.

Four specimens of $BaSO_4$ were prepared, one inactive, and three active, the activity of the latter at the time of preparation being 96, 101, and 85 mC /g, respectively. These specimens were degassed in the adsorption system at 200° prior to experiment [7]. The specific surface $\underline{s}$ of each was determined in this same system following the BET low-temperature nitrogen and argon adsorption method. The characteristics of these specimens are shown in the table.

The adsorbates were n-hexane, benzene, methanol, nitrogen, and (in certain instances) argon. Data on the adsorption of vapors of n-hexane* and benzene are presented below. The adsorption of benzene is largely due to electrokinetic (dispersional) interaction with the adsorbent surface. The adsorption of benzene on a surface carrying electrical charges and dipoles involves interaction not only of electrokinetic and weak electrostatic induction forces but also a supplementary interaction of the electron cloud of the benzene molecule (principally from the π-bonds) with the surface dipoles and ions [9, 10].

Isotherms showing the absolute adsorption of vapors of n-hexane and benzene (per unit surface, as determined from nitrogen adsorption) on inactive $BaSO_4$ and on the three active specimens of $BaSO_4$, each degassed at 200°, are given in Fig. 1. The adsorption of these substances per unit area was greater for the radioactive specimens than for the inactive in the region of monomolecular coverage, the difference being especially pronounced at low coverage. An absolute adsorption twice as great for $Ba^{*}SO_4$-1 as for the inactive specimen was obtained at $p/p_s = 0.005$ in the case of the weakly adsorbed hexane and at $p/p_s = 0.0005$ with the strongly adsorbed benzene.

The table shows that the radioactive specimens differed principally in age at the time of determination of the adsorption isotherms. These specimens had approximately the same initial radioactivity but differed markedly in activity at the time of developing the adsorption isotherms. Figure 1 shows the isotherms for adsorption of hexane on $Ba^{*}SO_4$-1 and $Ba^{*}SO_4$-2 to be almost identical although these specimens differed in specific activity prior to measurement (21

* The adsorption of n-hexane vapors on barium sulfate has been studied earlier in [8].

Characteristics of the Working Specimens of $BaSO_4$.

Specimen	Initial radioactivity, mC /g	Specific surface, m^2/g, from nitrogen adsorption	Age up to the beginning of adsorption measurements, days		Radioactivity prior to measurement of adsorption, mC /g	
			hexane	benzene	hexane	benzene
Degassed at 200°						
$BaSO_4$	0	4,3	—	—	—	—
Ba^*SO_4-1	96	4,6	187	167	21	25
Ba^*SO_4-2	101	8,0	42	56	72	65
Ba^*SO_4-3	85	7,3	7	10	80	77
Suppl. degassing at 400°						
$BaSO_4$	0	3,3	—	—	—	—
Ba^*SO_4-1	96	3,9	—	—	—	—
Ba^*SO_4-2	101	4,4	75	71	56	57
Ba^*SO_4-3	85	5,0	92	86	41	43

and 72 mC /g) while there was a marked difference between the isotherms for adsorption of this same vapor on Ba^*SO_4-2 and Ba^*SO_4-3 which had approximately equal activities (72 and 90 mC/g). Thus, the activity of a specimen at a given instant is practically without effect on the adsorption. This conclusion was confirmed by special experiments on the effect of holding time on the adsorption capacity of the radioactive specimens. After developing the adsorption isotherms for benzene on Ba^*SO_4-1 and Ba^*SO_4-3, these specimens were held for two months and similar measurements then repeated on them. The results of these measurements are shown in Fig. 2, from which it is clear that long holding did not alter the adsorption capacity of either the Ba^*SO_4-3 which had been freshly prepared or the Ba^*SO_4-1 which had already undergone holding. This indicates that possible alterations in the surface state of a solid sulfate resulting from β-decay of S^{35} are without influence on the adsorption of benzene, a substance which is extremely sensitive to changes in the electrical field of the adsorbent surface [7, 9, 10].

At the same time, Fig. 1 shows the adsorption of vapors of benzene and hexane per unit surface to increase with increasing initial radioactivity of the specimen in the region of low surface coverage.

These results justify the assumption that activation of the solution used in preparing Ba^*SO_4 by introduction of $^*SO_4^{2-}$ leads to the formation of a precipitate whose surface activity for adsorption is higher than of an inactive specimen.

If this enhanced adsorption capacity of the radioactive specimens of barium sulfate were due to higher nonuniformity* of the surface, it could be anticipated that the relative diminution of this factor resulting from removal of the nonuniformity would be greater for the radioactive specimens than for the inactive specimen. In order to test this assumption, the specimens which had been degassed at 200° were given an additional 30-hour degassing at 400° in the system at the end of the experiments. The specific surface of each was checked by low temperature nitrogen adsorption. The specimen characteristics are given in the table. This table shows that vacuum heating reduced the specific surface, the reduction being higher for the more highly dispersed radioactive specimens.

The isotherms for the absolute adsorption of vapors of hexane and benzene on specimens which had been degassed at 200 and 400° are compared in Figs. 3 and 4. Heating in vacuum sharply diminished the adsorption capacity of each specimen with respect to hexane and benzene, this reduction per unit area being greater in the radioactive specimens than in the inactive. Thus, elevation of the temperature from 200 to 400° reduced the adsorption of hexane vapors at a relative pressure of 0.005 by a factor of 1:3 in the case of the inactive specimen and by a factor of 1:7 in the case of the radioactive specimen Ba^*SO_4-2.

The elevation of the temperature from 200 to 400° markedly altered not only the magnitude of the adsorption but also the character of the isotherm, the latter passing from convex to almost linear in the region of low values of

*This nonuniformity can be either geometrical or chemical, the first type arising from the structure of the precipitate and the second from the structural details of the surface and hydrate film.

p/p_s. This also confirms the above assumption that the surface of a specimen which has been degassed at 200° is highly nonuniform, the nonuniformity being greater in the radioactive specimens than in the inactive. Degassing at 400° led to a sharp reduction in the nonuniformity of each specimen.

Thus, the study of the adsorption of vapors on specimens which had been subjected to supplementary heating in vacuum at 400° confirms the above assumption that the addition of radioactive $Na_2\overset{*}{S}O_4$ leads to the formation of a precipitate having enhanced adsorption capacity and a surface of highly nonuniform structure, this nonuniformity being greater than in the case of an inactive specimen. On the other hand, heating in vacuum at 400° makes the surface of each specimen considerably more uniform and gives practically the same adsorption capacity to each.

LITERATURE CITED

1. Vikt. I. Spitsyn, Izvest. Akad. Nauk SSSR, Otdel Khim. Nauk 1958, 1296.
2. Vikt. I. Spitsyn and I. E. Mikhailenko, Doklady Akad. Nauk SSSR 121, 319 (1958).
3. A. A. Balandin, Vikt. I. Spitsyn, et al., Doklady Akad. Nauk SSSR 121, 495 (1958).
4. Vikt. I. Spitsyn, Izvest. Akad. Nauk SSSR, Otdel Khim. Nauk 1960, 1325.
5. Vikt. I. Spitsyn and V. V. Gromov, Doklady Akad. Nauk SSSR 123, 722 (1958), Radiokhimiya 1, 181 (1959).
6. Vikt. I. Spitsyn, I. E. Mikhailenko, et al., Izvest. Akad. Nauk SSSR, Otdel Khim. Nauk 1960, 1311.
7. L. D. Belyakova and A. B. Kiselev, Zhur. Fiz. Khim. 33, 1534 (1959).
8. N. N. Avgul', G. I. Berezin, et al., Izvest. Akad. Nauk SSSR, Otdel Khim. Nauk 1960, 11, 1948.
9. A. V. Kiselev and D. P. Poshkus, Doklady Akad. Nauk SSSR 120, 834 (1958).
10. A. V. Kiselev, Ya. Koutetski, and I. Chizhek, Doklady Akad. Nauk SSSR 137, No. 3 (1961); Ya. Kontetski and I. Chizhek, Zhur. Fiz. Khim. 35 (1961).

All abbreviations of periodicals in the above bibliography are letter-by-letter transliterations of the abbreviations as given in the original Russian journal. *Some or all of this periodical literature may well be available in English translation.* A complete list of the cover-to-cover English translations appears at the back of this issue.

THE RADIO-THERMAL CRACKING OF LIQUID HYDROCARBONS

A. M. Brodskii, K. P. Lavrovskii, Corresponding Member
Acad. Sci. USSR, and V. B. Titov

Institute of Petroleum Chemistry Syntheses, Academy of Sciences, USSR
Translated from Doklady Akad. Nauk SSSR, Vol. 138, No. 5,
pp. 1143-1146, June, 1961
Original article submitted February 18, 1961

The present work treats effects arising from the joint action of heat and high energy radiation on the gas oil fractions of mixed hydrocarbons which boil over the interval from 200 to 350°. These experiments were carried out in the VVR reactor. Heated evacuate quartz ampules [1,2], 250 mm in length and 10 mm in internal diameter, approximately one-third filled with liquid, were used in this work. The contents of each ampule were carrefully deaerated prior to sealing. The results of these experiments are in agreement with those obtained in [3] insofar as they show radiolysis of liquid hydrocarbons to be associated with a characteristic ln G, 1/T relation (G is the number of molecules destroyed through the absorption of 100 ev of energy) of the type indicated in Fig. 1. The quantity G alters comparatively slowly with temperature below a certain limiting value T_p (stage I in Fig. 1). G begins to rise rapidly at T_p (approximately 600°K), the energy of activation being 20 ± 5 kcal/mole (stage II). The transition from stage I to stage II occurs quite sharply over a narrow but continuous interval of the curve. The process of stage II gradually passes over into thermal cracking (stage III) with further elevation of temperature. The degree of decomposition in stage III is no longer fixed by the total dose of absorbed energy as is the case with stages I and II but begins to depend more and more on the dose rate, i.e., the length of stay in the reaction zone.

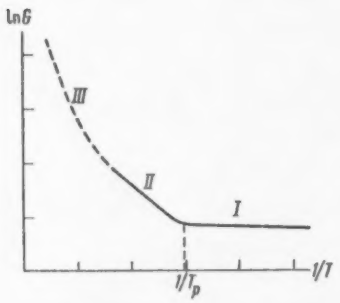

Fig. 1. Schematic representation of the ln G vs 1/T relation; T_p is the critical point.

The existence of stage II in the radiolysis of gaseous hydrocarbons was first noted in the work of L. S. Polak and his collaborators [4] where it was designated as radio-thermal cracking. The data of this work would indicate that a stage I type of G, temperature relation is not met in the radiolysis of gaseous hydrocarbons and the latter therefore differs from the radiolysis of liquid products which is under investigation here where the activation energy is equal to several kilocalories*.

Our experimental data show the temperature dependence of the rate of formation of high-molecular products ("polymers") to be of a peculiar type. Figure 2 give the relation between 1/T and ln G_h (G_h is the number of molecules of parent hydrocarbons which are converted into high-molecular products) for the radiolysis of gas oil. The yield of high-molecular products was determined by molecular distillation under high vacuum of 10^{-5} mm of Hg. The figure shows that the radiochemical yield of high-molecular products from saturated hydrocarbons begins to diminish rapidly at T_p.

The fact that the yield of various low molecular destruction products shows a different type of temperature dependence is of importance for an analysis of the processes which are involved in radio-thermal decomposition. The experimentally established temperature dependence of the radio-chemical yields from destruction processes is shown in Fig. 3.

The interaction of radiation with hydrocarbon molecules can result in two types of reactions which may proceed independently of one another.

*An alteration in the mechanism of hydrocarbon decomposition with elevation of the temperature was noted in the work of M. A. Mokul'skii [7] although no account was there taken of the radical reactions which are fundamental to the case now under study.

hydrocarbon + radiation → . . .

. . . → excited molecule + final stable products (1)

hydrocarbon + radiation → . . .

. . . → thermal hydrocarbon radicals → radical reaction products (2)

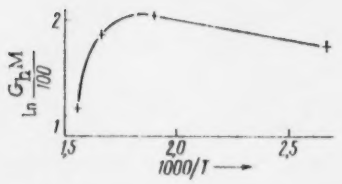

Fig. 2. The temperature dependence of the radiochemical yield of high-molecular products.

Reaction (1) corresponds to the so-called direct path for radiochemical decomposition, and reaction (2) to the radical path. A determination of the detailed mechanisms of those intermediate steps which are indicated by dots in the above scheme is not necessary to the further discussion. The intermediate steps may involve the formation of either ions or hot radicals; they have not, as yet, been fully analyzed. It is essential, however, that the rate of formation of final products in reaction (1) is only weakly dependent on the temperature over the interval which includes the stages indicated as I and II above, the excitation energy being much greater than kT. Thus reaction (1) makes a fixed contribution to the hydrocarbon decomposition in stages I and II which is independent of the temperature.

The further history of the hydrocarbon radicals which are formed in reaction (2) is quite different in stages I and II. In the first case, the radicals are stable and the predominant reaction is that of mutual recombination while the aliphatic or mixed radicals which are formed in stage II decompose to a considerable extent to olefins and radicals of lower molecular weight which then undergo further substitution and decomposition.

We will now obtain an expression for the temperature T_p at which stage I begins to pass over into stage II. We will first consider those cases in which cage and similar effects can be neglected. A special instance of this type is found in the radiolysis of gaseous hydrocarbons. Here it can be considered that radio-thermal cracking will begin when the rate of radical decomposition $k_d [R]$ becomes equal to the rate of the reactions which are taking place in stage I. Thus the temperature T_p of transition from stage I to stage II corresponds to

$$k_d [R] \simeq a_1 G_1 I, \tag{3}$$

where $k_d^0 e = k_d e^{-E_d/RT_p}$ is the mean rate constant for radical breakdown, [R] is the concentration of the thermal high-molecular radicals formed in reaction (2), G_1 is the radiochemical yield of reaction (1), I is the dose rate at which radiation is absorbed by the unit volume, and a_1 is a constant of the order of unity. Under the conditions contemplated here a stationary condition is established for the active radical concentration, and the equation of balance for the high-molecular radicals can be written in the form*:

$$I G_R - k_d [R] - k_T [R] [\overline{R}] = 0, \tag{4}$$

where $[\overline{R}]$ is the total radical concentration as determined from the equation:

$$I G_{\overline{R}} - \overline{k}_T [\overline{R}]^2 = 0 \tag{5}$$

G_R is the radiochemical yield of the R radicals from reaction (2), and $G_{\overline{R}}$ is the total radical yield.

The recombination constants k_T and $\overline{k}_T$ can be considered as independent of the temperature [5] and in the final evaluation of T_p it will be supposed that $\overline{k}_T \simeq k_T$.

It follows from Eqs. (4) and (5) that

$$T_p = E_d / R \ln (k_d^0 b / \sqrt{k_T I G_{\overline{R}}}). \tag{6}$$

where the constant $b = (1 - a_1 G_1 / G_R) > 0$ is independent of the temperature. The value of this constant is close to unity and can be neglected. Equation (6) shows the value of T_p to be almost independent of the choice of a_1, a fact which accounts for the comparatively sharp transition from radiolysis to radio-thermal cracking and the weak dependence of T_p on an inhibition which alters the G_R / G_1 ratio. The value of T_p is proportional to E_d and alters only slowly with changing dose rate I. Substitution into (6) of the values: $G_{\overline{R}} \sim 5$ (per 100 ev), $k_T = 10^{-11}$ cm^3/(mole·sec), $k_d^0 = 10^{13}$ sec^{-1}, and E = 25-30 kcal/mole [5] leads to a value of 600°K for T_p, in agreement with the experimental data which have been cited above**.

*Here it is considered that the radicals are predominantly consumed in the formation of low-molecular radicals (CH_3, C_2H_5) and olefin molecules.

**The increase of T_p with I results from the fact that the rate of reaction (1) rises more rapidly than that of reaction (2) as the dose rate is increased.

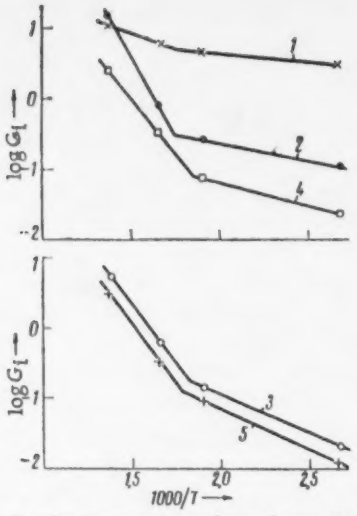

Fig. 3. The temperature dependence of the radiochemical yield of certain gaseous radiolysis products (E is the energy of activation of the process in question in kcal mole):1) Hydrogen, E = 0.5 (stage I), E = 3-4 (stage II); 2) methane, E = 2 (stage I), E = 20 (stage II); 3) propane, E = 4 (stage I), E = 12-13 (stage II); 4) propylene, E = 2-3 (stage I), E = 13-14 (stage II); 5) n-butane, E = 4 (stage I), E = 12-13 (stage II).

We will now analyze the condition for transition from stage I to stage II in the case of liquid hydrocarbons. Equation (6) will still be a valid expression for T_p in the one limiting case in which it is possible to neglect the cage effect. Here it should be kept in view that the value of k_T is several orders less in liquids than in gases [6]. The more rapid dissipation of the energy in liquids results in values of G_1, $G_{\bar{R}}$, and $G_{\bar{\bar{R}}}$ which are less than those found for gases, but this is compensated for in Eq. (6) by the fact that the dose rate at which energy is absorbed by unit volume is generally higher. The second limiting case in that in which there is a strong cage effect*. Here the radical concentration $[\bar{R}]$ must be split into two terms: $[\bar{R}] = [\bar{R}'] + [\bar{R}'']$ (with $G_{\bar{R}} \simeq G_{\bar{R}'}$), the first of which designates the number of radicals per unit volume located pairwise in the cage along with other radicals which were formed at the same time, and the second designates the concentration of the high-molecular radicals which have now diffused outside the cage. The balance equation for the radicals can be written in the form:

$$G_{\bar{R}'} I - 1/\tau_T [\bar{R}'] - k_d [\bar{R}'] = 0, \tag{7}$$

where τ_T designates the time within which recombination reduces $[\bar{R}']$ by a factor 1:e. For this limiting case radical diffusion will be neglected in the balance equation (7). At temperatures in the neighborhood of T_p, the balance equation for $\bar{R}''$ will take the form:

$$1/\tau_D [\bar{R}'] - k_d [\bar{R}''] - k_T [\bar{R}]^2 = 0, \tag{8}$$

where $1/\tau_D$ is the reciprocal of the time required for diffusion of the radical out of the cage.

Equations (7) and (8) show that the rate of destruction to olefins is in this case equal to:

$$G \quad I = k_d [\bar{R}] = k_d ([\bar{R}'] + [\bar{R}'']) \simeq (k_d + 1/\tau_D) G_{\bar{R}'} I (1/\tau_T + k_d)^{-1} \tag{9}$$

direct reactions of type (1) and recombination within the cage both being neglected, the latter in view of the low value of the various liquid steric factors.

It follows from Eq. (8) that the temperature dependence of the destruction reactions will be comparatively weak when $k_d \ll 1/\tau_D \ll 1/\tau_T$. The activation energy must then be equal to the activation energy for diffusion of those light radicals which pass out of the cage. This last fact explains why there is a certain acceleration in the formation of destruction products in stage I of liquid radiolysis which diminishes with the molecular weight of the product in question (see Fig. 3). Equation (9) shows that there will be a rapid increase in the rate of the destruction processes and passage from stage I to stage II at the temperature where

$$k_d = k_d^0 \exp(-E_d / RT_p) \simeq 1/\tau_D \tag{10}$$

this temperature being independent of the dose rate. The temperature dependence of the radiolysis of stage II will be fixed by that of the multiplying factor $k_d/(1/\tau_T + k_d) \simeq k_d \tau_T$ when $k_d \gg 1/\tau_D$, since for the most part $k_d \ll 1/\tau_T$. Equation (10) can be used to evaluate the dimensions of the cage from the expression for the kinetic constants and the experimental data on the radiolysis at various temperatures.

We will now apply these consideration to the case of the radiolysis of gas oil. A study of Fig. 3 and the simplest of kinetic considerations show that the activation energy for the destruction of high-molecular radicals to CH_3 radicals which then react further to form CH_4 must be equal to ~ 20 kcal. Entering Eq. (10) with E = 20 kcal/mole, $k_d^0 = 10^{13} sec^{-1}$, $1/\tau_D = D/d^2$ (d is the cage diameter), and $T_p = 600°K$, one finds a value of 10^{-6} cm for d when $D = 10^{-5} cm^2/sec$. These figures justify the conclusion that the cage effect is quite significant for the radiolysis of liquid hydrocar-

*The term liquid structural cage is to be understood in the sense of [8,9].

bons. It is to be noted that this conslusion is confirmed by the fact that there is an increase in the polymer yield in stage I with energy of activation when the latter is near to the activation energy for diffusion. In conclusion it must be emphasized that the study of stage II (radio-thermal cracking) could be an important and quite simple means of determining the detailed characteristics of a number of elementary acts in chemical reactions.

LITERATURE CITED

1. Yu. G. Nikolaev, Transactions, First Geneva Conference on the Peaceful Uses of Atomic Energy [in Russian] (Moscow, 1955), Vol. 2.
2. M. B. Fiveiskii, M. A. Mokul'skii and Yu. S. Lazurkin, Atom. Énergiya, 9, 4, 321 (1960).
3. P. J. Lucchessi and B. L. Tarmy, Ind. and Eng. Chem., 50, 874 (1958).
4. A. V. Topchiev, L. S. Polak, et al., Doklady Akad. Nauk SSSR, 130, 4, 789 (1960).
5. E. W. P. Steacie, Atomic and Free Radical Reactions, 2nd Ed. (New York, 1954).
6. N. N. Semenov, Certain Problems in Chemical Kinetics and Reactivity [in Russian] (Acad. Sci. USSR Press, 1958).
7. M. A. Mokul'skii, Vysokomolek. Soed. 2, 1, 119 (1960).
8. E. Rabinowitch, Trans. Farad. Soc. 33, 1225 (1937).
9. B. Williamson and V. K. LaMer, J. Am. Chem. Soc. 70, 2, 717 (1948).

All abbreviations of periodicals in the above bibliography are letter-by-letter transliterations of the abbreviations as given in the original Russian journal. *Some or all of this periodical literature may well be available in English translation.* A complete list of the cover-to-cover English translations appears at the back of this issue.

ELECTRICAL DOUBLE LAYER RESULTING FROM DONOR-ACCEPTOR BONDING AT THE CONTACT SURFACE BETWEEN AMORPHOUS SOLIDS

V. P. Smilga

Institute of Physical Chemistry, Academy of Sciences USSR
(Presented by Academician A. N. Frumkin, February 8, 1961)
Translated from Doklady Akad. Nauk SSSR, Vol. 138, No. 5,
pp. 1147-1150, June, 1961
Original article submitted January 19, 1961

In previous papers [1] the role of electrical double layers in adhesion phenomena on crystalline solids was examined. However, from a practical standpoint it is more interesting to examine adhesion processes on polymers and amorphous solids, which generally have a very complicated and irregular molecular structure. It is therefore imperative that one investigate the formation of electrical double layers at the contact surface between two polymers or amorphous solids.

We will assume that the layers adjacent to the surface of one of the two solids in contact are saturated with donor molecules, while the other solid has similarly located acceptor molecules. The number of donor and acceptor molecules per 1 cm^2 will be denoted by N_d and N_a respectively. We will assign certain average positions to the donor and acceptor centers (see Fig. 1). The curve gives the electronic energy, where the energy well N_d corresponds to the ground state of an electron in the donor center and N_a the ground state in the acceptor center; d_1 and d_2 are the distances from the donors and acceptors respectively to the interface; W_0 is the difference between the energy levels for electrons in the donor and acceptor centers. When the energy level of an electron in the acceptor center lies below the level of the donor center the heat of reaction W_0 will be positive.

An important feature of the problem is that the reaction takes place over the entire surface, and consequently every donor-acceptor pair finds itself in an electrostatic field generated by other pairs which had already reacted. This field changes the difference between the electron energy levels, and the heat of reaction will therefore depend on the number of pairs which have reacted. The difference between the potential energy of an electron in a donor center and that of an electron in an acceptor is given by the expression

$$W(n) = W_0 - e\Delta V(n); \tag{1}$$

where $\Delta V(n)$ is the energy difference between the bottoms of the potential wells for electrons in the donor and acceptor centers, both located in the field of other donor-acceptor pairs which had already reacted.

Let us take as a specific example a case where the density of acceptor centers exceeds that of the donor centers ($N_d < N_a$). We will assume that the acceptor centers are so closely packed on the surface that an electron from a donor center can be transferred to the nearest acceptor center located across or "almost across" from the donor center. We would like to point out that all our subsequent derivations are equally valid for the case where the electron of a given donor can "choose" among several acceptors. Let us also point out that from now on it will always be assumed that electrons can not move freely along the surface.

The equilibrium state is defined as one at which the free energy (which is a function of the number of reacted donor-acceptor pairs) of the system is at a minimum. To be more specific the free energy of the system is

$$F = F_0 + \Delta F(n) = F_0 + \Delta E(n) - T\Delta S(n) \tag{2}$$

and the state of equilibrium satisfies the relationship $(\partial F/\partial n)_T = 0$, where $\underline{n}$ is the number of reacted donor-acceptor pairs per 1 cm^2.

The increase in entropy during the reaction is given by the relationship

$$\Delta S(n) \quad k \ln \frac{N_d!}{(N_d - n)!\, n!} \approx k\,[N_d \ln N_d - (N_d - n)\ln(N_d - n) - n \ln n]. \tag{3}$$

Of course, if we have fewer acceptors than donors then N_d in Eq. (3) should be replaced by N_a.

In cases where the electron of every donor center can chose among several acceptor centers the expression for $\Delta S(n)$ will change a little, and in the limiting case where the electron of any one donor may end up on any acceptor the equation will become

$$\Delta S(n) = k\left[\ln \frac{N_d!}{(N_d - n)!\, n!} + \ln \frac{N_a!}{(N_a - n)!\, n!}\right]. \tag{3a}$$

We will confine our investigation primarily to those cases where Equation (3) holds, since all the typical features of the reaction are fully represented by this model, and also in dealing with real problems we find the model very plausible. The change in the internal energy of the system will be $\Delta E(n) = -n[W_0 - e\Delta V]$. Differentiating the free energy with respect to n and evaluating at the minimum we get

$$\left(\frac{\partial F}{\partial n}\right)_T = -W_0 + e\Delta V(n) + en\frac{\partial \Delta V(n)}{\partial n} - kT \ln \frac{N_d - n}{n} = 0, \tag{4}$$

from which we get

$$\frac{n}{N_d - n} = \exp\left[\frac{W_0 - e\Delta V(n) - en\dfrac{\partial \Delta V(n)}{\partial n}}{kT}\right]. \tag{5}$$

In order to determine n we have to know the form of the function $\Delta V(n)$. If the number of reacted pairs is very small at the equilibrium state $\Delta V(n)$ is practically zero; when n increases, the function $\Delta V(n)$ generally becomes quite complicated, since one has to take into account the discrete structure of the double layer. The determination of $\Delta V(n)$ is somewhat similar to the solution of micropotential problems, which are of considerable importance in electrochemistry. Let us note, however, that in our case it is hardly necessary to carry out a rigorous determination of $\Delta V(n)$ with the discrete structure of a double layer taken into account even though the problem can be reduced to a rather tedious though basically simple set of calculations (see, for example [2]).

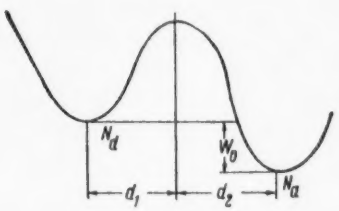

Fig. 1.

As a matter of fact, in the first place, when a double layer with a discrete structure is analyzed one has to postulate some sort of a concrete model (for example, one in which the reacted pairs form a plane hexagonal lattice) so that the $\Delta V(n)$ function will still remain somewhat arbitrary. In the second place, if the number of reacted pairs is large enough (and this in fact is the case we are mostly interested in) one would presumably get a good approximation by representing the double layer as a condenser with the charge "smeared" along one plane. Finally, since there is practically no experimental data at the present time on the nature of donor-acceptor bonding at the interface between two solids, it is hardly necessary to aim at an imaginary rigorous treatment, but instead one should try to provide a qualitative description of the process and to determine to what extent donor-acceptor reactions do influence the forces of adhesion.

The postulated "plane condenser" is entirely satisfactory for our purpose. In such a case $\Delta V(n) = \frac{4\pi en}{\alpha} \times \left(\frac{d_1}{\varepsilon_1} + \frac{d_2}{\varepsilon_2}\right)$. The coefficient α is introduced to take into account the fact that $\Delta V(n)$ depends exclusively on the field of external reacted pairs, while the portion of the "smeared-out charge" connected with the donor-acceptor pair for which $\Delta V(n)$ is determined should not enter into the calculation.

It is very simple to show that as long as the charge density remains large $(1/\sqrt{n} \approx d_1 + d_2)$; the factor α will be a slowly varying function of n and have a value close to one. Once we know the function $\Delta V(n)$ we can derive the equation:

$$\frac{n}{N_d - n} = \exp\left[\frac{W_0 - e\beta V(n)}{kT}\right], \tag{6}$$

where $V(n) = 4\pi en\left(\frac{d_1}{\varepsilon_1} + \frac{d_2}{\varepsilon_2}\right)$ is the potential difference between the faces of the double layer, and $\beta = 2/\alpha$ is independent of n and is close to one in magnitude.

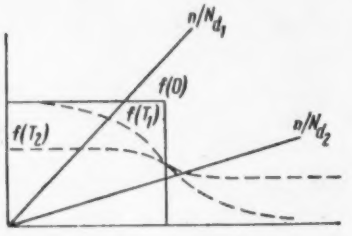

Fig. 2. $f = \frac{1}{1 + \exp\{-[W_0 - \gamma n]/kT\}}$, $N_{d_1} < N_{d_2}$, $T_1 < T_2$.

Equation (6) shows that to find n we have to solve a transcendental equation, which can be done graphically by assigning discrete values to the parameters. One of our problems involves the determination of the order of magnitude of n, and therefore we have to make some reasonable assumptions with regard to the parameters and see what solutions they yield for n.

If we take $d_1 + d_2 \approx 5 \cdot 10^{-8} - 10^{-7}$ cm, $W_0 \approx 0.5$ -1 ev, $N_d \approx 10^{13} - 10^{14}$ cm^{-2} and $\epsilon_1 \approx \epsilon_2 \approx 10$, then one can readily see that n will be a number on the order of 10^{11}-10^{13}. Values of n of this magnitude correspond to a charge density of the double layer of 10^{-2}-10^{-4} CGSE and would provide adhesive forces of hundreds of kilograms per square centimeter.

Hence it is conceivable that in certain cases donor-acceptor bonding and the resulting double layer play a dominant role in adhesion phenomena. An essential prerequisite for the formation of a sufficiently dense double layer is that one of the reacting surfaces be saturated with donor-type and the other with acceptor-type functional groups before coming into contact with each other.

There is quite a large number of known molecules and functional groups with distinct donor or acceptor properties and by selecting appropriate pairs and saturating the surface with them one can count on producing strong adhesion. We would like to point out that N. A. Krotova and L. P. Morozova [4] have already observed a relationship between the density of the electrical double layer and adhesive properties on one hand and chemical modifications of the surface on the other.

In particular, it is well known [3] that long molecules containing conjugated double bonds and nitrogen can readily lose an electron, and it would thus be interesting to examine the adhesive properties of polymers containing such functional groups.

From Eq. (6) one can deduce some very interesting facts pertaining to the formation of double layers. One unique feature of the examined reaction is that the formation of a double layer is a self-quenching process. Whereas initially the transfer of an electron from the donor to the acceptor results in the absorption of energy ($W_0 < 0$) and the reaction is endothermic, as the newly formed double layer grows in size the heat of the reaction becomes more and more negative. As a result one achieves a state of equilibrium at much lower values of n than would be the case if the heat of the reaction remained constant. If $W_0 > 0$ the reaction is initially exothermic. As the double layer grows the heat of reaction declines and it is possible that even before equilibrium is attained the reaction will change from exothermic to endothermic [as soon as $e\Delta V(n)$ exceeds W_0].

We will now introduce the symbol $\gamma = 4\pi e^2\beta\left(\frac{d_1}{\varepsilon_1} + \frac{d_2}{\varepsilon_2}\right)$ and transform Eq. (6) into the form

$$\frac{n}{N_d} = \frac{1}{1 + \exp\{-[W_0 - \gamma n]/kT\}}. \tag{7}$$

Regarding n as a function of T it can easily be shown that if the root of Eq. (7) is such that $\gamma n < W_0$ then n is inversely proportional to T. On the other hand if the root is such that $\gamma n > W_0$ then n is a montonically increasing function of temperature. This can be best demonstrated by a graphical analysis of Eq. (7) (see Fig. 2). The point of intersection between the line $y = n/N_d$ and the curve representing the right hand side of Eq. (7) yields the root of the equation.

One can see in the graph that if the initial concentration of donor centers (keeping other conditions fixed) is increased an exothermic reaction can be changed to an endothermic.

This last result is of particular interest, since it is quite possible that a similar situation arises in chemisoption problems whenever the latter depend on donor-acceptor bonding and in problems connected with the formation of a double layer at a solid-electrolyte interface.

Before concluding we would like to point out that if the change of entropy follows Eq. (3a), then the free energy minimum yields instead of Eq. (5) the expression

$$\frac{n^2}{(N_d - n)(N_a - n)} = \exp\left[\frac{W_0 - e\Delta V(n) - en\,\partial\Delta V(n)/\partial n}{kT}\right]. \quad (8)$$

We wish to thank B. V. Deryagin for his interest in this work.

LITERATURE CITED

1. V. B. Sandomirskii and V. P. Smilga, Fiz. Tverd. Tela 1, 2 (1961); B. V. Deryagin and V. P. Smilga, Doklady Akad. Nauk SSSR 121, No. 5 (1958); V. P. Smilga and B. V. Deryagin, Doklady Akad. Nauk SSSR 122, No. 6 (1958).
2. O. Esin and I. Shikhov, Zhur. Fiz. Khim. 17, 236 (1943).
3. S. Reed, Excited States in Chemistry and Biology [Russian translation] (IL, 1960).
4. N. A. Krotova and L. P. Morozova, Doklady Akad. Nauk SSSR 129, No. 1 (1959).

All abbreviations of periodicals in the above bibliography are letter-by-letter transliterations of the abbreviations as given in the original Russian journal. *Some or all of this periodical literature may well be available in English translation.* A complete list of the cover-to-cover English translations appears at the back of this issue.

A STUDY OF THE SURFACE OF AN IRON ELECTRODE BY MEASURING THE POTENTIAL DECAY AFTER SWITCHING OF THE CURRENT

V. V. Sobol' and Z. A. Iofa

M. V. Lomonosov Moscow State University
(Presented by Academician A. N. Frumkin, February 2, 1961)
Translated from Doklady Akademii Nauk SSSR, Vol. 138, No. 5,
pp. 1151-1154, June, 1961
Original article submitted January 27, 1961

The capacity of an electrode can be calculated from the rate of potential decay after switching off the polarizing current. The capacity is calculated from the formula

$$\Delta\eta_t = b \lg\left(1 + \frac{2{,}3 i_0 t}{Cb}\right), \tag{1}$$

where $\Delta\eta_t$ is the potential decay up to time t, i_0 is the polarizing current density, C is the capacity of the electrode, and b is the coefficient in the Tafel equation. Equation (1) is strictly applicable only under the condition that the electrode self-discharge current depends on the potential in accordance with the Tafel equation, and the capacity of the electrode is assumed to be constant in the investigated overvoltage range. Retardations or plateaus on the curve of the potential in relation to time after switching off the current indicate a disturbance of the normal electrode self-discharge process.

For measurements in the case of large capacities or not very high i_0 values, when the initial portion of the decay curve lasts for not less than 10^{-3} sec, we used an MPO-2 loop oscillograph with electronic amplification of the direct current in the loop with natural oscillation frequency of 2000 cps. In the case of the calculation of small capacities it was necessary to discard some of the points in the initial portion of the decay curve where it was observed that the curve was distorted. An electron oscillograph, with the aid of which it was possible to measure the change in potential after an interval of $5.4 \cdot 10^{-6}$ sec, was used for plotting the curves of decay proceeding at high rate. The errors in the calculation of capacities under different conditions of amplification and scanning rates amounted to 5-7% for the loop oscillograph and 3-4% for the electron oscillograph.

An increase in the overvoltage η_0 was observed in the case of protracted cathodic polarization of iron and also nickel electrodes in alkalies at high current densities, which in [1,2] was considered to be due to increased hydrogen absorption on the electrode and the formation of surface hydrides. In [3] the increase in overvoltage on the iron electrode was explained by surface changes and penetration of hydrogen into the metal. In [4] the authors considered that the increase in overvoltage on iron and nickel was connected to a considerable degree with impurities leached out of the glass cells because the increase in overvoltage was considerably reduced in polystyrene cells. The substances which poisoned the metallic electrodes and increased the overvoltage could also increase the absorption and diffusion of hydrogen into the metal [5,6].

We drew the potential decay curves from experiments carried out with an iron electrode in 1N KOH and 1N LiOH, and also with an iron electrode poisoned with mercury in the same solutions and in 1N H_2SO_4. The experiments were carried out under hydrogen in a polystyrene cell.

Hilger Company iron, plates of which, with observable surface 0.2-0.5 cm^2, were used in our experiments, was reduced in a current of hydrogen at 800-900°. The relationship between the capacity of the iron electrode, calculated from Eq. (1), and the overvoltage in 1N KOH is shown in Fig. 1. With decrease of the starting overvoltage η_0 the capacity, calculated from the initial portions of the decay curves, increased, but after η_0 had fallen to 0.4 v the capacity decreased anew; at this potential the curve is seen to have a maximum.

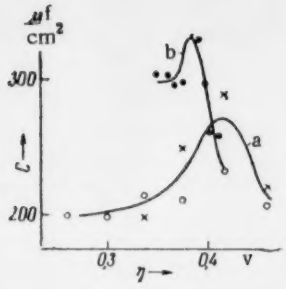

Fig. 1. Relationship between the capacity of the iron electrode in 1N KOH and overvoltage η. a) Capacity calculated from the initial portions of the decay curves (different symbols pertain to different experiments); b) capacity calculated from different protions of a decay curve after polarization at current density 10^{-2} amp/cm^2.

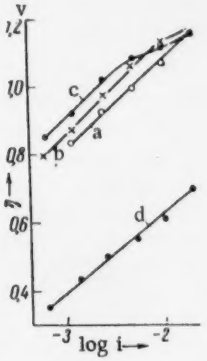

Fig. 2. Stationary polarization curves for an iron electrode poisoned with mercury in 1N KOH for periods: a) 30 sec; b) 3 min; c) 10 min; d) poisoned for 10 min, curve recorded immediately after switching off the current.

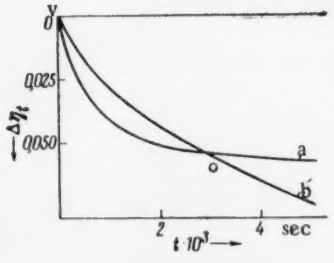

Fig. 3. Dependence of potential decay $\Delta\eta_t$ on time for an iron electrode polarized at current density $i_0 = 10^{-2}$ amp/cm^2. a) Electrode poisoned with mercury for 10 min; b) nonpoisoned electrode in 1N KOH.

The values of the capacity calculated from different portions of a decay curve as a rule increased with time elapsed after switching off the current and also passed through a maximum, but at a somewhat lower overvoltage (Fig. 1b). The high value of the capacity of the electrode in comparison with that of the double layer, and also the increase of capacity with time elapsed after switching off the current, indicated that the electrode surface was highly charged withadsorbed hydrogen; the extent of the charging amounted to 15-20% [4]. The reduction of the capacity when $\eta_0 = 0.4$-0.35 v was probably associated with the fact that the quantity of hydrogen absorbed in the surface, and consequently also its rate of ionization, decreased at these potentials.

For experiments with an iron electrode poisoned with mercury, the electrode was electroplated with mercury by cathodic polarization in 1N KOH solution saturated with HgO, in a separate cell, with current density 10^{-3}amp/cm^2. The extent of the poisoning was determined by the duration of the cathodic polarization. Polarization curves obtained with an iron electrode poisoned to different extents with mercury are shown in Fig. 2. With considerable poisoning, the polarization curves consisted of two parts. At the higher current densities of $2\cdot10^{-2}-5\cdot10^{-3}$ amp/cm^2 the coefficient b = 0.12-0.13, at the lower current densities of $5\cdot10^{-3}-6.3\cdot10^{-4}$ amp/cm^2 the coefficient b fluctuated in the range 0.23-0.26. Similar polarization curves were obtained in [7]. Plateaus were observed on the potential decay curves for highly poisoned electrodes and $i_0 = 2\cdot\cdot10^{-2}-1\cdot10^{-2}$ amp/cm^2. After switching off the current the electrode potential fell at first only by 50-70 mv and then was almost constant for a definite period (of the order of 0.1-1.0 sec), after which it again slowly fell (Fig. 3). With decrease of η_0 the specified plateau disappeared, and the value of the capacity was 100-150 μf/cm^2. With further decrease of i_0 to values of $2.5\cdot\cdot10^{-3}-6.3\cdot10^{-4}$ amp/cm^2, the capacity of the electrode fell to 25-35 μf/cm^2, i.e., to values close to the capacity of the double layer. With weak poisoning for 30 sec [8] the capacity at all current densities did not exceed 35 μf/cm^2.

In experiments for studying the diffusion of hydrogen through the iron plate, it was found that the overvoltage of the electrode poisoned with mercury decreased with diffusion of the hydrogen through it [8]. As was shown by A. N. Frumkin [9], this is possibly due to small charging of the surface with atomic hydrogen as a result of an increase in the rate of electrochemical desorption. The value of the capacity found by us also indicated insignificant charging of the surface of the iron electrode poisoned with mercury with absorbed hydrogen.

The plateaus on the decay curves indicated the presence of anodic processes, occurring when the current was switched off, which retarded the potential decay. The amount of material ionizing when there is a potential plateau can be approximately calculated from the equation

$$n = \frac{i\Delta t}{q}, \qquad (2)$$

where n is the number of ionized atoms, i is the current corresponding to the potential plateau on the polarization curve, Δt is the duration of the delay, and q is the electron charge.

The value of n obtained from decay curves with plateaus was $3\text{-}6\cdot10^{16}$. It is easy to see that plateaus and excessive values of the capacity were observed only after reaching the portion of the polarization curve with coefficient b = 0.12-0.13 and η_0 = 1.0-1.1 v. It may be surmised that at high overvoltages a potassium amalgam formed on the electrode surface in 1N KOH. The amalgam decomposed when the current was switched off, and the electrode potential remained close to the decomposition potential of the amalgam. Ionization of the potassium dissolved in the mercury is an anodic process, as a result of which a plateau was formed on the decay curve.

The value η_0 = 1.1-1.2 v is evidently sufficient for formation of the amalgam since it corresponds to −2.19 v relative to the normal calomel electrode, and the half-wave potential of the potassium ion equals −2.17 v relative to the normal calomel electrode.

The polarization curves shown in Fig. 2 a-c were obtained after protracted polarization. Immediately after switching off the current the polarization curve, even in the case of the greatest poisoning, was considerably below the stationary values (Fig. 2d). In the course of 1.5-2 hours η_0 increased, and the polarization curve assumed the form shown in Fig. 2c. Because when plotting the decay curves the plateaus were obtained only when η_0 had reached 1.1 v, in the case of the electrode conditions corresponding to Fig. 2d, when this value of η_0 was not attained, the capacity after switching off the current for all original current densities, was similar to that when the electrode was weakly poisoned, i.e., 25-35 $\mu f/cm^2$.

Measurements from the initial portions of the decay curves for an iron electrode in 1N LiOH gave values of the capacity of the electrode close to those obtained in 1N KOH, i.e., they amounted to 150-200 $\mu f/cm^2$, the capacity increasing with time elapsed after switching off the current. However in 1N LiOH, even in the case of the electrode poisoned to the highest degree with mercury, a plateau or increased capacity of the electrode in comparison with that of the double layer was not observed on the decay curve. The capacity of the electrode fluctuated in the range 15-25 $\mu f/cm^2$. The absence of a plateau on the decay curve for an electrode in lithium lye can be explained by the fact that lithium amalgam was not formed at the overvoltages attained in the experiment because the half-wave potential of the lithium ion is −2.34 v relative to the normal calomel electrode.

We also measured the capacity of an iron electrode poisoned with mercury in 1N H_2SO_4 with the aid of an electron oscillograph. It was shown that with any degree of poisoning and i_0 values from $8\cdot10^{-2}$ to $6.3\cdot10^{-4}$ amp/cm^2 the capacity of the electrode amounted to 17-20 $\mu f/cm^2$. Hence, plateaus on the decay curves were obtained only in the presence of alkali metal ions which can form amalgams under the given conditions; in all other cases the capacity of the iron electrode poisoned with mercury was close to the capacity of the double layer.

In conclusion we express our sincere thanks to Academician A. N. Frumkin for his kindness and advice given during the execution and discussion of this work.

LITERATURE CITED

1. J. O'M. Bockris and E. C. Potter, J. Chem. Phys. 20, 614 (1952).
2. G. P. Loshchinina, B. N. Kabanov and A. M. Murtazaev, Doklady Akad. Nauk Uzbek.SSR 8, 17 (1956).
3. E. M. Kuchinskii and I. E. Veselovskaya, Trudy Chetvertogo Soveshchaniya po Elektrokhim., Moscow, 1956, (1959) p. 96.
4. V. É. Past and Z. A. Iofa, Doklady Akad. Nauk SSSR 106, 1050 (1956); V. É. Past and Z. A. Iofa, Zhur. Fiz. Khim. 33, 1230 (1959).
5. D. V. Alekseev and M. N. Polukarov, Zhur. Russ. Fiz. Khim. Obshchestva 58, 511 (1926).
6. F. Korber and H. Ploum, Z. Elektrochem. 39, 252 (1933).
7. N. E. Buyanova and G. A. Tsyganov, Trudy Chetvertogo Soveshchaniya po Elektrokhim., Moscow, 1956, (1959) p. 827.
8. I. A. Bagotskaya, Doklady Akad. Nauk SSSR 110, 397 (1956).
9. A. N. Frumkin, Zhur. Fiz. Khim. 31, 1875 (1957).

THE RETARDING EFFECT OF THE URANYL ION IN THE RADIATION-CHEMICAL OXIDATION OF BIVALENT IRON

V. G. Firsov

Institute of Theoretical and Experimental Physics, Academy of Sciences, USSR
(Presented by Academician A. I. Alikhanov, January 23, 1961)
Translated from Doklady Akad. Nauk SSSR, Vol. 138, No. 5,
pp. 1155-1157, June, 1961
Original article submitted January 23, 1961

In the papers [1, 2]it was shown that the uranyl ion retards the radiation oxidation of tetravalent uranium solutions, while the retardation kinetics may be quantitatively described by using the model of an irradiated solution proposed by Allen. In connection with this it appeared important to study the retarding effect of the uranyl ion in the radiation oxidation of bivalent iron.

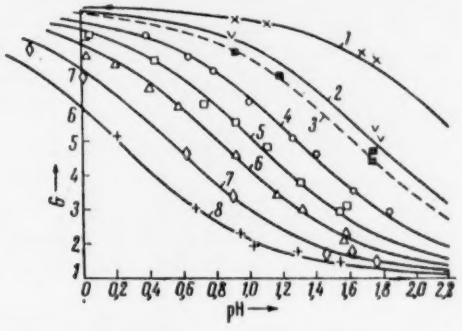

Fig. 1. Dependence of the oxidation yield of Fe^{2+} on UO_2^{2+} concentration and pH of the medium. The curves drawn were calculated from equation (2) using $k_4/k_6 = 0.84$.

Curve No.	1	2	3	4
$[UO_2^{2+}]$, g-eq 10^{-3}	4.26	14.91	20.02	42.60
$[Fe^{2+}]$, g-eq 10^{-3}	50.05	50.50	26.0	50.05
Curve No.	5	6	7	8
$[UO_2^{2+}]$, g-eq 10^{-3}	77.63	129.4	258.8	517.5
$[Fe^{2+}]$, g-eq 10^{-3}	50.05	50.05	50.05	50.05

Experiment. Carefully outgassed solutions of bivalent iron mixed with uranyl sulfate in sulfuric acid were put into quartz ampoules closed with a ground plug in the form of a capillary with a widening. The presence of the capillary secures levelling of the pressure inside and outside without admission of oxygen into the system. The solutions were exposed to the action of γ-rays from a Co^{60} source with a radiation intensity of $1.5\ 10^{19}$ ev/liter·sec [3].

The influence of the UO_2^{2+} concentration upon the oxidation of Fe^{2+} was studied at various acidities of the solution. The results of the measurements, which are given in Fig. 1, show that the yield of Fe^{2+} oxidation falls noticeably when the UO_2^{2+} concentration is raised or the H^+ ion concentration is decreased. The curves of $G_{Fe^{3+}}$ versus the uranyl ion concentration at various pH were obtained from the data of Fig. 1 and plotted in Fig. 2.

Discussion. In the literature, generally, the following scheme is proposed for the radiolytic oxidation of aqueous Fe^{2+} solutions in the presence of O_2 (see, for instance, the papers [4-9]):

$$(n + 2k)\,H_2O \equiv (m + 2l)\,H_2O = nH + m\,OH + k\,H_2 + l\,H_2O_2; \quad (I)$$

$$Fe^{2+} + OH \rightarrow Fe^{3+} + OH^-; \quad (II)$$

$$Fe^{2+} + H_2O_2 \rightarrow Fe^{3+} + OH + OH^-; \quad (III)$$

$$H + H^+ \rightarrow H_2^+; \quad (IV)$$

$$Fe^{2+} + H_2^+ \rightarrow Fe^{3+} + H_2. \quad (V)$$

The retarding action of the UO_2^{2+} ions upon the oxidation of Fe^{2+} obviously is brought about by the reactions:

$$UO_2^{2+} + H \rightarrow UO_2^+ + H^+; \quad (VI)$$

$$UO_2^+ + OH \rightarrow UO_2^{2+} + OH^-, \quad (VII)$$

which have been proposed in the paper [1] for uranyl ion concentrations above 0.05 M. The presence of pentavalent uranium in an irradiated solution of uranyl salts has been proved later on by N. B. Miller, V. I. Veselovskii and V. A. Vorotyntsev*.

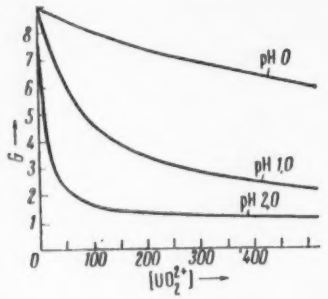

Fig. 2. Influence of the UO_2^{2+} concentration upon $G_{Fe^{3+}}$ at various pH.

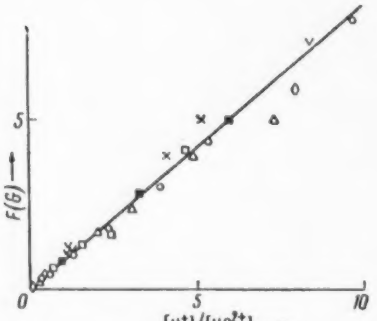

Fig. 3. Relation between $[H^+]/[UO_2^{2+}]$ and $F(G) = \frac{1/2\,G - k}{n + k - 1/2\,G}$

The idea that UO_2^{2+} may compete with Fe^{2+} for the oxidizing radiolysis components, as was assumed in [1] for solutions of tetravalent uranium, leads to the conclusion that the yield of Fe^{2+} oxidation should not depend upon the acidity of the medium. Since this conclusion is contradicted by the results of the present study, such a retardation mechanism has not been taken into account here. Retardation effected by Fe^{3+} is not discussed, since only the initial oxidation yields were determined.

By using the method of stationary states and assuming that $G_{H_2^+} = 0$, one finds when taking into account the reactions (I)-(VII) that G is a function of the concentrations of only two solution components, namely H^+ and UO_2^{2+}:

$$\frac{k_4}{k_6}\,\frac{[H^+]}{[UO_2^{2+}]} = \frac{1/2\,G - k}{n + k - 1/2\,G} = F(G). \quad (1)$$

According to equation (1) a plot of G versus log $[H^+]$ or log $[UO_2^{2+}]$ at a constant concentration of the second component may be obtained in the way [10], as given in the paper [11], namely by plotting G versus log F. Such a curve at all values, for instance, of the UO_2^{2+} concentrations will have the shape of the experimental curve for G versus log $[H^+]$ and differ from the latter only by its position relative to the axis of abscissas. By matching such a theoretical curve to the experimental one the ratio of the constants k_4/k_6 may be calculated. Agreement between the theoretical curve constructed in this way and all experimental curves measured at various values of the UO_2^{2+} concentration is found actually, as is evident from Fig. 1. The curves of Fig. 1 have been calculated from equation (1), while for n and k the values used in the paper [1] have been taken. The extent to which equation (1) is in agreement with the experiment is more clearly visible in Fig. 3 where F(G) is plotted versus the ratio $[H^+]/[UO_2^{2+}]$. The points obtained lie on a straight line passing through the origin, and the slope $k_4/k_6 = 0.84 \pm 0.04$.

*Reported at the Second All-Union Conference on Radiation Chemistry in 1960.

Attention should be drawn to the dashed curve of Fig. 1: it coincides just as well with the theoretical curve although it was obtained by halving the Fe^{2+} concentration. The good quantitative agreement between theory and experiment that is found when the UO_2^{2+} and H^+ concentrations are varied over more than two orders of magnitude proves that the radiolysis model proposed by Allen is fruitful.

It must be supposed that the assumed mechanism of oxidation retardation by the uranyl ion will also be right for other systems. The mechanism adopted for small UO_2^{2+} concentrations in the paper [1] possibly results from the fact that the rate of the reaction U^{4+}+OH is smaller than that of the reaction Fe^{2+}+OH.

I express my gratitude to B. V. Ershler for valuable advice and comments in the discussion and presentation of the results of the present study.

LITERATURE CITED

1. V. G. Firsov and B. V. Érshler, Atomnaya Énerg. 4, 4, 343 (1958).
2. V. G. Firsov and B. V. Érshler, Transactions of the First All-Union Conference on Radiation Chemistry [in Russian] (Moscow, 1958), p. 60.
3. V. G. Firsov, Atomnaya Énerg. 2, 2, 182 (1957).
4. A. O. Allen, Rad. Res. 1, 85 (1954).
5. J. Weiss, Nature 165, 728 (1950).
6. T. Rigg, G. Stein, and J. Weiss, Proc. Roy. Soc. A211, 375 (1952).
7. F. S. Dainton and H. C. Sutton, Disc. Farad. Soc., No. 12, 121 (1952).
8. A. O. Allen, and H. A. Schwarz, Proc. Intern. Conf. on the Peaceful Uses of Atomic Energy, Geneva, 14, 179 (1955).
9. W. G. Rothschild and A. O. Allen, Rad. Res. 8, 101 (1958).
10. B. V. Érshler, Doklady Akad. Nauk SSSR, 129, 866 (1959).
11. B. V. Érshler, M. A. Nezhevenko and G. G. Myasishcheva, Doklady Akad. Nauk SSSR 126, 126 (1959).

All abbreviations of periodicals in the above bibliography are letter-by-letter transliterations of the abbreviations as given in the original Russian journal. *Some or all of this periodical literature may well be available in English translation.* A complete list of the cover-to-cover English translations appears at the back of this issue.

ADSORPTION ISOSTERES IN THE POTENTIAL THEORY

B. P. Bering, Academician M. M. Dubinin,

and V. V. Serpinskii

Institute of Physical Chemistry, Academy of Sciences, USSR
Translated from Doklady Akad. Nauk SSSR, Vol. 138, No. 6,
pp. 1373-1376, June, 1961
Original article submitted March 22, 1961

It is well known that the adsorption isosteres, that is, the curves expressing the relation between equilibrium pressure and temperature at a constant amount adsorbed, when plotted in the coordinates log p versus 1/T are usually in a more or less broad temperature range satisfactorily approximated by straight lines. For examples, it will suffice to point to several papers [1-3] in which sets of linear adsorption isosteres are given for many substances on various adsorbents. In all cases where in some temperature range the state of the adsorbed substance does not change, the adsorption isostere remains practically linear in this range. A break in the isostere or a smoother change of its slope in a narrow temperature range is characteristic of the appearance of a phase transition in the adsorbed substance. Thus, the nearly linear character of the adsorption isosteres in the existence region of a homogeneous adsorbed phase may be considered as an experimental fact of very general importance. When studying the adsorption equilibrium one usually measures the relation between adsorption and pressure at a constant temperature, that is, one determines the adsorption isotherm. Only recently in isolated cases has anyone started to carry out direct experimental measurements of the adsorption isosteres [4, 5]. In some respects the adsorption isostere is a more important characteristic of the adsorption equilibrium than is the traditional isotherm, since the former allows one to determine the differential heat and entropy of adsorption. The nearly linear character of the isosteres, as is found experimentally, is not an obvious consequence of the basic ideas of physical adsorption theory. The best known isotherm equations either do not contain in an explicit form the relation between the equation parameters and T or they give a complicated relation between the pressure p and the temperature T at a = const, from which it does not follow that in the general case the isosteres will be linear. The potential theory, which in principle enables one to find the relation between adsorption and temperature from the characteristic curve and to construct the adsorption isosteres, is an exception. However, until now the question of the shape of these isosteres has not been discussed. Below we will examine the conditions under which the linearity of the isosteres follows from the potential theory.

As is well known, the development of the potential theory in the papers [6,7] enabled us to obtain thermal equations for vapor adsorption on two structural types of sorbents; these equations give an explicit relation between adsorption and temperature. First we will discuss the equation for adsorbents of the first structural type:

$$a = (W_0 / v) \exp |- (BT^2 / \beta^2) \lg (p_s / p)|, \tag{1}$$

where W_0 and B are constants characterizing the adsorbent and v, p_s and β are the molar volume of the adsorbate, its saturated vapor pressure and the affinity coefficient of the characteristic curve, which coefficient can be approximated as the ratio between the adsorbate parachor and that of the standard substance [7]. Equation (1) may be written in the following form:

$$\ln p = \ln p_s - 2{,}30\, \beta B^{-1/2} [\ln (W_0 / av)]^{1/2} \cdot 1 / T, \tag{2}$$

which at a = const gives the equation of the adsorption isostere in the coordinates ln p and 1/T, where v is considered to be a function of T. In agreement with the vast amount of experimental data we will start from the assumption that the latent heat of vaporization may always be taken constant in a more or less broad temperature range, that is,

$$\lambda = Rd \ln p_s / d (1 / T) = \text{const}, \tag{3}$$

and consequently:

$$\ln p = - (\lambda / R) \cdot 1 / T + C_s. \tag{4}$$

By differentiating equation (2) with respect to 1/T at $\underline{a}$ = const we obtain:

$$Q = -R\left(\frac{\partial \ln p}{\partial (1/T)}\right)_a = \lambda + 2{,}30\beta RB^{-1/2}\frac{\partial}{\partial (1/T)}\left[\left(\ln\frac{W_0}{av}\right)^{1/2}\frac{1}{T}\right]_a, \tag{5}$$

where by Q we denote the differential isosteric heat of adsorption. Let us find the shape of the function v(T) at which Q = const and, consequently the isostere (2) is linear, that is, is expressed by an equation of type (4). It is evident from equation (5) that under the condition (3) Q will be a constant, if at $\underline{a}$ = const

$$[\ln (W_0/av)]^{1/2}\cdot 1/T = K/T + D$$

or

$$F_1(T) = [\ln (W_0/av)]^{1/2} = [\ln (v_m/v)]^{1/2} = K + DT. \tag{6}$$

Because of this

$$\ln v = \ln v_m - (K + DT)^2, \tag{7}$$

where K and D do not depend upon T, and $v_m = W_0/a$. The value of v_m represents the highest possible value for the molecular volume $\underline{v}$ of the adsorbed substance, and at this value for a given isostere the entire volume of the adsorption space is filled at some temperature T_m. It is evident that the substitution of this equation for ln $\underline{v}$ into equation (2) gives a linear relation of the type of equation (4) for the isostere. From equation (7) it follows that isosteres (6) will be exactly linear only if the molar volume of the substance in the adsorbed state is a function of temperature of the form

$$\ln v = m + \alpha T + cT^2, \tag{8}$$

where $\alpha > 0$ and $\underline{c} < 0$.

Generally, the molar volume of a substance in the normal three-dimensional state is satisfactorily approximated by equation (8), but, however, with a positive rather than a negative value of the coefficient $\underline{c}$. From this it follows that when one substitutes the value of ln $\underline{v}$ from equation (8) for the normal three-dimensional phase (with $\underline{c} > 0$) into equation (2), the isosteres will deviate somewhat from linearity (especially near T_{cr}). However, calculations by means of equation (2) which we have carried out, for example, for the isosteres of benzene adsorption on activated charcoal have shown that these deviations, even in the range 0-170°, are still very small and the isosteres remain practically linear. It should be noted that the linear relation for the volume of the adsorbed substance v^* as a function of T between T_{boil} and T_{cr}, as was introduced in the paper [8], may be approximated by equation (8) with a coefficient $\underline{c} < 0$, and therefore substitution of ln v^* into equation (2) in a good approximation will result in a linear isostere even at temperatures close to T_{cr}.

In a narrower range of T (not very close to T_{cr}) for many substances the quadratic term in equation (8) is small (especially in the region in which the solid phase exists) and it may be neglected. Under this condition

$$\ln v = m + \alpha T, \tag{9}$$

and consequently the actual expansion coefficient α is a constant:

$$\alpha = \frac{1}{v}\frac{dv}{dT} = \text{const}. \tag{10}$$

Calculations which we have carried out for various particular cases (for instance, for the adsorption of alkanes from C_4 to C_8 on zeolites from data of [1]) show that upon substituting ln $\underline{v}$ from equation (9) into the relation (6) and then expanding the function $F_1(T)$ obtained in a power series of T one may restrict oneself with a good degree of accuracy to the term containing the first power of T. Therefore, if in a given temperature range ln $\underline{v}$ may be represented by equation (9), then F_1 will be satisfactorily approximated by a linear function of T, and consequently the isostere (2) will be nearly linear.

Now we will look at the thermal equation of the adsorption potential theory for adsorbents of the second structural type [7]:

$$a = (W_0'' / v) \exp [- (AT / \beta) \lg (p_s / p)], \tag{11}$$

where W_0'' and A are constants not depending upon temperature and characteristic for the adsorbent, and v, β and p_s have the same meaning as in equation (1). Just as above, it is sufficient to solve equation (11) with respect to ln p at a = const in order to obtain the equation of the adsorption isostere:

$$\ln p = \ln p_s - \frac{2{,}30\beta}{A} \frac{1}{T} \ln \frac{W_0'}{av}. \tag{12}$$

As we did above, we will assume that in the temperature range given, condition (3) is met, that is, λ = const. Under this condition the isostere equation (12) will be linear, and consequently the heat of adsorption Q = const, if $F_2(T) = \ln (W_0''/av)$ is a linear function of temperature. When we use equation (9) for the relation between v and T, we obtain:

$$F_2'(T) = \ln \frac{W_0'}{av} = \ln \frac{W_0'}{a} - m - \alpha T = l - \alpha T. \tag{13}$$

Upon substituting F_2 into equation (12) we obviously get a strictly linear isostere equation of the type of relation (4).

Thus, if in the temperature range given the conditions

$$\lambda = \text{const}, \quad \alpha = d \ln v / dT = \text{const} \tag{14}$$

are met, that is, if the latent heat of vaporization and the actual expansion coefficient are constants, then in this approximation both for adsorbents of the first [equation (1)] and for those of the second structural type [equation (11)] the adsorption isosteres are linear and the isosteric heats of adsorption are constant. The deviation from linearity of ln v in equation (8) at $c > 0$ in both cases results in some bending of the isostere over a broad temperature range.

If in the temperature range considered the conditions

$$\lambda = \text{const}, \quad Q = \text{const} \tag{15}$$

are met, then it is easy to show that along an isostere a = const the differential adsorption entropy is constant. In fact, let us write down Gibbs-Helmholtz equation for the adsorption equilibrium

$$q = Q - \lambda = \varepsilon - T\Delta S = \varepsilon - T (\partial \varepsilon / \partial T)_a, \tag{16}$$

where ϵ is the adsorption free energy and ΔS the differential adsorption entropy. If we choose the liquid at the temperature T as standard state, then

$$\varepsilon = RT \ln (p_s / p). \tag{17}$$

At the same time

$$\Delta S = (\partial \varepsilon / \partial T)_a. \tag{18}$$

By differentiating equation (16) with respect to T under the condition of (15) and taking into account (18) we obtain

$$(\partial^2 \varepsilon / \partial T^2)_a = (\partial \Delta S / \partial T)_a = 0,$$

from which it follows that at a = const the differential entropy ΔS = const. We note that a similar result has been obtained in the paper [2] where the gas phase at 1 atm pressure was chosen as the standard state. In this paper by studying the adsorption of hydrocarbons on the synthetic zeolite faujacite it was found that for all substances examined the value ΔS was constant along the linear isosteres. Similarly, constant values of ΔS along the linear isosteres of CO_2 adsorption on silica gel were obtained by us when we treated the experimental data of the paper [3].

Thus, if in some temperature range simultaneously λ = const and Q = const or if $q = Q - \lambda$ = const, then along the isostere the differential adsorption entropy remains constant independent of the particular form of the equation for the adsorption isostere. Consequently, linear adsorption isosteres are characterized by the fact that the differential

heat and entropy of adsorption are simultaneously constant. From the discussion above it may be confirmed that in the approximation given the linearity of the isosteres and the constancy of the Q and ΔS values are consequences of the basic equations (1) and (11) of the adsorption potential theory.

LITERATURE CITED

1. A. Titow, Zs. phys. Chem. 74, 641 (1910).
2. R. M. Barrer and J. W. Sutherland, Proc. Roy. Soc. A237, 439 (1956).
3. B. N. Vasil'ev, B. P. Bering, M. M. Dubinin and V. V. Serpinskii, Doklady Akad. Nauk SSSR 114, 131 (1957).
4. B. R. Puri, Y. P. Myer and D. D. Singh, Trans. Farad. Soc. 53, 503 (1957).
5. C. Hodgson and R. McIntosh, Canad. J. Chem. 38, 958 (1960).
6. M. M. Dubinin, E. D. Zaverina and L. V. Radushkevich, Zhur. Fiz. Khim. 21, 1351 (1947); M. M. Dubinin and E. D. Zaverina, Zhur. Fiz. Khim. 23, 1129 (1949).
7. M. M. Dubinin, Studies in the Field of Gas and Vapor Adsorption by Hydrocarbon Adsorbents, Lectures Held in Upsala [in Russian] (Acad. Sci. USSR Press, 1956).
8. M. M. Dubinin and K. M. Nikolaev, Izvest. Akad. Nauk SSSR, Otdel. Khim. Nauk, No. 10, 1665 (1958).

All abbreviations of periodicals in the above bibliography are letter-by-letter transliterations of the abbreviations as given in the original Russian journal. *Some or all of this periodical literature may well be available in English translation.* A complete list of the cover-to-cover English translations appears at the back of this issue.

THE EFFECTS OF ALKALI METAL CATIONS ON THE HYDROGEN OVERVOLTAGE AT A MERCURY ELECTRODE IN ACID SOLUTIONS

É. A. Maznichenko, B. B. Damaskin

and Z. A. Iofa

The M. V. Lomonosov Moscow State University

(Presented by Academician A. N. Frumkin, February 8, 1961)
Translated from Doklady Akad. Nauk SSSR, Vol. 138, No. 6,
pp. 1377-1380, June, 1961
Original article submitted February 3, 1961

Investigation of the relation between the capacity of the electric double layer and the nature of the alkali metal cation [1,2] has shown that there is a somewhat more than equivalent adsorption of large radius cations at the surface of the mercury electrode. This is in agreement with the results of studies on the effects of cations on the kinetics of electrochemical processes [3-9]. It was therefore of interest to investigate the effects of alkali metal cations on cathodic hydrogen evolution at a mercury electrode, since the theory of this process has been more completely developed.

The hydrogen overvoltage η was measured at a dropping mercury electrode for the following solutions: 0.01 N HCl alone and with 0.1, 0.33, and 1 N LiCl, NaCl, KCl RbCl, and CsCl; 0.001 N HCl alone and with 0.001, 0.01, and 0.033 N LiCl, KCl, and CsCl.

In 0.001 N HCl the polarization curves were corrected for concentration polarization by the method of Meiman and Bagotskii [10]. In 0.01 N HCl, the measured current I was considerably less than the limiting value, so that concentration polarization could be neglected. In this case, the current density i, corresponding to a definite η, was calculated from the measured current $\bar{I}$ and the mean drop area as given by the formula $\bar{s} = 0.509\,(m\tau)^{2/3}$, where m is the flow rate of mercury from the capillary, and τ is the mercury drop time at the given potential. The η, log i curves obtained in this way agreed with curves recorded for a stationary mercury electrode, so that the method of calculation allowed for the correction associated with the use of a dropping electrode [11].

In the dilute solutions, the ohmic fall in potential was calculated from the formula:

$$\Delta\varphi = \frac{\bar{I}}{4\pi\varkappa}\left[\frac{4{,}82a}{m^{1/3}\tau^{1/3}} - 1\right],$$

where $\varkappa$ is the specific electrical conductivity, and a is the distance between the tip of the Luggin capillary and the drop center.

A linear relation between η and log i was observed in the region of current density investigated, $10^{-4.8}$ to $10^{-3.5}$ amp/cm^2. The slope of the curves was 0.110-0.111 v for salt concentrations up to 0.33 N, and 0.116 v for normal solutions. The experiments were carried out at negative potentials, when there should be no adsorption of the Cl^- anion. The reproducibility in the values of η from experiment to experiment was ± 3 mv.

Table 1 shows the values of η for all the HCl and salt concentrations investigated, for log i = −4 and t = 22°. It is clear that for solutions of the same concentration η increased from Li^+ to Cs^+. According to the fundamental equation of the theory for delayed discharge

$$\eta = \text{const} + \frac{RT}{\alpha F}\ln i + \frac{1-\alpha}{\alpha}\left(\psi_1 - \frac{RT}{F}\ln[H^+]\right) \qquad (1)$$

and increase in η is associated with a shift of the ψ_1 potential in the positive direction. Since the total electrolyte concentration remained constant, it is evident that the ψ_1 potential became more positive in value as the result of an increase in cation adsorption with increase in cation radius.

TABLE 1. Hydrogen Overvoltage η (in Volts)

	0,001 *N* HCl			0,01 *N* HCl			
	Metal cation concentration						
	0,001 *N*	0,01 *N*	0,033 *N*	0	0,1 *N*	0,33 *N*	1 *N*
—	—	—	—	0,964	—	—	—
Li^+	0,976	1,000	1,022	—	0,999	1,022	1,034
Na^+	—	—	—	—	1,009	1,030	1,042
K^+	0,980	1,011	1,033	—	1,011	1,033	1,044
Rb^+	—	—	—	—	1,025	1,048	1,057
Cs^+	0,994	1,037	1,059	—	1,036	1,059	1,069

Let us consider the relation between η and supporting electrolyte concentration for each cation, andcompare it with the increase in overvoltage $\Delta\eta$ for the change from pure acid to a solution of the given composition, as calculated from the equation based on the diffusion theory of the double layer. Ignoring the nature of the cation, then the value of $\Delta\eta$ should be given by the approximate formula

$$\Delta\eta = \frac{1-\alpha}{\alpha}\frac{RT}{F}\ln\frac{C}{[H_3O^+]}, \qquad (2)$$

where C is the total electrolyte concentration; this formula gives a value close to the theoretical with $\alpha = 0{,}527$ [13].

It follows from equation (1) that with ln i = constant and pH = constant, then $\Delta\eta = \Delta\psi_1$. We can thus compare our experimental values of $\Delta\eta$ and those obtained from equation (2) with the corresponding values of $\Delta\psi_1$, i.e., the increases in ψ_1 on changing from pure HCl to HCl of the same concentration with added salts, calculated from capacity data in accordance with Grahame's theory. The experimental and calculated results for acid solutions of LiCl, KCl, and CsCl are given in Table 2. It is clear that for all electrolyte concentrations except the highest the closest agreement between the experimental values of $\Delta\eta$ and the theoretical values of $\Delta\eta$ and $\Delta\psi_1$ was obtained with KCl solutions. Our experimental values of $\Delta\eta$ for KCl were approximately 10% lower than those of Bagotskii [15], possibly because we obtained higher η values in pure HCl.

TABLE 2

HCl concn.	Salt concn.	$\Delta\eta$ experimental, mv	$\Delta\eta$ from Eq. (2), mv	$\Delta\psi_1$ from capacity, mv	$\Delta\psi_1$ from Brodowsky-Strehlov theory, mv
0,001 *N*	0,001*N* LiCl	12		17,6	
	0,001*N* KCl	16	16	16,8	
	0,001*N* CsCl	30		15,8	
0,001 *N*	0,01*N* LiCl	36		56,2	
	0,01*N* KCl	47	55	55,2	
	0,01*N* CsCl	73		53,3	
0,001 *N*	0,033*N* LiCl	58		84,7	
	0,033*N* KCl	69	81	82,9	
	0,033*N* CsCl	95		78,3	
0,01 *N*	0,1*N* LiCl	35		58,6	52
	0,1*N* KCl	47	55	56,5	60
	0,1*N* CsCl	72		53,7	
0,01 *N*	0,33*N* LiCl	58		82	
	0,33*N* KCl	69	81	81,5	
	0,33*N* CsCl	95		78,2	
0,01 *N*	1*N* LiCl	70		104,4	94
	1*N* KCl	80	106	104,1	117
	1*N* CsCl	105		101	

All the experimental values of $\Delta\eta$ for LiCl were lower and those for CsCl higher than the theoretical, suggesting that the cation concentrations in the double layer were lower for Li^+ than for K^+, and higher for Cs^+. Thus the Li^+ ions evidently showed negative specific adsorption, probably owing to their high tendencey to hydration; they would be more likely to be in the bulk of the solution, where they are fully hydrated, than in the double layer, where

TABLE 3

Salt cation	0,001N HCl						0,01N HCl					
	Salt cation											
	0,001 N		0,01 N			0,033 N		0,1N		0,33 N		1 N		
	$\Delta\Delta\eta$ exp., mv	$\Delta\Delta\psi_1$ calc., mv, a)	$\Delta\Delta\eta$ exp., mv	$\Delta\Delta\psi_1$ calc., mv		$\Delta\Delta\eta$ exp., mv	$\Delta\Delta\psi_1$ calc., mv, a)	$\Delta\Delta\eta$ exp., mv	$\Delta\Delta\psi_1$ calc., mv		$\Delta\Delta\eta$ exp., mv	$\Delta\Delta\psi_1$ calc., mv, a)	$\Delta\Delta\eta$ exp., mv	$\Delta\Delta\psi_1$ calc., mv	
				a	b				a	b				a	b
Li^+	4	—1,3	11	—2	9	11	—3,6	12	—3	13	11	—1,2	10	—0,8	22
K^+	14	—2,3	26	—3,9		26	—5,7	25	—4,3		26	—5	25	—4	
Cs^+															

Note: a) Grahame theory; b) Brodowsky-Strehlov theory.

partial dehydration of cations can occur. The increased concentration of Cs^+ ions in the double layer, which is in accordance with literature data, is probably due to specific adsorption.

It is evident from Table 2 that when the supporting electrolyte concentration was increased to 1 N the experimental values of $\Delta\eta$ in KCl solutions were considerably less than the theoretical, which in this case agreed better with the experimental values for CsCl. According to the differential capacity literature data [2], this may be due to an attraction of Cl^- anions into the double layer, which reduces the effect of the specific adsorption of Cs^+ cations.

It is interesting to compare experimental values of $\Delta\Delta\eta$ for replacement of Li^+ by K^+ ions and of K^+ by Cs^+ ions in solutions of the same concentration with the theoretical values of $\Delta\Delta\psi_1$ for the solutions. It is evident from Table 3 that electrostatic calculations of $\Delta\Delta\psi_1$ based on Grahame's theory, assuming no specific adsorption of cations, give negative values, which is in conflict with experimental kinetic data.

Tables 2 and 3 show values of $\Delta\psi_1$ and $\Delta\Delta\psi_1$ for K^+ and Li^+ ions calculated from the Brodowsky-Strehlov theory [16,17]. The calculations were carried out graphically, using the following values for the effective ionic radii: H^+ and Li^+ r = 5 A, K^+ and Cs^+ r = 3 A*. According to this theory, the value of $\Delta\psi_1$ for a high supporting electrolyte concentration is close to that calculated from the diffusion theory of the double layer (Table 2). On the other hand, $\Delta\Delta\psi_1$ for the change from Li^+ to K^+ has the same sign as the experimental value of $\Delta\Delta\eta$ (Table 3). In dilute solutions there was quantitative agreement between theory and experiment.

The increase in η on changing from Li^+ to K^+ can be explained theoretically [16,17] by the more positive value of ψ_1 in KCl due to the high concentration of K^+ ions in the double layer as the result of their small effective volume. However, it follows from this theory that the increase in η should be greater on changing from Li^+ to K^+ than from K^+ to Cs^+, since the difference in effective ionic radius, as calculated from the mobilities [19], is very much greater in the first case than in the second. It is evident from Table 3 that this deduction is contrary to the experimental data: the experimental value of $\Delta\Delta\eta_{Cs^+-K^+}$ is more than twice $\Delta\Delta\eta_{K^+-Li^+}$. Thus the theoretical premises of Brodowsky and Strehlov are inadequate to account for the value of $\Delta\Delta\eta_{Cs^+-K^+}$. It is evidently necessary to take into account the effect of specific adsorption.

In our experiments the effect of cations on the rate of the process was less specific than in the reduction of the $S_2O_8^{2-}$ anion. This can be explained in part on the basis of the delayed discharge theory, since the effect of cations is greater the greater the absolute value of the ψ_1 potential coefficient. This coefficient is $(n-\alpha)/\alpha = -8.1$ for the $S_2O_8^{2-}$ anion and $(1-\alpha)/\alpha = +1$ for hydrogen reduction. At the same time, $\Delta\Delta\psi_1$, as calculated from the delayed discharge theory for the change from 0.01 N KCl to 0.01 N CsCl, is 65 mv for reduction of 0.001 N $S_2O_8^{2-}$ and 37 mv for reduction of 0.001 N H^+. This divergence is evidently associated with the approximate character of the ψ_1 potential in the vicinity of the adsorbed ions.

We are very grateful to Academician A. N. Frumkin for his deep interest in this work and to his valuable advice in discussions on the experimental results.

* These values for the effective ionic radii were gross approximations to the radii of the F^- and Cl^- anions, since they have only been determined for these ions. The ratios of the ionic radii were determined (except for H^+) from the ratios of the mobilities. Calculation of the absolute effective ionic radii from Stokes's equation and the mobilities [18] gave considerably lower values which eliminated the difference between the Grahame and Brodowsky-Strehlov theories.

LITERATURE CITED

1. D. C. Grahame, J. Electrochem. Soc., 98, 343 (1951).
2. A. N. Frumkin, B. B. Damaskin, and N. V. Nikolaeva-Fedorovich, DAN, 115, 751 (1957); DAN, 121, 129 (1958).
3. A. N. Frumkin, Usp. Khim., 24, 933 (1955).
4. N. V. Nikolaeva and B. B. Damaskin, Proceedings of the Fourth Conference on Electrochemistry [in Russian] (Izd. AN SSSR, 1959), p. 150.
5. I. Žežula, Chem. Listy, 47, 492 (1953).
6. S. I. Zhdanov, V. I. Zykov, ZhFKh, 32, 644 (1958).
7. N. A. Izgaryshev, Kh. M. Ravikovich, ZhRFKhO, 62, 255 (1930); I. A. Izgaryshev and E. Ya. Maiorova, ZhOKh, 6, 1208 (1936).
8. S. V. Gorbachev and R. M. Vasenin, ZhFKh, 28, 135, 1795, 1922, 1928, 2157 (1954).
9. P. Herasimenko and P. Šlendyk, Zs. phys. Chem., A 149, 123 (1930).
10. N. Meiman, ZhFKh, 22, 1454 (1948); V. S. Bagotskii, ZhFKh, 22, 1466 (1948).
11. Z. A. Iofa and A. N. Kolychev, ZhFKh, 14, 58 (1939).
12. A. N. Frumkin, V. S. Bagotskii, Z. A. Iofa and B. N. Kabanov, Kinetics of Electrode Processes [in Russian] (Moscow, 1952).
13. A. N. Frumkin, ZhFKh, 24, 244 (1950).
14. D. C. Grahame, Chem. Rev., 41, 441 (1947).
15. V. S. Bagotskii, DAN, 58, 1387 (1947).
16. H. Brodowsky and H. Strehlov, Zs. Elektrochem., 63, 262 (1959).
17. H. Brodowsky and H. Strehlov, Zs. Elektrochem., 64, 891 (1960).
18. E. Guggenheim and J. Prue, Physico-Chemical Calculations [Russian translation] (Moscow, 1958).
19. R. Parsons, Handb. Electrochemical Constants (London, 1959).

All abbreviations of periodicals in the above bibliography are letter-by-letter transliterations of the abbreviations as given in the original Russian journal. *Some or all of this periodical literature may well be available in English translation.* A complete list of the cover-to-cover English translations appears at the back of this issue.

THE PHOTOCONDUCTIVITY KINETICS OF CHLOROPHYLL AND GREEN LEAF PIGMENTS

E. K. Putseiko

(Presented by Academician A. N. Terenin, December 26, 1960)
Translated from Doklady Akademii Nauk SSSR, Vol. 138, No. 6,
pp. 1381-1384, June, 1961
Original article submitted December 12, 1960

In the paper by Nelson [1], who studied the photoconductivity of chlorophyll and of methylchlorophyllide a; the rise and decay of the photocurrent with time had two time constants, one less than a second and the order of the order of several minutes. He attributed the two time constants to two different forms of aggregation of the pigment – colloidal and crystalline.

In the present work the relaxation processes in solid films of chlorophyll and its analogues were studied for the initial stages of the rise and decay of the photocurrent. Crystalline films of chlorophyll (a + b) and methylchlorophyllide (a + b), isolated in the Botanical Institute, Academy of Sciences, USSR, were used for the investigation. In addition the green leaf pigments of nettles and jasmine, isolated from acetone extracts were studied. Such extracts contained in addition to chlorophylls a and b, the prinicipal leaf carotinoids (β-carotene, lutein, violaxanthin, and neoxanthin) and the lipoprotein fraction of the disintegrated chloroplasts. Although in the process of extraction the lipoprotein complex is broken down, it may be expected that the chlorophyll still remains bound with the carotinoids, and its phytyl chain with the lipoids.

The films to be studied were precipitated from concentrated solutions of the pigments in chloroform or acetone onto quartz plates carrying on their surfaces coated platinum electrodes in the form of two combs with 0.1-mm gaps. To the photoresistant electrodes was applied a voltage of 100-200 v. The film thickness varied from 0.01 to 1μ.

Relaxation of the photoconductivity of the chlorophyll films as well as of phthalocyanins [2] was investigated by the τ-meter method [3] permitting observation of the entire course of the rise and decay of the photocurrent in the time range $5 \cdot 10^{-6}$ to 10^{-2} sec. Illumination was effected with visible light, modulated at a 100 cps frequency from a SVDSh-120 mercury vapor lamp, passed through a ZhS-12 yellow light filter (thickness 2 mm). Illumination power was from 10^{-3} to 10^{-5} watt/cm.

1. Investigation of the photoconductivity kinetics of crystalline films of chlorophyll (a + b) in air at room temperature showed that the rise and decay of photocurrent for all samples studied occurred over a wide time range, from a few microseconds up to seconds and minutes. In Fig. 1 are shown the oscillogram photographs of the relaxation curves for the rise and decay of photocurrent with time, for samples of crystalline chlorophyll (a + b) in air, as the linear (A) and exponential (B) evolutes. For an illumination with a rectilinear light impulse lasting 10^{-2} sec the photoconductivity in the chlorophyll (a + b) films in air did not reach a steady value. The photocurrent rise curves in the majority of cases were symmetrical with the decay curves. Part of the inertia component was large and was almost 80% of the "maximum" value of the photocurrent. In general the character of the rise and decay of photocurrent was not exponential.

By means of the exponential evolute on separate sections of the decay curve it was possible to distinguish three exponents, one with a short time constant: $\tau_1^{\text{Decay}} = 3 \cdot 10^{-5}$ sec, and the others with longer constants, $\tau_2^{\text{Decay}} = 6 \cdot 10^{-3}$ sec, $\tau_3^{\text{Decay}} = 1.7 \cdot 10^{-2}$ sec. Determination of the law governing the photocurrent decay in the materials studied was made by means of a graph of the "instantaneous" relaxation times [4]. In Fig. 2, 1 is represented the decay of photocurrent with time for a chlorophyll (a + b) film in air measured on the τ-meter by means of the exponential evolute by the method of "partial times". On curve 1 of the same figure are shown the "instantaneous" relazation times θ, characterizing the reciprocal logarithmic derivative of the photocurrent with time. Analysis of the decay curves by means of such graphs showed that in the rapid time range from a few microseconds up to 10^{-3} sec the photocurrent decay was hyperbolic, $I_{\text{Decay}} = I_0/(1 + at)^{\alpha}$, which indicated the process of recombination of charges to be bimolecular. This fundamental result was obtained for different crystalline chlorophyll films under a variety of conditions.

The experiments showed that for the same chlorophyll (a+b) film after evacuating the air, the lag was already sharply reduced at room temperature. In Fig. 1b are shown curves of the photocurrent variation with time for one of the described crystalline chlorophyll (a+b) films under vacuum with and without illumination as linear (A) and exponential (B) evolutes.

From the given results is is seen that the slow component part of the photocurrent decay in vacuum is 50% of the steady value, and the inertia of the rapid and slow components is reduced by a factor of 5 or more. In the initial stages the rise and decay of the photocurrent took place with rapidity, exceeding the time constant of the apparatus itself. In the photocurrent rise curves under vacuum conditions, "instantaneous" jumps in the photocurrent were observed, apparently caused by supplementary electron transitions, having a longer duration the more finely divided the crystal levels.* Rise of the photocurrent proceeded more rapidly than the decay.

In the exponential evolute it was possible to distinguish on separate sections of the decay curves three exponents, one with very short (less than microseconds) and the others with longer times $\tau_{\frac{1}{2}}^{HL} = 10^{-4}$ sec** and $\tau_3^{Decay} = 1.2 \cdot 10^{-2}$ sec. As in air, the photocurrent decay in chlorophyll films in vacuum after cutting off illumination was described by a hyperbolic law(Fig. 2, 2 and 2'). The phenonomen was reversible and after admission of air the duration of the photoelectric processes was again increased (Fig. 1c). The adsorped vapor of quinone at a pressure of about 0.02 mm of mercury had the same effect on the photoconductivity kinetics as air. In contrast to this, admission of water vapor at a pressure of 14 mm of mercury to previously evacuated chlorophyll samples did not have any marked effect on the photoconductivity relaxation. Apparently in air or in quinone vapor the electrons in the chlorophyll molecules are localized in coherent levels which increase the duration of the recombination processes.

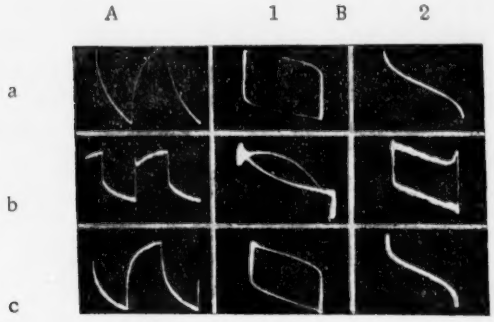

Fig. 1. Photoconductivity kinetics of chlorophyll (a+b): (a) Chlorophyll (a+b) in air at 20°, $\tau_1^{Decay} = 3 \cdot 10^{-5}$ sec (1) $\tau^{HL} = 5 \cdot 10^{-3}$ sec. (2); (b) The same film as in (a), in a vacuum of 10^{-5} mm of mercury, $\tau_1^{Decay} < 5 \cdot 10^{-6}$ sec (1), $\tau_3^{Decay} = 2 \cdot 10^{-2}$ sec (2); (c) The same film as in (b) after admission of air, $\tau_1^{Decay} = 5 \cdot 10^{-6}$ sec (1), $\tau^{HL} = 2.6 \cdot 10^{-3}$ sec (2).

2. Experiments with films of crystalline methylchlorophyllide (a+b) containing a small amount of carotinoids—lutein and violaxanthin, showed that rise and decay of the photocurrent, in the same way as for chlorophyll, took place over a wide time range. In Fig. 3a are shown typical curves of the rise and decay of photocurrent with time for methylchlorophyllide (a+b) as the linear (A) and exponential (B) evolutes with two different time constants. $\tau_1^{Decay} = 2 \cdot 10^{-4}$ sec (B, 1); $\tau_{\frac{1}{2}}^{HL} = 1.3 \cdot 10^{-3}$ sec (B, 2).

Just as in the case of chlorophyll (a+b), removal of air from the methylchlorophyllide films appreciably decreased the inertial lag. Under vacuum conditions the rapid part of the component reached 50% of the steady photocurrent value, and the lag of the slow component was reduced by a factor of 3 or more (Fig. 3b).

Analysis of the photocurrent decay curves for methylchlorophyllide films by means of a graph of the "instantaneous" relaxation times showed that, both in air and under vacuum the initial stages of decay of photoconductivity followed a hyperbolic law (Fig. 4, 1 and 1).

3. In contrast, crystalline films of chlorophyll and methylchlorophyllide (a+b) leaf pigments isolated from an extract of the green leaves of plants already in air exhibit considerably decreased relaxation times. In Fig. 3c are shown the curves of the rise and decay of photocurrent in leaf pigments with time, with and without illumination at 0.02-sec time intervals. As seen from these curves, for leaf pigments containing a mixture of chlorophyll (a+b) with carotinoids (β-carotene, violaxanthin, lutein and neoxanthin) and a lipoprotein fraction of disintegrated chloroplasts the photocurrent rise occurred more rapidly than the decay. Similarly to chlorophyll under vacuum, in the photocurrent rise curve of leaf pigments in air "instantaneous" jumps were observed. For a 10^{-2} sec illumination the photocurrent very rapidly reached a steady value. After cutting off illumination in the initial moment the photocurrent sharply

* This problem will require a more detailed investigation.

** $\tau_{\frac{1}{2}}^{HL}$ = half-life time.

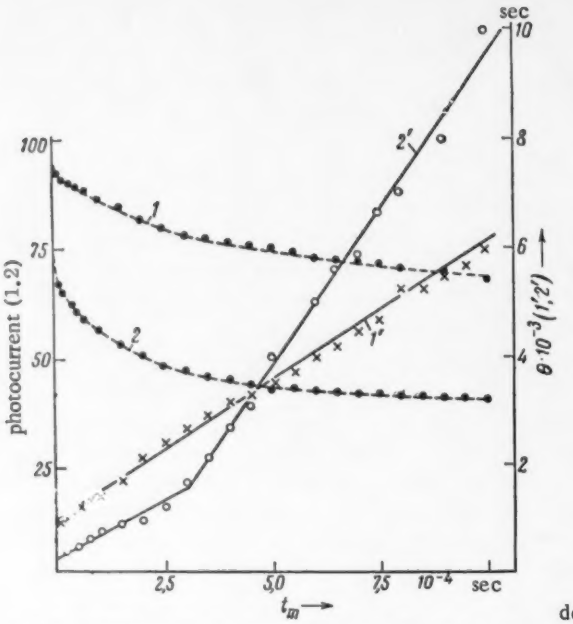

Fig. 2. 1) Photocurrent decay of chlorophyll (a + b) in air as the exponential evolute; 2) The same as 1) in vacuum. "Instantaneous relaxation times" of chlorophyll (a + b): 1' in air ($\alpha = 0.28$), 2' in vacuum ($\alpha_1 = 0.45$ and $\alpha_2 = 0.125$).

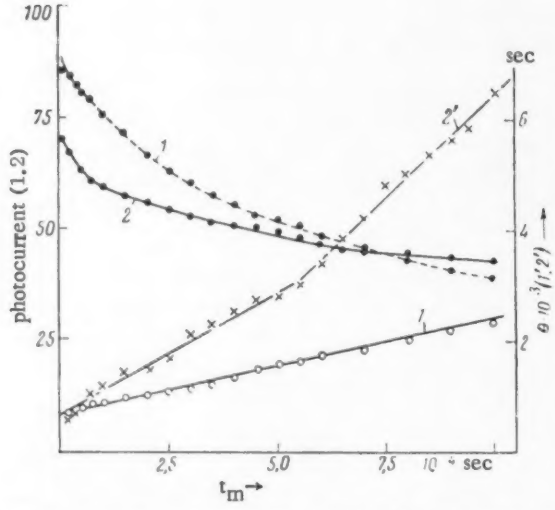

Fig. 4. 1) Photocurrent decay of methylchlorophyllide (a + b) with carotinoids (lutein, violaxanthin) in vacuum as the exponential evolute; (2) the same as (1) for green leaf pigments: "instantaneous relaxation times": 1') methylchlorophyllide (a + b) ($\alpha = 0.8$), 2) green leaf pigments ($\alpha_1 = 0.32$ and $\alpha_2 = 0.20$).

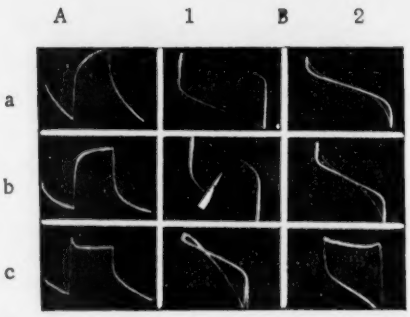

Fig. 3. Photoconductivity kinetics of (a) methylchlorophyllide (a + b) admixed with carotinoids (leutein, violaxanthin) in air at 20°, $\tau_1^{Decay} = 2 \cdot 10^{-4}$ sec (1), $\tau^{HL} = 1.3 \cdot 10^{-3}$ sec (2); (b) the same film as (a) in vacuum of 10^{-5} mm of mercury, $\tau_1^{Decay} = 7 \cdot 10^{-5}$ sec (1), $\tau^{HL} = 8 \cdot 10^{-4}$ sec (2); (c) green leaf pigments in air at 20°. $\tau_1^{Decay} = 4 \cdot 10^{-6}$ sec (1), $\tau_3^{Decay} = 1.2 \cdot 10^{-2}$ sec (2).

decreased, passed through a bend and then slowly approached the original value. In the exponential evolute in separate sections of the photocurrent decay two time constants can be distinguished: one very short $\tau_1^{Decay} = 4 \cdot 10^{-6}$ sec and a longer one $\tau_3^{Decay} = 10^{-2}$ sec.

Similarly to crystalline chlorophyll (a + b) in vacuum the photocurrent decay in the case of an extract of green leaf pigments in the time range of 10^{-5} to 10^{-3} sec in air can be approximated to the sum of two hyperbolas (Fig. 4, 2 and 2') with $\alpha_1 = 0.32$ and $\alpha_2 = 0.20$.

The establishment in this work of a small lag in the processes of liberation and loss of electronic vacancies (positive holes) in solid films of chlorophyll (a + b), methylchlorophyllide (a + b) and leaf pigments [5] shows that we are dealing with the primary process. The expressed dependence of the relaxation of photoconductivity by these pigments on adsorped vapors and gases indicated a trapping of the electrons from excited chlorophyll molecules in traps present in crystalline pigments. Experiments with the extract of green leaf pigments showed that the residues of the lipoproteins of the chloroplasts in which are fixed carotinoids and chlorophyll not only prevented the movement of charges, but this process proceeded in air with less inertial lag.

The author expresses his deep thanks to Academician A. N. Terein for his interest in the work and valuable advice, and also Prof. D. I. Sapozhnikov and I. A. Popova for the preparation of chlorophyll.

LITERATURE CITED

1. R. Nelson, J. Chem. Phys. 27, 864 (1957).
2. E. K. Putseiko, Doklady Akad. Nauk SSSR 132, 1299 (1960).

3. N. A. Tolstoi and P. P. Feofilov, Uspekhi Fiz. Nauk 41, 44 (1950).
4. N. A. Tolstoi, Izvest. Akad. Nauk SSSR, ser. fizich 15, 712 (1951).
5. A. N. Terenin and E. K. Putseiko, J. Chim. Phys. 55, 681 (1958).
6. E. K. Putseiko and A. N. Terenin, Doklady Akad. Nauk SSSR 136, No. 5 (1961).

All abbreviations of periodicals in the above bibliography are letter-by-letter transliterations of the abbreviations as given in the original Russian journal. *Some or all of this periodical literature may well be available in English translation.* A complete list of the cover-to-cover English translations appears at the back of this issue.

THE SEPARATION OF THE HYDROGEN ISOTOPES ON A PALLADIUM CATHODE

G. N. Trusov, N. A. Aladzhalova,

and V. I. Veselovskii

L. Ya. Karpov Institute of Physical Chemistry

(Presented by Academician A. N. Frumkin, August 1, 1960)
Translated from Doklady Akad. Nauk SSSR, Vol. 138, No. 6,
pp. 1385-1388, June, 1961
Original article submitted July 18, 1960

The electrochemical separation of the hydrogen isotopes has been treated in [1-5]. There is, however, a considerable spread in the experimentally determined values of the separation coefficient, S, which are cited in the literature. The theoretical work which had been published [6-9] does not give an entirely satisfactory explanation of the variation of S with the conditions of electrolysis. A series of experiments which have been carried out in the laboratories of the L. Ya. Karpov Institute of Electrochemistry [1,10] has shown that S is potential dependent for hydrogen-adsorbing metals. It was concluded here that there is some complex relationship between the separation coefficient and an electrochemical process whose mechanism and kinetics are dependent on the state of the electrode surface. Hydrogen is present on the surfaces of Fe, Ni, Pt, and Pb cathodes and fixes the energy conditions of each such surface by the nature of its bonding with it. This bonding is, in turn, determined by the treatment of the specimen and the conditions of electrolysis [11-13].

The present work aims at an elucidation of the effect of the properties of the electrode surface layer of hydrogen on the value of S. A palladium cathode was used in this study. The following information is available concerning such a cathode: 1) the activity of the hydrogen on the cathode surface is known from measurements of the palladium overvoltage (see [14]); 2) the centers of discharge and recombination of the palladium surface are known to be spatially delineated [15,16]; 3) the rate of isotopic exchange between the hydrogen of the palladium surface and an alkali electrolyte is known to be equal to 10^{-4}-10^{-5} amp/cm^2. This last fact justifies the assumption that isotopic exchange on a palladium cathode in alkaline solution is without effect on the magnitude of S at electrolyzing currents of the order of 10^{-3} amp/cm^2 [17].

Measurements were made of the deuterium-tritium* separation coefficient. The test electrode was prepared from palladium foil to which a fine platinum wire connector had been attached by polyethylene. The outer wall of a palladium test tube served as the anode, this wall being saturated with hydrogen from the inside. With this arrangement it was certain that the anodic reaction would be that of hydrogen ionization, and at the same time the possibility of entrance of oxygen into the tube was eliminated.

The characteristics of the electrode were determined by developing so-called "rapid" oscillographic overvoltage curves on which the current altered by three orders in 1.5 seconds. These curves were developed by connecting the cell in series with a condenser which had been charged to 4 kv and allowing the latter to discharge through an auxiliary resistance of 160 kilohm. The strength of the discharge current passing through the cell dropped off exponentially with time. It is obvious that the emf of the cell could not distort this exponential relation, at least to within four orders, since the polarizability of the electrodes was comparatively low. The alteration of the overvoltage was recorded on a low frequency ÉNO-1 oscillograph.

This technique made it possible to delineate clearly the two components, η_1 and η_2, of the total palladium overvoltage and determine the relation between these components and the separation coefficient**.

* The tritium concentration was determined with an internally filled Geiger-Muller counter, using both electrolytic hydrogen and hydrogen prepared by complete breakdown of the water of the electrolyte [10].

** The component η_1 arises from retardation of the discharge step in the evolution of hydrogen, and the component η_2 from the activity of the hydrogen carried by the surface.

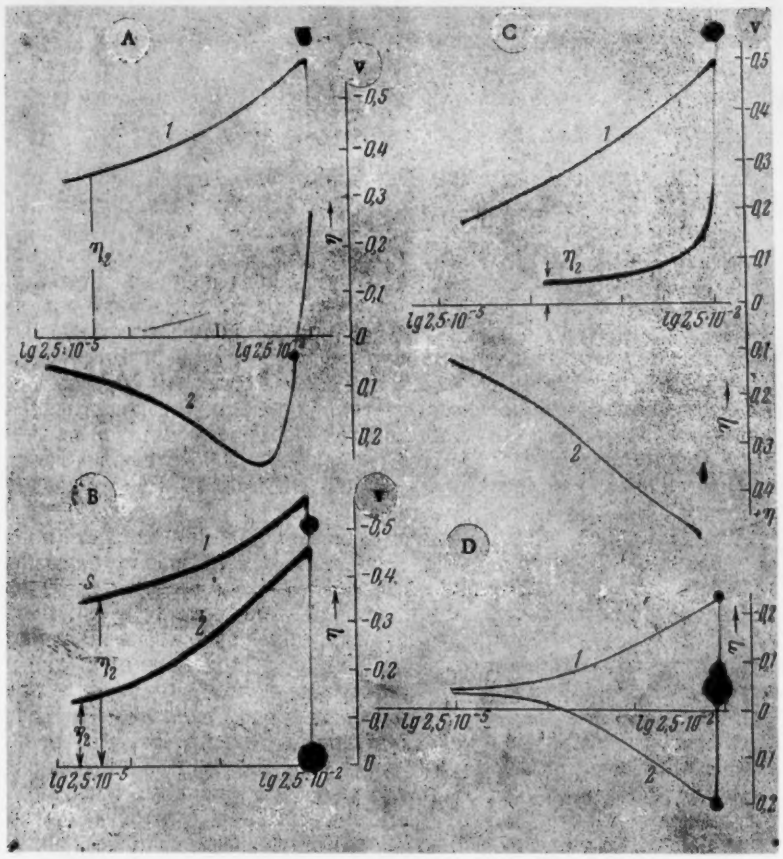

Fig. 1. Cathodic and anodic overvoltage curves: A) On electrodes which had not been given any previous anodic treatment but had been saturated with a direct current of 50 ma/cm^2; B) on a cathode after saturation with a current of 50 ma/cm^2 which was direct for Curve 1 and intermittent for Curve 2; C) during saturation of the electrode by an alternating current (cathodic impulse, 50 ma/cm^2, anodic impulse +3 ma/cm^2), Curve 3 being for fall-off (t = 1.4 sec); D) on an activated palladium electrode.

Measurements of the overvoltage and the coefficient S were carried out simultaneously. Both of these quantities are strongly dependent on the treatment of the electrode and on the means employed for saturating it with hydrogen. Each of these factors affects the ratio between the number of centers for recombination and for discharge on the electrode surface, thus altering the total value of the overvoltage and the magnitude of S (see also [19]). Alteration of S can also be brought about by resorting to certain techniques for polarizing the surface which would change the ratio of η_1 and η_2 but not the over-all overvoltage.

It was observed that the overvoltage increased during cathodic polarization if the palladium sheet had not been first subjected to strong oxidation by anodic polarization. The curve moved into the cathodic region by 100-200 mv during passage from the initial into the stationary state. The oscillographic overvoltage curves developed during approach to the stationary state (Fig. 1 A) indicate that the value of η_2 is high (Curve 1). The presence of a considerable quantity of active hydrogen on the electrode is indicated by the form of the anodic curve for hydrogen ionization developed on the same surface (see initial segment of Curve 2 of Fig. 1 A). The separation coefficient S on these electrodes ranged from 6.5 to 11.

It was found that the overvoltage diminished and the curve was displaced in the anodic region by 50-150 mv when an electrode of this same type was cathodically polarized with intermittent instead of direct current and the

frequency of interruption was so chosen that the effective current strength was approximately 20% less than in the preceding experiment. A comparison of Curve 2 and Curve 1 of Fig. 1 B shows that reduction of the total overvoltage in intermittent polarization is achieved at the expense of the component η_2. The corresponding value of S is thereby increased by 1-2 units and ranges from 7 to 12.

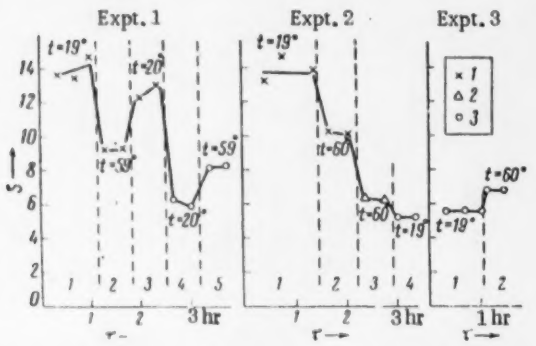

Fig. 2. The relation between S, the method of polarization and the temperature: 1) Polarization by an alternating current of 50 ma/cm² with an anodic impulse of + 3 ma/cm² (Fig. 1 B); 2) polarization by an intermittent current of 50 ma/cm² (Fig. 1 C); 3) polarization by direct current of 50 ma/cm² (Fig. 1 A).

The oscillographic overvoltage curve has the form shown in Fig. 1 C when the electrode is polarized by applying an alternating current, while maintaining the effective current density at approximately the same value as before by having the cathodic impulse 10 times greater than the anodic impulse. The fall-off curve 3 shows that such an electrode has a low η_2, while the value η_1 is much higher than in the other cases. The value of S for this electrode falls between 15 and 20.

An active palladium electrode suface shows a low value of the total overvoltage. Surface activation is achieved by alternate cathodic and anodic polarization at low current density (0.001 amp/cm²) with subsequent slight anodic oxidation of the metal. The overvoltage curves for the activated electrode are shown in Fig. 1 D and indicate low values for both the total overvoltage and its components. The S value for an electrode whose surface has been treated in this manner varies between 3.5 and 7.

Figure 2 illustrates the results which were obtained

Expt. No.	S, gas from bulk Pd	S, gas from electrolyte	Expt. No.	S, gas from bulk Pd	S, gas from electrolyte
1	1,46	6,5	5	1,3	8
2	1,15	7,5	6	1	15,6
3	1	9,6	7	1	19,8
4	1,1	9			

Note: 1,2,3,4, and 5 were electrodes having high values of η_2 (Fig. 1 A); electrodes 6 and 7 had low values of η_2 (Fig. 1C).

in certain separation experiments which were carried out at 19 and 59°. Columns 1,2, and 3 of Experiment 1 and columns 1 and 2 of Experiment 2 show values of S obtained at various temperatures with high-coefficient electrodes (characteristic curves in Fig. 1C). The figure indicates that the value of the coefficient is considerably higher at 19-20° than at 59-60°. The value of S should diminish with rising temperature according to the well-known expression $S = k\exp(\Delta E/RT)$[20].

It is observed that S increases with the temperature in the case of electrodes with high η_2 where the coefficient is markedly affected by hydrogen. This is to be seen from columns 4 and 5 of Experiment 1 and from columns 1 and 2 of Experiment 3 (Fig. 2). Naturally, elevation of temperature brings about a decrease in the coefficient even here, but this effect is masked by an increase in S which is probably related to an accelerated desorption of hydrogen from the surface.

The most clear-cut decision as to the stage of the reaction responsible for isotopic separation in electrolysis is that which follows from an analysis of the isotopic composition of the gas evolved from the electrode and the gas absorbed in the bulk of the metal*. The gas specimens must obviously be collected after attainment of a stationary state of cathodic saturation. The technique which we have developed involves removal of the hydrogen-saturated electrode from the electrolyte followed by immersion in liquid nitrogen. The frozen electrode with its residue of electrolyte is then inserted in a previously cooled ampoule and evacuated. The electrode is thawed, the water frozen

*It is clear that earlier measurements of the isotopic composition of the hydrogen absorbed by palladium [18] are less trustworthy.

out, and the ampoule heated to 300°, analysis being made of the evolved hydrogen. This procedure eliminates loss of hydrogen during transfer of the electrode from the electrolytic cell to the analytical system.

The data of the table makes it clear that S is approximately equal to unity for the recombination step. In view of this fact and the results obtained in [16] it can be considered that the principal contribution to the kinetic separation coefficient on palladium must arise from rupture of the H-OH bond during discharge of the water molecule. Experiment shows that the variation of the value of S on palladium is due to alteration in the conditions for discharge of the water molecule, these conditions being determined by the state of the surface hydrogen and the character of the water adsorption.

Low and medium values of S are shown by inactive electrodes which have high overvoltage and still retain high chemical potential of the surface adsorbed water (Fig. 1 A). Very high S values are shown by electrodes which retain high overvoltage while undergoing reduction of the potential of the surface-adsorbed hydrogen as the result of application of anodic impulses (Fig. 1 C). Low, and even very low, values of S are shown by activated electrodes on which both the chemical potential of the adsorbed hydrogen and the total overvoltage have been reduced by the application of the various methods described for activation (Fig. 1 D).

LITERATURE CITED

1. I. E. Veselovskaya, Dissertation (L. Ya. Karpov Institute of Physical Chemistry, 1952).
2. J. Takahashi, S. Oka, and M. O. Kawa, Bull. Chem. Soc. Japan, 31 220 (1958).
3. M. Stakelberg and W. Jahns, Zs. Elektrochem., 62, 349 (1958).
4. J. Brun, Th. Varberg, W. Gundersen, and R. Solli, Kgl. Norske Vid. Selskab. forh., 29, 5 (1956).
5. Post and Hiskey, J. Am. Chem. Soc., 73, 161 (1951).
6. J. Horiuti and T. Nakamura, J. Res. Inst. Catalysis Univ. Hokkaido, 3, 73 (1951).
7. T. Keii and T. Kodera, ibid., 5, 105 (1957).
8. B. E. Conway and J. O'M. Bockris, Canad. J. Chem., 35, 1124 (1957).
9. B. E. Conway, Proc. Roy. Soc., A 247, 400 (1958).
10. N. P. Vasilistov, Dissertation (L. Ya. Karpov Institute of Physical Chemistry, 1957).
11. E. M. Kuchinskii and I. E. Veselovskaya, Transactions, Fourth Conference on Electrochemistry (Moscow, 1959), p. 96.
12. J. O'M. Bockris and E. C. Potter, J. Chem. Phys., 20, 614 (1952).
13. a) P. D. Lukovtsev and S. L. Levina, Zhur. Fiz. Khim., 21, 325 (1947); b) V. É. Past and Z. A. Iofe, Zhur. Fiz. Khim., 33, 1230 (1959).
14. A. N. Frumkin and N. A. Aladzhalova, Zhur. Fiz. Khim., 18, 492 (1944).
15. M. Stackelberg and H. Bischoff, Zs. Elektrochem., 59, 467 (1955).
16. G. N. Trusov and N. A. Aladzhalova, Zhur. Fiz. Khim., 34, 11 (1959).
17. G. N. Trusov and N. A. Aladzhalova, Doklady Akad. Nauk SSSR, 130, 2, 370 (1960).
18. A. Farkas, Trans. Farad. Soc., 33, 553 (1937).
19. A. I. Fedorova and T. N. Rzhishcheva, Zhur. Fiz. Khim., 34, 684 (1960).
20. J. Bockris, Certain Problems in Modern Electrochemistry [Russian translation] (Moscow, 1958), p. 294.

All abbreviations of periodicals in the above bibliography are letter-by-letter transliterations of the abbreviations as given in the original Russian journal. *Some or all of this periodical literature may well be available in English translation.* A complete list of the cover-to-cover English translations appears at the back of this issue.

THE THERMAL EXPANSION OF WATER IN MICROCAPILLARIES

N. N. Fedyakin

Kostroma Textile Institute
(Presented by Academician A. N. Frumkin, February 17, 1961)
Translated from Doklady Akad. Nauk SSSR, Vol. 138, No. 6,
pp. 1389-1391, June, 1961
Original article submitted January 19, 1961

It has been shown repeatedly [1-3] that the interface between a polar liquid and a solid body is a singular phase which differs from the bulk liquid in both structure and properties. Thus, it is to be anticipated that there will be an alteration in properties when a liquid passes into a body in which the pore diameter is commensurate with the depth of this transition phase. Study of the properties of water in porous materials [4,5] has suggested that various liquid structures might be met in pores. Capillary nonuniformities and the solubility of various salts in water have, however, made it impossible to reach definite conclusions about the existence or properties of a special structure in microcapillaries.

The thermal expansion is a property which is extremely sensitive to structural changes. Thus, in studying the structure of transition layers it is desirable to investigate the volume expansion of the liquid in capillaries whose radii are of the same order of magnitude as the depth of this layer itself, i.e., in capillaries whose radii fall within the interval ranging from 0.1 to 0.01μ [1-8].

We will pause briefly on the technique which was employed here in measuring the capillary diameter since this is the fundamental difficulty involved in such experiments. The empty canal of a capillary whose diameter is less than the wavelength of light will scatter light from an intense bundle of rays which is directed toward it from the side, and a brilliant field will be observed when it is then viewed under a low power microscope with a magnification of the order of 100-150. The canal will scatter light only weakly when it is filled with liquid. It is possible to use these facts for detecting displacement of a liquid meniscus.

A cavity was blown on one end of the capillary whose diameter was to be measured (Fig. 1), and this cavity was then filled with liquid. Knowing the volume V of this cavity and observing the increase in length Δl of the liquid column in a certain section of the capillary resulting from heating the cavity through $\Delta t°$, the mean radius of this segment could be obtained from the equation:

$$r = \sqrt{\frac{V\Delta t\beta}{\pi\Delta l}},$$

in which β is the coefficient of volume expansion of the liquid. The volume of the cavity could be calculated from its projection if the cavity was assumed to have the form of a solid of rotation, a point which could be checked by photographing in two mutually perpendicular planes. It was, of course, necessary to allow for the magnification of the glass walls of the capillary, a factor which has been shown both theoretically and experimentally to be equal to 1.5. The uniformity of the canal over the segment in question could be judged from the value of $\Delta t/\Delta l$ read off of the experimentally developed graph showing Δl as a function of Δt.

Measurements of this kind were carried out over various portions of the capillary, and a segment with cylindrical walls then selected for use in subsequent work. The selected segment was partially filled with water and sealed at both ends in such way that only one end was free of liquid.

The apparatus for measurement of the volume coefficient of expansion consisted of: two cylindrical glass tubes set one inside of the other; a thin nichrome heating coil which was inserted between these tubes; a microscope which was equipped with a long range objective and mounted horizontally; an illuminator which was directed downward and emitted an intense bundle of light rays; and a filter which was set in the path of these rays to absorb the infrared portion of the spectrum.

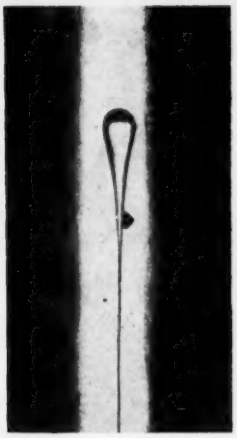

Fig. 1. Cavity at the end of capillary.

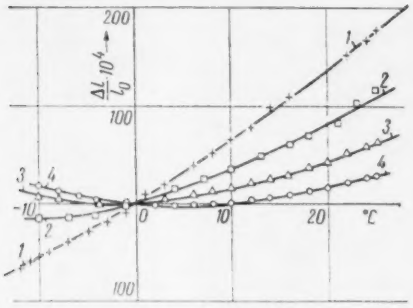

Fig. 2. Relation between $\Delta l/l_0$ and t: 1) r = = 0.022 μ, 2) 0.08 μ; 3) 0.19 μ; 4) water.

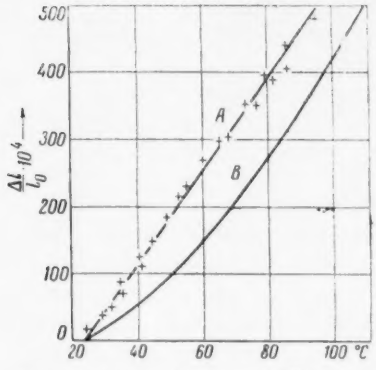

Fig. 3. Relation between $\Delta l/l_0$ and t, reduced to 23°; A) r = 0.022 μ; B) from tables of data on water.

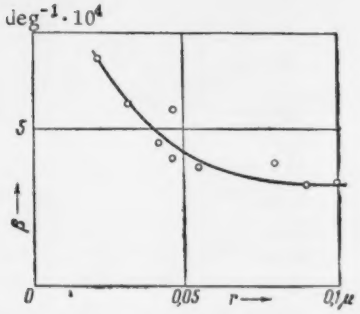

Fig. 4. Relation between β and r at 23°.

The capillary was fixed in the inner tube and a thermocouple so introduced that its tip was in contact with the middle of the capillary (this thermocouple could, however, be moved into any desired position). The tube was filled with either alcohol or glycerine, depending on the temperature interval over which measurements were to be made. The whole was so mounted in a specimen holder that the tube was in a horizontal position and perpendicular to the axis of the microscope. The temperature of the liquid in the tube, i.e., the temperature of the capillary, was measured with the thermocouple after thermal equilibrium had been established, and the expansion of the column of liquid was read off from a screw-operated micrometer eyepiece. The temperature dependence of the relative increase in length was determined in this manner.

In a cylindrical capillary the coefficient of volume expansion will be given by the equation $\beta = \Delta l/l_0 t$. It is possible to neglect the thermal expansion of the glass in this case since it is two orders less than that of water, even at 100°.

Figure 2 shows that the coefficient of volume expansion is only weakly dependent on the temperature in the case of capillaries with radii less than 0.1μ, the dependence on the radius being much more pronounced. Experimental data on the expansion of water in a capillary with 0.022 μ radius are given in Fig. 3 and compared with the bulk expansion of water, with reduction to 23°. In this capillary the coefficient of volume expansion remained constant from 10 to 120°, the maximum working temperature.

The coefficient of volume expansion over the interval from 23 to 50° is shown by Fig. 4 to rise in comparison with that of water in bulk as the capillary radius diminishes. Coldmann and Polanyi have also detected departures from the expansion of water in bulk in their measurements of the expansion of adsorbed films in porous materials from 0 to 5° [9]. X-ray studies on water [10] have shown that this material has three basically different structures, each of which is characteristic of a certain temperature interval. Passage from one structure into another is observed during heating. This is the explanation of the anomaly in the thermal expansion.

Figures 2 and 3 show that there is no anomaly of expansion in capillaries whose radii are of the order of 0.02μ. This indicates that the liquid structure remains constant here and that it is therefore different from that of water in bulk.

On the basis of these results it can be concluded that the specific volume of water in narrow pores is by no means the same as that of water in bulk since it depends differently on the temperature and varies with the pore radius as well.

LITERATURE CITED

1. B. V. Deryagin, V. V. Karasev, and Z. M. Zorin, The Structure and Physical Properties of Materials in the Liquid State (Material from a meeting in Kiev, May 28-30, 1953) [In Russian] (Kiev, 1954).
2. V. V. Karasev and B. V. Deryagin, Zhur. Tekh. Fiz., 33, 1 (1959).
3. B. V. Deryagin, V. V. Karasev, et al, Zhur. Tekh. Fiz., 27, 5 (1957).
4. A. F. Lebedev, Subsurface Water [in Russian] (Moscow-Leningrad, 1936).
5. A. A. Rode, Soil Moisture [in Russian] (Moscow, 1952).
6. B. V. Deryagin, Zhur. Fiz. Khim., 5, 2-3 (1984).
7. B. V. Deryagin and M. M. Kusakov, Izvest. Akad. Nauk SSSR, ser. Khim., No. 5 (1936).
8. B. V. Deryagin, V. I. Gol'donskii, and V. V. Karsaev, Doklady Akad. Nauk SSSR, 57, 7 (1947).
9. F. Coldmann and M. Polanyi, Zs. phys. Chem., 132, 321 (1928).
10. V. I. Danilov, The Structure and Crystallization of Liquids (Collected Papers) [in Russian] (Kiev, 1956).

All abbreviations of periodicals in the above bibliography are letter-by-letter transliterations of the abbreviations as given in the original Russian journal. *Some or all of this periodical literature may well be available in English translation.* A complete list of the cover-to-cover English translations appears at the back of this issue.